# SOLID STATE ABSTRACTS

*an abstract journal devoted to the theory, production and use of solid state materials and devices*

VOLUME 1 NUMBERS 10 – 11

PHYSICS

METALLURGY

ELECTRONICS

SEMICONDUCTORS

PHOSPHORS

MAGNETICS

DIELECTRICS

SUPERCONDUCTORS

METALS

# SOLID STATE ABSTRACTS

VOLUME 1, NUMBERS 10-11

July/August 1961

Abstracts 8580–9150


## TABLE OF CONTENTS

### Abstracts of the Solid State Literature


**Metallurgy and Chemistry of Solids**

Thermodynamic Properties . . . 443
Crystal Structure . . . 444
General . . . 444
Disordered Atomic Arrangements . . . 445
Chemical Impurities . . . 448
Crystal Growth . . . 450
Crystal Surfaces . . . 451
Environmental Effects . . . 452

**Solid State Physics**

General . . . 454
Crystal Physics . . . 454
Binding Properties . . . 454
Energy Band Structure . . . 454
Lattice Vibrations . . . 455
Electronic Properties . . . 456
Electrical Properties . . . 456
Dielectric Properties . . . 456
Carrier Properties . . . 459
Conductivity (Resistivity) . . . 463
Superconductivity . . . 466
Magnetoelectric (Galvanomagnetic) Properties . . . 469
Other Electrical Properties . . . 471
Magnetic Properties . . . 472
General . . . 472
Ferro- and Ferrimagnetism . . . 472
Paramagnetism . . . 479
Diamagnetism . . . 482
Optical Properties . . . 483
General . . . 483
Absorption (Transmission) . . . 483
Radiation (Luminescence) . . . 486
Photoelectronic Properties . . . 489
Electromagnetic Properties . . . 490
Thermal Properties . . . 491
Mechanical Properties . . . 494

**Solid State Devices**

Diodes and Rectifiers . . . 497
Point Contact . . . 497
Junction . . . 497
Area Contact . . . 501
Transistors . . . 502
General . . . 502
Point Contact . . . 502
Junction . . . 502
Surface Barrier . . . 505
Magnetoelectric Devices . . . 505
Other Conductive Devices . . . 506
Photodevices . . . 506
Thermal Devices . . . 507
Ferro- and Ferrimagnetic (Ferrite) Devices . . . 508
Paramagnetic Devices (Masers and Lasers) . . . 509
Other Solid State Devices . . . 510

**Basic Solid State Device Circuits**

General . . . 510
Amplifiers . . . 511
Oscillators . . . 513
Switching Circuits . . . 514
Signal Converters . . . 515
Wave Generators . . . 516
Other Circuits . . . 516

**Applications of Solid State Devices**

Commercial and Space . . . 517
Radio and Television . . . 518
Telephony . . . 518
Other Communications Type Applications . . . 519
Computers . . . 519
Power Applications . . . 520
Control Applications . . . 521
Instrumentation . . . 522

**Subject Index** . . . 524

**Author Index** . . . 532



**Editor: GEOFFREY KNIGHT, JR., Ph.D.**

**Assistant Editor: JOHN A. MURPHY**

**PUBLISHED MONTHLY BY**

Cambridge Communications Corporation, 238 Main Street, Cambridge 42, Massachusetts, Tel. 491-0710

Subscription Rate: $25.00 per year. Single Copies and Back Issues: $5.00. Advertising Rates on Request.

Cambridge Communications Corp. is not prepared to furnish copies of the articles abstracted. However, there are many libraries throughout the country which maintain photocopying services.


**SYMBOLS USED IN THE ABSTRACTS**

L: Letter to the Editor. A: Only an abstract is given in the reference. R: Only a review is given in the reference. E: Erratum.

The reference numbers in the indices are the abstract numbers, not the page numbers.


Copyright 1962 by Cambridge Communications Corp. Printed in the U.S.A. by the University Press, Inc.

# ABSTRACTS OF THE SOLID STATE LITERATURE

## METALLURGY AND CHEMISTRY OF SOLIDS

### THERMODYNAMIC PROPERTIES

8580 PHASE EQUILIBRIA IN THE SYSTEM ZnO-$TiO_2$ by F. H. Dulin and D. E. Rase (Alfred U.); J. Am. Ceram. Soc., Vol. 43, pp. 125-131, Mar. 1960

An investigation of the system ZnO-$TiO_2$ using quenching, hydrothermal, strip furnace, and solid state reaction techniques is reported. Two compounds were found: $Zn_2TiO_4$, which melts congruently at 1549°C, and $ZnTiO_3$, which dissociates hydrothermally at 945°C to give $Zn_2TiO_4$ and rutile. Two eutectics were found: one between ZnO and $Zn_2TiO_4$ at 32 mole per cent $TiO_2$ and 1537°C and the other between $Zn_2TiO_4$ and $TiO_2$ at 58 mole per cent $TiO_2$ and 1418°C. Rutile was the only modification of $TiO_2$ observed. Reported solid solutions of $TiO_2$ in $Zn_2TiO_4$ and $ZnTiO_3$ were not found and explanations of this discrepancy are proposed.

8581 PHASE EQUILIBRIA IN THE FERRITE REGION OF THE SYSTEM FeO-MgO-$Fe_2O_3$ by A. E. Paladino (Raytheon); J. Am. Ceram. Soc., Vol. 43, pp. 183-191, Apr. 1960

An investigation of phase equilibria in the ferrite region of the system FeO-MgO-$Fe_2O_3$ at temperatures up to 1300°C over an oxygen pressure range of 1.0 to 0.01 atmospheres is reported. The five most important features of the equilibria in this system are: (1) the spinel phase can exist with a deficiency of oxygen in the high magnesium compositions, (2) $Mg^{2+}$ replaces $Fe^{2+}$ in $Fe_3O_4$ beyond the "stoichiometric $MgFe_2O_4$," corresponding to the formula $(MgO)_xMgFe_2O_4$, where $x = 0.092 \pm 0.004$ and is independent of temperature, (3) the spinel field does not include a single phase composition corresponding to $MgFe_2O_4$, (4) the lattice constant of spinels in this system depends on cation distribution, and the extent of distribution changes as a function of temperature in turn depends on the Mg concentration in the spinel, and (5) the spinel field near its terminus has little or no width.

8582 SOLID-VAPOR EQUILIBRIA FOR THE COMPOUNDS $Cd_3As_2$ AND $CdAs_2$ by V. J. Lyons and V. J. Silvestri (IBM); J. Phys. Chem., Vol. 64, pp. 266-269, Feb. 1960

Measurements which show that $Cd_3As_2$ and $CdAs_2$ thermally dissociate according to the reactions $Cd_3As_2 \rightleftarrows 3Cd + 1/2\,As_4$ and $CdAs_2 \rightleftarrows 1/3\,Cd_3As_2 + 1/3\,As_4$ are discussed. Dissociation pressures were measured by a dew-point technique and by a direct pressure method employing a quartz Bourdon gauge. The dissociation of $Cd_3As_2$ in the gas phase was observed through a comparison of the data obtained from the two methods and the gaseous species was identified from this. The experimental data may be represented by the equation $\log P_{mm} = -6600/T + 9$ ($\Delta H = 106$ kcal/mole). In contrast to $Cd_3As_2$, thermal dissociation of $CdAs_2$ is readily observed. The compound dissociation pressures measured by the two techniques were in good agreement and the data may be represented by the equation $\log P_{mm} = 7100/T + 11$ ($\Delta H = 11$ kcal/mole).

Melting Points of HgTe-CdTe Mixed Crystals - See 8867

8583 HETEROGENEITIES IN SOLID SOLUTIONS by A. Griunier (U. Paris); Solid State Phys.-Adv. Res. and Appl., Academic Press, 1959, Vol. 9, pp. 293-398

The structure of homogeneous, disordered substitutional metallic solid solutions is discussed. The principles of the method of studying lattice faults and a brief indication of the experimental techniques for the application of these principles are given. The typical equilibrium case consists of an alloy kept at a temperature in the range of a stable, single phase, or a disordered solid solution that is maintained above the critical temperature of ordering. The theories are compared with experimental data. It is possible to describe the statistical distributions of atoms in a solid solution accurately from experimental information. The most important non-equilibrium case is the super-saturated solution when it is still a single phase. Continuous and discontinuous precipitation and pre-precipitation are discussed. Variations in the properties of solid solutions in the pre-precipitation stage are caused by heterogeneities in the distribution of the dissolved atoms. The excess dissolved atoms have a tendency to form "zones". The arrangement of the atoms in the zones as determined with X-rays is described in detail. With the aid of this structure, it is possible to explain certain properties and the laws governing their growth and transformation.

Solid Solutions of:
GaSe and GaS - See 8900
$Fe_2O_3$ and $FeVO_3$ - See 8631

Dielectric Properties of Solid Solutions Based on $NaNbO_3$ - See 8677

Superconducting Transitions in Thallium Solid Solutions - See 8743

8584 THE DISTRIBUTION OF IONS AND THEIR VALENCIES IN MAGNESIUM MANGANESE FERRITES by J. Broz (Czech.

Acad. Sci.); Czech. J. Phys., Vol. 10B, No. 6, pp. 428-438, 1960

A model of the distribution of cations and valencies in non-stoichiometric Mg-Mn ferrites is proposed and its validity is verified by measurements of the saturation magnetic moments. The results of measuring the moment in stoichiometric ferrites to a certain extent also confirm the correctness of the proposed model for this type of Mg-Mn ferrite. In a discussion of the distribution coefficient for Mn ions the close connection between this coefficient and the average valency of the Mn is indicated. The question of the dependence of the distribution coefficient of Mg ions on the composition is solved by introducing the maximum values of this coefficient and assuming that a simple proportionality holds for all compositions between the actual value of this coefficient and its maximum value.

Stoichiometry of Alloys - See 8653

8585 ON THE POSSIBILITY OF GRADUAL PHASE TRANSITIONS IN SOLIDS by J. W. Allen and D. M. Eagles (Services Electronics Res. Lab.); Physica, Vol. 26, pp. 492-500, July 1960

The possibility that some substances can change from one crystal structure at low temperature to a second structure at high temperature through a continuous range of mixed structures is discussed. Simple models are used as illustrations. The thermodynamics of the process is considered to determine the conditions which the system must obey in order to show this behavior. A comparison of the theoretical predictions with some experimental results on ZnS is presented.

Phase Transformations in $Mn^{3+}$ Spinels - See 8590

8586 SEMICONDUCTING PROPERTIES OF GREY TIN by G. A. Busch and R. Kern (Eidgenossische Tech. Hoch., Zurich); Solid State Phys.-Adv. Res. and Appl., Academic Press, 1960, Vol. 11, pp. 1-40

The $\alpha \leftrightarrow \beta$ transition of tin is discussed. The $\alpha$-phase, which is stable below 13.2°C, forms spontaneously if metallic or $\beta$-tin is kept below this temperature for a sufficiently long time. Density measurements reveal that the process is never completed. This is also true for the reverse transformation. During the incubation period, nuclei of the $\alpha$ phase are formed. This nucleation time is followed by the spherical growth of each nucleus. A number of observations indicate that the $\alpha \leftrightarrow \beta$ transformations are of the diffusionless or martensitic type. The methods of preparation of grey-tin powder, coherent samples and single crystals are reviewed. The semiconducting properties of grey tin and the experimental results of conductivity, the Hall effect, magnetoresistance, thermoelectric power, magnetic susceptibility, and photoconductivity are discussed. The determination of characteristics and the effects of impurities on intrinsic and extrinsic properties are considered.

## CRYSTAL STRUCTURE

### GENERAL

8587 THE STRUCTURE OF CRYSTALS by A. F. Wells (Imp. Chem. Ind., England); Solid State Phys.-Adv. Res. and Appl., Academic Press, 1958, Vol. 7, pp. 425-503

A topological approach to the problem of the structure of crystals is presented. The basic geometry underlying the structures of crystals is outlined. Periodic networks of connected points, space filling by polyhedra, open packings of polyhedra and the closest packing of equal spheres are discussed. Crystals of different formula types $MX_n$, which arise by filling different proportions of the octahedral holes in the close packing of X atoms, form the octahedral coordination of metal atoms in close-packed oxides and halides. The structures of many complex oxides and halides are based on close-packed layers. Structures with very high coordination numbers and those based on 3-connected nets, 4-connected nets, 6-connected nets, and 8-connected nets are considered. It is shown how other structures are related in a topological sense to certain fundamental 3-dimensional networks.

8588 NUCLEAR MAGNETIC RESONANCE IN CRYSTALS by D. W. McCall and R. W. Hamming; Acta Cryst., Vol. 12, p. 81, 1959

Nuclear magnetic resonance techniques in crystal analysis are examined from the point of view of Van Vleck's theory for the second moment of the resonance absorption as applied to single crystals. Assuming only dipolar interactions to be important and assuming a rigid lattice, a procedure for acquiring and analyzing the second moments is developed. The second moment may be completely described by fifteen parameters in the most general type of the crystal and thus only fifteen structural parameters can be uniquely determined from second moment data. The fifteen experimental parameters are related to fifteen sums over internuclear coordinates. The fifteen lattice sums must be equal to the corresponding theoretical lattice sums (from Van Vleck's theory) for the correct crystal structure. Thus a trial-and-error technique may be employed to determine nuclear coordinates. Formulae are given by which one may find the adjustments required in the nuclear coordinates of the trial structure when the structure is known approximately. The calculations are well suited for programming on a high-speed digital computer.

Lattice Parameters of HgTe and CdTe - See 8867

Lattice Constants of:
$Y_{3-x}Yb_xFe_5O_{12}$ - See 8817
$FeO-MgO-Fe_2O_3$ Ferrites - See 8581

8589 ON THE STRUCTURE OF ZnSb by K. Toman (Czech. Acad. Sci.); J. Phys. Chem. Solids, Vol. 16, pp. 160-161 (L), Nov. 1960

X-ray powder diffraction measurements made on ZnSb are discussed. Considerable disagreement was found between the coordinates of the zinc atoms and the coordinates measured by Almin and between the Zn-Zn distance (2.82 ± 0.02A) and that measured by Almin (2.59A). The interatomic distance measurements have the following similarities with measurements in CdSb: (1) long (non-bonding) Zn-Zn distance, (2) two short (bonding) Zn-Sb distances, and (3) one longer (presumable non-bonding) Zn-Sb distance. This suggests that the bonding scheme of Mooser and Pearson for CdSb also holds for ZnSb.

Crystal Structure of:
$CrF_2$ and $CrCl_2$ - See 8821
$FeVO_3$ - See 8631

8590 CRYSTAL DISTORTION IN SPINELS CONTAINING

$Mn^{3+}$ IONS by K. S. Irani, A. P. B. Sinha and A. B. Biswas (Natl. Chem. Lab., India); J. Phys. Chem. Solids, Vol. 17, pp. 101-111, Dec. 1960

The effect of chemical composition on tetragonal-cubic spinel transformations in the systems $Mn_3O_4$-$MgAl_2O_4$ and $MgMn_2O_4$-$MgAl_2O_4$ has been studied by X-ray diffraction. The unit cell dimensions of the various compounds have been determined at room temperature. The c' and a' values do not change linearly with composition but show an abrupt change at a critical composition, beyond which c' = a', and the systems have the cubic spinel structure. The cation distribution has been worked out from an analysis of the X-ray diffraction intensities, and thus a correlation between the actual number of distorting $Mn^{3+}$ ions at the octahedral sites and the degree of distortion has been obtained. The critical number of $Mn^{3+}$ ions required at these sites to maintain the tetragonal spinel structure at room temperature has been accurately determined.

Effects of Polytypism on the Electron Paramagnetic Resonance of $K_3Co(CN)_6$ - See 8831

## DISORDERED ATOMIC ARRANGEMENTS

8591 IMPERFECTION IONIZATION ENERGIES IN CdS-TYPE MATERIALS BY PHOTOELECTRONIC TECHNIQUES by R. H. Bube (RCA Labs.); Solid State Phys.-Adv. Res. and Appl., Academic Press, 1960, Vol. 11, pp. 223-260

An investigation of crystal imperfections by photoelectronic techniques is reported. Those techniques useful in determining the location of energy levels which cannot be located by standard methods are emphasized. There are three effects of impurities on conductivity, namely: changing the photosensitivity; changing the speed of response; and extending the spectral response of photoconductivity to the long wavelength side of the absorption edge. Various photoelectronic techniques for obtaining ionization energies, including the measurement of variation of conductivity and the Hall constant with temperature, are described. Measurements of optical absorption, of photoconductivity with light intensity, of thermally stimulated luminescence or conductivity, and of space-charge-limited currents, are reported. The assignment of observed ionization energies to specific imperfections is difficult in some cases. Approximate correlation between the observed ionization energies and the individual cation and anion constituents of the material is made. Some indications of complex ionization processes are discussed.

Lattice Faults in Solid Solutions - See 8583

8592 SMALL ANGLE INTENSITIES FROM DOUBLE-BRAGG REFLECTIONS IN COLD-WORKED METALS by B. E. Warren (MIT); Austl. J. Phys., Vol. 13, pp. 376-383, July 1960

The small angle intensity from a cold-worked polygrain metal is treated in terms of double Bragg reflections. It is assumed that cold work breaks up the original grains into subgrains with varying orientations, such that a first reflection in one subgrain can be followed by a second reflection in another subgrain of the original grain. For an initial sample which is polygrained with random orientation, the small angle intensity resulting from cold work is given in absolute units in terms of two parameters; an average initial grain size G, and a subgrain correlation function $p(\phi)$ giving the distribution in orientation of subgrains with respect to any average subgrain of the original grain. Under favorable conditions, both of these quantities can be obtained from the small angle intensity curve. For polygrained metals small angle scattering is a useful tool for obtaining the subgrain correlation function $p(\phi)$, a quantity not obtainable from the usual high angle measurements.

8593 WAVE FUNCTIONS FOR ELECTRON-EXCESS COLOR CENTERS IN ALKALI HALIDE CRYSTALS by B. S. Gourary and F. J. Adrian (Johns Hopkins U.); Solid State Phys.-Adv. Res. and Appl., Academic Press, 1960, Vol. 10, pp. 127-247

Wave functions for electron-excess color centers in alkali halides of the NaCl structure are considered. The approximations made in reducing this many-electron problem to an effective one-electron problem and the various methods used in the solutions of the one-electron problem are surveyed. A brief discussion of polarization experiments, electron spin resonance and electron nuclear double resonance is given. Various calculations based on continuum models and semicontinuum models are discussed. Calculations based on these models allow for the failure of the effective mass approximation and the dielectric constant concept. Treatment of color center problems by molecular orbital techniques and the point-ion-lattice approximation are discussed. It is concluded that the foundation of the one-electron approximation is still shaky. The quasi-adiabatic approximation should be put on a firmer foundation.

Theory of the F-Center - See 8895

Annealing of Radiation-Induced Color Centers in LiF - See 8647

Coloration of Glass by $\gamma$-Rays - See 8648

Paramagnetic Resonance of F-Centers - See 8835, 8836, 8837, 8839, 8840

Optical Absorption of Color Centers - See 8856, 8857, 8858, 8859, 8860

Luminescence of Color Centers - See 8885 and 8886

8594 ON THE EFFECT OF NONEQUILIBRIUM VACANCIES ON THE KINETICS OF KIRKENDALL DIFFUSION by H. Fara and R. W. Balluffi (U. Illinois); J. Appl. Phys., Vol. 30, pp. 325-329, Mar. 1959

A nonequilibrium vacancy diffusion model which predicts nonparabolic kinetics is described. The kinetics approach those of the equilibrium model when either the vacancy lifetime approaches zero or the diffusion time becomes large. The applicability of the equilibrium model depends on the particular system and the diffusion time. It is concluded that non-parabolic effects are of little importance in fcc metallic systems when $Dt > 10^{-5}\,cm^2$.

8595 A THEORY OF THE CONDENSATION OF EXCESS VACANCIES DURING THE COOLING OF SOLIDS by V. I. Vladimirov (Leningrad Physicotech. Inst.); Soviet Phys.-Solid State, Vol. 2, pp. 145-153, July 1960

The condensation of vacancies in a solid during a temperature decrease is considered. It is shown that the condensation of vacancies can produce macroscopic imperfections $\gtrsim 10^3 a$, where "a" is the lattice constant. A relation between the dimensions of the imperfections and the rate of cooling is calculated. The effect of the vacancies escaping toward the surface of the solids is evaluated.

Clustering of Vacancies in NaCl - See 8729

8596 CLASSICAL NONLINEAR LATTICE-STATICS OF DISLOCATIONS. Part II. CALCULATIONS [in German] by F. Wahl; Z. Naturforsch., Vol. 15a, pp. 983-993, Nov. 1960

The layers of the lattice elements and the dislocation energy are calculated for a dislocation in the KCl crystal. The resulting displacements are clearly displayed in a diagram. The basic calculations are carried through, but not in all details. A series of mathematical tools is derived. Problems of convergence and divergence are investigated, and the results are discussed. In the energy calculations some detailed considerations are still necessary.

8597 THE BASIC EQUATIONS OF THE DYNAMICS OF THE CONTINUOUS DISTRIBUTION OF DISLOCATIONS. Part I. GENERAL THEORY by E. F. Holländer (Welding Res. Inst.) Czech. J. Phys., Vol. 10B, No. 6, pp. 409-418, 1960

The basic equations for the continuous distribution of dislocations are derived for the dynamic case (especially for small deformations) and for the Poisson ratio equal to zero in a continuum, infinite with respect to space and time, using the variational method and the formal apparatus of the special theory of relativity.

8598 OBSERVATION OF DISLOCATIONS IN NON-METALLIC LAYER STRUCTURES by S. Amelinckx and P. Delavignette; Nature, Vol. 185, pp. 603-604, Feb. 27, 1960

A study of dislocations in $Bi_2Te_3$, $Sb_2Te_3$, graphite, muscovite and talc by the electron microscope thin film transmission technique is reported. Within the resolution of the microscope available, dislocations appear to be undissociated in $Sb_2Te_3$ with a slight suggestion of dissociation in $Bi_2Te_3$. Extensive beam-induced movement of dislocations was observed both on the c-plane and on the pyramidal glide planes. In muscovite the electron beam appears to cause gas bubbles to precipitate on the dislocations. In graphite and talc dislocations are split into partials. In the latter the equilibrium separation is about 0.2μ, corresponding to a very low stacking energy.

Effect of Crystal Polarity on the Detection of Dislocations by Etching - See 8639, 8640, 8641

Dislocation Etch Pits on P-Type PbTe - See 8642

8599 THE FORMATION OF DISLOCATIONS BY A SPARK DISCHARGE by B. Sestak and S. Libovicky; Czech. J. Phys., Vol. 10, No. 10, pp. 759-764, 1960

A study of the arrangement of dislocations formed in a single crystal of the alloy Fe-4.2 per cent Si by a spark discharge in air is reported. The dislocations were made visible by etching on the surfaces perpendicular and parallel to the axis of the crater. The results of the observations are explained on the basis of microphysical concept of plastic deformation.

Density of Dislocations in Annealed Alloys - See 8916

8600 THE ORIENTATION DEPENDENCE OF WORK-HARDENING IN CRYSTALS OF FACE-CENTERED CUBIC METALS by L. M. Clarebrough and M. E. Hargreaves (CSIRO); Austl. J. Phys., Vol. 13, pp. 316-326, July 1960

It is shown that the principal features of the observed orientation dependence of work-hardening can be accounted for in terms of the likelihood of formation of Lomer-Cottrell sessile dislocations in two directions in the primary slip plane. This is deduced from the known variation of resolved shear stress with orientation, for the possible secondary slip systems, and metallographic observations of slip and deformation bands.

8601 HARDENING DUE TO THE RECOMBINATION OF DISLOCATIONS by G. Saada; Acta Metal., Vol. 8, pp. 841-847, Dec. 1960

Two simplified models which show how the recombination of dislocations influences hardening are discussed. It is established that, in a dislocation "forest", the piercing of attracting "trees" results in stresses which are decidedly greater than those accompanying the penetration of repulsing "trees". The recombination mechanism is responsible for the formation of vacancies or interstitials, the role played by thermal activation being negligible. It is supposed that the dislocations are not dissociated.

8602 PHYSICS OF THE STRENGTH OF CRYSTALLINE MATERIALS by R. I. Garber and I. A. Gindin (Acad. Sci., USSR); Sov. Phys.-Uspekhi, Vol. 3, pp. 41-77, July-Aug. 1960

Present physical ideas about the strength of crystalline materials, the reasons for the low strengths of real materials, and also the main ways of increasing their strengths are discussed. The discrepancies between the various theories of strength and the experimental results are examined. Structural defects, such as dislocations, are fully discussed in their relation to the strength of materials. Surface or interior cracks are treated in detail. Other factors influencing the strength, e.g., size or environment, are considered. It is concluded that while a strict quantitative theory of the strength of solid materials on the basis of ideas about real crystals has not yet been developed, the available experimental data is in satisfactory agreement with such ideas.

Dislocation Damping in Si and Ge - See 8946

8603 DISLOCATION NETS IN BISMUTH AND ANTIMONY TELLURIDES by P. Delavignette and S. Amelinckx (Ctr. d'Etude Energie Nucl., MOL Belgium); Phil. Mag., Vol. 5, pp. 729-744, July 1960

Extended dislocation patterns revealed by electron microscopic examination of thin foils of $Sb_2Te_3$ and $Bi_2Te_3$, prepared by repeated cleavage, are discussed. Since the C-plane is simultaneously glide and cleavage plane, the dislocation arrangements are preferentially situated in the plane of observation. This is of considerable advantage in the study of configurations due to glide. Sets of concentric dislocation lines are often observed, but they invariably originate in some invisible source outside the crystal. In the C-plane very extended nets are often observed. The multiplication of dislocations and the resulting formation of networks, as well as the elimination of dislocations, are observed while in progress. The latter phenomenon is due to a combination of glide and climb. Some contrast effects are also mentioned.

8604 RADIATION LIMITED DISLOCATION MOTION IN CRYSTALS by R. Thomson (U. Illinois); J. Appl. Phys., Vol. 31, p. 617(L), Mar. 1960

The case where a dislocation, moving with nearly zero average velocity, traverses a Peierls hill structure is considered.

The radiation loss per atom length of line of the dislocation in moving from the bottom of one hill to the top of the next is computed and compared with the energy gained as it moves one atomic distance through the stress field. The energy radiated is found to be much larger than the energy gained for any crystal with a critical shear stress of the usual magnitude. The ratio of the energies approaches unity only when the stress approximates the Peierls value. The observed critical shear stress at which dislocations become mobile seems, therefore, not due to the dynamic motion of the dislocation but the dislocations may be thermally activated through the lattice hill and valley structure.

8605 THEORY OF DISLOCATION CLIMB IN METALS by J. Lothe (U. Fysiske Inst., Oslo); J. Appl. Phys., Vol. 31, pp. 1077-1087, June 1960

An estimate of the climb motions of dislocation jogs which takes into account the fact that dislocations are pipes of easy diffusion is given. The climb of dislocations under near-equilibrium conditions is then discussed. A new estimate is made of the jog concentration for which vacancy equilibrium will be established along the entire dislocation. It is argued that the dislocation line tension is an important driving force both in high-temperature creep and in whisker dekinking. Under quench conditions it must be expected that a great number of jogs are nucleated at the nodes of the dislocation network.

8606 THE INTERACTION OF PARALLEL EDGE DISLOCATIONS WITH A SIMPLE TILT DISLOCATION WALL by J. C. M. Li; Acta Metal., Vol. 8, pp. 296-311, May 1960

An elastic theory analysis of the interaction of a dislocation wall (tilt substructure boundary) with parallel approaching dislocations whose slip vectors are the same as those of the dislocations in the wall is reported. It is found that such a wall fully or partially pinned is a less effective barrier for the penetrations of dislocations than a single pinned dislocation on the same slip plane as an approaching dislocation. Quantitative results for the equilibrium positions of the free dislocations in the wall and the forces exerted on the approaching dislocation in various cases are presented. Free dislocations in the wall usually reduce the resistance of the wall to the penetration of approaching dislocations. The interaction between a wall and a solute atom is found to be less than that between the single nearest dislocation with the same solute atom. It is suggested that the experimental evidence which leads to the concept of hardening by substructures of this kind needs further interpretation. The segregation of vacancies and solute atoms to the dislocations probably plays a more important role in the hardening effect than the appearance of substructure.

8607 ON THE INTERACTION BETWEEN A FIXED DISLOCATION AND A MOBILE DISLOCATION IN ITS SLIP PLANE by G. Saada; Acta Metal., Vol. 8, pp. 200-208, Mar. 1960

A model is proposed for the detailed study of the passage of a dislocation moving in its slip plane through a dislocation "forest." In the absence of exterior constraints, there does not exist, in the slip plane, a stable loop enclosing one of the "trees" of this "forest." It is also shown that the passage of a repulsive "tree" is made without a significant modification of the shape of the line. If slip is not too difficult, the jog created by the passage of a "tree" will produce an appreciable number of vacancies only if the "tree" is attractive. Several applications in the study of hardening are cited. It is shown, in particular, that the dislocations situated in slip planes near those of the moving dislocations exert constraints of the same order as those due to "trees" cutting the slip plane.

8608 THE INTERACTION OF DISLOCATIONS IN SILICON OBSERVED WITH THE AID OF SHADOWING by L. S. Milevskii (Baikov Inst. Metall., USSR); Sov. Phys.-Cryst., Vol. 4, pp. 742-743, May 1960

The interaction of dislocations belonging to different glide systems in Si single crystals is described. A decoration technique using a precipitate of Cu was employed. Read and Cottrell have stated theoretically that if two dislocations intersect during the process of glide formation, then the character of the interaction is determined by their orientation in the crystal and also by the type of dislocation. This is corroborated, along with Cottrell's further statements about the case in which two screw dislocations intersect.

8609 DISLOCATIONS IN FERROELECTRIC GLYCINE SULFATE SINGLE CRYSTALS by H. Toyoda (Nippon Tel. and Tel.); J. Phys. Soc. Japan, Vol. 15, p. 1539(L), Aug. 1960

Dislocation etch pits observed on the surfaces of glycine sulfate crystals are discussed. Rapid etching with water has revealed cone-shaped etch pits on (010) faces and pits with trapezoidal bases on the (001) and (110) faces. Pits on opposite (010) cleavage surfaces were found to match each other. A nearly perfect match was found between pits on (110) and (001) faces produced by cutting the crystals with a wet thread. The density of the pits varies from $10^2$ to $10^6$ $cm^{-2}$ on all crystal faces. Experimental evidence indicates that there is some relationship between the dislocation density and the domain structure.

Effect of Dislocations on Carrier Transport in Bicrystals - See 8708

8610 THE STRUCTURE AND PROPERTIES OF GRAIN BOUNDARIES by S. Amelinckx and W. Dekeyser (Cryst. Lab., Belgium); Solid State Phys.-Adv. Res. and Appl., Academic Press, 1959, Vol. 8, pp. 325-499

Dislocation models of small-angle boundaries and the geometry of dislocation arrays are discussed. The density of dislocation in a boundary is directly proportional to the angle of rotation and the lines are straight, equally spaced, and parallel. Stable boundary models in which the boundary has the lowest energy are derived for the primitive lattice, face-centered cubic and body-centered cubic structures. Methods restricted to observation of the surface and methods which permit observation of dislocations in the bulk are discussed. Mechanics of grain boundaries, as well as the problem of stability, are considered in detail. For a high-angle case, any variation of energy with the angle is incompatible with the existence of an amorphous transition zone. The mechanism for the formation of dislocations in melt-grown crystals and deformed crystals is discussed. Diffusion phenomena have a direct bearing on the structure of grain boundaries, and the interpretation of experimental results is discussed. Theoretical and experimental aspects of the segregation and precipitation of solutes at grain boundaries are presented. The specific electrical properties of boundaries which are associated with the presence of dangling bonds, most pronounced in semiconductors, are discussed.

8611 MODELS OF GRAIN BOUNDARIES IN THE DIAMOND LATTICE. Part II. TILT ABOUT <001> AND THEORY by

J. Hornstra (Philips); Physica, Vol. 26, pp. 198-208, Mar. 1960

Models for large angle grain boundaries with a <001> tilt axis in the diamond lattice are discussed. For all angles of tilt, dislocations without dangling bonds can be used in the construction of the models. One model may be considered either as an array of edge dislocations or as an array of 45° dislocations. The crystallography of regular grain boundaries is discussed, the grain boundary index is introduced, and the application of the transformation matrix to grain boundary problems is illustrated.

Electrical and Photoelectrical Properties of Grain Boundaries - See 8896

Electroluminescence at Grain Boundaries in GaP - See 8882

8612 ELECTRONIC PROCESSES IN ZINC OXIDE by G. Heiland and E. Mollwo (U. Erlangen, Germany) and F. Stockmann (Tech. Hoch., Darmstadt, Germany); Solid State Phys.- Adv. Res. and Appl., Academic Press, 1959, Vol. 8, pp. 191-323

The applications, lattice structure and various physical properties of ZnO are discussed. It can be used as a catalyst and photocatalyst, and it plays a subordinate role as a semiconductor and photoconductor. ZnO has hexagonal wurtzite lattice structure, in which oxygen ions are arranged in closest hexagonal packing, and Zn ions occupy half of the tetrahedral interstitial positions. Optical and electrical properties are described in detail. The results of diffusion of defects are discussed in connection with observations of the so-called tarnishing reactions of metallic Zn and oxygen. Absorption and refraction are discussed for material with and without admixtures. The properties of photoconductivity cannot be explained by considering only processes which play an important role in producing luminescence radiation. The conductivity in thermal equilibrium and the methods of measurement are discussed for three cases: 1) thin layers, 2) sintered specimens, and 3) single crystals. Various influences on the conductivity are considered.

## CHEMICAL IMPURITIES

8613 MASS SPECTROGRAPHIC STUDIES OF IMPURITIES ON SURFACES by A. J. Ahearn (Bell Labs.); 1959 Vacuum Symp. Trans., Pergamon Press, 1960, pp. 1-5

A mass spectrograph which can detect and identify surface contaminants at concentrations of less than the equivalent of 0.01 monatomic layer is described. The spectrograph is a double focusing instrument of the Mattauch type that uses a vacuum spark as its source of positive ions. It was built primarily for the study of bulk impurities in solids which it can detect at concentrations below $10^{-7}$ atomic fraction. It can also distinguish between bulk impurities and surface contaminants. Typical studies of surface contaminants on semiconductors and on insulators are presented.

8614 SPECTROGRAPHIC ANALYSIS OF HIGH PURITY SILICON CARBIDE by G. H. Morrison, R. L. Rupp and G. L. Klecak (Genl. Tel. Electronics); Analyt. Chem., Vol. 32, pp. 933-935, July 1960

A direct spectrographic method for the determination of trace impurities in semiconductor grade SiC with limits of sensitivities for many elements in the range 10 to 300 ppb is described. Through selective volatilization of many impurity elements from the SiC matrix, it has been possible, under proper conditions, to increase the sensitivity several orders of magnitude over previous spectrographic methods. Conditions of analysis, working curves, and limits of sensitivities for 15 impurity elements are presented.

8615 ANALYSIS OF BISMUTH-ANTIMONY-TELLURIUM-SELENIUM COMBINATIONS by J. F. Reed (Westinghouse); Analyt. Chem., Vol. 32, pp. 662-664, May 1960

Techniques for separating Bi, Sb, Se, and Te during analysis of mixtures containing these elements are described. Se and Te are separated at different acidities with $SO_2$ and weighted as the free elements. Bi is titrated with (ethylenedinitrilo) tetraacetic acid using thiourea as the indicator. Sb is titrated potentiometrically with potassium permanganate. The accuracy and precision are within 1 to 2 parts per thousand.

8616 VAPOR-ZONE REFINING by L. R. Weisberg and F. D. Rosi (RCA); Rev. Sci. Instr., Vol. 31, pp. 206-207, Feb. 1960

The vapor-zone refining technique for purifying elements which have a high vapor pressure at their melting temperature and elements, such as As, which melt only under high pressures is discussed. In this technique, a section of the ingot to be purified is vaporized and repetitively passed unidirectionally through the ingot. Vapor-zone refining apparatus and its use are described. The apparatus has been used for zone refining As. In six passes under non-optimum conditions, the concentrations of Si, Fe, Al, and Cu are increased roughly by a factor of three at the front end of the ingot. Concentrations of Pb and Bi were increased by a factor of three at the tail end of the ingot and the concentrations of Mg and Ag remained uniform throughout the ingot. The total impurity concentration in the middle of the ingot was decreased by at least a factor of two compared to the starting material. Elements which can be vapor-zone refined include Ca, Cd, I, Mg, P, S, Sb, Te, and Zn.

8617 MODIFIED BOAT DESIGN FOR RAPID ZONE PURIFICATION by L. R. Johnson and W. Zimmerman, III (U.S. Naval Res. Lab.); Rev. Sci. Instr., Vol. 31, pp. 203-204, Feb. 1960

The use of the migration of charge during zone refining to improve the refining process is discussed. A modified boat incorporating an overlow trap is utilized. As each succeeding zone freezes at the end of its travel, it forces a small amount of the liquid to leave the main charge and land in the overflow trap. As a result, the concentration of those impurities with a segregation factor less than 1.0 is reduced automatically in the final zone on each pass. It has been found that one filling of the overflow trap with either Ge or one of the III-V compounds requires 10 to 15 single zone passes and results in an average purity equivalent to that obtained after cutting off the last 20-25 per cent of an ingot after 30 to 40 single zone passes.

Purification of Hg by Distillation and Zone Purification - See 8867

8618 PURIFICATION OF ALKALI HALIDE CRYSTALS THROUGH FRACTIONAL DISTILLATION AND NORMAL FREEZING by H. Kanzaki and K. Kido (U. Tokyo); J. Phys.

Soc. Japan, Vol. 15, pp. 529-530(L), Mar. 1960

The growth of high purity alkali halide crystals is discussed. The alkali halide is first purified by means of fractional distillation in a transparent quartz tube under high vacuum. The first fraction is collected in a receiver nearest the liquid nitrogen trap and the middle fraction is collected in the next section. The concentration of multivalent cations in the middle fraction is always about one-tenth of that in the starting material. The middle fraction is then sealed in a quartz tube under high vacuum immediately after distillation and the melt is solidified by lowering the sealed ampoule very slowly (2 mm/hr) along a temperature gradient. No reaction between the molten alkali halide and the quartz tube has been observed and the crystals do not stick to the walls on cooling to room temperature. The effectiveness of the method in removing multivalent cationic impurities is shown by low temperature conductivity measurements on KCl crystals.

8619 METHOD FOR SEPARATING AND PURIFYING GERMANIUM FROM SUBSTANCES CONTAINING METALLIC GERMANIUM by O. Rösner; U.S. Pat. 2,892,700, Issued June 30, 1959

A technique for removing Ge from materials containing metallic Ge is described. The Ge-containing material is heated to a high temperature, preferably greater than 800°C in a stream of $CO_2$. The volatile GeO in the reaction evaporates and condenses on the cooler parts of the reaction container. Metallic Ge can then be recovered from the GeO.

8620 DIFFUSION IN SEMICONDUCTORS by R. A. Swalin (U. Minnesota); NASA Symp. on the Theory and Mechanism of Diffusion in Solids, Oct. 1960

The theory of impurity diffusion in Ge and Si for both substitutionally and interstitially dissolved impurities is developed. With regard to interstitially dissolved impurities, it appears that the activation energy can be discussed in terms of coulombic repulsion between the interstitial and solvent ions. In general, unlike diffusion in metals, elastic strain energy is not an important factor in the activation energies for diffusion in semiconductors because of the open nature of the crystal. This is particularly true for interstitial diffusion.

8621 ON THE DETERMINATION OF THE DIFFUSION COEFFICIENT OF BORON IN SILICON by J. Yamaguchi, S. Horiuchi, K. Matsumura (Osaka U.), and Y. Ogino (Osaka Inst. Tech.); J. Phys. Soc. Japan, Vol. 15, pp. 1541-1542 (L), Aug. 1960

Determination of the diffusion coefficient of B in Si from measurements of the surface conductance of a diffused layer both before $\sigma(0)$ and after $\sigma(x)$ removing a thickness x of the layer is discussed. D can be determined from $u = x/2\sqrt{Dt}$, where u is given by $\sigma(x)/\sigma(0) = 1/0.565 \int_u^\infty \text{erfc}\, u\, du$. The procedure can be used with a smaller penetration depth than with the method of Fuller and Ditzenberger. A diffusion coefficient $D = 17.1 \exp\left(-\frac{84{,}800}{RT}\right)$ cm²/sec) was found. Good agreement was obtained with the activation energies measured by Fuller and Ditzenberger. The values of D in the present investigation are, however, 80 per cent larger over the temperature range studied.

8622 INCORPORATION OF Au INTO VAPOR-GROWN Ge by W. E. Baker and D. M. J. Compton (IBM); IBM J. Res. and Dev., Vol. 4, pp. 296-298(L), July 1960

The incorporation of Au into Ge grown by the vapor-growth process, using the closed-tube method, is discussed. The deposition was carried out using high-purity Ge as the source and a thin wire of radioactive Au as doping agent. The temperature of the seed zone was kept at 405°C and that of the source zone at 555°C for 5 days in an evacuated tube sealed at a pressure of $1 \times 10^{-5}$ mm. Depositions were made on an n-type (111) wafer and on a p-type (211) wafer. Single crystal deposits, epitaxial to the substrate, were obtained. Thin, polycrystalline films were produced at the surface and their thickness was greatest at the end of the seed nearest the source zone, next greatest at the opposite end, and thinnest in the middle. The Au was not distributed homogeneously in the deposit and the maximum concentration was much higher than that previously reported for Au in Ge grown from the melt. Electrical measurements indicate that not all the incorporated Au is electrically active. An explanation is offered for the observation of Au incorporation during the closed-tube process but not in the open-tube process.

8623 DIFFUSION OF CADMIUM INTO GALLIUM ARSENIDE by F. A. Cunnell and C. H. Gooch (SERL); Nature, Vol. 188, p. 1096(L), Dec. 24, 1960

An investigation of the diffusion of Cd into GaAs is reported. $Cd^{115}$ was diffused from a saturated vapor into a carefully prepared specimen measuring approximately 1 cm x 0.4 cm x 0.2 cm in a quartz tube 2 cm³ in volume. Diffusion profiles obtained after diffusion for 40 hrs at 1000°C with the Cd source held at 750°C are shown. The concentration initially decreases very rapidly from $2 \times 10^{19}$ cm$^{-3}$ at the surface, falls to a minimum, rises to a maximum, and then gradually decreases. Fitting the initial portion of the concentration-depth curve to a complementary error function gives an approximate diffusion coefficient $D = 3 \times 10^{-12}$ cm$^2$sec$^{-1}$. The concentration at the maximum has ranged between $4 \times 10^{18}$ cm$^{-3}$ and $\sim 10^{16}$ cm$^{-3}$. Differences between these results and those obtained by Goldstein are discussed and some experiments being undertaken to explain the behavior of Cd in GaAs are briefly outlined.

8624 DIFFUSION OF COPPER IN AlSb by R. H. Wieber, H. C. Gorton and C. S. Peet (Battelle); J. Appl. Phys., Vol. 31, p. 608(L), Mar. 1960

An investigation by radio tracer techniques of the diffusion of Cu in AlSb in the temperature range 150°-500°C is described. The samples were prepared by lapping on 600 grit SiC paper, polishing to a mirror finish with dry Linde A on photographic blotting paper, etching for 1 min in 4:4:1 HCl:$HNO_3$:H tartaric and for 2-3 sec in 1:1 HCl:$HNO_3$, and drying in alcohol. $Cu^{64}$ was plated on one surface of the samples and the plated samples were heated in quartz containers in an argon atmosphere. Excess Cu was removed from the surface after diffusion and the activity of successive layers was counted. A value for $D_0$ of $3.5 \times 10^{-3}$ cm$^2$/sec and an activation energy of 0.36 ev were obtained. Because of the extremely high diffusion rate of Cu in AlSb, Cu cannot be used in devices intended for high temperature operation and care must be taken to prevent Cu contamination during the processing of AlSb crystals for device application.

8625 INTERACTIONS BETWEEN LITHIUM AND OXYGEN IN SILICON by E. M. Pell (GE); Solid State Phys. in Elec-

tron. and Telecommun., Academic Press, 1960, Vol. 1, pp. 261-276

Chemical interactions between Li and oxygen in Si are described in detail. Experiments indicate that oxygen, itself electrically inactive, can affect the behavior of electrically active Li which is simultaneously present. Oxygen affects the nucleation of Li precipitates and the diffusion rate, and also leads to the formation of Li-O donor complexes. The precipitation kinetics of the various reactions and the behavior of the 9μ peak during precipitation are described.

Effects of Si in GaAs - See 8762

## CRYSTAL GROWTH

8626 SINTERING REACTION OF ZINC OXIDE by V. J. Lee and G. Parravano (U. Notre Dame); J. Appl. Phys., Vol. 30, pp. 1735-1740, Nov. 1959

A study of the sintering of ZnO spheres at 700°-900°C in air, oxygen, He and hydrogen is reported. Fresh ZnO sinters rapidly in air and oxygen, but it does not sinter appreciably in He at the same temperature range. ZnO spheres annealed separately in air may not be sintered in air at temperatures as high as 1100°C. On the other end, fresh spheres, separately air annealed and subsequently treated in an hydrogen atmosphere, do sinter in the range 700°-900°C. These facts are explained on the basis of a mechanism involving the diffusional transfer of stoichiometric excess of Zn ions. The diffusion equation for Zn ions is derived, and the experimental points fit the equation satisfactorily. The treatment shows that the relationship between the width of bridges connecting sintering spheres and time varies with extent of sintering. This fact invalidates the use of this relationship as an unequivocal diagnostic criterion for the sintering mechanism in non-stoichiometric oxides.

8627 A NEW ELECTRON GUN FOR THE VACUUM EVAPORATION OF METALS AND DIELECTRICS by R. Thun and J. B. Ramsey (USAERDL); 1959 Vacuum Symp. Trans., Pergamon Press, 1960, pp. 192-196

A new electron gun evaporation source which focuses the electron beam by a spherical field between cathode and anode is described. The advantages of such a design over a conventional gun with a grid cylinder are greater ruggedness and simplicity, higher energy output and the possibility of a full analytical treatment of its characteristics. The source makes possible the evaporation of difficult materials such as Si.

8628 EPITAXIAL GROWTH OF SILICON by E. S. Wajda, B. W. Kippenhan and W. H. White (IBM); IBM J. Res. and Dev., Vol. 4, pp. 288-295 (L), July 1960

Layers of Si grown by the disproportionation of $SiI_2$ are discussed. Growth takes place by two distinct processes, the transport of vapor from the source zone to the crystal surface, and nucleation and growth of a new layer on the substrate surface. It has been found that single crystal vapor deposited layers can be grown with the same orientation as the substrates. The thickness and structure of the deposited films depend on the duration of the crystallization process, temperature, concentration of Si vapors, and the content of impurities in the system.

Growth of Heavily Doped Ge - See 8955

Epitaxial Deposition of Au-Doped Ge - See 8622

Growth of Monoclinic α-Se Crystals - See 8908

Preparation of:
- BP - See 8732
- InSb Single Crystals - See 8897
- GaSb-InSb Alloys by Directional Freezing - See 8725
- HgTe and Mixed Crystals of HgTe-CdTe - See 8867
- $Bi_2Te_3$ - See 8928

8629 FILM STRIPPING TECHNIQUE FOR MAKING THIN SILICA WINDOWS by E. Tannenbaum (Bell Labs.); J. Appl. Phys., Vol. 31, p. 940 (L), May 1960

A technique for producing transparent silica windows with thickness ranging from 1000 to 100,000 A and areas as large as 1 $cm^2$ is described. An amorphous $SiO_2$ layer is removed from the desired area on one side of a Si slice by masking and exposing to HF vapor. The slice is then exposed to hot chlorine gas which etches the exposed Si by forming $SiCl_4$. The technique can also be used for cutting Si into shapes too difficult for mechanical machining or conventional liquid etching.

Preparation of MnSi, $CrSi_2$ and CoSi - See 8931

8630 PREPARATION OF FERROMAGNETIC CHROMIUM DIOXIDE by B. Kubota (Matsushita Electronic Ind.); J. Phys. Soc. Japan, Vol. 15, p. 1706 (L), Sept. 1960

The preparation of ferromagnetic $CrO_2$ by the thermal decomposition of $CrO_3$ under a high oxygen pressure caused by the oxygen liberated from the $CrO_3$ is discussed. Chemically pure $CrO_3$ was heated at 10°C per hour in a stainless steel high pressure bomb. Crystals of $Cr_3O_8$, $Cr_2O_5$, $CrO_2$, and $Cr_2O_3$ were produced as the temperature was progressively increased. The pressure-temperature relation was found to exhibit a step-like character. The magnetic properties of $CrO_2$ prepared by heating $CrO_3$ at 480°C for 4 hours under oxygen pressure of about 560 $kg/cm^2$ were measured in the temperature range 77° to 500° K. The Curie temperature, the saturation magnetization at 0°K, and the Bohr magneton number of a $Cr^{4+}$ ion were found to be 117°C, 133.7 ± 2 gauss/gram, and 2.01 ± 0.03, respectively.

Preparation of $Y_{3-x}Yb_xFe_5O_{12}$ - See 8817

8631 ANTIFERROMAGNETIC $FeVO_3$ by C. R. Berry and C. M. Combs (Kodak); J. Appl. Phys., Vol. 31, p. 1130 (L), June 1960

The preparation and properties of the compound $FeVO_3$ are discussed. Complete conversion to $FeVO_3$ was obtained by heating for 1 hour in vacuum at 1200°C appropriate quantities of Fe, $Fe_2O_3$, and $V_2O_5$. From a consideration of X-ray diffraction data and the ionic radii of $V^{3+}$ and $Fe^{3+}$ it is concluded that the valences in the compound are $Fe^{2+}$ and $V^{4+}$. Traces of the B-H curve of dispersions of $FeVO_3$ did not show any ferromagnetism at room temperature. Additions of 20, 40, and 50 mole per cent of $Fe_2O_3$ to $FeVO_3$ were investigated. X-ray diffraction indicated solid solution over the entire range of compositions and a spinel component, apparently $Fe_3O_4$. The superlattice lines (003) or (011) were not found in $FeVO_3$ or in the solid solutions and the only ferromagnetism found was that associated with the spinel component of the mixtures. These latter results indicate that $FeVO_3$ and its solid solutions have the disordered ilmenite structure.

8632 GROWTH FROM THE MELT. Part I. INFLUENCE OF SURFACE INTERSECTIONS IN PURE METALS by G. F. Bolling and W. A. Tiller (Westinghouse Res. Labs.); J. Appl. Phys., Vol. 31, pp. 1345-1350, Aug. 1960

The effect of the solid-liquid interface shape during growth from the melt for pure metals in the vicinity of external and internal surfaces is discussed. The cases of isotropy and anisotropy of solid-liquid interfacial energy have been considered. From these considerations it is possible to determine some effects associated with interface and external surface anisotropy. For example, a preferred direction of growth, a surface layer phenomenon and stray-crystal formation during seeding and normal crystal growth may arise as a result of the solid-liquid interface configuration.

Growth of Quartz Crystals - See 8944

Preparation of Triglycinsulphate - See 8691

## CRYSTAL SURFACES

8633 STUDY OF SURFACES BY USING NEW TOOLS by J. A. Becker (Bell Labs.); Solid State Phys.-Adv. Res. and Appl., Academic Press, 1958, Vol. 7, pp. 379-424

Two new tools used to study the surface phenomena are described; one is an ion gauge, the other a field-emission microscope. With the ion gauge one can easily measure the rates of absorption and desorption, and the amount absorbed for a steady state. With the field emission microscope one can determine how the electron work function varies with the crystallographic plane and how it is affected by the absorption of foreign materials. The location of individual atoms on metal surfaces can also be observed. The various techniques and results of studies on simple systems are reported. A list of major questions regarding the surface phenomena are answered, based on the results of experiments. The field ion microscope is also described.

8634 ON THE OXIDATION PROCESSES IN MANGANESE FERRITES [in German] by A. Braginski (Zaklad Mat. Mag., Warsaw); Solid State Phys. Electronics and Telecommun., Academic Press, 1960, Vol. 3, pp. 114-125

An investigation of the oxidation processes in powdered manganese ferrites at the relative state of equilibrium in air is described. The following was determined: 1) The oxidation of $MnFe_2O_4$ between 300° and 600°C leads to the formation of solid solutions with deformed spinel lattice. 2) Between 600° and 1050°C a decomposition of the spinel lattice into separate phases of $\alpha$-$Fe_2O_3$ and $\beta$-$Mn_2O_3$ or into solid solutions of these phases occurs because of the oxidation. 3) Over 1050°C various solid solutions with defect spinel lattice form which with rising temperature become liquid $MnFe_2O_4$. 4) The lattice relaxation at the transformation point of manganese oxide probably facilitates the decomposition and resynthesis of the spinel lattice. 5) The oxidation processes occur in a similar manner in the region of the solid solutions of $0.55\ MnO \cdot 0.45\ Fe_2O_3$ to $0.45\ MnO \cdot 0.55\ Fe_2O_3$. 6) The oxidation of the ferrite is accompanied by complicated simultaneous reactions. The change of the magnetic properties resulting from the decomposition reaction cannot be calculated.

8635 THE OXIDATION OF INTERMETALLIC COMPOUNDS. Part III. THE ROOM-TEMPERATURE OXIDATION OF $A^{III}B^{V}$ COMPOUNDS by A. J. Rosenberg (Lincoln Lab.); J. Phys. Chem. Solids, Vol. 14, pp. 175-180, July 1960

The oxidation of vacuum-crushed InSb, GaSb, AlSb, InAs, GaAs and InP is discussed. The kinetics are analyzed in terms of the empirical function, $\eta \equiv -\partial \log V / \partial X$. (The general utility of $\eta$ and the associated function, $\epsilon = \eta X$ in the kinetics analysis of protective surface reactions is discussed in detail.) Maxima in $\eta$ are observed at $2.5 \times 10^{15}$ and $1.35 \times 10^{15}$ oxygen atoms/cm$^2$ on the antimonides and the arsenides, respectively. The reaction of InP exhibits no distinct maximum in $\eta$; otherwise, it resembles that of the arsenides. The results are interpreted in terms of metastable surface complexes whose formation precedes the initiation of true oxide growth. The composition of these intermediates is dictated largely by the nature of the $B^{V}$ atom in the substrate. The associated kinetics depend systematically, however, upon the $A^{III}$ atoms. Thus, the rate of complex formation decreases in the order Al>In>Ga, while the rate of oxide formation decreases in the order In>Ga>Al.

8636 EFFECTS OF OXYGEN PARTIAL PRESSURE ON THE OXIDATION OF SILICON CARBIDE by P. J. Jorgensen, M. E. Wadsworth and I. B. Cutler (U. Utah); J. Am. Ceram. Soc., Vol. 43, pp. 209-212, Apr. 1960

An investigation of the rate of oxidation of SiC at different partial pressures of oxygen is discussed. The diffusion rate constant was found to vary with the logarithm of the partial pressure of oxygen according to the theory of oxidation of thin films proposed by Engell and Hauffe. An alternative explanation based on the change of free energy with surface coverage was also found to fit the data.

8637 THE ION BOMBARDMENT, OXIDATION AND REGENERATION OF GERMANIUM SURFACES by S. P. Wolsky and E. J. Zdanuk (Raytheon); J. Phys. Chem. Solids, Vol. 14, pp. 124-130, July 1960

Use of a sensitive quartz microbalance and an omegatron type mass spectrometer in an ultra-high vacuum system to investigate the interaction of oxygen and ion-bombarded Ge surfaces is described. The omegatron mass spectrometer provided valuable information concerning the nature and effect of experimental procedures upon the sample ambient. Such knowledge is necessary for developing the proper experimental technique and for interpreting the experimental data. It is concluded that adsorption investigators must work with atomically clean surfaces of known crystal orientation and degree of perfection in order to obtain a more detailed knowledge of the oxygen-germanium interaction.

8638 STRUCTURE AND ADSORPTION CHARACTERISTICS OF (111) AND (11$\bar{1}$) SURFACES OF InSb CLEANED BY ION BOMBARDMENT AND ANNEALING by D. Haneman (Brown U.); J. Phys. Chem. Solids, Vol. 14, pp. 162-168, July 1960

Low energy electron diffraction studies of five (111) and (11$\bar{1}$) surfaces of InSb cleaned by argon ion bombardment and annealing are discussed. From the diffraction patterns obtained in both (110) and (112) azimuths, a double-spaced structure of surface atoms appears to be present on (111) and (11$\bar{1}$) surfaces. Exposure to oxygen resulted in a gradual decrease in intensity of all beams, indicating that an amorphous layer of oxygen was formed. The sticking coefficient for oxygen on the cleaned surfaces has a maximum value of $10^{-5}$, and appears to be similar on both (111) and (11$\bar{1}$) surfaces. The cleaned surface

pattern could be regenerated by heating the crystal at about 330°C for approximately 1 hr.

8639 EFFECT OF THE POLARITY OF THE III-V INTERMETALLIC COMPOUNDS ON ETCHING by J. W. Faust, Jr. and A. Sagar (Westinghouse); J. Appl. Phys., Vol. 31, pp. 331-333, Feb. 1960

Studies of etch pit effects are reported for several etches on InSb, InAs, GaSb, and GaAs. For the III-V intermetallic compounds, the <111> directions are polar axes. The shape of etch pits bounded by crystallographic planes and the presence or absence of pits at dislocations are influenced by the effect of the polar axes on the etch rates. Correlation of these studies with published X-ray investigations shows that these etches reveal dislocations and truncated pyramidal pits only on {111} surfaces that are at the group III end of the polar axis. A difference in the shape of the pits on opposite {100} surfaces was found and is explained by means of the polar axes.

8640 ETCHING AND INHIBITION OF THE {111} SURFACES OF THE III-V INTERMETALLIC COMPOUNDS: InSb by H. C. Gatos and M. C. Lavine (Lincoln Lab.); J. Phys. Chem. Solids, Vol. 14, pp. 169-174, July 1960

In oxidizing etching media, the {111} surfaces of InSb are much less reactive than the $\{\bar{1}\bar{1}\bar{1}\}$ surfaces as determined by direct dissolution rates and by etching of spheres. Related to this difference in reactivity is the fact that dislocation etch pits appear on the {111}, but not on the $\{\bar{1}\bar{1}\bar{1}\}$ surfaces. Inhibitors such as stearic acid and primary amines appreciably decrease the dissolution rate of only the $\{\bar{1}\bar{1}\bar{1}\}$ surfaces. Furthermore, etching inhibitors lead to the formation of new dislocation etch pits on the {111} and also on the $\{\bar{1}\bar{1}\bar{1}\}$ surfaces. Similar effects have been observed in GaAs. These phenomena are discussed in terms of the atomic configuration of the surfaces involved and the relative reactivity of the group III and group V atoms.

8641 ETCH PITS IN GALLIUM ARSENIDE by J. L. Richards and A. J. Crocker (Philco); J. Appl. Phys., Vol. 31, pp. 611-612(L), Mar. 1960

Etchants which reveal dislocations on the A face, the B face, or both faces in GaAs are discussed. Acidic oxidizing etchants reveal etch pits on the A faces only and $HF/HNO_3$ etchants to which silver ions are added reveal etch pits on the B faces or on both the A and B faces depending on the etch composition. The relative rates of attack on the different crystal planes have been observed by etching small spheres.

8642 DISLOCATION ETCH PITS ON P-TYPE LEAD TELLURIDE by B. B. Houston and M. K. Norr (U.S. Naval Ord. Labs.); J. Appl. Phys., Vol. 31, pp. 615-616(L), Mar. 1960

Two etches for producing etch pits in PbTe at points where dislocations intersect the surface are discussed. One etch is prepared by dissolving 5 gm of NaOH in 10 ml of distilled water and adding 0.2 gm of $I_2$ while the solution is still hot. The etch pits produced by etching fresh cleavage surfaces of p-type PbTe for 5 min at 94°-98°C are approximately 5μ across. The second etch is prepared by mixing 10 ml of 0.5 per cent $NaIO_3$ solution and 5 gm of NaOH. The etch pits produced by this etch under the same conditions as the other etch are 7μ across. Pits have been observed along small angle grain boundaries, along traces of active slip planes, and at isolated points on the surface. Dislocations introduced by plastic deformation are found to be attacked at about the same rate as those already present. In several as-grown crystals the two surfaces formed by the same cleavage are almost perfect mirror images of one another. The etches must be used on fresh cleavage surfaces, i.e., surfaces unspoiled by mechanical damage or chemical contamination.

Dislocation Etch Pits in Ferroelectric Glycine Sulfate Single Crystals - See 8609

8643 GAS ETCHING AND ITS EFFECT ON SEMICONDUCTOR SURFACES by J. G. Gualtieri, M. J. Katz and G. A. Wolff (USASRDL); Z. Krist., Vol. 114, pp. 9-22, June 1960

Etching of single crystals of diamond, Si and Ge in the halogens, chalcogens, hydrogen halides, $ClF_3$ and other gaseous etchants is reported and light reflectograms obtained from the etched surfaces are discussed. After prolonged etching, only the chemically resistant planes remain and they account for the light reflections or reflectograms. These reflectograms yield direct information about the elementary and kinetic processes of the etching. The possible reaction mechanisms involved in the etching with halogens and chalcogens are discussed.

## ENVIRONMENTAL EFFECTS

Heat Treatment Effects in InAs - See 8726

8644 THE INTERDEPENDENCE OF SOLID STATE PHYSICS AND ANGULAR DISTRIBUTION OF NUCLEAR RADIATION by R. Heer and T. B. Novey (U. Rochester); Solid State Phys. Adv. Res. and Appl., Vol. 9, Academic Press, 1959, pp. 199-255

The necessary formalism connected with the field-free angular correlation problem is presented. In this formalism, the intermediate lifetime of a nuclear state is assumed to be so short that nothing happens to the nucleus, i.e., the orientation of its spin does not change. The way to predict the anisotropic angular distribution of radiation emitted from an oriented state is described. The possible sources of change in spin orientation and the resulting effect in the angular distribution are discussed. The extranuclear effects on angular correlation of successive nuclear radiation are considered in detail. Experimental methods of measuring the angular distribution of nuclear radiation and various techniques for orienting the nuclei are described. It is pointed out that angular distribution of nuclear radiation is a useful tool in solid state physics. A few problems which might be attacked advantageously with these methods are suggested.

Radiation-Induced Acceptor Levels in Si - See 8645

8645 EFFECT OF DISSOLVED OXYGEN ON RADIATION DAMAGE IN N-TYPE SILICON by E. Sonder and L. C. Templeton (Oak Ridge Natl. Lab.); Bull. Am. Phys. Soc., Ser. II, Vol. 5, pp. 196-197(A), Mar. 21, 1960

The gamma-radiation damage in n-type Si containing dissolved oxygen and in Si of low oxygen content was compared using Hall-effect measurements. In the case of 2 ohm-cm oxygen-containing material, one discrete net acceptor level located 0.17 ev below the conduction band is introduced by the irradiation at the rate of approximately $1.3 \times 10^{-3}$ trap/incident photon. However, in Si of similar resistivity containing less

than $10^{16}$ oxygen atoms per $cm^3$, there is clear evidence of the introduction of two net acceptor levels, one at 0.17 ev and another at 0.47 ev below the conduction band. The introduction rate of these is $0.8 \times 10^{-3}$ and $1.0 \times 10^{-3}$ trap/incident photon, respectively.

8646 LIGHT SCATTERING BY NEUTRON IRRADIATED SILICA by R. D. Maurer (Corning); J. Phys. Chem. Solids, Vol. 17, pp. 44-51, Dec. 1960

The intensity of light scattered by fast neutron irradiated fused silica indicates that the damaged volume per primary struck atom is about $(67 A)^3$. There is dissymmetry of scattering showing that this small volume is strung out in a long thin, or rodlike, region in order to give interference effects. The angular dependence of scattering for the $H_h$ and $V_v$ components is different and can be accounted for by assuming that strain surrounds the damaged region. Theories of the strain scattering effect are developed to give a quantitative account of the scattering. These indicate how the angular dependence of scattering may be interpreted to discriminate between the effect of strain and the effect of the length of the rodlike regions. The length is found to be approximately 1800 A.

Slow Neutron Scattering in Lattices - See 8666

8647 PARAMAGNETIC RESONANCE STUDY OF RADIATION DAMAGE IN LITHIUM FLUORIDE by W. Känzig (GE Res. Labs.); J. Phys. Chem. Solids, Vol. 17, pp. 88-92, Dec. 1960

Paramagnetic resonance studies of the low temperature annealing processes in LiF crystals X-rayed at 77°K are discussed. Four types of hole centers (V-type centers), the structures of which are known from previous work, play an important part; namely, the self-trapped holes, the H-centers, the $V_F$-centers and the $V_4$-centers. The relative concentrations of these defects have been measured after X-irradiation at 77°K and after subsequent pulse annealing at successively higher temperatures. Four temperature intervals were found in which the paramagnetic resonance spectra undergo significant changes in intensity. There seems to be a one-to-one correspondence between the annealing processes observed by means of paramagnetic resonance and those detected by other investigators by means of thermoluminescence, conductivity, changes of the optical absorption and of the crystal volume.

Radiation-Induced Paramagnetic Centers - See 8835, 8836, 8837, 8838, 8839

8648 RADIATION-INDUCED DEFECTS IN LEAD SILICATE GLASS by R. S. Barker, D. A. Richardson, E. A. G. McConkey, and R. E. Yeadon (Pilkington Bros.); Nature, Vol. 188, p. 1181 (L), Dec. 31, 1960

The process of coloration of glass by γ-radiation is discussed. A sample of lead silicate glass which had previously been used was given a γ-radiation dose of $10^8$ rads and its optical density was measured over the wave length range 360 - 1000 mμ at intervals of time during the week following irradiation. The induced coloration was bleached by exposure to light from a mercury lamp until the optical density of the glass was not significantly different from that measured before the irradiation. The sample was then given a further dose of $10^8$ rads and the optical absorption remeasured. In all cases the optical density of the sample after bleaching and re-irradiation is greater than that obtained after the first irradiation. This agrees with a proposed mechanism for the coloration.

8649 HIGH-ENERGY ELECTRON IRRADIATION OF GERMANIUM AT 78°K BY V. A. J. van Lint, E. G. Wikner, J. W. Harrity and H. Horiye (Genl. Dynamics); Bull. Am. Phys. Soc., Ser. II, Vol. 5, p. 196 (A), Mar. 21, 1960

Studies made during the conversion of n-type Ge to p-type due to irradiation by 25 Mev electrons at 78°K were discussed. Measurements performed during irradiation included conductivity, Hall coefficient, and excess-carrier lifetimes. The following conclusions have been made from these data: (1) Appreciable annealing of the radiation-induced changes occurred during a few minute warming to 275°K, (2) The initial change of Hall coefficient implied a carrier removal rate of 4.0 electron/cm of 25 Mev electron path, (3) When the Fermi level crosses a point 0.10 ev below the conduction band, the carrier removal rate falls to 0.019 electron/cm of path, (4) The electron mobility is decreased markedly during irradiation by impurity scattering but the hole mobility remains at the value determined by lattice scattering, (5) Two-hole trapping levels were observed at 78°K having activation energies of 0.27 ev and 0.15 ev.

Effect of γ-Radiation on the Dielectric Properties of Insulating Materials - See 8674 and 8675

Ionic Conductivity of γ-Irradiated NaCl - See 8729

Effect of Neutron Radiation on the Magnetoresistance of GaAs - See 8765

Effects of Neutron Irradiation on the Magnetic Properties of Fe-Ni Alloys - See 8793

Effect of Radiation on the Thermoelectric Power of $Bi_2Te_3$ - See 8925, 8926, and 8927

8650 ANNEALING OF X-RAY INDUCED SURFACE HARDENING IN NaCl by R. Cuypers and S. Amelinckx (Lab. voor Kristalkunde); Acta Metal., Vol. 8, pp. 551-553, Aug. 1960

The surface hardening of NaCl crystals due to X-irradiation and the resoftening due to annealing at different temperatures are discussed. The activation energy of the process associated with the annealing in the temperature range 150°-300°C is derived. Clusters of point defects are probably the principal cause of the surface hardening, a conclusion which agrees with that of other workers. For annealing temperatures below 300°C the resoftening would mainly result from the growth in size of these aggregates and their corresponding decrease in number.

8651 ANNEALING KINETICS OF NEUTRON-IRRADIATED ALUMINUM AND COPPER by T. H. Blewitt, R. R. Coltman, and C. E. Klabunde (Oak Ridge Natl. Lab.); Austl. J. Phys., Vol. 13, pp. 347-353, July 1960

Measurements of the activation energies for the annealing of Cu and Al following reactor bombardment near 4°K in the range from 10° to 40°K, are reported. Both the change in slope method and the isothermal technique method were utilized with the assumption that a constant activation energy existed. Computations of the number of jumps involved from the measured activation energy result in an impossibly small number. It is obvious that the method for determination of the activation energies is not applicable, probably because of the non-uniqueness of the activation energy.

# SOLID STATE PHYSICS

## GENERAL

8652 SOLID-STATE RESEARCH AT LOW TEMPERATURES. Part I. INTRODUCTION by J. Volger (Philips); Philips Tech. Rev., Vol. 22, No. 6, pp. 190-195, 1960-61

A number of examples are given to demonstrate that a system may be said to be at a low temperature when kT is smaller than a certain characteristic energy. This is the energy quantum $h\nu$ for the specific heat of a system of quantized harmonic oscillators, the heat of fusion (per mole) for the fusion of a solid, the energy $\mu_B H$ for the magnetization of a paramagnetic substance, and the Fermi energy $E_F$ for the electrical conductivity of metals and semiconductors. Many solid-state processes, e.g., the orientation of electron spins in a paramagnetic substance, are slowed down at low temperature.

8653 MINERALS AS MODELS FOR NEW SEMICONDUCTOR COMPOUNDS by G. Busch and F. Hulliger (ETH, Zurich); Helv. Phys. Acta, Vol. 33, No. 6/7, pp. 657-666, 1960

The combining of binary semiconductors to obtain new semiconductor compounds is discussed. In determining likely mixing proportions, the natural nonmetallic sulpho minerals indicate possible stoichiometric ratios in ternary and quarternary selenide and telluride semiconductors. A partial substitution of the elements appearing in the minerals with chemically related elements leads to a great number of new semiconductors with lowest melting points and activation energies from 0.1 to 3 ev. The lattice constants for some highly symmetrical compounds can be determined from powder patterns.

## CRYSTAL PHYSICS

### BINDING PROPERTIES

8654 ON THE CHEMICAL BOND WITH "COMMON-VALENCE" WITH A SPECIAL CONSIDERATION OF THE ZnS AND WURTZITE PHASES [in German] by O. G. Folberth (Siemens-Schuckert); Z. Naturforsch., Vol. 15a, pp. 425-431, May/June 1960

According to older views, the chemical bond of crystals with ZnS structure is mainly covalent. However, in recent years it has been increasingly pointed out that these views had to be modified, when it became known that the share of ion-band in these compounds is much higher than it was hitherto assumed. Yet, it cannot be ignored that the original concept displayed some very engaging arguments in its favor. Additionally, this concept has been deeply rooted through historical tradition, and has been adopted by almost all papers on the subject. Hence this view should not be discarded lightly, but it should be attempted to refute the alleged arguments in its favor. This paper is dedicated to this purpose.

Nature of the Bonds in ZnSb - See 8589

### ENERGY BAND STRUCTURE

8655 GENERALIZATION OF BAND THEORY TO INCLUDE SELF-ENERGY CORRECTIONS by G. W. Pratt, Jr. (Lincoln Lab.); Phys. Rev., Vol. 118, pp. 462-467, Apr. 15, 1960

A one-particle Schrödinger-like equation is found whose eigenvalues in certain cases are identical with the energies of the many electron states of a semiconductor or insulator including self-energy corrections. The one particle Hamiltonian is expressed in terms of the Coulomb interaction as modified by polarization processes. The relation between the modified Coulomb interaction and the dielectric function which is the generalization of the classical dielectric constant is given. Suggestions are made as to how the one-particle equation including self-energy effects might be solved in practice.

8656 SYMMETRY PROPERTIES OF THE ENERGY BANDS OF CRYSTALS WITH CHALCOPYRITE STRUCTURE [in Russian] by V. A. Chaldyshev and V. N. Pokrovskii (SFTI, Tomsk U.); Izv. VUZ Fiz., No. 2, pp. 173-181, 1960

Characters of the irreducible representations of the simple and double space groups of crystals having the chalcopyrite lattice are determined. Tables of superposition are constructed and the influence of spin-orbital interaction on the structure of the spectrum is discussed.

8657 THE ENERGY SPECTRUM OF AN AMORPHOUS SUBSTANCE by P. Phariseau (Lab. voor Krist. en Studie van Vaste Stoffen, Ghent); Physica, Vol. 26, pp. 1185-1191, Dec. 1960

The energy spectrum of an electron moving in a one-dimensional model of an amorphous solid consisting of atoms of the same kind, each represented by a Dirac's δ-function, is discussed by means of a Green's function method. The integration of the Schroedinger equation is reduced to the integration of a linear and homogeneous equation of the second order. By means of a continued fraction method, the existence of allowed energy bands in amorphous solids is shown. Amorphous solids have extra localized energy levels in the forbidden energy regions.

Energy Band Structure of:
- Bi - See 8907
- AlSb - See 8861
- Cubic-Hexagonal ZnS - See 8902
- $Bi_2Te_3$ - See 8919
- Ge-Si Mixed Crystals - See 8824

Valence Band Contours in Ge - See 8864

Conduction Band of GaSb - See 8724

8658 ON THE INTERPRETATION OF THE ΔE VALUES OF ZnS PHASES [in German] by O. G. Folberth (Siemens-Schuckert); Z. Naturforsch., Vol. 15a, pp. 432-434, May/June 1960

If the widths of the forbidden zone ΔE of semiconductor compounds with ZnS structure are compared, it is found that, other factors remaining equal, those compounds with the smaller cation and the larger anion display the larger forbidden zone ΔE. This regularity is interpreted with consideration of more recent findings on the subject which, contrary to hitherto prevalent views, make a much higher ion concentration of the ZnS probable.

Energy Gap of:
- CdTe - See 8764
- SiC - See 8865
- BP - See 8732
- GaP - See 8872
- $Bi_2Te_3$ - See 8928

Energy Gap of:
(In, Ga) As Alloys - See 8932
CdS-ZnS Mixed Crystals - See 8899
GaSe-GaS Mixed Crystals - See 8900
Alumina - See 8678

8659 STATISTICAL PROBLEMS IN SEMICONDUCTORS. Part II. by P. T. Landsberg (U. Aberdeen); Solid State Phys. in Electronics and Telecommun., Vol. 1, Academic Press, 1960, pp. 436-455

The following topics are discussed: the statistics of localized and non-localized impurity states, the transition from localized to non-localized impurity states, the effect of statistics on the inferred concentration dependence of impurity activation energies, the donor paramagnetic susceptibility, the effect of a magnetic field on the electron populations, the statistics of recombinations via traps, the introduction of the non-localized Fermi probability into the statistics of localized centres, and the effective energy levels of localized "flaws".

Impurity Levels in InSb - See 8731

Photoelectric Analysis of Energy Levels in CdS Type Crystals - See 8591

Magnetic Susceptibility of Donors in Si and Ge - See 8823

Fermi Surface of Mg - See 8849

8660 SURFACE STATES OF ONE-DIMENSIONAL CRYSTALS. Part I. by E. Aerts (Lab. voor Krist. en Studie van Vaste Stoffen, Ghent); Physica, Vol. 26, pp. 1047-1056, Dec. 1960

Energy levels at the surface of a one-dimensional semi-infinite crystal are calculated by means of the scattering matrix method of Saxon and Hutner for the case in which the potential of the surface atom is asymmetric. The formula of Tamm is obtained. In an analogous calculation for a linear crystal with a surface contaminated by an impurity atom the same number of possible solutions is found as in the previous case. The position of the levels is, however, different. An explanation for the n-type or p-type surface conductivity of an intrinsic semiconductor is proposed.

8661 SURFACE STATES OF ONE-DIMENSIONAL CRYSTALS. Part III. by E. Aerts (Lab. voor Krist. en Studie van Vaste Stoffen, Ghent); Physica, Vol. 26, pp. 1063-1072, Dec. 1960

Localized surface energy levels for crystal models with a symmetric potential for the surface atom are computed by the scattering matrix method of Saxon and Hutner. In the case of a clean surface, no levels are found in agreement with the results of Shockley. If, however, the surface is covered with an adsorbed impurity, surface levels are found when the potential of the impurity is weaker than that of the bulk atoms. Theoretical evidence for the existence of interface states at the junction of two semi-infinite one-dimensional crystals is given. They occur only when the first forbidden energy gap of one crystal corresponds with the second forbidden energy gap of the other.

8662 SURFACE STATES IN A ONE-DIMENSIONAL CRYSTAL MODEL by E. Aerts (Lab. voor Kristal., Ghent); Solid State Phys. in Electronics and Telecommun., Vol. 1, Academic Press, 1960, pp. 628-638

The following topics are treated: the surface states in a one-dimensional crystal model, the energy levels in an infinite one-dimensional crystal, models of the potential energy function, the effects of imperfections on δ-function energy model, the surface states of a semi-infinite perfect one-dimensional crystal under the assumption of a δ-function potential energy model, the wave functions associated with the problem, and the matrix associated with the scattering of an electron by a potential step. It is deduced that the number of extra energy levels depends on the lattice parameter, the height of the surface barrier, and the potential strength. The solutions are presented graphically. The surface states of a semi-infinite one-dimensional perfect crystal with an impurity adsorbed at the surface are also discussed quantum-mechanically, and graphical solutions are given. The derivations of the wave functions for the surface states of a semi-infinite perfect linear crystal both with and without an impurity at the surface are given.

8663 SURFACE MEASUREMENTS ON FRESHLY CLEAVED SILICON P-N JUNCTIONS by G. W. Gobeli and F. G. Allen (Bell Labs.); J. Phys. Chem. Solids, Vol. 14, pp. 23-26, July 1960

Silicon (111) faces 1.5 mm x 6 mm in area and free of visible imperfections, containing a p-n junction, have been produced by cleavage in high vacuum. The cleavage features and the technique are discussed. Contact potential difference (Kelvin method) across the junction indicates bending of the bands at the surface due to surface states by many tenths of a volt.

8664 ENERGY LEVEL DIAGRAMS FOR GERMANIUM AND SILICON SURFACES by P. Handler (U. Illinois); J. Phys. Chem. Solids, Vol. 14, pp. 1-8, July 1960

The concept of localized atomic orbitals is used to show how the structure and type of binding of surface atoms to the crystal may affect the energy level diagram of the surface region. In particular it is shown in a qualitative way that the s or p character of the non-bonding orbitals of the surface atoms may determine the energy of the surface state bands and the type of space charge region at cleaned germanium and silicon surfaces. The transport data of the p-type space charge region of the cleaned germanium are used to determine the parameters, $N_0$, the density of states per $cm^2 ev$, and $(E_F - E_0)$, the degree of degeneracy of a two-dimensional surface state band. Using the value of these parameters obtained from the transport data and the simple model of a two-dimensional surface state band, it is shown that the linear temperature dependence of the thermionic emission data of Allen on silicon may be predicted to within a factor of 2 or 3.

## LATTICE VIBRATIONS

8665 CORRECT ENUMERATION OF VIBRATION FREQUENCIES IN THE BRILLOUIN ZONE by B. Dayal and S. P. Singh (Banaras Hindu U.); Proc. Phys. Soc., Vol. 76, pp. 777-779, Nov. 1960

In order to calculate the vibration frequencies by Born's method the Brilluoin zone is sub-divided into a number of points. The actual number of frequencies used by the workers for the calculation of $C_v$ is, however, different from the number of points of the zone, resulting in a non-uniform distribution of points. It has been shown that this results in an incorrect value

of the specific heat. As an example Hsieh's theoretical results have been used to recalculate the specific heat of silicon with a proper number of frequencies. The difference between these revised results and Hsieh's original calculations is found to be large.

8666 INTERACTION OF THERMAL NEUTRONS WITH SOLIDS by L. S. Kathan and K. S. Singwi (Atomic Energy Estab., India); Solid State Phys.-Adv. Res. and Appl., Vol. 8, Academic Press, 1959, pp. 109-190

The theoretical aspects of the interaction of slow neutrons with lattice vibrations and the application of the general theory to the study of lattice dynamics are presented. The mechanism of slowing down thermal neutrons in solids is discussed. The scattering in the thermal energy region can be divided into two types, elastic and inelastic. Both types can give rise to "coherent" and "incoherent" scatterings. The cross sections of these scatterings are derived. The variation of transport cross section with energy mean logarithmic energy decrement, energy loss per collision, slowing-down age, and the energy spectrum of neutrons in solid moderators are discussed. The cold neutron scattering is purely inelastic so the testing of the theory of neutron-phonon interaction can be made in this cold region. It is shown that the dispersion relation, the polarization of a phonon, and, in certain cases, the frequency distribution function can be determined by studying the angular and energy distribution of inelastically scattered neutrons. The slowing-down properties of a medium are calculated based on a gas model. The calculated results agree reasonably well with experiments for neutron energies larger than Debye energy. For smaller energies, more refined calculations are necessary.

8667 LATTICE FREQUENCY OF IONIC CRYSTALS by S. S. Mitra and S. K. Joshi (The University, Allahabad); J. Phys. Soc. Japan, Vol. 15, pp. 1575-1576, Sept. 1960

Using an inverse power type repulsive potential two different expressions for the lattice frequency of ionic crystals are obtained, one in terms of the cohesive energy and the other in terms of the compressibility of the crystal.

Anharmonicity of Lattice Vibrations in Ionic Crystals - See 8910

Lattice Vibrations in GaP - See 8855

## ELECTRONIC PROPERTIES

8668 HARTREE-FOCK EQUATIONS WITH A PERTURBING FIELD by L. C. Allen (U. California); Phys. Rev., Vol. 118, pp. 167-175, Apr. 1, 1960

The Hartree-Fock equations under the action of an arbitrary field for any order of perturbation are set up in an integro-differential form. This form appears particularly advantageous for practical computation in such problems as electronic polarizability and electronic structure perturbations caused by nuclear moments. The equations are explicitly written down for a uniform perturbing field and a comparison is made with previous formulations. A wide variety of other applications is also discussed.

8669 ON THE DETERMINATION OF THE POLARIZATION ENERGY IN ION LATTICES [in German] by T. Neugebauer (Roland Eötrös U., Budapest); Acta Phys. Hung., Vol. 12, pp. 279-289, 1960

The known quantum-mechanical results concerning the fractions of the polarization energy still present in the coordination lattices and the higher moment thereby induced are briefly reviewed. From these considerations it follows that it would be unprofitable to solve the same problem according to the classical theory. Accordingly, a simple product-eigenfunction and the spherically symmetric determinant-eigenfunction are introduced into the derived formulas; it is shown that the result for spherically symmetric ions can be put into a form so simple that the actual calculation reduces to an averaging of the even powers of r over the charge density.

## ELECTRICAL PROPERTIES

### DIELECTRIC PROPERTIES

8670 A GRAPHICAL METHOD FOR MEASURING DIELECTRIC CONSTANTS AT MICROWAVE FREQUENCIES by C. B. Sharpe (U. Michigan); IRE Trans., Vol. MTT-8, pp. 155-159, Mar. 1960

A graphical method for measuring the real and imaginary parts of the dielectric constant $\epsilon/\epsilon_0 = \epsilon' - j\epsilon''$ of materials at microwave frequencies is described. The method is based on the network approach to dielectric measurements proposed by Oliner and Altschuler in which the dielectric sample fills a section of transmission line or waveguide. In contrast to their method, the network representing the dielectric sample is analyzed in terms of the bilinear transformation

$$\Gamma' = \frac{a\Gamma + b}{c\Gamma + d};\ ad - bc = 4.$$

The analysis proceeds from the geometric properties of the image circle in the $\Gamma$ plane obtained by terminating the output line in a calibrated sliding short. The technique described retains the desirable features of the network approach but avoids the necessity of measuring both scattering coefficients. As a result the procedure is more direct and, in the case of the TEM configuration, leads to an entirely graphical solution in which the complex dielectric constant can be read from a Smith chart overlay.

8671 METHOD FOR MEASURING TIME CHANGES IN PERMITTIVITY OF FERROELECTRIC MATERIALS by V. Janousek and J. Tomik [in Czech]; Cs. cas. fys., Vol. 10A, pp. 41+, 1960

A description of a method for the constant measurement of rapid changes in $\epsilon$ and tan $\delta$ of dielectrics is given. The accuracy of measurement is calculated and the limits of applicability of the method are determined.

8672 DIELECTRIC CONSTANT MEASUREMENTS IN Ge AND Si AT RADIO FREQUENCIES AS A FUNCTION OF TEMPERATURE AND PRESSURE by M. Cardona, W. Paul and H. Brooks (Harvard U.); Solid State Phys. in Electronics and Telecommun., Vol. 1, Academic Press, 1960, pp. 206-214

Measurements of the dielectric constant of Ge and Si at radio frequencies are presented. The temperature and pressure dependence of the dielectric constant are reported. The resistivity of typical samples of Au doped Si and Mn doped Ge is given as a function of temperature. The corrected pressure

variation of the dielectric constant of Si is $-0.4 \pm 0.0\%$ in 10,000 kg/cm$^2$. The corrected pressure variation of the dielectric constant of Ge is $-1.2 \pm 0.3\%$ in 10,000 kg/cm$^2$. The temperature coefficient gives a change of 0.4% in the dielectric constant for 100 degrees Kelvin for both Si and Ge.

8673 ON THE DIELECTRIC CONSTANT OF GERMANIUM AT MICROWAVE FREQUENCIES by A. C. Baynham, A. F. Gibson and J. W. Granville (Roy. Radar Estab.); Proc. Phys. Soc., Vol. 75, pp. 306-309, Feb. 1960

Measurements of the dielectric constant of germanium at room temperature in the frequency range 30.40-36.62 Gc are reported. Values of $15.35 \pm 0.10$, $14.94 \pm 0.05$, $14.90 \pm 0.10$, and $17.4 \pm 0.5$ were found at 36.62, 34.75, 32.78, and 30.40 Gc, respectively. The experimental techniques are discussed. The experimental values and those of other workers are plotted together with a theoretical dispersion curve. The experimental values verify the existence of a small dispersion region.

Dielectric Constant of GaP - See 8855

8674 INFLUENCE OF GAMMA RADIATION ON THE DIELECTRIC PROPERTIES OF CERTAIN ELECTRICAL INSULATION MATERIALS. Part II. PHENOL-FORMALDEHYDE PLASTICS [in Russian] by K. A. Vodop'ianov, B. I. Vorozhtsov and G. I. Potakhova (SFTI, Tomsk U.); Izv. VUZ Fiz., No. 3, pp. 133-137, 1960

Results of an investigation of the dielectric permeability, angle of dielectric loss and electrical strength of a number of phenol-formaldehyde plastics before and after the effect of gamma radiation are presented. It is shown that after the effect of the gamma rays, a change in the loss angle is observed in the low frequency and high temperature ranges. The effects observed diminish as the temperature at which exposure occurs rises. No change was detected in the dielectric permeability and the electrical strength.

8675 INFLUENCE OF GAMMA RADIATION ON THE DIELECTRIC PROPERTIES OF CERTAIN ELECTRICAL INSULATION MATERIALS. Part III. LACQUERS [in Russian] by K. A. Vodop'ianov, B. I. Vorozhtsov and T. G. Mikhailova (SFTI, Tomsk U.); Izv. VUZ Fiz., No. 4, pp. 152-155, 1960

Results of an investigation of the influence of gamma radiation on the dielectric permeability and the dielectric loss-angle of some electrical insulating lacquers are presented. The irradiation was at +20°, +60°, −60°C and under tropical humidity conditions. It is shown that the dielectric permeability and the dielectric loss-angle of the lacquers are characteristics which are quite resistant to the effect of gamma radiation.

8676 IMPROVEMENT IN THE CHARACTERISTICS OF INSULATOR CERAMICS BY DIMINISHING THE INHOMOGENEITY [in Russian] by M. M. Nekrasov (Kiev Polytech. Inst.); Izv. VUZ Fiz., No. 3, pp. 146-153, 1960

A method of diminishing the inhomogeneity of the internal field by the injection of admixtures of certain oxides is related. This has a favorable effect on the electrical characteristics of insulator ceramics (the voltage distribution across both the thickness of the dielectric and over the insulator surface is hence improved). All the other characteristics of the insulator are improved (the dielectric losses, the electrical conductivity, the absorption capacity are diminished; the breakdown voltage and the discharge voltage over the surface are raised).

8677 SOLID SOLUTION DIELECTRICS BASED ON SODIUM NIOBATE by R. M. Glaister (G. V. Planer); J. Am. Ceram. Soc., Vol. 43, pp. 348-353, July 1960

The dielectric properties of some twenty solid solution systems based on sodium niobate are described. The additives are classified into $ABO_3$, $AB_2O_6$, and $A_2B_2O_7$ types. Properties of the systems $NaNbO_3$-$BaTiO_3$, $NaNbO_3$-$SrTiO_3$, and $NaNbO_3$-$Sr_2Ta_2O_7$ are described in some detail. A composition in the last system has permittivity and loss tangent values at 1600 cps of 2600 and 0.003, respectively, at 20°C and 1600 and 0.025, respectively, at 200°C. The system $NaNbO_3$-$SrTiO_3$ undergoes a phase transition from orthorhombic to cubic symmetry at 15 to 20 mole per cent $SrTiO_3$ accompanied by a change from $NaNbO_3$-type behavior to para-electric behavior. Results on some mixed crystal systems are also reported.

8678 DIELECTRIC PROPERTIES OF ALUMINA AT HIGH TEMPERATURES by J. V. Florio (Genl. Tel. Electronics); J. Am. Ceram. Soc., Vol. 43, pp. 262-267, May 1960

Measurements in air of the dielectric constant and dissipation factor of both single crystal and polycrystalline alumina over the frequency range $10^2$ to $3 \times 10^5$ cps in the temperature range 900° to 1300°C are reported. The three electrode guard ring method was used. The observed dielectric losses were due predominantly to free electron conduction mechanisms. The volume conductivity of single crystal and polycrystalline alumina has been calculated from the high frequency data. The temperature dependences of the volume conductivity for two single crystals of different thicknesses are similar. The large thermal activation energy indicates intrinsic conductivity. The energy gap is calculated to be approximately 7.3 ev. The bulk conductivities of the polycrystalline alumina are considerably higher than the single crystal values, presumably because of impurities in the polycrystalline material. The results are compared with previously reported values.

8679 STATIC SPACE-CHARGE DISTRIBUTIONS by J. R. MacDonald (Texas Instr.); Solid State Phys. in Electronics and Telecommun., Vol. 1, Academic Press, 1960, pp. 389-406

Static space-charge distributions in solids and liquids are discussed in detail and methods of measuring the spatial dependence of potential within these materials are described. Solutions of the space-charge equations for charge-containing materials are given for two cases: (1) one plane, blocking electrode; and (2) two plane, blocking electrodes. The effects of charge mobility on the quasistatic space charge distribution and the measurement of static and differential capacitances as functions of a dc potential bias are discussed. These measurements are used to determine potential distributions in space-charge regions of small dimensions. Materials to which the theory may be applied include electroluminescent materials, photoconducting alkali and silver halides, impure ice, plastic insulators, glass, and extrinsic semiconductors.

8680 SPACE CHARGE FIELDS IN $BaTiO_3$ by S. Triebwasser (IBM); Phys. Rev., Vol. 118, pp. 100-105, Apr. 1, 1960

Experiments on: (1) hysteresis loops, (2) double loops above the Curie point, (3) Kerr electro-optic effect above the Curie point and (4) capacitance above the Curie point in $BaTiO_3$, all

made in the presence of dc electric field bias, are reported. The purpose of these experiments was to determine field distributions in the crystal under an externally applied difference of potential and to examine the extent to which space-charge surface layers cancel the bulk field. The first three types of observations were qualitative in nature. The biased hysteresis loops show normal behavior with no evidence of field cancellation. Double loop measurements show some evidence of field cancellation, while Kerr electro-optic measurements show strongly nonuniform fields, indicating anomalous space-charge fields. The measurements of capacitance above the Curie point indicate that surface layers build up in the presence of a dc field, and these surface layers have a capacitance that varies with applied voltage. The results can be understood qualitatively if simple Schottky exhaustion barriers are assumed at the two metal electrode-crystal contacts. Observed asymmetries with respect to the applied fields are discussed.

8681 A NOTE ON THE THEORY OF SPACE CHARGE LIMITED CURRENTS by C. Rhys-Roberts and R. H. Tredgold (U. Coll. N. Wales); Proc. Phys. Soc., Vol. 76, pp. 497-501, Oct. 1960

In order to explain the observed non-ohmic conductivity in barium titanate and cadmium sulfide, it is necessary to assume that the current is space charge limited. Previous work on space charge limited currents has failed to predict the correct thickness dependence. In this paper a model is proposed wherein there are thin layers of uncharged traps at the surface of the dielectric uniformly distributed in space and of one energy depth; the bulk of the material contains no traps. Using this model the observed experimental results can be explained.

8682 THE ELECTRICAL CONDUCTIVITY OF BARIUM TITANATE SINGLE CRYSTALS by A. Branwood and R. H. Tredgold (U. Coll. N. Wales); Proc. Phys. Soc., Vol. 76, pp. 93-98, July 1960

Measurements of the electrical conductivity of a number of barium titanate single crystals as a function of temperature, applied field, electrode material, thickness, and time are reported. Tentative theories for the observed activation energies, the striking non-ohmic nature of the conductivity, and the influence of the electrode material are suggested. Results for some doped crystals are also given.

8683 ON THE ORIGIN OF BARKHAUSEN PULSES IN $BaTiO_3$ by R. C. Miller (Bell Labs.); J. Phys. Chem. Solids, Vol. 17, pp. 93-100, Dec. 1960

An experimental investigation of the domain phenomena which give rise to ferroelectric Barkhausen pulses in $BaTiO_3$ is described. Through direct observation of the domain structure, and simultaneously the Barkhausen pulses, specific domain phenomena have been correlated for the first time with particular Barkhausen pulse shapes. It is found that Barkhausen pulses occur under a variety of different circumstances. Among these are: the nucleation of a reversed domain, the initial growth step of a small reversed domain, the collision of two reversed domains, and the formation of a small backswitched domain which produces a negative Barkhausen pulse. With the average crystal, each of these origins is operative at some point during polarization reversal. It has also been observed with some crystals that Barkhausen pulses continue to occur for times of the order of hours in the absence of an applied field. The duration of the Barkhausen events range from 2 μsec to about 300μsec and the charge involved during the event is of the order of $10^{-13}$ C. The theoretical aspects of the problem have not been treated, but several driving forces which may be responsible for the pulses are suggested.

8684 MEASUREMENT OF MICROWAVE DIELECTRIC CONSTANTS OF FERROELECTRICS. Part I. DIELECTRIC CONSTANTS OF $BaTiO_3$ SINGLE CRYSTAL AT 3.3 KMc/s by E. Nakamura and J. Furuichi (Hokkaido U.); J. Phys. Soc. Japan, Vol. 15, pp. 1955-1960, Nov. 1960

An extension of Horner et al's method of dielectric measurement in the microwave region to cylindrical specimens of arbitrary cross-sections with relatively high loss tangent and high permittivity is described. As the first application of this method, dielectric constants of $BaTiO_3$ single crystal have been measured from room temperature to 170°C at a frequency of 3.3 KMc/s. Above the Curie point, dielectric constants measured at 3.3 KMc/s agree well with those measured at 24 KMc/s by Benedict and Durand, while the loss tangents slightly above the Curie point are 0.01 ± 0.007 compared to 0.1 in the case of Benedict and Durand.

8685 THEORETICAL STUDY ON THE PROPERTIES OF COERCIVE FIELD OF $BaTiO_3$ SINGLE CRYSTAL by R. Abe (Nagoya U.); J. Phys. Soc. Japan, Vol. 15, pp. 795-801, May 1960

The coercive field properties of $BaTiO_3$ single crystals are investigated theoretically using a previous result on the domain wall motion. The dependences of the coercive field on applied field, crystal thickness and temperature are derived. A further study on the shape of hysteresis loop is made and it is concluded that the particular shapes of the hysteresis loop, such as the double hysteresis loop, are caused by the effects of internal stresses.

8686 EFFECT OF HYDROSTATIC PRESSURE ON THE DIELECTRIC PROPERTIES OF $BaTiO_3$ by J. Klimowski and J. Pietrzak (A. Mickiewicz U.); Proc. Phys. Soc., Vol. 75, pp. 456-459, Mar. 1960

Measurements of the effect of hydrostatic pressure on the dielectric permittivity of both single crystal and ceramic $BaTiO_3$ above and below the Curie point are discussed. In the single crystals the changes in the Curie point and the Curie-Weiss temperature were found to be $-4.1 \times 10^{-3}$ deg $cm^2 kg^{-1}$ and $-3.6 \times 10^{-3}$ deg $cm^2 kg^{-1}$, respectively, as the pressure was increased. The Curie constant was $1.1 \times 10^4$°C and did not change with pressure. In $BaTiO_3$ ceramics the changes in Curie point and Curie-Weiss temperature with increasing hydrostatic pressure were $-4.5 \times 10^{-3}$ deg $cm^2 kg^{-1}$. In both single crystals and the ceramics the reciprocal of the permittivity is a linear function of hydrostatic pressure at a fixed temperature. Below the Curie point, $1/\epsilon$ decreases linearly as the pressure rises, with the rate of change being temperature dependent. Above the Curie point, $1/\epsilon$ increases linearly with pressure, with the rate of change being independent of temperature.

Surface Layers on $BaTiO_3$ Single Crystals - See 8854

8687 INFLUENCE OF THE ADDITION OF $Fe_2O_3$, $V_2O_5$ AND $SnO_2$ ON THE DIELECTRIC PROPERTIES OF BARIUM TITANATE CERAMICS [in French] by G. Lapluye, G. Morinet and P. Palla; Comptes Rendus, Vol. 250, p. 79, Jan. 4, 1960

It is reported that the inclusion of $Fe_2O_3$, $V_2O_5$ and $SnO_2$ in a barium titanate of molecular ratio $TiO_2/BaO = 1.05$ modifies

very sensitively the dielectric properties, especially for low concentrations of $2.5 \times 10^{-2}$ impurity atoms per molecule of titanate.

8688 EFFECTS OF THE INCORPORATION OF METALLIC OXIDES ON THE PROPERTIES OF A BARIUM TITANATE by G. Lapluye, G. Morinet and P. Palla; Comptes Rendus, Vol. 250, p. 305, Jan. 11, 1960

It is reported that the addition of oxides of lanthanum, molybdenum, and tungsten to a barium titanate containing 51.2 per cent molecular composition of $TiO_2$ considerably modifies its dielectric properties.

8689 DIELECTRIC PROPERTIES OF MANGANESE DIOXIDE. Part I. by V. G. Bhide and R. V. Damle (Roy. Inst. Sci., Bombay); Physica, Vol. 26, pp. 33-42, Jan. 1960

The variation with temperature, frequency, and voltage of the electric conductivity, the dielectric constant, and the loss factor of pyrolusite, $MnO_2$, is discussed. The material behaves as a semiconductor. The dc and ac conductivities show an anomaly about 50°C. At this temperature the value of the dielectric constant is a maximum. The loss factor has a minimum value in this temperature region. This behavior indicates that the substance becomes ferroelectric below 50°C. This ferroelectricity is discussed in connection with the crystal structure.

8690 DIELECTRIC PROPERTIES OF MANGANESE DIOXIDE. Part II. by V. G. Bhide and R. V. Damle (Roy. Inst. Sci., Bombay); Physica, Vol. 26, pp. 513-519, July 1960

Measurements of the dielectric hysteresis in manganese dioxide in dc and ac fields as a function of temperature and the biasing field are reported. At a temperature near 50°C the dielectric constant is maximum and the loss factor $\tan\delta$ is minimum. In the same temperature region, the saturation polarization and the coercive field calculated from the hysteresis loop fall to a low value. These results give further indication of the ferroelectric properties of manganese dioxide.

8691 PHYSICAL PROPERTIES AND PREPARATION OF FERROELECTRIC TRIGLYCINSULPHATE by V. Janovec, B. Brezina, and H. T. Arend [in Czech]; Cs. cas. fys., Vol. 10A, pp. 63+, 1960

Data concerning the preparation and physical properties of ferroelectric triglycinsulphate and its isomorphous compounds are given and possible uses for these substances are pointed out.

8692 THERMAL EXPANSION OF TRIGLYCINE SULPHATE by S. Ganesan (Indian Inst. Sci., Bangalore); Nature, Vol. 185, pp. 757-758(L), Mar. 12, 1960

An investigation of the ferroelectric transition in triglycine sulphate by means of thermal expansion measurements in 4 crystallographic directions is discussed. It was found that the crystal expands along the c- and the a-axes and perpendicular to the a-axis as it is heated to the transition point. The expansion coefficient becomes larger as the transition point is approached. Above the transition point the crystal contracts along these directions. Along the b-axis, the crystal contracts while being heated to tne transition point and expands above the transition point. The experimental results indicate that the transition is of the second order, that the anomaly is of the $\lambda$-type, and that the direction of maximum expansion coefficient coincides nearly with the direction of the shortest hydrogen bond. The transition point was found to vary slightly along different directions but all the measurements taken as the crystal was heated were between 51° and 53°C. This differs from the value of 47°C found by Matthias et al.

Domain-Dislocation Relationship in Ferroelectric Glycine Sulphate - See 8609

8693 PIEZOELECTRICITY AND CONDUCTIVITY IN ZnO AND CdS by A. R. Hutson (Bell Labs.); Phys. Rev. Lett., Vol. 4, pp. 505-507(L), May 15, 1960

The effect of piezoelectric scattering on the temperature dependence and magnitude of the phonon drag effect in ZnO and CdS is discussed. The piezoelectric constants were measured in both crystals. The experimental techniques and results are given. The temperature dependence of the electron mobility limited only by piezoelectric scattering is $\mu \cong 50\,(m/m^*)^{3/2}\,(300/T)^{1/2}\,cm^2/v\text{-sec}$ in ZnO and $\mu \cong 120\,(m/m^*)^{3/2}\,(300/T)^{1/2}\,cm^2/v\text{-sec}$ in CdS. Piezoelectric scattering can produce large phonon drag with a small effective mass.

8694 SOURCES OF SOUND IN PIEZOELECTRIC CRYSTALS by E. H. Jacobsen (GE); J. Acoust. Soc. Am., Vol. 32, pp. 949-953, Aug. 1960

The production of sound in piezoelectric crystals is examined from the viewpoint of the inhomogeneous wave equation. It is shown that sound is generated by a gradient in the piezoelectric stress and that consequently the free surface of a piezoelectric crystal are usually the most effective wave sources. The excitation of sound at microwave frequencies is also discussed and is shown to be equivalent to the case of RF excitation at low frequencies.

## CARRIER PROPERTIES

Magnetic Susceptibility of Free Carriers in Si and Ge - See 8848

8695 EXCITON ENERGY LEVELS IN GERMANIUM AND SILICON by T. P. McLean (RRE) and R. Loudon (Clarendon Lab.); J. Phys. Chem. Solids, Vol. 13, pp. 1-9, May 1960

The energies of the lowest-lying levels of the direct exciton in germanium and the indirect excitons in germanium and silicon are calculated in the effective-mass approximation by a variational procedure. These energies are compared with the experimental values obtained from optical absorption experiments.

Magneto-optics of Excitons - See 8850

8696 ON THE DISTRIBUTION OF CARRIERS IN A SEMICONDUCTOR by Z. Bodó (Ind. Res. Inst. Telecommun. Tech., Budapest); Acta Phys., Vol. 11, No. 1, pp. 1-33, 1960

The distribution of carriers and change of potential in the interior of a semiconductor considered semi-infinite when minority carriers of arbitrary distribution have been generated on the surface is investigated. The results are obtained for the case of not too strong generation in the form of exact integrals. As a special case the light-spot diameter dependence of the

photovoltage for generation by a circular light spot is calculated. It is possible to determine the inner recombination and the surface recombination velocity from measurements of this effect.

8697 ONE-DIMENSIONAL OVERLAP FUNCTIONS AND THEIR APPLICATION TO AUGER RECOMBINATION IN SEMICONDUCTORS by A. R. Beattie and P. T. Landsberg (U. Aberdeen and Texas Instr.); Proc. Royal Soc., Vol. 258, Ser. A, pp. 486-495, Nov. 8, 1960

The theoretical lifetime of excess carriers in semiconductors limited only by the Auger recombination mechanism depends on a temperature-independent parameter which involves certain overlap integrals. These integrals are calculated on the basis of a Kronig-Penney model. The value of the parameter obtained is shown to be rather insensitive to many details of the model used. When the value found is inserted into the previously published theory of lifetimes in InSb, very good agreement is obtained with experimental results. This suggests that the dominant recombination mechanism in InSb at elevated temperatures has been identified. A more general analysis of the properties of the overlap integrals is also given.

8698 PHOTOCONDUCTIVE EFFECTS IN INDIUM ANTIMONIDE by D. W. Goodwin (Roy. Radar Estab.); Solid State Phys. in Electronics and Telecommun., Vol. 2, Academic Press, 1960, pp. 759-767

Methods for measuring electron and hole lifetimes in n- and p-type InSb are described. In n-type material the electron and hole lifetimes are equal, and recombination takes place through impurity sites which are associated with acceptor density. In p-type material the electron and hole lifetimes are equal for temperatures greater than 160°K; at lower temperatures the electron and hole lifetimes differ by several orders of magnitudes. A formula governing fluctuation noise in n-type InSb is given and photoconductive decay is discussed.

8699 ANALYSIS OF LOW-LEVEL SEMICONDUCTOR LIFETIME DECAY WAVESHAPES by J. Mandelkorn (USASRDL); Rev. Sci. Instr., Vol. 31, p. 455, Apr. 1960

The measurement of lifetime in semiconductors by the photoconductive decay method when the photoconductivity decay curves displayed on an oscilloscope are low in amplitude is discussed. The hum and noise level of the measurement system makes analysis of these curves difficult. A system which overcomes this difficulty by generating a reference waveshape in the same hum and noise level as the sample output waveshape and by displaying this reference waveshape alternately with the sample decay waveshape on the same baseline of the oscilloscope is briefly discussed. The system has features which permit a thorough analysis of the coincidence regions of the two waveforms.

8700 DETERMINATION OF THE MINORITY CARRIER LIFETIME IN SEMICONDUCTORS by Z. Bodó (Ind. Res. Inst. for Telecommun. Technique, Budapest); Solid State Phys. in Electronics and Telecommun., Vol. 1, Academic Press, 1960, pp. 194-198

The carrier and potential distribution in the interior of an infinite semiconductor is determined for the case in which electron-hole pairs are generated in an arbitrary distribution on the surface. The concentration of holes in the center of the applied light spot is calculated theoretically. A suitable method for measuring changes in the surface recombination rate of a Ge sample without destroying the crystal is developed.

8701 MEASUREMENT OF LIFETIME IN Ge FROM NOISE by S. Okazaki and H. Oki (Okayama U.); Phys. Rev., Vol. 118, pp. 1023-1024, May 15, 1960

A method of determining the lifetime of minority carriers from a noise measurement based on the liberation of hole-electron pairs by light is described. A convenient experimental arrangement is suggested and a typical plot of the experimental results is shown. The curves of the results are compared with the calculated curves.

Carrier Lifetime in:
Au-Doped Ge - See 8864
PbSe - See 8898

Carrier Recombination in Si and Ge - See 8945 and 8946

8702 FREQUENCY FACTOR AND ENERGY DISTRIBUTION C SHALLOW TRAPS IN CADMIUM SULPHIDE by J. J. Brophy a R. J. Robinson (Armour); Phys. Rev., Vol. 118, pp. 959-960, May 15, 1960

Current noise and photoconductivity measurements taken under uniform 5200 A illumination of CdS single crystals are used to derive the energy distribution and frequency factor of shallow traps in the range 0.3 to 0.6 electron volt below the conduction band for samples of different CuCl impurity content. Trap densities varying from $10^{12}$ to $10^{17}$ $cm^{-3}$ $ev^{-1}$ and total trap concentrations of $10^{16}$ $cm^{-3}$ with discrete levels at 0.36, 0.43, and 0.60 ev below the conduction band have been observed. In a moderately doped, good photosensitive crystal, the traps also have a continuous distribution in energy and all have the same frequency factor, $10^{11}$ $sec^{-1}$, which suggests the traps are structurally similar. The results imply that a photoelectron may experience several thousand retrapping transitions on the average before recombining. It is possible to account semiquantitatively for the 1/f noise spectrum observed in some crystals at high frequencies in terms of the near exponential trap distributions and constant frequency factor derived from low-frequenc noise measurements.

Statistics of Recombination via Traps - See 8659

8703 THE INFLUENCE OF THE AMBIENT ATMOSPHERE ON THE SURFACE RECOMBINATION ON SILICON by H. U. Harten (Radiorohrenfabrik, Hamburg-Lokstedt); Solid State Phys. in Electronics and Telecommun., Vol. 1, Academic Press, 1960, pp. 624-627

The effect of the composition of a gas adjacent to a Ge or Si surface on the position of the Fermi level at the semiconductor oxide-interface is discussed. Surface recombination has been investigated by measuring the photo-voltaic effect of a p-n junction alloyed to one surface of a thin silicon disk which is illuminated on the other surface with non-penetrating light. To have an indication of the surface potential, the "surface photovoltage" is measured, i.e., the alternating voltage originated by periodically interrupted light at a transparent electrode which is separated from the illuminated silicon surface by a mica spacer. The sign of the variations of surface recombination and surface photovoltage due to ambient cycles agrees with the model assuming recombination centers at the surface.

Method of Determining Diffusion Length and Surface Recombination Velocity - See 8730

8704 CASCADE CAPTURE OF ELECTRONS IN SOLIDS by M. Lax (Bell Labs.); Phys. Rev., Vol. 119, pp. 1502-1523, Sept. 1, 1960

Enormous capture cross sections in the range $10^{-15}$ cm$^2$ to $10^{-12}$ cm$^2$ have been observed for a wide variety of Coulomb attractive centers in Si and Ge, some involving binding energies many times the Debye energy. Whereas multiphonon transitions to the ground state yield cross sections five to ten orders of magnitude too small, capture into excited states of large radius followed by a cascade of one-phonon transitions leads to cross sections of the right order of magnitude. The initial capturing event is likely to involve an optical phonon or an intervalley collision in the room temperature range, but the acoustic phonon contribution will predominate at low temperatures. Subsequent collisions may eject the electron or cause it to increase its binding energy. The "sticking probability," or probability of eventual capture into the ground state, becomes significant for binding energies of order kT. As the temperature is reduced capture into orbits of larger radius becomes effective and, at least for the acoustic phonon case, the cross section increases rapidly with decreasing temperature and with decreasing electron energy. The large cross sections $10^{-17}$ cm$^2$ to $10^{-15}$ cm$^2$ found for neutral centers can be explained on a similar basis, the attractive potential in this case being provided by the large polarizability of the neutral center.

8705 BAND DYNAMICS AND ZENER EFFECT by G. H. Wannier (Bell Labs.); Solid State Phys. in Electronics and Telecommun., Vol. 1, Academic Press, 1960, pp. 340-342

The basis of the effective mass formalism for semiconductor carriers is discussed. A pseudo-classical kind of band dynamics is presented as a method in problem-solving for experimental purposes. The theory of the Zener breakdown is considered and the nature of the bands in an electric field is discussed.

8706 VALENCE BAND PARAMETERS IN SILICON FROM CYCLOTRON RESONANCES IN CRYSTALS SUBJECTED TO UNIAXIAL STRESS by J. C. Hensel and G. Feher (Bell Labs.); Phys. Rev. Lett., Vol. 5, pp. 307-309(L), Oct. 1, 1960

The determination of the valence band inverse mass parameters in p-type silicon by measurements of the anisotropy of the effective mass m* under uniaxial stress is discussed. It is shown that the application of a uniaxial stress decouples the degenerate bands and makes the measurements possible. Measurements were made at ~9000 Mc and 1°-26° K in samples subjected to uniform, compressive stresses up to 1000 kg/cm$^2$ applied in the [001] or the [111] directions. The anisotropy was independent of the crystallographic plane. In the [001] direction the following were measured with stress T = 1220 kg/cm$^2$: $m_{\parallel}/m = 0.196 \pm 0.001$, $m_{\perp}/m = 0.264 \pm 0.001$, $A = (-4.23 \pm 0.002)\hbar^2/2m$, and $|B| = (0.87 \pm 0.2)\hbar^2/2m$. In the [111] direction and T = 1090 kg/cm$^2$, the following results were obtained: $m_{\parallel}/m = 0.128 \pm 0.001$, $m_{\perp}/m = 0.401 \pm 0.001$, $A = (-4.26 \pm 0.02)\hbar^2/2m$, and $|N| = (10.64/0.04)\hbar^2/2m$.

Negative Effective Mass Cyclotron Resonance Experiments - See 8769

Anisotropy in the Effective Mass of Excitons - See 8909

Density of States Mass in (In, Ga) As Alloys - See 8932

Effective Mass in:
- Ge-Si - See 8824
- AlSb - See 8861
- InSb - See 8911
- InAs and InP - See 8912
- ZnSb and CdSb - See 8768
- $Bi_2Te_3$ - See 8914

8707 THEORY OF ELECTRON TRANSPORT PROCESSES IN SOLIDS by J. M. Richardson (Hughes Aircraft); Solid State Phys. in Electronics and Telecommun., Vol. 1, Academic Press, 1960, pp. 356-379

The theory of electron transport processes in solids is discussed in detail. The author's formulation of irreversible statistical mechanics is applied to a simplified model of the motion of electrons in crystals. The derivation of a closed set of equations describing the spatial and temporal variation of the number and energy densities in each band is given. Electrical conductivity is defined on a new set of observables. Transport properties are derived directly from the microscopic equations of motion instead of starting with the Boltzmann equation.

8708 ANISOTROPY OF CARRIER TRANSPORT IN SEMICONDUCTOR BICRYSTALS by H. F. Mataré (Sylvania); Solid State Phys. in Electronics and Telecommun., Vol. 1, Academic Press, 1960, pp. 73-96

The electrical effects of dislocations and dislocation planes on carrier transport phenomena in semiconductor bicrystals are discussed. The fundamental edge and screw dislocations are described, and some of the properties of grain boundaries are deduced on the basis of the edge dislocation. The model presented reveals two major causes for the strong electrical influence of dislocations: mechanical deformation resulting in changes in the band structure, and free bonds with their acceptor level and possible recharging character. Methods of measuring the lifetime anisotropy in bicrystals are discussed. Theoretical calculations and experimental data are presented.

8709 A REVERSED CARRIER TRANSPORT EFFECT IN GERMANIUM by A. C. Prior (Roy. Radar Estab.); Proc. Phys. Soc., Vol. 76, pp. 465-480, Oct. 1960

The difference in the behavior of electrons and holes in germanium in the degree of departure from linearity of their drift velocity-electric field relationships is shown theoretically and experimentally to influence substantially the motion of a density distribution in near intrinsic material at high fields. In n-type germanium the normal motion can be reversed. A consequence is that injection or extraction, depending on the nature of the contact, can occur from the negative end of an n-type specimen. Cross section variations can also act as sources of injection or extraction. An apparent negative resistance has been observed, and a tentative explanation is given. Changes in mobility ratio due to mechanical stress can have an appreciable effect at high fields, and it is shown that even at low fields interpretation of piezoresistance measurements could be influenced by these considerations.

8710 SURFACE TRANSPORT IN SEMICONDUCTORS by R. F. Greene, J. Zemel (U.S. Naval Ord. Lab.) and D. R. Frankel (Genl. Tel. Electronics); Phys. Rev., Vol. 118, pp. 967-975, May 15, 1960

A transport theory for electrons and holes in space-charge

layers at semiconductor surfaces is given. For diffuse surface scattering, the effective surface mobilities may differ significantly from the bulk mobility for any strength of space-charge layer. Agreement with Schrieffer's formulas is found only for strong space-charge layers and the discrepancy is explained. The results are extended to cover an arbitrary degree of diffuseness of surface scattering and to cover samples of small thickness.

8711 NEW DERIVATION OF BARDEEN-SHOCKLEY FORMULA FOR MOBILITY OF ELECTRONS IN HOMOPOLAR SEMICONDUCTORS by L. Hrivnák (Komensky U., Bratislava); Czech. J. Phys., Vol. B10, p. 633, Sept. 1960

The Bardeen-Shockley formula for the mobility of an electron or hole in a homopolar semiconductor is derived in a different way to that in which its authors obtained it. The interaction energy of the electron with the acoustic lattice oscillations is derived in an original way. A new possibility for determining the energy gap is given.

8712 ON THE THEORETICAL VARIATION OF ELECTRON MOBILITY WITH APPLIED ELECTRIC FIELD IN SEMICONDUCTORS by R. Stratton (Metropolitan-Vickers); Solid State Phys. in Electronics and Telecommun., Vol. 1, Academic Press, 1960, pp. 343-355

The variation of the electron mobility in a semiconductor with the magnitude of the applied field ("hot electron effect") is treated theoretically. The assumption of elastic electron-phonon scattering of previous theories is considered well satisfied for essentially all electron energies when the electrons are scattered by acoustic phonons, but not when they are scattered by optical phonons. The theory presented discards the assumption of elastic scattering for optical phonons. A method of solving the more complicated integro-differential Boltzmann equation is presented.

8713 FIELD DEPENDENT ELECTRON MOBILITY IN IONIC CRYSTALS by J. F. Barnes and R. H. Tredgold (U. Coll., N. Wales); Proc. Phys. Soc., Vol. 76, pp. 261-266, Aug. 1960

The Boltzmann equation for electronic conduction in an ionic crystal is set up and an approximate solution is obtained through terms in the cube of the field. Explicit results for values of $\hbar\omega_0$ of 2kT and 1/2kT, where $\omega_0$ is the angular frequency of longitudinal optical modes, are obtained. It is shown that for fields less than the known breakdown fields the mobility decreases with increasing field. The non-ohmic effects will always be negligible for fields less than $10^5$v $cm^{-1}$.

Effect of Electron Irradiation on Mobility in Ge - See 8649

8714 MICROWAVE METHODS OF MEASURING MOBILITY IN SEMICONDUCTORS by H. M. Barlow and J. Brown (U. Coll., London); Solid State Phys. in Electronics and Telecommun., Vol. 1, Academic Press, 1960, pp. 199-205

Microwave methods of measuring carrier mobility in semiconductors are described. The determination of charge carrier density at low frequencies by use of the Hall effect, and at high frequencies by use of radiation pressure, is discussed. The relation between radiation pressure and the Hall EMF is derived. The Hall effect microwave mixer provides a simple alternative to Faraday rotation for the measurement of mobility.

Derivation of Hole Mobility in InSb from Galvanomagnetic Measurements - See 8759

8715 A COMPARISON OF DRIFT MOBILITY, CARRIER LIFETIME AND HALL EFFECT MEASUREMENTS ON p-TYPE SILICON by F. W. G. Rose, E. L. Heasell and F. Paton (Brit. Thomson-Houston); Solid State Phys. in Electronics and Telecommun., Vol. 1, Academic Press, 1960, pp. 230-239

The rather low values of electron drift mobility sometimes observed in high resistivity Si are discussed. These low values are explained by a high concentration of compensated donor and acceptor type scattering centers. Combined measurements of the room-temperature drift mobility and of the temperature dependence of the carrier lifetime and Hall effect have been made on some samples.

Hall Mobility in Ge - See 8761

Mobility in (In, Ga) As Alloys - See 8932

Hall Mobility in CdTe - See 8764

8716 TWO-PHONON INDIRECT TRANSITIONS AND LATTICE SCATTERING IN Si by W. P. Dumke (IBM); Phys. Rev., Vol. 118, pp. 938-939, May 15, 1960

The probability of indirect transitions with the emission of two phonons is calculated. Several of the intensity maxima in the intrinsic low-temperature emission spectrum of Si are explainable in terms of these transitions. Scattering matrix elements obtained from an analysis of the observed emission spectrum indicate that intervalley scattering is the dominant scattering mechanism for electrons in Si, with 0.023 ev and 0.046 ev longitudinal acoustic mode phonons umklapp scattering electrons between valleys on the same and on different crystal axes, respectively. The valleys are approximately 82 per cent of the way from the center to the edge of the Brillouin zone. Optical mode scattering in the valence band is largely responsible for the anomalous temperature dependence of the intrinsic hole mobility.

8717 KINETIC THEORY OF IMPACT IONIZATION IN SEMICONDUCTORS by L. V. Keldysh (P. N. Lebedev Phys. Inst.); Soviet Phys.-JETP, Vol. 10, pp. 509-518, Mar. 1960

The effect of impact ionization processes on the distribution function for electrons and holes in a strong electric field is discussed. It is shown that the energy dependence of the impact ionization probability near the threshold is essentially different for crystals with small and high dielectric constants. The kinetic equation is solved for both these cases. Expressions for the equilibrium number of carriers in a strong field, the impact-ionization coefficient, and the critical field are obtained and the dependence of the breakdown field on temperature, specimen thickness, and the electron-lattice interaction law is found. The relation of the derived expressions to the breakdown criteria of Froelich and von Hippel is determined. It is shown that increasing the electric field causes a decrease in the recombination speed, as a result of which the equilibrium number of carriers starts growing as the field increases long before the appearance of impact ionization.

Impurity Scattering in Metal Alloys at Low Temperatures - See 8920

Isotope and Impurity Scattering in $Bi_2Te_3$ - See 8919

Scattering Processes in the PbS Group - See 8918

Piezoelectric Scattering in ZnO and CdS - See 8693

## CONDUCTIVITY (RESISTIVITY)

8718 HEITLER-LONDON APPROACH TO ELECTRICAL CONDUCTIVITY AND APPLICATION TO d-ELECTRON CONDUCTIONS by J. Yamashita and T. Kurosawa (U. Tokyo); J. Phys. Soc. Japan, Vol. 15, pp. 802-821, May 1960

Conduction by the movement of an extra electron which is tightly bound to an ion in an ionic lattice is discussed. The wave function of the electron is assumed to be localized closely around an ion and the motion of the electron is so slow that lattice polarization is induced around the electron. Further, the potential in the lattice is assumed to deviate slightly from a perfectly periodic arrangement owing to the existence of many impurity-ions. In these circumstances the current is connected with a hopping motion of the electron from ion to ion rather than with a translational motion of the electron in a nearly perfect lattice. The self-trapped state of a positive hole in a polar lattice with a fluctuating potential is discussed. A theory of the transition of the hole from ion to ion by using the non-adiabatic approximation is developed and the same problem is discussed using the adiabatic approximation. In the last section the theory is compared with experimental results. The electrical conduction through d-electrons in crystals such as $Li_xNi_{1-x}O$, $LaMnO_3 + SrMnO_3$, magnetite and $CoFe_2O_4$ is regarded as a good example to which the Heitler-London conduction mechanism is applicable. The impurity conduction in germanium is discussed from a similar point of view.

8719 SEMICONDUCTION IN $Li_xNi_{(1-x)}O$ by S. Van Houten (Philips); J. Phys. Chem. Solids, Vol. 17, pp. 7-17, Dec. 1960

NiO is an insulator which may be made conducting by the addition of lithium oxide. This behavior is explained in terms of an energy level scheme consisting of full, localized $Ni^{2+}$ levels with empty $Ni^{+}$ levels approximately 5 ev above them. The consequence of introducing lithium into the lattice is that the $Li^{+}$ ions are compensated by $Ni^{3+}$ ions, giving $Li^{+} \cdot Ni^{2+}$ acceptor levels at approximately 0.03 ev above the $Ni^{2+}$ levels. Electrical conduction, which is always p-type, may be described in terms of a thermally activated diffusion of holes from one nickel ion to another. The activation energy is connected with self-trapping by the polarization induced by the hopping hole itself. A detailed account is given of the calculation of the energy levels, starting from the ionization energies of the free ions and combining them with Madelung potentials. Corrections are made for the polarization of the lattice and for differences in crystal field stabilization between the Ni ions of different valencies. Measurements of Seebeck effect and electrical resistance as a function of temperature and lithium concentration are discussed in terms of this model. It is shown that the oxygen band, lying much lower than the $Ni^{2+}$ levels, does not give any contribution to the electrical conduction.

8720 ON THE NATURE OF ELECTRICAL CONDUCTION IN GERMANIUM AT LOW TEMPERATURES; NON-EQUILIBRIUM BULK AND CONTACT PHENOMENA by S. H. Koenig (IBM); Solid State Phys. in Electronics and Telecommun., Vol. 1, Academic Press, 1960, pp. 422-431

The theory of electrical conduction in Ge at low temperatures is developed. The processes which determine the speed of response of any proposed devices utilizing the non-linear conduction of Ge are considered and the factors that determine the relation of the switching time to physically adjustable parameters are discussed. Contact effects on switching time are considered.

8721 A DIELECTRIC APPROACH TO IMPURITY CONDUCTION by D. G. H. Frood (U. Liverpool); Proc. Phys. Soc., Vol. 75, pp. 185-193, Feb. 1960

Impurity conduction is formulated on a dielectric basis. It is assumed that the condition for the transition from insulator to metal is provided by the dielectric catastrophe which occurs through the polarizability of the neutral particle. On the basis of the Onsager formula, the contribution to the permittivity arising from the hydrogenic donor atoms is calculated, assuming all catastrophic excited states merge with the continuum. The upper temperature limit of the phase transition from N discrete levels to N-1 discrete levels can then be estimated. The donor activation energy is found to be a stepwise decreasing function of both temperature and donor concentration. The dielectric theory is then extended to include screening by the conduction electrons. With an appreciable number of carriers present the hydrogen model breaks down and there is no polar contribution to the dielectric constant. The donor activation energy decreases smoothly and more rapidly with increasing temperature and donor concentration than it would do had only the unscreened catastrophe been operative in producing the band model.

8722 THE ANISOTROPY OF THE CONDUCTIVITY OF HOT ELECTRONS AND THEIR TEMPERATURE IN GERMANIUM by E. G. S. Paige (Roy. Radar Estab.); Proc. Phys. Soc., Vol. 75, pp. 174-184, Feb. 1960

A method of analyzing the anisotropy of the conductivity of electrons in germanium at high electric fields is discussed and applied to Koenig's data on a specimen having a free carrier concentration of $6.5 \times 10^{14}\ cm^{-3}$. The electron temperatures in each valley are obtained and the mobility and population of carriers within the valleys are calculated. These electron temperatures are compared with electron temperatures calculated from an energy balance equation applied to each valley as though it existed independently of the other valleys. The comparison shows that there is interaction between electrons in different valleys. Estimates of the rate of energy transfer between valleys are made.

8723 ANISOTROPIC CONDUCTION IN SOLIDS NEAR SURFACES by P. J. Price (IBM); IBM J. Res. Dev., Vol. 4, pp. 152-157, Apr. 1960

A reduction in the electrical conductivity of a solid results from "diffuse" reflection of electrons from the surfaces. The effect occurs for specular reflection also, if the operative electron-energy surfaces are not spherical. A theory of the latter case is given. The average conductivity of a thin crystal tends to a finite limit (rather than zero) as the thickness tends to zero. The Hall effect for the same circumstances is also treated.

8724 EFFECTS OF HYDROSTATIC PRESSURE ON THE PIEZORESISTANCE OF SEMICONDUCTORS: i-InSb, p-Ge, p-InSb, AND n-GaSb by R. W. Keyes and M. Pollak (Westinghouse);

Phys. Rev., Vol. 118, pp. 1001-1007, May 15, 1960

A method for measuring the piezoresistance of a sample under high hydrostatic pressure by comparison with the piezoresistance of intrinsic InSb is described. The method is tested by a measurement of the piezoresistance of p-type germanium and p-type InSb up to 13,000 kg/cm$^2$. The piezoresistance of these materials is found to be independent of pressure, in good agreement with predictions based on other experiments. Measurement of the piezoresistance of n-GaSb as a function of pressure up to 12,000 kg/cm$^2$ confirms the correctness of the model of the conduction band which has been proposed by Sagar. Values for certain parameters of the conduction band of GaSb are deduced.

Effect of Grain Sizes on the Resistivity of Pressed $Bi_2Te_3$ Powders - See 8929

Electrical Properties of Grain Boundaries - See 8610

Photoelectric Analysis of Conductivity in CdS-Type Crystals - See 8591

Theory of Surface Conductivity - See 8660

8725 ELECTRICAL PROPERTIES OF GaSb-InSb ALLOYS by J. C. Woolley and C. M. Gillett (U. Nottingham); J. Phys. Chem. Solids, Vol. 17, pp. 34-43, Dec. 1960

Production of reasonably homogeneous, polycrystalline, solid ingots of GaSb-InSb alloys by slow directional freezing techniques, and their use to investigate the variation of electrical properties as a function of composition are described. Values of extrapolated thermal energy gap $E_0$, electron mobility, and mobility ratio have been determined for some 25 specimens covering the complete composition range. Estimates have been made of the variation of effective mass values and, by comparison with optical energy gap values, of the energy gap temperature coefficient $\beta$. From the variation of mobility with temperature, values of mobility temperature exponent x have been obtained. At the InSb-rich end of the composition range, the results indicate a smooth variation of the various parameters with composition, without any appreciable change in the band structure from that of InSb. The results at the GaSb-rich end of the range are complicated, first by the presence in GaSb of two conduction bands of only small energy separation, and second by an effect which extends over a considerable range of composition and is thought probably to be due to ordering in the alloys. As a result, correlation of the optical and electrical results is difficult in this range of composition.

8726 HEAT TREATMENT EFFECTS IN INDIUM ARSENIDE by J. T. Edmond and C. Hilsum (Services Electronics Res. Lab.); J. Appl. Phys., Vol. 31, pp. 1300-1301 (L), July 1960

Experiments conducted to determine the impurity responsible for the heat treatment-induced conductivity type changes observed in InAs are described. Heat treatments were carried out in tubes of Vitreosil, a normal grade of silica, and of Spectrosil, a synthetic high purity silica. In the Vitreosil tubes the usual effects were observed (i.e., the material became more n-type upon heat treatment and less n-type after annealing). The specimens heated in Spectrosil became more p-type and showed only a small amount of annealing after heat treatment. To determine whether S or Cu is the donor impurity responsible for the changes observed in the Vitreosil tubes, InSb samples with similar electrical properties were heated in Spectrosil tubes doped with Cu and S and in an undoped tube for 17 hrs at 850°C. The specimen heated in undoped Spectrosil became less n-type and the other two more n-type. After annealing the specimen heated in Cu-doped Spectrosil showed the same annealing characteristics of normal heat-treated material. The others showed no appreciable change. Heat treatment in normal silica then produces two changes, a permanent change by an unknown mechanism and a temporary change due to copper contamination.

8727 SIZE EFFECT FOR CONDUCTION IN THIN BISMUTH CRYSTALS by A. N. Friedman (Columbia U. and IBM) and S. H. Koenig (IBM); Bull. Am. Phys. Soc., Ser. II, Vol. 5, p. 150(A), Mar. 21, 1960

Measurements of the electrical conductivity $\sigma$, Hall constant $R_H$, and magnetoresistance at liquid helium temperatures for thin single crystals of bismuth of varying orientation, and lateral dimension (~0.2 - 5.0 mm) of the order of the electron mean free path were reported. The Hall data were taken with the magnetic field parallel to the thin direction. Both $\sigma$ and $R_H$, as a function of thickness, level off to a "saturation" value in the thin limit. The existence of this saturation, the magnitude of which is dependent upon the crystallographic orientation relative to the sample geometry, indicates that the surface reflection of the carriers is specular. The results, when compared with theory, are consistent with current ideas regarding the structure of the conduction band if the contribution of the holes to the conductivity is assumed negligible. Specific results for the galvanomagnetic effects, mean free path, and scattering time were presented.

Temperature Dependence of the Resistance of Thin Be Films - See 8757

8728 INCONSTANCY OF THE ELECTRICAL PARAMETERS OF SELENIUM SAMPLES WITH A BROMINE IMPURITY AS A FUNCTION OF THEIR STORAGE TIME [in Russian] by V. N. Romankevich and V. G. Sidiakin (Kiev Polytech. Inst.); Izv. VUZ, Fiz., No. 3, pp. 180-184, 1960

The influence of bromine on the electrical properties of selenium is discussed. It is shown that bromine is bound weakly to the hexagonal selenium and is liberated at room temperature. The bromine liberation slowly changes the electrical parameters of the selenium sample with the bromine impurity. This fact should be taken into account in operating with a semiconductor device fabricated from brominated selenium.

Semiconducting Properties of:
ZnO - See 8612
Gray Tin - See 8586

Resistivity of MnSi, $CrSi_2$, and CoSi - See 8931

8729 IONIC CONDUCTIVITY OF GAMMA IRRADIATED SODIUM CHLORIDE by H. S. Ingham, Jr. and R. Smoluchowski (Carnegie Inst. Tech.); Phys. Rev., Vol. 117, pp. 1207-1215, Mar. 1, 1960

Results of subjecting single crystals of NaCl to about $5 \times 10^5$ roentgens of $Co^{60}$ gamma irradiation at 5°C, then rapidly heating and maintaining them at a fixed temperature in the range of 65° to 135°C are given. The dc ionic conductivity at this temperature was measured by means of a vibrating reed electrometer as a function of time. It decreased in the temperature range 65° to 80°C during a period of several hours to a value that was less than the preirradiation conductivity by a factor which was typically about 30. The conductivity is

presumed to be a direct measure of the number of positive ion vacancies. The data fit a rate equation describing the bimolecular process A + B → AB, with an activation energy approximately equal to that of the mobility of the positive ion vacancies. This confirms the supposition that the change of conductivity reflects the clustering of the positive ion vacancies with other imperfections at a rate controlled by the diffusion of these vacancies. Above 100°C, many of the clusters appear to break up again with an accompanying increase of conductivity. The conducting vacancies appear to be localized in a rather small fraction of the total volume of the crystal.

Low Temperature Conductivity of Highly Purified KCl - See 3618

8730 SURFACE RECOMBINATION AND DIFFUSION PROCESSES IN CATHODOLUMINESCENCE AND ELECTRON BOMBARDMENT INDUCED CONDUCTIVITY by Gy. Gergely (Res. Inst. Telecommun., Budapest); J. Phys. Chem. Solids, Vol. 17, pp. 112-116, Dec. 1960

The voltage dependence of cathodoluminescence and electron bombardment induced conductivity is analyzed, taking into consideration the surface recombination and diffusion processes. The diffusion equation of DeVore is combined with Young's and Feldman's laws relating to the penetration and energy loss of incident electrons. A good agreement was obtained between the theoretical and experimental brightness vs voltage curves. By the analysis of this curve the diffusion length L and the surface recombination velocity S may be determined. It was found that L = 0.05 −0.15 micron and S = $5 \times 10^3$-$5 \times 10^5$ cm/sec for several phosphors.

8731 SOME OBSERVATIONS ON THE ELECTRICAL PROPERTIES OF INDIUM ANTIMONIDE AT LOW TEMPERATURES by E. H. Putley (Roy. Radar Estab.); Solid State Phys. in Electronics and Telecommun., Vol. 2, Academic Press, 1960, pp. 751-758

Measurements of the conductivity and Hall effect of intrinsic and p-type crystals of InSb are reported. Two impurity levels are present in the p-type material, one at 0.0075 ev and the other at 0.02 ev above the valence band. These crystals deviate from Ohm's law at fields greater than 0.5 volt/cm. The temperature variation of the Fermi level and of the concentration of impurity scattering centers in several samples of n-type InSb over the range of 20°-100°K are also given and the mobility data between these temperatures are analyzed. Results obtained for the transverse magnetoresistance of an n-type specimen at helium temperatures are given and the effects of high electric fields at low temperatures are described.

8732 SEMICONDUCTING PROPERTIES OF CUBIC BORON PHOSPHIDE by B. Stone and D. Hill (Monsanto); Phys. Rev. Lett., Vol. 4, pp. 282-284(L), Mar. 15, 1960

The properties of cubic BP crystals prepared by the vapor phase reaction of boron compounds with phosphorus compounds or phosphorus vapors and by the slow cooling of a melt containing dissolved boron and phosphorus are discussed. Optical absorption measurements on thin polycrystalline films indicate that the energy gap is almost 6 ev. Crystals grown by the slow cooling of a melt are p-type with a carrier concentration ranging from 1 to $5 \times 10^{18}$ carriers/cm$^3$. The Hall coefficient is essentially constant from about 900°K down to about 160°K. Needle-shaped crystals grown by the vapor phase reaction are n-type with an impurity level about $10^{17}$ carriers/cm$^3$. The thermoelectric power of both n- and p-type crystals is about 300 μv/°C.

8733 CONDUCTIVITY OF THE OXIDES OF IRON AT HIGH TEMPERATURES by D. S. Tannhauser (MIT); Bull. Am. Phys. Soc., Ser. II, Vol. 5, p. 278(A), Apr. 25, 1960

Measurements of the conductivity and thermoelectric power of wüstite and magnetite between 1000° and 1450°C were reported. A thin sheet of Puron iron, with platinum electrodes attached, was oxidized under a suitable oxygen pressure. The sample converted reversibly into the various oxides of iron, the ratio Fe:O and therefore $Fe^{2+}$:$Fe^{3+}$ inside the various oxide phases was controlled by the oxygen pressure. The conductivity of wüstite is practically proportional to the concentration of $Fe^{3+}$ in the lattice, and that of magnetite is proportional to the $Fe^{1+}$ concentration. The thermoelectric power against platinum changes sign near the boundary between the two phases and indicates p-type conduction in wüstite and n-type conduction in magnetite. The conductivity of the two phases is almost the same on the two sides of the boundary, even though the ratio $Fe^{2+}$:$Fe^{3+}$ changes from 2:1 in wüstite to 1:2 in magnetite. The conductivity depends only very slightly on the temperature. It was inferred that the charge carriers are essentially free and that their concentration is equal to that of $Fe^{3+}$ in wüstite and that of $Fe^{2+}$ in magnetite. The mean free path by the Drude theory is less than 1 A; therefore a band picture is probably not appropriate.

8734 ELECTRICAL PROPERTIES OF PSEUDO-BINARY SYSTEMS OF $Ag_2VI'S$; $Ag_2Te_xSe_{1-x}$, $Ag_2Te_xS_{1-x}$, AND $Ag_2Se_xS_{1-x}$ by S. Miyatani (Niigata U.); J. Phys. Soc. Japan, Vol. 15, pp. 1586-1595, Sept. 1960

The electrical properties such as the electronic and ionic conductivities, Hall coefficients, etc. of the alloys $Ag_2$(Te, Se; Te, S; Se, S) are studied with use of the galvanic cell Ag | AgI | specimen | Pt, the excess Ag content being controlled by sending a current across the cell. The electrical properties of these alloy systems change continuously in the α phase as the mixing ratio x is varied, while they change discontinuously or rapidly at certain x's in the β phase. The experimental results are compared with theory under simplifying assumptions such as the energy-independent relaxation time and the energy-momentum relation given by $\mathcal{E} = \hbar^2k^2(1-Bk^2)/2m^*$.

8735 ORGANIC SEMICONDUCTORS. Part I. SOME CHARACTERISTICS OF THE P-PHENYLENEDIAMINE-CHLORANIL COMPLEX by M. M. Labes, R. Sehr, and M. Bose (Franklin Inst.); J. Chem. Phys., Vol. 32, pp. 1570-1572(L), May 1960

Electrical conductivity, thermal conductivity, and Seebeck coefficient measurements performed on microcrystalline samples of the p-phenylenediamine-chloranil complex are discussed. Measurements were made on rectangular samples measuring 2 x 0.5 x 0.2 cm and on round samples with the dimensions 1.3 cm diameter x 0.3 cm. From the temperature dependence of the electrical conductivity, an activation energy of 0.57 ev was found. The Seebeck coefficient was measured on one round and one rectangular sample. A mean value of $1.1 \times 10^{-3}$ v deg$^{-1}$ ± 20 per cent, which is the highest thus far reported for organic materials, was found. A thermal conductivity of 2.0 $\times 10^{-3}$ w cm$^{-1}$ deg$^{-1}$ with an accuracy of about 15 per cent was found. These values give a figure of merit of $Z = S^2\sigma/\kappa \approx 10^{-11}$ even though S and κ are better than inorganic thermoelectric materials.

8736 ELECTRICAL RESISTIVITY OF DYSPROSIUM SINGLE CRYSTALS by P. M. Hall, S. Legvold and F. H. Spedding (Iowa State U.); Phys. Rev., Vol. 117, pp. 971-973, Feb. 15, 1960

Resistivity measurements on two single crystals of hcp dysprosium metal in the temperature range 1.3°K are reported. The two magnetic transitions at 90°K and 175°K are very evident in the resistivity. Significant anisotropy is observed only above 175°K, which is the paramagnetic range; at 400°K, $\rho_{\perp}/\rho_{\parallel} = 1.5$. A prediction for the resistivity of polycrystalline dysprosium based on these measurements is seen to be in good agreement with the resistivity of a polycrystalline sample.

## SUPERCONDUCTIVITY

8737 DISPERSION OF PLASMA FREQUENCIES AND SCREENED EXCHANGE ENERGY IN THE SUPRACONDUCTIVE STATE [in German] by L. Tewordt (München U.); Z. Naturforsch., Vol. 15a, pp. 490-502, May/June 1960

The theory of superconductivity by BCS (Bardeen, Cooper, Schrieffer) is continued, based on the description by Bardeen and Pines. For the BCS semi-particle pairs, the equation of the motion with the complete Electron-Hamilton Operator (BCS fundamental part, plus the interaction between electron pairs with a total impulse different from zero, and total spin zero, which was neglected by BCS) is obtained by the method of the generalized random phase approximation. Hereby one is able to determine the corrections of the matrix elements of the density variations relative to the matrix elements with BCS excitation. These corrected matrix elements are inserted in the general expressions for the longitudinal dielectric constant and the screened exchange energy, following from the random phase approximation in a formulation analogous to Nozieres and Pines. The resultant sums can be transformed into integrations and evaluated by the Wentzel transformation. The results are: the plasma frequencies and the components of the screened exchange energy with small wave number are not influenced by the transition from normal to supraconductive. Hence, the result by BCS regarding the condensation-energy of the supraconductive state at the absolute zero of temperature and the consequent conclusions remain correct within the approximation used, when the energies of the far reaching Coulomb interaction are also considered.

8738 ON THE INTERMEDIATE STATE OF FERROMAGNETIC SUPERCONDUCTORS by G. F. Zharkov (P.N. Lebedev Phys. Inst.); Soviet Phys.-JETP, Vol. 10, pp. 1259-1262, June 1960

The range of external magnetic field values for which a single domain ferromagnetic ellipsoid can exist in the intermediate state is found and the structure of the intermediate state for the case of a ferromagnetic superconducting plate is examined using the "unbranched" model.

8739 STRONG-COUPLING LIMIT IN THE THEORY OF SUPERCONDUCTIVITY by D. J. Thouless (U. California); Phys. Rev., Vol. 117, pp. 1256-1260, Mar. 1, 1960

The Hamiltonian used by Bardeen, Cooper, and Schrieffer in their theory of superconductivity is studied in the strong-coupling limit. The complete set of energy levels can be found by using group theory, even for a finite system. An expression for the grand partition function can immediately be written down, and this expression can be evaluated in a simple manner for a large system. The results are in qualitative agreement with the weak-coupling theory, and in quantitative agreement with the strong-coupling limit of the expressions derived by Bardeen, Cooper, and Schrieffer. The second-order phase transition is a simple consequence of the form of the grand partition function. There is an energy gap independent of the total number of particles which goes to zero as the temperature approaches the critical temperature. The normal state is not metastable below the critical temperature.

8740 ON TAKING THE COULOMB EFFECTS INTO ACCOUNT IN THE THEORY OF SUPERCONDUCTIVITY by D. V. Shirkov (Joint Inst. Nuc. Res.); Soviet Phys.-JETP, Vol. 10, pp. 127-131, Jan. 1960

Through a transition from the energy operator to the S matrix, the compensation equation for dangerous electron diagrams is brought into a symmetric form, which is expressed in terms of the usual Green functions. In the high-density electron gas approximation, the summation of the Coulomb singularities in the kernel of the compensation equation is performed by the renormalization group method. In the lowest approximation the result of the summation is the same as the formulas obtained previously by qualitative means.

8741 THE CRITICAL SUPERCOOLING FIELD IN SUPERCONDUCTIVITY THEORY by L. P. Gor'kov (Inst. Phys. Problems); Soviet Phys.-JETP, Vol. 10, pp. 593-599, Mar. 1960

It is shown that the magnitude of the critical supercooling field $Hc_1$ is larger than or smaller than the critical field Hc, depending on whether the superconductor in a weak field is of the London or the Pippard type. The superconductor in the first case must display a behavior similar to that of alloys in a strong field. The magnitude of the ratio $Hc_1/Hc$ depends weakly on the temperature in the whole temperature range.

8742 ON THE PHASE TRANSITION OF A SUPERCONDUCTOR by G. Wentzel (Bell Labs.); Helv. Phys. Acta, Vol. 33, No. 8, pp. 859-871, 1960

In previous studies of the statistical mechanics of a superconductor, only the 'reduced Hamiltonian' of the BCS theory has been used which ignores the vast majority of the electron-electron interactions. Here, the Hamiltonian is extended by including the other interactions as perturbations up to the second order. As a preliminary step, omitting all but the first order terms in the Hamiltonian, a rigorous expression for the free energy is derived. Then, to take account of the second-order perturbations, a variational method is used. Particular attention is paid to the behavior of the free energy near the critical temperature.

8743 SUPERCONDUCTING TRANSITION TEMPERATURE IN DILUTE THALLIUM SOLID SOLUTIONS by J. I. Budnick and D. J. Quinn (IBM Res. Lab.); Bull. Am. Phys. Soc., Ser. II Vol. 5, p. 164(A), Mar. 21, 1960

A study of the variation of the superconducting transition temperature with composition in dilute thallium solid solutions with several nonmagnetic solutes, namely, lead, indium, tin, and bismuth, was reported. All of these impurities produced a small increase (initially proportional to the concentration in the range from 0.01 to 0.1 atomic per cent) in the superconducting transition temperature. The change in critical

temperature at a fixed residual resistance ratio depends on the specific impurity added. This behavior is to be contrasted with the initial decrease in the transition temperature generally found by Serin, Lynton, and co-workers when small amounts of nonmagnetic impurities were added to tin, aluminum and indium.

8744 FURTHER EXPERIMENTS CONCERNING THE SPIN-ELECTRON INTERACTIONS IN SUPERCONDUCTORS by B. T. Matthias, H. Suhl and E. Corenzwit (Bell Labs.); J. Phys. Chem. Solids, Vol. 13, pp. 156-159, May 1960

The lowering of the superconducting transition temperature of lanthanum by dissolving in it the rare earths Ce, Nd, Sm, Eu, Tb, Ho and Er is reported and discrepancies regarding previous theoretical considerations are pointed out.

8745 THEORY OF SUPERCONDUCTING ALLOYS IN A STRONG MAGNETIC FIELD NEAR THE CRITICAL TEMPERATURE by L. P. Gor'kov (Inst. Phys. Problems); Soviet Phys.-JETP, Vol. 10, pp. 998-1004, May 1960

The equations of the phenomenological Ginzburg-Landau theory of superconducting alloys near $T_c$ are derived from the Bardeen-Cooper-Schrieffer theory. As in the case of pure superconductors, a double charge is encountered in the equations. The relation between the constant $\kappa$ of the alloy with $\kappa_0$ of the pure superconductor is found under the assumption that the shift in $T_c$ is small. For a sufficiently "impure" alloy, $\kappa$ depends only on the coefficient in the linear law for the electronic specific heat of the metal. Agreement between the theory and experiments has been found to be satisfactory.

8746 THE VOLUME DEPENDENCE OF THE ELECTRON LEVEL DENSITY AND THE CRITICAL TEMPERATURE IN SUPERCONDUCTORS by J. L. Olsen and H. Rohrer (ETH, Zurich); Helv. Phys. Acta, Vol. 33, No. 8, pp. 872-880, 1960

Experimental work on the volume dependence of the critical magnetic field in superconductors and on the volume change at the transition is summarized and discussed. The best values for $d \ln T_c/d \ln v$ and $d \ln \gamma/d \ln v$ ($T_c$ = transition temperature, $\gamma T$ = electronic specific heat per mole, $v$ = molar volume) are estimated. $d \ln \gamma/d \ln v$ is many times greater than the free electron value. No correlation between $d \ln T_c/d \ln v$ and $d \ln v$ could be seen, but the relation $d \ln (T_c/\theta)/d \ln v = \text{const.}$ $\ln (\theta/T_c)$ is approximately obeyed for the soft superconductors ($\theta$ = Debye temperature).

8747 EFFECT OF OXYGEN ON THE CRITICAL FIELDS OF SUPERCONDUCTING TIN FILMS by H. L. Caswell (IBM Res. Ctr.); Bull. Am. Phys. Soc., Ser. II, Vol. 5, p. 164(A), Mar. 21, 1960

Tin films of 4500 to 6000 A thickness have been evaporated through a glass mask onto room-temperature substrates of fused quartz at pressures less than $2 \times 10^{-9}$ torr and in various partial pressures of oxygen by bleeding in reagent grade oxygen. The critical, external magnetic field extrapolated to 0°K required to switch a film from the superconducting to normal state as determined by the introduction of electrical resistance was found to increase from 380 oe for a pure film to 410, 500, 600, and 820 oe for films evaporated under conditions where the ratio of oxygen molecules to tin atoms striking the substrate was 1, 4, 7, and 10 per cent respectively. The effect is due to a decrease in surface mobility of tin atoms in the edges of the film. With pure films tin atoms in this region form discontinuous grains so that electrically the film appears to be of uniform thickness. Oxygen inhibits this breakup resulting in the formation of a continuous edge gradient whose thinner portions require higher switching fields. Mechanical removal of the edges reduces the field value to approximately that of a pure film.

8748 CRITICAL FIELD CURVES OF MERCURY, TIN, AND INDIUM by D. E. Mapother, D. K. Finnemore and R. W. Shaw (U. Illinois); Bull. Am. Phys. Soc., Ser. II, Vol. 5, p. 163(A), Mar. 21, 1960

Deviations from the law of corresponding states of the BCS theory are readily observed in precise measurements of the critical field curve. Most superconductors (including Sn and In) show a critical field which falls below a parabola drawn through $H_0$ and $T_c$, in general agreement with BCS. However, measurements which show Hg to be similar to Pb in having a positive deviation from the parabolic relations were presented. Given a reliable value of $\nu$ (the temperature coefficient of the normal electronic specific heat), the critical field data permit a precise determination of the temperature dependence of $C_{es}$ (the superconducting electronic specific heat). The present work indicates an appreciable entropy contribution from the superconducting electrons at the lowest temperatures of observation (about 1.1°K), which makes the $\nu$ values uncertain. Thus significant comparisons of $C_{es}(T)$ for various elements by this method must await the extension of critical field measurements to temperatures well below 1°K.

8749 ENERGY GAP IN SUPERCONDUCTORS MEASURED BY ELECTRON TUNNELING by I. Giaever (GE); Phys. Rev. Lett., Vol. 5, pp. 147-148(L), Aug. 15, 1960

Measurements of the energy gaps of superconducting lead, tin, and indium are reported. The tunnel current between aluminum/aluminum oxide/lead sandwiches both when the lead was normal and when it was a superconductor. The ratio of the slope $dI/dV$ of a sandwich in which lead is a superconductor to one in which it is normal is plotted against the potential difference. Half the energy gap is given approximately by the point at which the relative slope $dI/dV = 1$. For lead the energy gap is $(4.2 \pm 0.1)\,kT_c$. Similar measurements in tin and indium indicate that the energy gap for these elements is about $4\,kT_c$.

Energy Gap of Superconducting Films - See 8853

8750 SURFACE IMPEDANCE OF SUPERCONDUCTORS by P. B. Miller (U. Illinois); Phys. Rev., Vol. 118, pp. 928-934, May 15, 1960

A detailed calculation of the surface impedance of superconductors based on the general theory of the anomalous skin effect in normal and superconducting metals given by Mattis and Bardeen is presented. It is found that there are large corrections to the extreme anomalous limit value of the superconducting to normal surface resistance ratio; corrections to the surface reactance ratio are much smaller. The theory is compared with recent experiments on the surface impedance of aluminum and of tin. It is found that the theory gives satisfactory agreement with experimental data on the surface impedance, both in absolute value and in its temperature and frequency dependence over a wide range of temperatures and frequencies.

8751 SURFACE IMPEDANCE OF A SUPERCONDUCTOR IN A MAGNETIC FIELD; THEORY by G. Dresselhaus and M. S. Dresselhaus (Cornell U.); Bull. Am. Phys. Soc., Ser. II, Vol. 5, p. 163(A), Mar. 21, 1960

A two-fluid model was used to calculate the quadratic term, i.e., $H^2$ term, in the variation of surface impedance with magnetic field. The superconducting electrons were assumed to satisfy the London equations while the normal electrons followed a nonlocal relation. Consideration was given to the two limiting cases of the classical and the extreme anomalous limit of the skin effect. Results were obtained in terms of the dimensionless parameter $\lambda/\delta n$ (static penetration depth/high frequency skin depth for normal electrons). Information on the band structure is implied, since for a given superconductor, experimental determination of $\lambda/\delta n$ yields a value for $m\nu_F$, in which m is the effective mass of the normal electrons in the superconducting state and $\nu_F$ is the Fermi velocity of these electrons.

8752 SURFACE IMPEDANCE OF A SUPERCONDUCTOR IN A MAGNETIC FIELD; EXPERIMENT by M. S. Dresselhaus and G. Dresselhaus (Cornell U.); Bull. Am. Phys. Soc., Ser. II, Vol. 5, p. 163(A), Mar. 21, 1960

Experimental data on tin at 1000 Mc/sec was compared with the two-fluid calculation of the magnetic field variation of the surface impedance. The Gorter-Casimir model was assumed for the normal electron concentration. The results in both longitudinal and transverse static magnetic fields imply that carriers of very small mass ($m/m \approx 10^{-3}$) are involved in the conduction processes in superconductors. A band structure for normal electrons in superconducting tin was proposed.

8753 ANALYSIS OF EXPERIMENTAL DATA RELATING TO THE SURFACE IMPEDANCE OF SUPERCONDUCTORS by A. A. Abrikosov, L. P. Gor'kov and I. M. Khalatnikov (Inst. Phys. Problems); Soviet Phys.-JETP, Vol. 10, pp. 132-134, Jan. 1960

The results of experimental measurement of the surface impedance of superconductors at various frequencies are compared with a new theory of superconductivity. Satisfactory agreement with the experiments has been found for all frequencies excluding the very lowest ones. At low frequencies the experimental values for the real part of the impedance near the critical temperature are several times larger than the theoretical values.

8754 USE OF SUPERCONDUCTING TRANSMISSION LINE FOR MEASURING PENETRATION DEPTHS by D. R. Young, J. C. Swihart, S. Tansal and N. H. Meyers (IBM); Bull. Am. Phys. Soc., Ser. II, Vol. 5, p. 163(A), Mar. 21, 1960

The penetration of the magnetic field into a superconducting film increases the inductance per unit length of a transmission line utilizing these films as conductors. This effect is large if the line is properly designed. Measurements of the velocity of propagation in a line of this type can therefore be used to determine the penetration depth. Preliminary measurements have been made using a pulse technique. The experiment is being modified to use a resonant technique to increase the accuracy of the results and to permit studies of the effect of a magnetic field on the penetration depth. Solutions of London's equations for a film thickness comparable to the penetration depth were presented.

Far Infrared Transmission Through Superconducting Films - See 8853

8755 MEASUREMENT OF THE UPPER LIMIT OF RESISTIVITY OF SUPERCONDUCTING LEAD by A. F. Hildebrandt and D. D. Elleman (CIT); Bull. Am. Phys. Soc., Ser. II, Vol. 5, p. 111(A), Mar. 4, 1960

Measurement by means of a nuclear magnetic resonance probe of the magnetic fields trapped in a superconducting lead cylindrical shell as a function of time was reported. A trapped field of 125 gauss was found to have variations of less than 4 milligauss over a period of 18 hr. By using these data, it was calculated that the resistivity of superconducting lead is less than $8 \times 10^{-25}$ ohm-m. The previous upper limit was given as $10^{-22}$ ohm-m by Grassmann. Measurements of the configuration of the magnetic field were discussed.

8756 ISOTOPE EFFECT IN SUPERCONDUCTING LEAD by R. W. Shaw, D. E. Mapother and D. C. Hopkins (U. Illinois); Bull. Am. Phys. Soc., Ser. II, Vol. 5, pp. 163-164(A), Mar. 21, 1960

Measurements of the isotope effect in Pb in the range from $T_c$ to 1.1°K were reported. Near $T_c$, the data follow the mass dependence, $T_c \propto M^p$, where $p = -0.457 \pm 0.024$. This value is about nine per cent lower than that previously reported, and the difference is believed due to a uniform improvement in the chemical purity of all specimens. An exponent of −0.475 for Pb has been calculated theoretically. Two specimens of nearly equal average mass but with drastically different mass distributions were found to exhibit nearly identical critical field curves over the entire temperature range. In these measurements only the similarity principle remains anomalous. Of seven specimens measured, five show good approximations to similarity in their critical field curves. The remaining two, while similar to each other, disagree with the rest.

Nuclear Spin Relaxation in Superconducting Al - See 8843

Thermal Conductivity of Superconducting Ga - See 8917

8757 SUPERCONDUCTIVITY OF BERYLLIUM AND ITS LOW-TEMPERATURE POLYMORPHISM by B. G. Lazarev, A. I. Sudovtsev and E. E. Semenenko (Physico-Tech. Inst.); Soviet Phys.-JETP, Vol. 10, pp. 1035-1036(L), May 1960

An investigation of the superconducting transition temperature and of the temperature dependence of the resistivity of Be films formed by evaporation on a substrate at liquid He temperature is discussed. Films 400 to 2500 A thick were found to become superconducting over the temperature region 7° to 9°K. The temperature dependence of the resistance was studied up to 400°K. All films showed a superconducting modification up to 20° - 30°K. Films heated to this temperature became superconducting again when recooled. Films which were heated to about 60°K showed an incomplete superconducting transition when subsequently cooled. Those heated above 60°K showed no superconductivity when later cooled. When the heating time was increased, the limiting temperature decreased.

8758 SUPERCONDUCTIVITY OF SIGMA AND ALPHA MANGANESE STRUCTURES by R. D. Blaugher and J. K. Hulm (Westinghouse Res. Labs.); Bull. Am. Phys. Soc., Ser. II, Vol. 5, p. 163(A), Mar. 21, 1960

The sigma and alpha manganese structures formed by binary alloys between group (V, Nb, Ta, Cr, Mo, W) and the group

(Mn, Fe, Co, Ni, Ru, Rh, Pd, Re, Os, Ir, Pt) were investigated for superconductivity down to 1°K. Nineteen new superconductors were found in these two systems with the majority occurring in the sigma phase. A plot of superconducting transition temperature of the sigma phases against the average number of valence electrons per atom exhibited a maximum at approximately $6\frac{1}{2}$ electrons per atom. This maximum is similar to those found for other structures by Matthias; however, it is displaced somewhat from the vicinity of 5 or 7 electrons per atom which Matthias indicated to be characteristic of other systems. The sigma phase data therefore suggests that in compound formation between pairs of transition elements, the d-band shape is preserved to some extent and is filled at an intermediate level by the available electrons.

## MAGNETOELECTRIC (GALVANOMAGNETIC) PROPERTIES

8759 GALVANOMAGNETIC EFFECTS IN THREE-BAND SEMICONDUCTORS – EXPERIMENTS WITH P-TYPE InSb by G. Fischer (U. Neuchatel); Helv. Phys. Acta, Vol. 33, No. 5, pp. 463-488, 1960

Measurements of the resistivity and Hall coefficient of p-type single crystal InSb as a function of magnetic field strength and temperature are reported. The ranges covered extend to ±8 koe and from 78° to 300°K. Equations are derived for the Hall effect and the magnetoresistance which are applicable to isotropic semiconductors containing an arbitrary number of non-interacting degenerate bands, and valid for any magnetic field strength. In particular a three-band model is discussed in detail and formulae are given by which it is possible to derive values for the density and mobility of the various charge carriers from the dependence of the Hall coefficient and resistivity on the magnetic field. This model appears valid for p-type InSb in the extrinsic range. It predicts the presence of two kinds of holes with highly different mobilities. In the intrinsic range the model fails by giving a negative concentration of high mobility holes. An alternative model consisting of only one band, but taking various scattering mechanisms into account, is found to be equally good at low temperatures, but also inadequate in the intrinsic range. The failure of these two models at high temperatures supports Ehrenreich's theory of predominantly polar scattering between 200° and 500°K.

Galvanomagnetic Effects in InSb - See 8933

8760 GALVANOMAGNETIC EFFECTS IN INDIUM ARSENIDE AND THEIR APPLICATIONS by R. P. Chasmar and E. Cohen (Metropolitan-Vickers); Solid State Phys. in Electronics and Telecommun., Vol. 2, Academic Press, 1960, pp. 659-670

Galvanomagnetic effects in InAs are discussed. The temperature invariance of the extrinsic Hall coefficient and the high electron mobility in InAs make this material particularly suitable for Hall effect devices. The Hall voltage produced across an InAs Hall plate in open circuit operation is shown to be a linear function of the plate current and the magnetic field. The efficiency of a Hall plate working into a matched load is discussed. Responsivity (the Hall voltage output in millivolts per unit plate current in mA and unit magnetic field in kilogauss) and a dissipation constant are defined as figures of merit for Hall plates. A simple linear Hall multiplier for use in analog computers and experimental multipliers using InAs Hall plates mounted in a gap in a ferrite core are described. The transverse magnetoresistance effect in InAs and its applications are discussed in detail.

8761 ANISOTROPIC HALL COEFFICIENTS IN N-TYPE GERMANIUM by H. Miyazawa and H. Maeda (Matsuda Res. Lab.); J. Phys. Soc. Japan, Vol. 15, pp. 1924-1939, Nov. 1960

Precise measurements of the Hall effect made at 77°, 90°, 195°, and 298°K up to 11,000 gauss on oriented single crystals of n-type germanium containing $5 \times 10^{14}$ antimony per $cm^3$ as donor centers are reported. The results principally indicate the variations of $\mu_H/\mu$ with the magnetic field and with the temperature, since the carrier concentration is practically constant under the experimental conditions. Absolute values of $\mu_H/\mu$ have been deduced from $R_\infty$ and $R_0$. $R_\infty$, for which $\mu_H/\mu$ always equals unity, is obtained by extrapolating $R_H^{<001>}$ (77°K) vs $1/H^2$ data. Then $R_H^{<001>}/R_\infty$ gives $\mu_H/\mu \cdot <001>_H$. On the other hand, $\mu_H/\mu$ for other orientations may be indirectly estimated from their extrapolated $R_0$ for which $\mu_H/\mu$ is independent of the orientation and should be equal to $R_0^{<001>}/R_\infty$ at corresponding temperatures, neglecting the effect due to slightly different impurity concentration between specimens. Values of $\mu_H/\mu$ thus determined are always smaller than unity, while those of $<001>_H$ approach unity most rapidly with increasing field and those of $<110>_H$ most slowly. They are of course temperature dependent and the zero magnetic field values are equal to 0.83 at 77°K, 0.84 at 90°K, 0.90 at 195°K and 0.92 at 298°K respectively. Numerical evaluation of the Boltzmann's equation taking account of ellipsoid model and mixed scatterings can give the observed values fairly well. It appears, however, preferable to introduce some correction term, e.g., a reasonable amount of optical phonon scattering, for the best agreement.

Hall Effect in a Thin Crystal - See 8728

8762 EFFECTS OF Si IN GaAs by J. M. Whelan, J. D. Struthers and J. A. Ditzenberger (Bell Labs.); Bull. Am. Phys. Soc., Ser. II, Vol. 5, p. 152(A), Mar. 21, 1960

The negative Hall coefficient of Si doped GaAs grown from the melt is inversely proportional to the Si content for concentrations less than $1 \times 10^{18}$ atoms $cm^{-3}$. For Si concentrations between 0.6 and $3 \times 10^{19}$ atoms $cm^{-3}$, the Hall coefficient is essentially independent of concentration although the solubility of Si in GaAs has been reported to be $1 - 2 \times 10^{20}$ atoms $cm^{-3}$. Si atoms located on Ga or As lattice sites act as either donors or acceptors, respectively. The preceding data are consistent with the fraction of total Si on either lattice site varying as a function of the Fermi level, as proposed by Longini and Greene for an amphoteric impurity. The applicability of this model is further supported by Hall data for GaAs specimens containing Si and either normal donor or acceptor impurities.

Hall Effect in Grey Tin - See 8586

Hall Constant and Magnetoresistance of Bi - See 8727

Photoelectric Analysis of Hall Constants in CdS Type Crystals - See 8591

8763 HALL EFFECT IN FERRITES NEAR THE CURIE POINT by K. P. Belov and E. P. Svirina (Moscow State U.); Soviet Phys.-JETP, Vol. 10, pp. 862-865, May 1960

Measurements of the Hall EMF in single crystal and polycrystalline nickel-zinc and manganese ferrites in the vicinity of the Curie temperature are reported. A new method for determining the ordinary Hall constant is described. The calculated values of the carrier density and mobility in the investigated ferrites agree in order of magnitude with the values obtained for non-ferromagnetic semiconductors. The Hall EMF is one order of magnitude greater in a single crystal specimen of manganese ferrite than in a polycrystalline specimen.

8764 ON THE ELECTRICAL AND OPTICAL PROPERTIES OF P-TYPE CADMIUM TELLURIDE CRYSTALS by S. Hamada (Shizuoka U.); J. Phys. Soc. Japan, Vol. 15, pp. 1940-1944, Nov. 1960

Measurements of the electrical and optical properties of p-type synthetic CdTe single crystals are reported. The Hall coefficients of the crystals were increased by heat treatment or growth in cadmium vapor. From these measurements it is shown that the intrinsic energy gap is about 1.43 ev, the ionization energy of acceptors is about 0.20 ev and the Hall mobility of holes is about 80 $cm^2$/volt-sec at room temperature. It seems that the data of Hall mobilities are in agreement with the theory of interaction with the optical mode of lattice vibrations.

8765 MAGNETORESISTANCE IN GALLIUM ARSENIDE by R. K. Willardson and J. J. Duga (Battelle); Proc. Phys. Soc., Vol. 75, pp. 280-290, Feb. 1960

The transverse magnetoresistance in n-type gallium arsenide as a function of impurity concentration and density of defects introduced by fast neutron irradiation is discussed. The data are consistent with theoretical predictions based on mixed scattering and a spherical energy surface model. The change in the magnetoresistance with fast neutron bombardment suggests the introduction of levels other than the deep-lying ones revealed by changes in the carrier concentration and that some of these levels may be multiply ionized.

8766 MAGNETORESISTIVE EFFECTS IN INDIUM ANTIMONIDE AND INDIUM ARSENIDE by H. P. R. Frederikse and W. R. Hosler (NBS); Solid State Phys. in Electronics and Telecommun., Vol. 2, Academic Press, 1960, pp. 651-658

Magnetoresistive effects in InSb and InAs are discussed. The Wilson-Sommerfeld formula governing the relative change of resistance as a function of electron mobility and magnetic field strength is given. The effects of (1) more than one type of carrier; (2) the scattering mechanism; (3) the degree of degeneracy; (4) anisotropic energy surfaces; (5) geometry; (6) high magnetic fields (quantum effects, "freeze-out"); (7) high electric fields ("breakdown"); and (8) temperature on the magnetoresistance are considered. Measurements of the magnetoresistance at 300°K, at 78°K, and at liquid helium temperatures are reported.

8767 MAGNETO-RESISTANCE EFFECT IN CADMIUM SULPHIDE by Y. Suge, S. Tanaka and T. Masumi (U. Tokyo); Solid State Phys. in Electronics and Telecommun., Vol. 2, Academic Press, 1960, pp. 872-879

Measurements of the magnetoresistance effect at several temperatures in impurity-doped hexagonal CdS single crystals, made as a function of the directions of the electric and magnetic fields with respect to the crystal axes, are discussed. Conducting flakes or blocks of CdS single crystals doped with Ga or Cl or with excess Cd were used as samples. The angular dependence of the magnetoresistance effects is given. The temperature dependence of the transverse magnetoresistance effect for different field directions is used to study scattering processes. Experimental results suggest the existence of anisotropic energy surface and scattering mechanisms.

Magnetoresistance of:
Grey Tin - See 8586
InSb - See 8897

8768 CYCLOTRON RESONANCE IN ZnSb AND CdSb by M. J. Stevenson (IBM); Bull. Am. Phys. Soc., Ser. II, Vol. 5, p. 117(A), Mar. 21, 1960

Observations of cyclotron resonance absorption in single crystals of the II-V intermetallic semiconductors ZnSb and CdSb were reported. Several p-type ZnSb crystals were pulled in a sealed tube from a melt of zinc and antimony of 99.999+ per cent purity. A single cyclotron resonance absorption line was observed at magnetic fields corresponding to an effective mass $m = 0.15 m_0$. The effective mass was almost isotropic in the three crystal planes with small anisotropy observed in the planes containing the b axis. The resonance can be interpreted in terms of an almost spherical energy surface for either the conduction or the valence band, depending on whether the resonance is associated with electrons or holes, respectively. The line width of the resonance revealed a very critical dependence on the crystal growth pattern, with the best resonance lines given by the relaxation time $\tau = 1.2 \times 10^{-11}$ sec. A single cyclotron resonance absorption line was also observed in p-type CdSb pulled from a melt of 99.999+ per cent pure triply distilled cadmium and 99.999+ per cent pure antimony. The resonance corresponded to an effective mass $m = 0.15 m_0$, the same value as for ZnSb. The resonance was almost isotropic as would be the case for a spherical energy surface. Very slight anisotropy was observed in planes containing the b crystal direction. The relaxation time $\tau$ was $1.5 \times 10^{-11}$ sec for the best resonances obtained.

8769 NEGATIVE EFFECTIVE MASS CYCLOTRON RESONANCE EXPERIMENTS by R. N. Dexter, D. Hensler, E. Hollar and M. Halloran (U. Wisconsin); Bull. Am. Phys. Soc., Ser. II, Vol. 5, p. 177(A), Mar. 21, 1960

Experiments at liquid helium temperatures which have been performed on germanium and silicon at 24 Kmc in unsuccessful attempts to confirm the work of Dousmanis which indicated emission due to negative effective mass heavy holes in germanium were described. No positive evidence of emission in several p-type samples was found using linearly or circularly polarized microwaves and wide ranges of microwave power and

light intensity and temperature variation between 1.3° and 5°K. There was extra absorption near breakdown which might correspond to absorption by negative mass carriers. For a [100]-directed magnetic field, the third-harmonic resonance of the heavy holes in germanium always absorbed energy resonantly under circular polarization conditions appropriate for electron resonance; the fifth-harmonic resonance of the heavy holes behaved like the light and heavy holes, however. The identification of the third-harmonic resonance as a hole resonance was confirmed by observing the effects of impact-ionization breakdown and carrier density augmentation as well as by resonance-field measurements.

8770 SPIN RESONANCE OF Ni, Pd, AND Pt IN SILICON by H. H. Woodbury and G. W. Ludwig (GE Res. Labs.); Bull. Am. Phys. Soc., Ser. II, Vol. 5, p. 158(A), Mar. 21, 1960

Spin resonance of some transition metal impurities ($V^{++}$, $Cr^{+}$, $Mn^{-}$, $Mn^{++}$, and $Fe^{0}$) in Si has been reported. Ni, Pd, and Pt impurity atoms in Si have also been found to be electrically active and, if properly compensated, each will show resonant absorption. Unlike the transition metal impurities, the resonance patterns of the Ni-group impurities must be described by an anisotropic g-tensor because of spontaneous distortions from the normal symmetrical lattice positions. Pd and Pt appear to be substitutional acceptors while Ni is an interstitial donor. The spectrum of $Pd^{-}$ in Si is similar to that of $Ni^{-}$ in Ge, with $g_1 = 1.919$, $g_2 = 2.059$, and $g_3 = 1.972$. Two different spectra due to $Pt^{-}$ have been seen; the one of present interest shows considerable anisotropy, the principal g-values being 1.427, 2.079, and 1.387. $Ni^{+}$ in Si is interesting in that only below 4°K does the distortion become fixed in the crystal; above this temperature a single isotropic line is observed because of motional averaging.

8771 SPIN RESONANCE OF $Mn^{++}$ IN CdTe by J. Lambe (Ford) and C. Kikuchi (U. Michigan); Bull. Am. Phys. Soc., Ser. II, Vol. 5, p. 158(A), Mar. 21, 1960

Following the suggestion by Dorain, single crystals of CdTe containing 0.01 per cent $Mn^{++}$ have been investigated in an X band ESR spectrometer at 300°, 78°, and 4.2°K. At room temperature, only the 6 broad Mn-55 hfs lines are observed. At 78°K, the lines narrow, the fine structure components are resolved and at 4.2°K, the principal hfs lines split into a number of superhyperfine structure components due to Cd nuclei. The cubic zero field splitting, 3a, for CdTe is 0.0084 $cm^{-1}$, compared to 0.00233 $cm^{-1}$ for ZnS, despite the fact that the anion-cation distances in CdTe and ZnS are 2.78 and 2.36 A, respectively. The g value shift is positive. The superhyperfine component spacing is 1.4 gauss, equal to that in CdS. The broadening of the lines at 300°K in CdTe is due to spin lattice interaction indicating a $T_1$ of about $10^{-8}$ sec, which is much shorter than is observed only when a fairly high number of conduction electrons are present. This effect is then due to an interaction between conduction electrons and $Mn^{++}$.

8772 SPIN RESONANCE OF CHARGE CARRIERS IN GRAPHITE by G. Wagoner (Natl. Carbon); Phys. Rev., Vol. 118, pp. 647-653, May 1, 1960

Observations of the electron spin resonance in perfect single crystals of graphite which clearly establish that the resonance arises from mobile charge carriers are reported. The line shape is of the Dysonian form which is characteristic of conduction electron spin resonance in metals. The intensity of the spin resonance agrees, both in absolute magnitude and in temperature dependence, with values calculated from the band model of graphite by McClure. The g value of the resonance shows a remarkably large anisotropy which depends strongly on temperature and on the position of the Fermi level with respect to the band edge. At room temperature in pure graphite, g varies from 0.0026 ± 0.0002 to 2.0495 ± 0.0002 as the magnetic field is shifted from perpendicular to parallel to the c axis. The g-value anisotropy increases with decreasing temperature; $g_{\parallel}$ becomes 2.127 at 77°K while $g_{\perp}$ remains constant. The line width of the resonance is a few gauss ($T_2 = 2.0 \times 10^{-8}$ sec) which is extremely narrow in comparison with the field shifts caused by changes of anisotropy with temperature. This indicates that for conduction states in graphite, the g value is a strong function of the wave vector and that the line is narrowed by an averaging process in k-space. This averaging is similar to that which occurs in motional and exchange narrowing.

## OTHER ELECTRICAL PROPERTIES

8773 FIELD EFFECT AT HIGH FREQUENCY by F. Berz (Mullard Res. Labs.); Solid State Phys. in Electronics and Telecommun., Vol. 1, Academic Press, 1960, pp. 380-388

The theory of the field effect at high frequencies in semiconductors is developed. The variation of surface charges with an impressed ac voltage, the variation of densities in the bulk, and the modulation of the conductivity are treated and an effective field effect mobility is defined. The theory is used to work out a numerical example from which the variation with frequency of the electron and hole charges induced in the front surface layer, the variation with frequency of the total electron charge induced in the bulk, and the variation with frequency of the field effect mobility are obtained.

8774 RECENT ADVANCES IN THE UNDERSTANDING OF SEMICONDUCTOR SURFACE PROPERTIES by H. Statz and G. A. Demars (Raytheon); Solid State Phys. in Electronics and Telecommun., Vol. 1, Academic Press, 1960, pp. 587-596

The effects of thick adsorbed layers of water vapor and vapors of acetone, methyl alcohol, pyridine, dioxane, and other liquids on semiconductor surface properties are discussed. These vapors produce outer surface states with a net positive charge. It is shown that in the case of a sufficiently thick adsorbed film the charge in the outer surface states is mobile. This finite mobility gives rise to diode characteristics which are markedly different in the reverse direction from those found on diodes with regular inversion layers. All experiments were carried out with n-p-n, grown junction Si bars. Similar effects are observed with Ge samples and the vapors of the above-mentioned liquids.

Temperature Dependence of the Thermionic Emission of Si - See 8664

## MAGNETIC PROPERTIES

### GENERAL

8775 MEASUREMENT OF MAGNETOSTRICTION WITHIN THE TEMPERATURE RANGE -196° TO +400°C by R.R. Birss (Imperial Coll. Sci. and Tech.) and E.W. Lee (U. Sheffield); J. Sci. Instr., Vol. 37, pp. 225-230, July 1960

An apparatus which permits the magnetostrictive constants of small single crystal or polycrystalline ferromagnetic specimens to be measured over the temperature range -196° to +400°C is described. Resistance strain gauges are employed and the performance of a number of gauges has been investigated at these temperatures. Details of the techniques used to obtain a reliable overall strain sensitivity of $2 \times 10^{-7}$ per mm deflection of the indicating galvanometer are given. The procedure by which the single crystal magnetostriction constants may be obtained from strain measurements at saturation is outlined for the case of a disk-shaped crystal in which the plane of the disk is normal to one of the three principal crystallographic directions.

Method of Measuring Magnetostriction - See 8809

8776 THE MAGNETOSTRICTION OF LITHIUM-CHROMIUM FERRITE IN THE NEIGHBORHOOD OF ITS COMPENSATION POINT by E.W. Lee and R.R. Birss (Nottingham U.); Proc. Phys. Soc., Vol. 76, pp. 411-412, Sept. 1960

Measurements of the magnetostriction of lithium-chromium ferrite ($Li_{0.5}Fe_{0.8}Cr_{1.7}O_4$) as a function of temperature on both sides of its compensation point (20°C) are reported. The measurements were made by observing the strain in a polycrystalline disc as it was rotated in a saturating field of 5000 oersteds. No anomalous behavior was observed at the compensation point and the magnetostriction was found to be essentially the same in both the antiferromagnetic and ferrimagnetic states. It is therefore concluded that the magnetostriction is determined by the magnetic moment of the individual sublattices and not by the net moment.

8777 THE TEMPERATURE DEPENDENCE OF MAGNETOSTRICTION IN POLYCRYSTALLINE GADOLINIUM by W.D. Corner and F. Hutchison (U. Durham); Proc. Phys. Soc., Vol. 75, pp. 781-788, May 1960

Measurements of the magnetostriction and magnetization of an ellipsoid of polycrystalline gadolinium in the temperature range 78° to 365°K are given. The results show that gadolinium has a large volume magnetostriction which is proportional to the square of the paramagnetic magnetization above the Curie point. The saturation magnetostriction shows an anomaly at 150°K and becomes zero at 233°K. The contribution of the volume magnetostriction to the thermal expansion of gadolinium is shown to be too small to account for the thermal expansion anomaly.

8778 LONG RANGE INTERACTIONS BETWEEN MAGNETIC MOMENTS IN SEMICONDUCTORS by W. Baltensperger and A.M. de Graaf (ETH, Zürich); Helv. Phys. Acta, Vol. 33, pp. 881-888, 1960

The interaction between magnetic moments embedded in a non-degenerate electron gas is calculated. In the fully degenerate gas the Ruderman, Kittel interaction applies whereas in the Boltzmann gas the interaction is ferromagnetic only and of comparatively long range. Between these extreme cases the behavior changes gradually. In a semiconductor an additional interaction comes from the virtual excitations of the valence band. These two interactions and the magnetic dipole interaction may be of comparable magnitude in dilute magnetic semiconducting alloys.

### FERRO- AND FERRIMAGNETISM

8779 NEW SOLUTION OF THE ISING PROBLEM FOR A RECTANGULAR LATTICE by C.A. Hurst and H.S. Green (U. Adelaide); J. Chem. Phys., Vol. 33, pp. 1059-1062, Oct. 1960

A new solution of the Ising problem for a rectangular lattice is derived from first principles. The solution, which is obtained algebraically, can be presented in a determinantal form different from though related to that found by Kac and Ward. By connecting the algebraic approach with the combinatorial solution, the latter is freed from dependence on topological conjectures. The new solution is considered to be fundamentally simpler than the others.

8780 RETARDING AND ADVANCING GREEN'S FUNCTION IN THE QUANTUM THEORY OF AN ISOTROPIC FERROMAGNET [in Russion] by Pu. Fu-Chouh, S.V. Tiablikov, and T. Shiklosh (Steklov Math. Inst. AN USSR, Joint Inst. Nuc. Res.); Acta Phys., Vol. 11, pp. 323-331, 1960

Retarding and advancing Green's functions for the computation of the fundamental theoretical characteristics of an isotropic ferromagnet are presented. Results have been obtained for the magnetization by this method which are suitable for the whole temperature range. In contrast to other works, a known orientation of the resultant magnetization relative to the direction of the external magnetic field is not assumed in advance which affords the possibility of investigating more complex problems in the theory of magnetism.

8781 EXCITATION OF SPIN WAVES IN FERROMAGNETS: EDDY CURRENT AND BOUNDARY CONDITION EFFECTS by P. Pincus (U. California); Phys. Rev., Vol. 118, pp. 658-665, May 1, 1960

The boundary condition for the transverse magnetization when there is a surface anisotropy field $H_s$ is derived. Writing the transverse magnetization as $a \sin kz + \beta \cos kz$ gives

$$\frac{a}{\beta} = -\frac{1}{2} ka + \left(\frac{H_s}{H_e ak}\right),$$

where $H_e$ is the exchange field and a the lattice constant. A similar result is found when there is an antiferromagnetic surface layer. For $H_s \neq 0$ spin-wave modes can be excited by a uniform RF field in a ferromagnet. The power absorbed in each mode in an insulator is calculated as a function of the surface anisotropy field. The excitation of the exchange modes is calculated for a metal with eddy-current damping. The eddy currents are found to have a large effect only on long wavelength spin waves. The line shape in a thick metal plate is calculated for $H_0$ normal to the plate.

8782 THEORY OF THE MAGNETIZATION CURVE OF A HEISENBERG FERROMAGNET by R. Brout and H. Haken (Cornell U.); Bull. Am. Phys. Soc., Ser. II, Vol. 5, p. 148(A), Mar. 21, 1960

A consistent approximate theory of the Heisenberg ferromagnet ($V = \Sigma v_{ij} S_i S_j$) which is a good high-density approximation and which passes continuously from the low temperature spin-wave region to the high temperature "classical" or Curie-Weiss region was formulated. This was done in the random-phase approximation as supplemented by the separate spherical-ization of the transverse and longitudinal sum rules. The result leads to a temperature-dependent spin-wave spectrum and a set of transverse excitations which are the usual spin waves at low T and become the classical spherical model normal modes at the Curie point. The longitudinal modes are always classical. For low T, the spin-wave spectrum is modified according to $\omega(q;T) = \omega(q;0)M(T)/M(0)$ where M(T) is the magnetization at temperature T.

8783 ROTATION OF THE PLANE OF POLARIZATION OF ELASTIC WAVES IN MAGNETICALLY POLARIZED MAGNETO-ELASTIC MEDIA by K.B. Vlasov and B. Kh. Ishmukhametov (Inst. Phys. Metals); Soviet Phys.-JETP, Vol. 10, pp. 531-534, Mar. 1960

Some peculiarities of the propagation of magnetoelastic waves in magnetically polarized media are discussed. A medium with uniaxial symmetry is considered. It is shown that a magnetoelastic wave propagated along the axis of symmetry consists of three waves, viz, a longitudinal wave and two circularly polarized waves whose speeds of propagation are different and are determined by the magnetic state of the medium. The treatment is based on phenomenological "equations of state" that describe the dynamic properties of magnetoelastic media. Some remarks are made regarding the physical meaning of the constants that determine the rotation of the plane of polarization in certain types of magnetoelastic media and the frequencies at which an appreciable effect is to be expected are estimated.

8784 NOTE ON PERTURBATION OF A UNIFORM MAGNETIC FIELD BY A CUBE OF MAGNETIC MATERIAL by F. Partovi (IBM); IBM J. Res. and Dev., Vol. 4, pp. 357-358(L), July 1960

The magnetic field around a rectangular parallelepiped of high permeability placed in a uniform magnetic field is derived and the theoretical results are compared with experimental measurements. The field about the parallelepiped, the volume of which is one-sixtieth of the volume in which the field might be considered uniform, was measured with a bismuth Hall probe the effective area of which is $10^4$ times smaller than one face of the parallelepiped. It was found that the theoretical derivation need not be carried beyond a first approximation.

8785 CRITICAL CONCENTRATION FOR THE EXISTENCE OF FERROMAGNETISM IN DILUTE ALLOYS by M. Coopersmith and R. Brout (Cornell U.); Bull. Am. Phys. Soc., Ser. II, Vol. 5, p. 148(A), Mar. 21, 1960

Estimates of the least concentration needed to support ferromagnetism in a dilute alloy of nearest neighbor exchange-coupled spins were reported. Diagrams have been summed so as to include all terms up to $0(x^5)$ for sc and bcc lattices, and up to $0(x^4)$ for fcc lattices. The following results were found for these three lattices, respectively: $x_0Z = 1.29, 1.39, 1.36$, where $x_0$ is the critical concentration and Z is the number of nearest neighbors. These results are in good accord with experiment.

8786 THEORY OF THE STABILITY OF MAGNETIC STATES OF FERROMAGNETIC MATERIALS IN THE MAGNETIZATION PROCESS by E.I. Kondorskii (Moscow State U.); Soviet Phys.-JETP, Vol. 10, pp. 790-793, Apr. 1960

The physical principles that determine the stability of magnetic states of a ferromagnetic single crystal with respect to external magnetic fields and to elastic forces are discussed. A formula for the minimum value of the magnetic fields and stresses at which the equilibrium of a domain wall passing near a magnetic inclusion is destroyed, and at which an irreversible change of magnetization occurs, is derived. An explanation for the strong magnetization of ferromagnets in weak magnetic fields by shocks or blows is given and formulas for estimating the irreversible changes of magnetization produced by elastic stresses are derived. An explanation for the observed stability, with respect to elastic forces, of magnetic states corresponding to the ideal magnetization curve is given.

8787 ULTRASONIC MEASUREMENT OF MAGNETIZATION IN Mn FERRITE SINGLE CRYSTAL by K. Husimi, K. Nishiguchi, and T. Suzuki (Elect. Commun. Lab., Tokyo); J. Phys. Soc. Japan, Vol. 15, p. 1341(L), July 1960

The use of the magnetostrictive output voltage of an ultrasonically excited ferrite crystal to measure the magnetic flux changes during switching in the ferrite is described. A block diagram of the measuring circuit is given and the experimental procedures are outlined. The relationship between the ultrasonic output voltage V and the magnetic flux density B is given approximately by $V \alpha B^{0.7}$.

8788 TEMPERATURE DEPENDENCE OF THE MAGNETOSTATIC PROPERTIES OF NICKEL-ZINC FERRITES [in Russian] by D.D. Mishin and L.D. Drobchenko (Ural U.); Izv. VUZ Fiz., No. 4, pp. 131-134, 1960

A magnetometric study of the temperature dependence of the magnetic susceptibility in the weak field region (initial permeability), the magnetization curve and the coercive force of two compositions of nickel-zinc ferrites in the -196° to 150°C temperature range is reported. The range of fields (in the initial section of the magnetization curve) in which the magnetization of ferrites is accomplished by reversible processes has been determined. The upper limit of this range is at about two-thirds the coercive force. A comparison of the theoretical temperature dependence obtained with the Kersten inclusion theory

$$\left( \mu_a(T) = C \frac{i_3^2(T)}{\sqrt{k(T)}} \right)$$

has shown that this theory cannot be used to determine the behavior of nickel-zinc ferrites. The temperature dependences of the magnetization and the coercive force curves of the ferrites investigated are qualitatively the same as for many metallic soft ferromagnets.

8789 LAW OF APPROACH TO SATURATION OF A SILICON IRON SINGLE CRYSTAL IN THE THREE PRINCIPAL DIRECTIONS [in Russian] by B.P. Khromov (Krasnoiarsk Polytech. Inst.); Izv. VUZ Fiz., No. 1, pp. 171-177, 1960

An experimental apparatus which permits the measurement of a differential susceptibility on the order of magnitude of $5 \cdot 10^{-4}$ in small size samples by an automatic photorecording method is described. It is shown that the law of approach to saturation for the [110] direction differs from the law of approach to saturation for the [100] and [111] directions. The coefficients of

magnetic rigidity are determined for the [100] and [111] direction; the magnitude of the susceptibility of the paraprocess is detected and measured.

8790 ANISOTROPY ENERGY AND REMANENT MAGNETIZATION OF A FROZEN BOLTZMANN DISTRIBUTION OF STONER-WOHLFARTH PARTICLES by F. West (Texas Instr.); Bull. Am. Phys. Soc., Ser. II, Vol. 5, p. 148(A), Mar. 21, 1960

When a specimen composed of N noninteracting ferromagnetic particles with anisotropy energy of the form $U = K \sin^2\theta$; e.g., Stoner-Wohlfarth particles, is quenched in the presence of a saturating magnetic field, the particles may be assumed to be frozen into a Boltzmann distribution. The bulk anisotropy energy E of such a distribution has been calculated and found to be of the uniaxial form $E(\phi, a) = A(a) + B(a) \sin^2\phi$; where $\phi$ is the angle between the quenching field direction (bulk anisotropy axis) and the saturation magnetization vector $M_s$;$a = K/kTo$;To is the temperature at which the distribution is frozen; and k is the Boltzmann constant. Expressions for A(a) and B(a) have been derived in terms of the tabulated function $y(x) = \exp(-x^2) \int_0^x \exp(t^2)dt$. Expressions for $m_{\parallel}(a)$ and $m_{\perp}(a)$, the remanent magnetizations parallel and normal to the anisotropy axis, as well as C(a), the magnetic specific heat of the distribution, have also been derived in terms of y(x). Accurately calculated curves for A(a), B(a), $m_{\parallel}(a)$, $m_{\perp}(a)$ and C(a) for the range $0.01 \leq a \leq 100$ were presented. Applications of some of these results to paramagnetic and superparamagnetic particles were also discussed.

8791 SUPEREXCHANGE INTERACTION IN FERRIMAGNETIC GARNETS AND SPINELS WHICH CONTAIN RANDOMLY INCOMPLETE LINKAGES by M.A. Gilleo (Lockheed); J. Phys. Chem. Solids, Vol. 13, pp. 33-39, May 1960

The variation of saturation moment, Curie temperature and susceptibility of ferrimagnetic compounds as a result of substitution of nonmagnetic ions for magnetic ions can be understood to good approximation on the basis of the random distribution of incomplete superexchange interactions. The two premises required for the understanding are that: (1) a magnetic ion actively participates in ferrimagnetism only if it interacts with two or more magnetic ions in different coordination and (2) the Curie temperature is determined by the number of complete interactions per active magnetic ion per formula unit. The requirement that a magnetic ion interact with at least two other magnetic ions in different coordination is implicit in the fact that ferrimagnetism is a cooperative phenomenon. Recent X-ray diffraction and magnetic studies of the yttrium-iron-calcium-iron-tin garnet system have provided the first firm basis for this understanding.

8792 DEMAGNETIZATION OF A FERRITE MEDIUM IN A MICROWAVE FIELD AT A LARGE SIGNAL LEVEL [in Russian] by K.P. Ivanov (Moscow Power Inst.); Izv. VUZ, Radiotek., Vol. 3, pp. 652-654, 1960

The use of the Bloch equation, neglecting the anisotropy fields of a crystal lattice, in the investigation of an infinite ferrite medium subjected to the effect of microwaves of a magnetic field, $h_o \cos \omega t$, directed along the Oy axis and a permanent field $H_o$ directed along the Oz axis which magnetizes the medium to saturation is discussed.

8793 APPLICATION OF A NÉEL-TANIGUCHI THEORY TO IRRADIATED MAGNETIC MATERIALS by A.I. Schindler and E.I. Salkovitz (U.S. Naval Res. Lab.); Bull. Am. Phys. Soc., Ser. II, Vol. 5, p. 189(A), Mar. 21, 1960

An investigation of neutron irradiation effects on the magnetic properties of iron-nickel alloys is described. All the results can be explained within the framework of the Néel-Taniguchi theory relating magnetic properties to directional ordering. If samples are irradiated for two weeks, short range directional order results, and the resulting hysteresis loops clearly show the domain distribution present during the irradiation. For samples irradiated with a saturating dc field present, the domains are aligned and rectangular hysteresis loops result. If no field is present during the irradiation, constricted hysteresis loops result but the amount of the constriction depends on the amount of domain alignment prior to irradiation. The differences are most evident for rectangular hysteresis loop material. If longer times of irradiation are employed, long range order appears to result which impedes the directional short range ordering and unconstricted but modified loops result.

8794 ON THE THEORY OF THE TEMPERATURE DEPENDENCE OF FERROMAGNETIC ANISOTROPY by E.A. Turov and A.I. Mitsek (Inst. Metal Phys.); Soviet Phys.-JETP, Vol. 10, pp. 801-805, Apr. 1960

The phenomenological spin wave theory is used to evaluate the temperature dependence of the magnetic anisotropy free energy in ferromagnets at low temperatures. It is shown that if the usual expressions for this free energy are used, the temperature dependence of the anisotropy constant of the $n^{th}$ order may depend substantially on the magnitude of the ratio at 0°K of the constants subsequent to the one given. The mixing of anisotropy constants of different orders in the equations for their temperature dependence disappears only when the anisotropy energy is written in the form of an expansion in homogeneous harmonic polynomials. It is found that at low temperatures the temperature dependence of the anisotropy constants derived theoretically by Zener is only approximately valid.

8795 THE INDUCED MAGNETIC ANISOTROPY IN EVAPORATED FILMS OF NICKEL-IRON ALLOYS by M. Prutton and E.M. Bradley (Intl. Computer and Tabulators); Proc. Phys. Soc., Vol. 75, pp. 557-574, Apr. 1960

The theories of the magnetic anisotropy of polycrystalline nickel-iron films in the permalloy region of composition are briefly reviewed and a simple model for the magnetic anisotropy which can be induced in such films during evaporation is described. The model includes the sum of the effects of iron-pair directional ordering and a constant linear stress lying along the annealing field. After a detailed description of the experimental technique used to prepare NiFe films about 1500 A thick in the region of composition 80 - 85 per cent nickel, the results of observations of the hysteresis loops measured at 400 cps are used to derive values of the anisotropy field $H_k$. These are then compared with values expected from the simple model. The experimental observation that increasing the substrate temperature moves the minimum in anisotropy energy to lower nickel content in the film is supported by the simple model. When the complicating effects of fiber growth are included, the main features of the observations are found to agree quite well with the model but the behavior of the induced anisotropy is shown to be complex and the possibility of contributions due to imperfection ordering is considered.

796 OBLIQUE-INCIDENCE ANISOTROPY IN EVAPORATED PERMALLOY FILMS by D.O. Smith, M.S. Cohen, and G.P. Weiss (Lincoln Lab.); J. Appl. Phys., Vol. 31, pp. 1755-1762, Oct. 1960

Magnetic anisotropy observed in evaporated Permalloy films deposited at oblique incidence of the vapor is discussed. Electron micrographs of such films reveal chains of crystallites whose long axes are oriented perpendicular to the vapor beam. A "self-shadowing" model is proposed to explain chain growth, i.e., the area behind a crystallite is left vacant because it is in the crystallite's shadow. Oriented crystallite chains are thus caused by a purely geometric process; their existence has also been demonstrated for Au, Pt, W, and Mg. Oriented chains give rise to a number of macroscopic effects: magnetic anisotropy, anisotropic resistance, dichroism, and anisotropic resonance linewidth. Experiments involving the stripping of oblique-incidence Permalloy films from their substrates indicate the presence of an anisotropic strain which, in conjunction with magnetostriction, gives another contribution to the magnetic anisotropy; this contribution explains the observed compositional dependence of the magnetic anisotropy. Surface tension, which tends to contract the crystallite chains, is postulated as the generating force of anisotropic strain; surface tension could similarly generate the isotropic strain which is found in normal-incidence films.

8797 "SPONTANEOUS MAGNETIC ANISOTROPY" IN POLYCRYSTALLINE THIN FILMS by W. Andrä, Z. Malek, W. Schüppel, and O. Stemme (Inst. Magnetic Materials, Jena, and Inst. Phys., Prague); J. Appl. Phys., Vol. 31, pp. 442-443(L), Feb. 1960

Measurements of the uniaxial magnetic anisotropy constant $K^*$ performed on evaporated and electrolytically-deposited nickel and permalloy films are reported. Nickel films electrolytically deposited under the same conditions but in different external magnetic fields had values of $K^* = K_1^* = (2.8 \pm 0.4) \times 10^3$ erg $cm^{-3}$. Evaporated permalloy and electrolytically-deposited nickel films shielded magnetically while being produced or shielded and rotating about an axis perpendicular to the surface while being produced had $K^*$ values smaller, but not an order of magnitude smaller, than $K_1^*$. Films rotated in a strong external magnetic field during production exhibited $K^*$ values an order of magnitude smaller than $K_1^*$. The application at room temperature of a magnetic field either parallel or perpendicular to the original axis (parallel to the film plane) of an electrolytically deposited nickel film caused $K^*$ to increase or decrease, respectively, in time. These observations can be explained by the formation of an easy axis parallel to the direction of spontaneous magnetization in each domain during and after film production.

8798 FLUX REVERSAL IN SOFT FERROMAGNETICS by E.M. Gyorgy (Bell Labs.); J. Appl. Phys., Suppl. to Vol. 31, pp. 110S-117S, May 1960

Many aspects of flux reversal in soft ferromagnetic materials may be interpreted in terms of three types of flux reversal processes: domain wall motion, nonuniform rotation, and uniform rotation. It has been shown that in general wall motion is the predominant mechanism for values of the applied magnetic field slightly in excess of the coercive field, that nonuniform rotation predominates for intermediate magnetic fields, and that uniform rotation predominates for large fields. The salient features of these three types of flux reversal are discussed and compared with experimental findings. Special emphasis is given to polycrystalline, square-looped ferrites and thin Permalloy films. The importance of geometric effects is illustrated in a review of detailed models for the uniform and nonuniform rotational processes. Specific limitations of the existing models are discussed, and possibilities for future advances are briefly outlined.

8799 ON THE QUESTION OF DETERMINING THE DEGREE OF PERFECTION OF TEXTURE IN POLYCRYSTALLINE FERROMAGNETS [in Russian] by I.P. Kudriavtsev (Ural Polytech. Inst.); Izv. VUZ Fiz., No. 1, pp. 203-207, 1960

New data have been obtained confirming the statement expressed earlier that it is most convenient to use the dispersion of the angle between the projection of the crystallographic direction [100] of crystallites on a flat sheet and the rolling direction as criteria of the degree of perfection of the crystallographic texture of cold-rolled electrotechnical steel since it is associated very simply with the amplitudes of the harmonics of the curve of the magnetic moment of the sample being investigated.

8800 DEPENDENCE OF THE MAGNETIC STRUCTURE OF A COBALT CRYSTAL ON ITS SIZE by G.S. Kandaurova, Ya. S. Shur, and F.V. Maslennikova (Ural State U.); Soviet Phys.-JETP, Vol. 11, pp. 45-47, July 1960

Changes in magnetic structure observed on the basal plane of a cobalt single crystal by means of powder patterns as the crystal thickness is progressively decreased by mechanical grinding followed by electrolytic polishing from 515 to 90 μ are discussed. It was found that at small thicknesses (< 200 μ) the domain width is proportional to the square root of the crystal thickness.

8801 STATISTICAL DYNAMICS OF BOUNDARY MOTION by R. Kikuchi (Hughes); Ann. Phys., Vol. 11, pp. 328-337, Nov. 1960

The motion of a domain wall between two magnetic domains of the Ising model induced by an external magnetic field is investigated by means of a statistical dynamics technique. It is assumed that each magnetic spin has a finite kinetic probability for changing its sign per unit time and that the spin system is in thermal contact with a heat bath. The path probability g for the change of state of the system for a short time interval is written in terms of a set of path parameters using the point approximation of the cluster-variation method, and then g is maximized with respect to the path parameters to determine the most probable change of state. When the profile of the domain wall is smooth, it is approximated by a continuous function of the distance and the change of the profile is written as a differentail equation. In the steady state when the domain wall is displaced parallel to itself, the differential equation takes the form of an eigenvalue equation with the velocity of the wall v playing the role of the eigenvalue. The eigenvalue equation is nonlinear, but it can be linearized when the applied magnetic field is weak and v is small. The equation for this case is solved and v is expressed in terms of known quantities. The technique developed is applicable to more realistic models of domain boundaries and can also be combined with better approximations of the cluster-variation method.

8802 DOMAIN WALL ENERGIES AND ENTROPIES FOR THE ISING MODEL AT 0°K by J.W. Cahn (GE Res. Lab.) and R. Kikuchi (Hughes Aircraft); Bull. Am. Phys. Soc., Ser. II, Vol. 5, p. 149(A), Mar. 21, 1960

The energy and entropy of domain walls at absolute zero in a number of two- and three-dimensional structures are computed for the Ising model as a function of orientation and compared with results of computations using various approximations. It is found that the Bragg-Williams approximation gives a poor estimate of surface entropy even at absolute zero. However, the pair approximation is found to be quite good at low temperatures, especially for structures of higher coordination.

8803 CHAIN WALL IN PERMALLOY THIN FILMS by Y. Gomi and Y. Odani (Nippon Tel. and Tel.); J. Phys. Soc. Japan, Vol. 15, p. 535, Mar. 1960

The origins of the displaced cross-tie and chain walls observed in evaporated 80 - 20 Permalloy films are discussed. The walls are caused by scratches or anisotropic inner stress. If there is no scratch, only cross-tie walls appear. If the scratch or the inner stress is comparatively small, either the cross-tie wall or the displaced cross-tie wall appears. When there is a large scratch or inner stress, either the chain wall or the displaced chain wall appears. The behavior of these walls in an applied dc magnetic field is being investigated.

8804 FINE STRUCTURE OF BLOCH WALLS by S. Shtrikman and D. Treves (Weizmann Inst. Sci.); J. Appl. Phys., Vol. 31, p. 1304(L), July 1960

A qualitative explanation of the zigzagging observed during the subdivision of 180° Bloch walls in an iron whisker into a periodic structure of right- and left-hand sections is proposed. Zigzagging is assumed to occur only near the surface of the sample. Near the surface the interaction of the volume charges in the wall with the surface charges cause a reduction of the magnetostatic energy if the wall is suitably tilted. It is shown that for a left-hand wall, the tilt should be left-handed when looking into the surface of the sample. For a right-hand wall a right-handed tilt is required. The wall, therefore, zigzags in opposite phases on opposite faces of the sample, as observed experimentally.

8805 ON THE MAGNETIZATION PROCESS IN FERROMAGNETS by L.V. Kirenskii, M.K. Savchenko, and I.F. Degtyarev (Phys. Inst. Siberian Div., Acad. Sci., USSR); Soviet Phys.-JETP, Vol. 10, pp. 437-441, Mar. 1960

The dynamics of the domain structure during magnetization, studied in crystals of silicon iron containing 30 per cent silicon by means of the powder figure method and the magneto-optical Kerr effect, are discussed. It is shown that magnetization is achieved in the general case by displacement of the domain walls, rearrangement of the domain structure, rotation of the magnetization vector in the direction of the field, and the paraprocess. The process of domain structure rearrangement plays an important role in the magnetization process. It is accompanied by a large number of Barkhausen jumps and corresponds to the maximum magnetic permeability.

Intermediate State of Ferromagnetic Superconductors - See 8738

8806 ON INHOMOGENEOUS BROADENING OF NUCLEAR RESONANCE IN MAGNETIC DOMAIN WALLS by H. Suhl (Bell Labs.); Bull. Am. Phys. Soc., Ser. II, Vol. 5, p. 175 (A), Mar. 21, 1960

The $Co^{59}$ NMR in cubic cobalt metal reported by Portis and Gossard, was found by them to be inhomogeneously broadene to about 400 oersteds at room temperature. A temperature-dependent mechanism for inhomogeneous broadening contribu ing some fraction to this total width was reported in this pape The participating nuclei reside in the domain walls. The ave age thermal deviation of the electronic spin density causing the hyperfine field at the nuclei was shown to vary through the wall. Consequently each nuclear spin sees a slightly dif ferent hyperfine field. For a simple model, with demagnetiz ing neglected, the fractional spread $\Delta H/H$ in hyperfine field is found to be $\Delta H/H \sim (E_A/kT)^{1/2}\delta M/M$ where $\delta M/M$ is the thermal deviation of M in the bulk sample. This formula assumes $kT >> E_A$; otherwise the root is replaced by unity. At room temperature, with $\delta M/M = 0.02^3$, $\Delta H$ for cubic cobalt ~40 oersteds. With demagnetizing the problem cannot be solved sufficiently generally, it may be argued that the effe is then enlarged. The zero point effect connected with quan tization of this mechanism is found to be negligible ($\Delta H \sim 1$ oersted).

8807 VOLUME DEPENDENCE OF THE NMR IN FERROMAGNETIC COBALT by R.V. Jones and I.P. Kaminow (Harvard U.); Bull. Am. Phys. Soc., Ser. II, Vol. 5, p. 175(A), Ma 21, 1960

Measurements of the NMR frequency of $Co^{59}$ in cubic cobalt metallic powder as a function of hydrostatic pressure to 6000 $kg/cm^2$ were given. At 296°K the pressure shift is quite line over this range can can be represented as $(\partial \ln \nu/\partial P)_T = 6.0$ $0.01 \times 10^{-7}$ $(kg/cm^2)^{-1}$. At 195°K the pressure shift is withi 3 per cent of this same value. From estimates of the volume compressibility of cubic cobalt the volume dependence of th resonance frequency is given by $\partial \ln \nu/\partial \ln = -1.19 \pm 0.06$. Marshall has given theoretical estimates of the various contributions to the magnetic field at the cobalt nucleus in hexa gonal cobalt. Following Portis and Gossard's adaptation of this model to the case of cubic cobalt and using previous ex perimental data, where available, the main source of the volume dependence of the resonance frequency has been in ferred. It was proposed that the main contribution arises fro an increase in the admixture of 4s wave functions into the 3 band with decreasing lattice constant.

8808 NUCLEAR MAGNETIC RESONANCE IN ANTIFERROMAGNETIC $MnF_2$ UNDER HYDROSTATIC PRESSURE by G.E Benedek and T. Kushida (Harvard U.); Phys. Rev., Vol. 11 pp. 46-57, Apr. 1, 1960

Measurement of the nuclear magnetic resonance frequency a the $F^{19}$ nucleus in antiferromagnetic $MnF_2$ in zero external field, as a function of pressure at 4.2°, 20.4°, and 35.7°K using a very high frequency variable frequency spectrometer reported. From these measurements the pressure dependence the hyperfine coupling constant (A) between the manganese electrons and the fluorine nucleus, and the pressure depend ence of the Néel temperature have been deduced. This dec tion gives $(1/A)(dA/dP) = +(1.9 \pm 0.1) \times 10^{-6}/(kg/cm^2)$ and $(1/T_N)(dT_N/dP) = +(4.4 \pm 0.3) \times 10^{-6}/(kg/cm^2)$. The com pressibility of $MnF_2$ has been measured. The magnitude and pressure dependence of A has been explained using the theo of Mukherji and Das, and Marshall and Stuart, which permi calculation of the dependence of A on the interatomic distan starting from the Hartree-Fock self-consistent field wave fu tions for $Mn^{++}$ and $F^-$ with the $Mn^{++}$ wave functions proper adjusted to bring it into agreement with neutron scattering form factor measurements. The theory is in very good agree ment with the experimental results.

8809 INFLUENCE OF ANISOTROPIC ELASTIC STRESSES ON FERROMAGNETIC RESONANCE IN POLYCRYSTALLINE FERRITES [in Russian] by Iu. N. Kotiukov and A.N. Burnysheva (SFTI, Tomsk U.); Izv. VUZ Fiz., No. 4, pp. 126-130, 1960

An experimental investigation of the influence of elastic stresses on ferromagnetic resonance absorption in polycrystalline ferrites is reported. A cylindrical sample was compressed along its axis and a permanent magnetic field was applied in the same direction. A relation between the magnitude of the resonance field and the magnitude of the applied stresses has been established for samples which went through different heat treatments. A new method for measuring magnetostriction based on the investigated effect is proposed.

Influence of Ferromagnetic Resonance on the Kerr Optical Effect - See 8906

8810 THE WALL EFFECT IN FERRIMAGNETIC RESONANCE EXPERIMENTS by W.B. Nash and K.J. Standley (U. Nottingham); Proc. Phys. Soc., Vol. 76, pp. 99-103, July 1960

Measurements of the shift in the applied magnetic field for resonance in ferrites caused by the presence of a conducting wall are reported. Small spheres of nickel ferrite and magnesium manganese ferrite were used at wavelengths of 0.87, 1.25, and 3.12 cm and of yttrium iron garnet at a wavelength of 3.12 cm only. The shift was always to lower fields and was independent of frequency within experimental error. Its magnitude at room temperature was 135 and 100 oersteds in nickel and magnesium manganese ferrites, respectively. In the garnet the shift was found to depend on the orientation of the steady field with respect to the conducting plane. A simple explanation which gives agreement with the experimental data in order of magnitude is presented.

8811 MEASUREMENT OF THE FERROMAGNETIC RESONANCE ABSORPTION LINEWIDTH IN POLYCRYSTALLINE FERRITES [in Russian] by Iu. N. Kotiukov and E.M. Smokotin (SFTI, Tomsk U.); Izv. VUZ Fiz., No. 4, pp. 173-177, 1960

An experimental study of the influence of the size and shape of ferrite samples on the width of the ferromagnetic resonance curve is discussed. It is shown that it is necessary to record the dependence of the ferromagnetic resonance curve width on the diameter of the sphere, when using spherical samples, for a correct experimental determination of the quantity $\Delta H$ and to extrapolate this dependence to zero diameter. A correspondence has been established between the change in $\Delta H$ of polycrystalline ferrites as a function of the sample shape and the theoretical results.

8812 FERRIMAGNETIC LINEWIDTH OF SINGLE CRYSTALS OF BARIUM FERRITE ($BaFe_{12}O_{19}$) by I. Bady, T. Collins, (USASRDL), D.J. DeBitetto and F.K. du Pré (Philips Labs.); Proc. IRE, Vol. 48, p. 2033(L), Dec. 1960

Two different linewidth measurements performed on single crystal barium ferrite are reported. In one measurement a small polished wafer 1 x 20 x 40 mils was placed in a rectangular waveguide and the variation in transmitted power was determined as a function of the applied field. The test frequency was 55.5 kMc, the narrowest linewidth was 50 oe, and the field required for resonance was 7600 oe. In the other measurement a small spheroid was placed one-half wavelength from the shorted end of a section of waveguide and the variation in VSWR was determined as a function of the applied field. The test frequency was 57.7 kMc, the narrowest linewidth was 53 oe, and the field required for resonance was 5000 oe.

8813 INFLUENCE OF COPPER AND COBALT ADMIXTURES ON THE CHARACTERISTICS OF NICKEL-CHROMIUM FERRITES [in Russian] by A.S. Khlystov and G.A. Petrakovskii (SFTI, Tomsk U.); Izv. VUZ Fiz., No. 1, pp. 222-227, 1960

Fundamental requirements which ferrites for the low-frequency microwave region must satisfy are analyzed. The influence of small Cu and Co admixtures on the characteristics of Ni-Cr ferrites with low saturation magnetization and high Curie temperature is investigated. The optimum admixtures to obtain ferrites with minimum ferromagnetic resonance curve width are obtained. Ni-Cr-Co ferrites with a 400°C Curie temperature are proposed which are suitable for use in resonance tubes of the 10 cm band.

8814 POLYCRYSTALLINE FERRITES [in Polish] by R. Waddas; Arch. Elektrotech., Vol. 9, No. 4, pp. 729-733(L), 1960

The effect of $Zn^{2+}$, $Cd^{2+}$, and $Co^{2+}$ ion concentration and temperature on the resonance characteristic $\Delta H$ of Ni-Cu ferrite is discussed. A linewidth $\Delta H = 80$ oe was measured in the ferrite $Ni_{0.4}Cu_{0.2}Zn_{0.4}Fe_2O_4$.

8815 INVESTIGATION OF THE MAGNETIC CHARACTERISTICS OF CERTAIN MIXED FERRITES [in Russian] by E.V. Siniakov, V.P. Avramenko, A. Iu. Kudzin, and A.F. Zuev (Dnepropetrov U.); Izv. VUZ Fiz., No. 1. pp. 80-86, 1960

The temperature dependences of the initial magnetic permeability $\mu_o$, $\tan\delta$ and the spontaneous magnetization, the dependences $B = f(H)$, $\mu = f(H)$ and the coercive forces of the following mixed ferrites have been investigated:

$nNiAl_2O_4 - 100\,NiFe_2O_4$ ; $nCoAl_2O_4 - 100\,NiFe_2O_4$
$nNiMn_2O_4 - 100\,NiFe_2O_4$ ; $nCoFe_2O_4 - 100\,MnFe_2O_4$.

One of the components in each case is nonmagnetic. It is established that the introduction of the nonmagnetic component lowers the Curie temperature, decreases the saturation magnetization and increases the coercive force. The results obtained agree with antiferromagnetism theory.

8816 MAGNETIC CHARACTERISTICS OF LITHIUM-ALUMINUM FERRITES [in Russian] by A.S. Khlystov and S.M. Zhiliakov (SFTI, Tomsk U.); Izv. VUZ Fiz., No. 2, pp. 151-153, 1960

The magnetic characteristics of $Li_{0.5}Fe_{2.5-a}Al_aO_4$ ferrites are presented. It is shown that the saturation magnetization varies between broad limits as a changes from zero to one. Therefore the Curie temperature changes slightly: from 640° to 470°C. The change in magnetization agrees with the assumption that the aluminum ions occupy the octahedral locations.

Ion Distributions and Valencies in Mg-Mn Ferrites - See 8584

Hall Effect in Ferrites - See 8763

8817 STUDY OF THE MAGNETIC PROPERTIES OF THE YTTRIUM-YTTERBIUM GARNET SYSTEM [in Chinese] by G. -D. Li, C. -Y. Zlai, H. -W. Xin, and Z. -R. Chen; Acta Phys. Sinica, Vol. 16, No. 5, pp. 281-288, 1960

An investigation of the yttrium-ytterbium garnet system $Y_{3-x}Yb_xFe_5O_{12}$ at the compositions for which $x = 0$, 0.75,

1.50, 2.25, and 3 is described. The samples were prepared by the co-precipitation method and sintered 7 hrs in an oxygen atmosphere at 1350° or 1400°C. Lattice constants and theoretical densities were determined from X-ray diffraction data. It was found that the whole system consisted of a single phase with the garnet structure and that the lattice constant decreased linearly from 12.371 A ($Y_3Fe_5O_{12}$) to 12.297 A ($Yb_3Fe_5O_{12}$). The static hysteresis loop, the initial permeability at 500 kc, the saturation magnetization between 500 Mc and 3000 Mc were observed as a function of composition. It was found that all the samples had high bulk densities (> 90 per cent theoretical densities) and high resistivities ($10^9$ - $10^{10}$ Ω cm) and that the saturation magnetization vs temperature curves had positive slopes at low temperature for $x \geq 1.50$.

8818 ON THE MAGNETIC PROPERTIES OF A $CrBr_3$ SINGLE CRYSTAL by I. Tsubokawa (Tohoku U.); J. Phys. Soc. Japan, Vol. 15, pp. 1664-1668, Sept. 1960

Measurements of magnetic properties of single crystals of $CrBr_3$ made with a magnetic balance and also with a torque magnetometer are reported. The ferromagnetic Curie point has been found to be 37°K from the temperature dependences of magnetization and of torque. Based on the data of the magnetic susceptibility above the Curie point, the paramagnetic Curie point $\theta_p$, Curie constant $C_M$ and the effective Bohr magneton number have been determined to be 47°K, 1.84 and 3.85 $\mu_B$ respectively. From the saturation magnetization at 42°K, the moment of chromium ion is estimated to be $3\mu_B$, coinciding with the spin moment obtained from the susceptibility measurement above the Curie temperature. Direction of easy magnetization lies along the c-axis of the hexagonal lattice, and the second order and the fourth order anisotropy constants are estimated to be $K_1 = -5.08 \times 10^5$ and $K_2 = 0.65 \times 10^5$ erg/cc respectively. In the present results, there is found a small deviation in the torque curves from simple sinusoidal form, $L = K \sin 2\theta$, which is discussed on the basis of the higher order term of magnetic anisotropy in the field strength range and also of the domain-theoretical consideration in the low field strength range.

8819 MAGNETIC SUSCEPTIBILITIES OF $Co(C_2H_3O_2)_2 \cdot 4H_2O$, $Ni(C_2H_3O_2)_2 \cdot 4H_2O$, AND $Mn(C_2H_3O_2) \cdot 4H_2O$ AT LOW TEMPERATURES by R.B. Flippen and S.A. Friedberg (Carnegie Inst. Tech.); Bull. Am. Phys. Soc., Ser. II, Vol. 5, p. 189 (A), Mar. 21, 1960

Measurements of the magnetic susceptibilities of powdered $Co(C_2H_3O_2)_2 \cdot 4H_2O$ and $Ni(C_2H_3O_2)_2 \cdot 4H_2O$ and of both powdered and single crystal $Mn(C_2H_3O_2)_2 \cdot 4H_2O$ in the liquid hydrogen and helium ranges by an ac bridge method were given. While all of these materials have monoclinic structures, only the nickel and cobalt salts are isomorphous. All three salts exhibit Curie-Weiss behavior between 14° and 20.2°K; for $Co(C_2H_3O_2)_2 \cdot 4H_2O$ this continues down to 1.3°K. Cooling this salt by adiabatic demagnetization reveals a sharp susceptibility peak near 0.6°K. The susceptibility of the nickel salt deviates from a Curie-Weiss law below 4.2°K without evidence of cooperative behavior. Significant cooling was not observed upon demagnetization from a field of ~5000 gauss at 1.3°K. Powdered $Mn(C_2H_3O_2)_2 \cdot 4H_2O$ exhibits a very large susceptibility peak at 3.18°K, the same temperature at which a lambda anomaly has been found in preliminary specific heat measurements. As the temperature is lowered through this point single crystal measurements in the a, b, and c directions show: $\chi_a$ passing thro a very sharp peak, $\chi_b$ going through a less pronounced peak, and $\chi_c$ changing only slightly before assuming a nearly constant value. These susceptibilities are strongly influenced b weak external fields. Hysteresis is found in the a direction

Ferromagnetic Properties of $CrO_2$ - See 8630

8820 SHIFT OF THE CURIE TEMPERATURE BY HYDROSTATI COMPRESSION OF MANGANESE AND COBALT FLUORID by D.N. Astrov, S.I. Novikova, and M.P. Orlova (All-Un Inst. Physico-Tech. and Electronic Measurements); Soviet Ph JETP, Vol. 10, pp. 851-854, May 1960

The shift of the Curie temperature in the antiferromagnetics $MnF_2$ and $CoF_2$ under the influence of hydrostatic compressio determined for polycrystalline specimens by measurement of magnetic susceptibility and of the change of the coefficients of linear expansion at the transition temperatures, is discusse For $MnF_2$ the shift is 1.5 ±0.2° at 1900 ± 100 atmospheres. For $CoF_2$ no shift was observed. The antiferromagnetic trans tion temperatures are 68° and 39°K for $MnF_2$ and $CoF_2$, resp tively.

8821 NEUTRON DIFFRACTION STUDIES OF ANTIFERRO-MAGNETISM IN $CrF_2$ AND $CrCl_2$ by J.W. Cable, M.K. Wilkinson, and E.O. Wollan (Oak Ridge Natl. Lab.); Phys Rev., Vol. 118, pp. 950-955, May 15, 1960

Neutron diffraction observations on powder samples of $CrF_2$ $CrCl_2$ from 298° to 4.2°K are reported. These materials, wh have crystal structures similar to rutile but distorted from tetr onality, become antiferromagnetic at low temperatures with different magnetic structures. For $CrF_2$ the magnetic unit ce is identical with the chemical cell and the moments at the c ner sites are directed oppositely to those at the center of the cell. The magnetic unit cell of $CrCl_2$ requires doubling of t b and c axes of the orthorhombic chemical cell and the mom at the corner sites are directed oppositely to those at the ce of the cell. The magnetic unit cell of $CrCl_2$ requires doubl of the b and c axes of the orthorhombic chemical cell and th structure consists of ferromagnetic (011) planes with adjacen planes antiparallel. In neither case were the intensities con patible with a magnetic axis directed along a simple crystall graphic direction. Unique magnetic axes could not be defin established but the data suggest that they lie parallel to the longest Cr-F and Cr-Cl bonds. Néel temperatures of 53° a 20°K were observed for $CrF_2$ and $CrCl_2$ respectively.

Antiferromagnetism of $FeVO_3$ - See 8631

8822 NEUTRON DIFFRACTION STUDY OF THE MAGNET PROPERTIES OF RARE-EARTH-IRON PEROVSKITES by W.C Koehler, E.O. Wollan, and M.K. Wilkinson (Oak Ridge N Lab.); Phys. Rev., Vol. 118, pp. 58-70, Apr. 1, 1960

A neutron diffraction study of the magnetic properties of the rare-earth-iron perovskites, $NdFeO_3$, $HoFeO_3$, and $ErFeO_3$ at temperatures ranging from 955° to 1.25°K is reported. Th iron ions in each of these compounds undergo a transition to antiferromagnetic configuration in which each moment has s oppositely directed moments at nearest neighbor distances. Néel temperatures are 760°, 700°, and 620°K, respectively, the compounds of Nd, Ho, and Er. The moment directions i $HoFeO_3$ and $ErFeO_3$ are parallel and antiparallel to the orth rhombic [100] direction at room temperature: at 43°K the mon

are found to be in a $(1\bar{1}0)$ plane. In $HoFeO_3$ the iron-ion moments at 1.25°K are parallel to [001]; in $ErFeO_3$ at the same temperature they are parallel to [110]. The magnitudes of the ordered iron moments at temperature saturation are $4.5_7$, $4.6_0$, and $4.6_2$ Bohr magnetons in NdFeOc, $HoFeO_3$, and $ErFeO_3$, respectively. In the liquid helium temperature range, magnetic ordering transitions of the rare-earth ions in $HoFeO_3$ ($T_N$ = 6.5°K) and ErFeOc ($T_N$ = 4.3°K) are observed. The $Er^{3+}$ ion moments form a nearly ideal antiferromagnetic configuration in which a chain of parallel moments is sourrounded by four chains of oppositely directed moments at nearest neighbor distances. In this compound, the $Er^{3+}$ ion moments are parallel and antiparallel to [001] and at 1.25°K have a magnitude of 5.8 Bohr magnetons. In $HoFeO_3$ the ions are ordered in a distorted antiferromagnetic configuration in which, at 1.25°K, each $Ho^{3+}$ moment with magnitude of 7.5 Bohr magnetons, makes an angle, in the (001) plane of about 27° with the [010] direction so as to produce a net ferromagnetic moment of 3.4 Bohr magnetons per $HoFeO_3$ molecule parallel to [100].

## PARAMAGNETISM

8823 MAGNETISM OF INTERACTING DONORS by E. Sonder and H.C. Schweinler (Oak Ridge Natl. Lab.); Phys. Rev., Vol. 117, pp. 1216-1221, Mar. 1, 1960

The magnetic susceptibility of donor centers in semiconductors is calculated for the case of small interactions between closely adjacent donors. A hydrogenic model is assumed for the donor centers. The random distribution of the centers, as well as the variation of the energy of interaction with separation distance of pairs of donors, is taken into consideration. A two-fold modification to the Curie law (which is correct for independent donors) is predicted by the resulting expression, namely, a curvature as well as a decrease of the slope of the Curie plot of the susceptibility versus inverse temperature. Both of these effects increase with the donor density, becoming appreciable in silicon with $10^{17}$ - $10^{18}$ donors/cm$^3$ and in germanium in the range around $10^{16}$ donors/cm$^3$. The theory is in good agreement with results of measurements.

8824 MAGNETIC SUSCEPTIBILITY OF Ge-Si MIXED CRYSTALS [in German] by G. Busch and O. Vogt (Eidgenossische Tech. Hochsch, Zurich); Helv. Phys. Acta, Vol. 33, No. 8, pp. 889-910, 1960

Measurements of magnetic susceptibilities as a function of temperature between 300° and 1200°K for a set of 34 Ge-Si mixed crystal samples are given. Assuming an ellipsoidal structure of the conduction band edge and two concentric spheres for the valence band edge it is possible to compare these results with measurements of cyclotron resonance and magnetoresistance. Effective masses for holes and electrons are calculated over the whole concentration range. Using the deformation potential formula it is furthermore possible to visualize the change of energy band edges as a function of composition.

Magnetic Susceptibility of Grey Tin - See 8586

8825 TEMPERATURE DEPENDENCE OF THE PARAMAGNETIC SUSCEPTIBILITY OF NICKEL-CADMIUM FERRITES [in Russian] by V.I. Chechernikov and R.F. Uchaikina (Moscow U.); Izv. VUZ Fuz., No. 3, pp. 39-42, 1960

The magnetic susceptibility of mixed nickel-cadmium ferrites in the high temperature range ($T \gg \theta_f$) and near the ferromagnetic Curie point ($\theta_f$) is examined. Investigations have shown that the temperature dependence of the paramagnetic susceptibility at high temperatures (up to ≈ 1400°K) follows the hyperbolic Néel law. The dependence of the constants $C$, $\sigma$, $\theta$ and $1/\kappa_o$ (which are in this law) on the ferrite composition is found. A transition region where the magnetic susceptibility depends not only on temperature but also on the magnetic field intensity, is detected near $\theta_f$.

8826 PROPOSAL FOR AN ELECTRON SPIN RESONANCE EXPERIMENT OF S-STATE IONS UNDER HIGH HYDROSTATIC PRESSURE by H. Watanabe (Hokkaido U.); Phys. Rev. Lett., Vol. 4, pp. 410-411(L), Apr. 15, 1960; p. 585(E), June 1, 1960

The cubic field splitting parameter a for S-state ions having the half-closed configuration $l^{(2l+1)}$ is analyzed. It is found that a should be proportional to the inverse tenth power of R, the interionic distance between the S-state ion and neighbor ions and should be positive regardless of the sign of $D_q$, a measure of the cubic field. Experimental results which confirm the analytical results with regard to the sign of a are presented. It is suggested that an electron spin resonance experiment on S-state ions under high hydrostatic pressure would be an excellent test of the prediction that a is proportional to the inverse tenth power of R.

Paramagnetic Resonance Detection of Trapping in a Photoconductor - See 8893

8827 MAGNETIC RESONANCE LINEWIDTH IN DILUTE PARAMAGNETIC SINGLE-CRYSTALS WITH ANISOTROPIC g-FACTOR [in Russian] by N.G. Koloskova and U. Kh. Kopvillem (Kazan U.); Izv. VUZ Fiz., No. 3 pp. 223-229, 1960

A formula is obtained for the computation of the fourth moment of the paramagnetic resonance curve in crystals with magnetically-equivalent ions which have an effective spin of one-half and an anisotropic spectroscopic splitting factor. All the internal interactions in paramagnets which can be described as tensor operators dependent on the spin variables of two paramagnetic ions are taken into account. As an example, tensor operators of dipole-dipole and anisotropic exchange interactions are presented. A comparison is made with experiment for the $Nd^{3+}$ ion in a lanthanum ethyl sulfate single crystal.

8828 RATIO OF SECULAR TO NONSECULAR BROADENING FOR EXCHANGE-NARROWED PARAMAGNETIC RESONANCES by G.E. Pake (Stanford U.); Bull. Am. Phys. Soc., Ser. II, Vol. 5, p. 252(A), Apr. 25, 1960

When the frequency of paramagnetic resonance is less than the correlation frequency describing the random modulation of the interactions responsible for line broadening, there are additional "nonsecular" contributions to the linewidth. For dipolar interactions, a motionally or exchange-narrowed line is broadened to 10/3 of its secular width (10/3 effect). Calculations which show that, if appreciable hyperfine interaction is present, the ratio departs from 10/3 were presented. Values of the ratio were given in terms of the relative amounts of isotropic and anisotropic hyperfine coupling; for purely isotropic coupling it is 2. Comparisons were made with the measurements of Rogers, Anderson, and Pake on solutions of stable free radicals.

8829 ON THE EFFECT OF SATURATION IN A PARAMAGNETIC SYSTEM WITH THREE AND FOUR LEVELS [in Russian] by K.S. Stankevich (NIRFI, Gor'kii U.); Izv. VUZ Radiofiz., Vol. 3, No. 5, pp. 764-773, 1960

Results of a computation of the magnetic permeability of a paramagnetic system with four levels in the presence of a strong auxiliary high-frequency field are given. The saturation effect is taken into consideration. The results obtained permit finding an expression for the magnetic permeability of a system with three levels.

8830 SATURATION OF THE MAGNETIC RESONANCE ABSORPTION IN DILUTE INHOMOGENEOUSLY BROADENED SYSTEMS by J.S. Hyde (MIT); Phys. Rev., Vol. 119, pp. 1492-1495, Sept. 1, 1960

The existing theory due to Portis for the saturation of inhomogeneously broadened resonances is discussed and a new theoretical formulation of the problem is developed using an expression for the transition probability first given by Rabi. For $\gamma H_1$ greater than both $T_1^{-1}$ and $T_2^{-2}$, the RF field interacts with spins precessing in the frequency interval $\gamma H_1$; this expression permits explicit calculation of the resulting magnetic loss. No assumption is made of the shape of the individual (homogeneously broadened) spin packets in weak exciting fields. For F centers in alkali halides the results are identical with those of Portis, but the underlying physical reasons differ.

8831 EFFECTS OF POLYTYPISM ON THE ELECTRON PARAMAGNETIC RESONANCE OF $K_3Co(CN)_6$ AND OTHER SPECTROSCOPIC IMPLICATIONS by J.O. Artman, J.C. Murphy (Johns Hopkins U.), J.A. Kohn, and W.D. Townes (USASRDL); Phys. Rev. Lett., Vol. 4, pp. 607-609(L), June 15, 1960

Unexpected splittings observed in the electron paramagnetic resonance spectra of $Cr^{3+}$ doped $K_3Co(CN)_6$ are discussed. A comparison of microwave and crystallographic data indicates that the ordinary lines correspond to the 2Or polytype and that the extraordinary lines correspond to the 1M polytype. Additional structures contribute to the O and E resonances as well as to the fifth and sixth (or more) resonances. It is pointed out that the $Cr^{3+}$ sphere of influence extends at least over a single 1M elementary cell volume. The polytype effect is not uniquely due to the presence of $Cr^{3+}$. Polytypism can explain some unexpected "hole burning" effects and linewidth vs concentration results recently found in the electron paramagnetic resonance of $Cr^{3+}$ doped $K_3Co(CN)_6$.

8832 EFFECT OF THERMAL TREATMENT OF PARAMAGNETIC RESONANCE SPECTRA OF RARE EARTH IMPURITIES IN CALCIUM FLUORIDE by E. Friedman and W. Low (Hebrew U.); J. Chem. Phys., Vol. 33, pp. 1275-1276(L), Oct. 1960

The effect of annealing on the symmetry of the paramagnetic resonance spectra of trivalent rare-earth ions in calcium fluoride is discussed. Experiments on calcium fluoride crystals containing 0.01 - 0.001 per cent gadolinium are described. Similar effects were also observed in crystals containing $Ce^{3+}$ and $U^{3+}$. When a crystal containing predominantly gadolinium in cubic sites was cooled slowly from 1200°C at a rate of 100° per hr, the gadolinium showed axial symmetry. The crystal was then heated again to 1200°C and quenched to room temperature in one to two hrs. The axial symmetry spectrum nearly disappeared and the cubic spectrum became stronger by a factor of thirty. The conversion from one symmetry to the other depends on the length of time the crystal is held at 1200°C.

8833 APPLICATION OF A REDUCED RELATIVISTIC WAVE EQUATION TO SPIN-LATTICE RELAXATION IN PARAMAGNETIC SALTS by R.J. Pendergast and W.A. Barker (St. Louis U.); Bull. Am. Phys. Soc., Ser. II, Vol. 5, p. 252(A), Apr. 25, 1960

As yet, no fully satisfactory theoretical treatment of spin-lattice relaxation in paramagnetic salts has been given. The object of the present work was to investigate more exhaustively than before possible relaxation mechanisms involving the interaction of one ion only with the lattice. To this end augmented relativistic one- and two-body wave equations were reduced to approximate form and the resulting terms combined in various ways. Those mechanisms which order of magnitude estimates indicated would be stronger were calculated more exactly for titanium and chrom alum, following the work of Van Vleck. The shortest relaxation time found exceeds the experimental value by $10^4$ and has the same incorrect field dependence as Van Vleck's. It seems, therefore, that unexplained features of spin-lattice relaxation are not due to any overlooked mechanism involving the interaction of only one ion with the lattice.

8834 A METHOD FOR THE MEASUREMENT OF LONG SPIN-LATTICE RELAXATION TIMES by M. Santini (U. Padova); Nuovo Cim., Suppl. to Vol. 16, Ser. 10, No. 2, pp. 232-239, 1960

A method for measuring long spin-lattice relaxation times which is based on a series of adiabatic fast passages is described. This method is particularly convenient in the case of exceptionally long times.

8835 MAGNETIC RESONANCE AND RAPID PASSAGE IN IRRADIATED LiF by J.S. Hyde (MIT); Phys. Rev., Vol. 119, pp. 1483-1492, Sept. 1, 1960

The experimental result of Portis that at room temperature the paramagnetic dispersion signal ($dX_m'/dH$) of radiation-induced paramagnetic centers in LiF has the shape of an undifferentiated Gaussian curve and lags the modulation field by 90 degrees is confirmed. His theory, explaining this result as a minifestation of rapid-passage behavior, has been tested over a range of experimental parameters and appears valid. In terms of this theory it was found that the spin-lattice relaxation time $T_1 = 1.5 \times 10^{-4}$ sec at room temperature. The prediction has been made by Portis that, if $\omega_m T_1 \gg 1$, where $\omega_m$ is the modulation frequency, the rapid-passage signal should lag the modulation field by 180 degrees. A lag of 130 degrees has been found at 4°K in LiF, using a modulation frequency of 23 cps, and the phase appears to approach a constant value. The same phase shift (130°) can be found at room temperature by using 400 cps modulation and can be interpreted as indicating that $T_1 = 2.6 \times 10^{-3}$ sec at 4°K. It seems more likely, however, that at 4°K the assumption made by Portis that $T_2 \gg T_1$ fails, and that spin-spin effects make the situation more complex. An argument is presented that the magnetic resonance arises from the F center. From its shape a value for the hyperfine splitting of $h_\gamma = 32 \pm 1$ gauss has been obtained. This result is compared with those of other workers who have reported resolved structure in LiF, and the conclusion is reached that the resolved structure resonances probably do not arise from the F center.

8836 ELECTRON SPIN PARAMAGNETIC RESONANCE (ESPR) OF IRRADIATED SINGLE CRYSTALS OF LiF by Y.W. Kim, R. Kaplan, and P.J. Bray (Brown U.); Bull. Am. Phys. Soc.,

Ser. II, Vol. 5, p. 252(A), Apr. 25, 1960

Thermal annealing has been found to change the width and Gaussian shape of the previously reported ESPR spectrum of irradiated LiF. The angular dependence of the remaining hyperfine structure upon annealing appears to be the same as before annealing. Similar angular variation of the hyperfine structure has also been observed together with Lorentzian envelopes of various widths from heavily irradiated LiF. It is very likely that two essentially independent centers are contributing to the characteristic ESPR hyperfine spectrum of neutron-irradiated LiF. Under certain conditions, the dipolar terms of the next nearest (fluorine) shell of Seitz's F center in LiF give a scheme of hyperfine levels whose angular dependence is similar to that observed. Other models for the two centers assumed to be responsible for the observed spectrum were discussed.

3837 PARAMAGNETIC RESONANCE OF THE ANTIMORPH OF THE F-CENTER by W. Känzig (GE Res. Lab.); J. Phys. Chem. Solids, Vol. 17, pp. 80-87, Dec. 1960

LiF crystals X-rayed at 77°K and then warmed up to a temperature between 130° and 220°K contain a new kind of a trapped hole center. Its electronic structure was studied by means of paramagnetic resonance. The center appears to consist of a hole trapped at a Li vacancy, and thus it may be considered as the "antimorph" of the F center. However, the electron deficiency is localized on but two neighboring fluoride ions adjacent to the Li vacancy, so that the symmetry is lower than that of the F center. The new center is closely related to the self-trapped hole, as it can also be described as an $F_2^-$ molecule-ion. However, owing to the vicinity of the Li vacancy the molecular bond is "bent," so that the center has the symmetry of an isosceles triangle lying in a (001) plane with the base along a [110] axis. The thermal stability is higher than that of the self-trapped hole because of the Coulomb field of the vacancy. The main optical absorption band is probably centered at about 3400 A just as for the self-trapped hole. So far, LiF is the only alkali halide in which a center of this type could be found.

8838 PARAMAGNETIC RESONANCE ABSORPTION IN SEVERAL ELECTRON-IRRADIATED MOLECULAR CRYSTALS by P.E. Wigen and J.A. Cowen (Michigan State U.); J. Phys. Chem. Solids, Vol. 17, pp. 26-33, Dec. 1960

Paramagnetic resonance in a series of hydrated and deuterated molecular crystals irradiated with one Mev electrons at liquid air temperature is attributed to a hole localized on the hydrogen bonded oxygen of the oxyion group. In each case hyperfine structure due to the hydrogen bonding proton is analyzed with the aid of a Hamiltonian containing an anisotropic term and an isotropic term and the results are interpreted to give the relative position of the nucleus and the paramagnetic center.

8839 PARAMAGNETIC RESONANCE AND OPTICAL ABSORPTION OF A V CENTER by W. Hayes and G.M. Nicols (Argonne Natl. Lab.); Phys. Rev., Vol. 117, pp. 993-997, Feb. 15, 1960

An investigation of the paramagnetic resonance and optical absorption spectra of KCl and KBr crystals containing divalent calcium strontium or barium ions is described. After X-irradiation at 195°K a resonance spectrum with three distinguishable centers is observed; the centers are similar and each has approximate axial symmetry about a different cube edge. The optical spectra show bands near 325 mμ in KCl and near 345 mμ in KBr which arise from the same centers. The centers are assigned to $Cl_2^-$ and $Br_2^-$ molecule ions and are closely related to the $Cl_2^-$ and $Br_2^-$ centers of Castner and Känzig.

8840 SATURATION AND RECOVERY OF A PORTION OF THE ELECTRON SPIN RESONANCE OF F CENTERS IN KCl AT 4°K by G.A. Noble (Zenith); Phys. Rev., Vol. 118, pp. 1028-1029, May 15, 1960

A method of photographing the inhomogeneously broadened magnetic resonance of F centers in additively colored potassium chloride using a field modulation which sweeps rapidly across the resonance as the absorption is displayed on the oscilloscope is described. The time between sweeps is long and adjustable. A concentration dependence of the spin lattice relaxation time has been observed at 4.2°K. In crystals with a concentration near $1 \times 10^{17}$ $cm^{-3}$, a portion of the resonance can be saturated without affecting the rest of the broad spectrum. The recovery time of this "hole burned in the resonance" is about a quarter of a minute. The results are compared with present theories on spin diffusion.

Paramagnetic Resonance of Radiation-Induced Color Centers in LiF - See 8647

Electron Spin Resonance of Color Centers in Alkali Halides - See 8593

8841 MAGNETIC RESONANCE IN SYSTEMS WITH ELECTRON AND NUCLEAR PARAMAGNETISM SIMULTANEOUSLY [in Russian] by A.A. Kokin (Ural Polytech. Inst.); Izv. VUZ Fiz., No. 4, pp. 198-205, 1960

Nuclear resonance in paramagnetic solutions and the influence of surrounding nuclei on electron resonance are analyzed using a previously published theory of magnetic resonance in systems containing two kinds of magnetic moments.

8842 NUCLEAR MAGNETIC RELAXATION IN IONIC CRYSTALS AT ELEVATED TEMPERATURES by P.P. Mahendroo and A.W. Nolle (U. Texas); Bull. Am. Phys. Soc., Ser. II, Vol. 5, p. 111(A), Mar. 4, 1960

Measurements of the nuclear magnetic spin-lattice relaxation time ($T_1$) in single crystals of NaCl, NaF, $BaF_2$, and LiF from room temperature to 500°C were reported. A magnetic recovery method was used, the magnetization being indicated by the induction signal following a "90° pulse." For $^{23}Na$ ions, the nuclear $T_1$ in appropriate temperature ranges is consistent with the quadrupolar relaxation theory of Van Kranendonk. However, above 375°C, $T_1$ is independent of temperature for both $^{23}Na$ and $^{19}F$ in NaF, suggesting that spin diffusion becomes dominant. A rapid decrease in $T_1$ for $^{19}F$ in NaF, between 210° and 300°C, can be explained by vacancy diffusion. For $^{19}F$ in $BaF_2$, a steady decrease of $T_1$ with increasing temperature is also tentatively ascribed to diffusion.

8843 NUCLEAR SPIN RELAXATION IN SUPERCONDUCTING Al by Y. Masuda (Columbia U.) and A. Redfield (IBM Watson Lab.); Bull. Am. Phys. Soc., Ser. II, Vol. 5, p. 176(A), Mar. 21, 1960

A systematic error in previously reported measurements of relaxation time was pointed out. The measurements have been repeated and extended to 0.36°K, using the same sample. The relaxation time is about 20 per cent greater than previously

reported, corresponding to the same gap of 3.25 $kT_c$ and a somewhat smaller value of the parameter r (about r = 10 instead of 15). According to the interpretation of a referenced paper, $r^{-1}$ is a measure of the anisotropy of the energy gap.

8844 NUCLEAR MAGNETIC RESONANCE OF SOLID HYDROGEN AND SOLID DEUTERIUM by R.M. Housley and G. W. Smith (Rice Inst.); Bull. Am. Phys. Soc., Ser. II, Vol. 5, p. 111(A), Mar. 4, 1960

Nuclear magnetic resonance studies of solid hydrogen ($H_2$) with ortho concentrations from 67 to 86 per cent and of solid deuterium ($D_2$) with para concentrations of 33 and 55 per cent were reported. The method of Cunningham et al. was used to produce the high concentrations ortho $H_2$ and para $D_2$. The temperature of rotational degeneracy in $H_2$ was found to shift to 2.18°K for 86 per cent ortho as compared to a value of 1.6°K for the normal concentration. $T_\lambda$ vs concentration data were found to join smoothly to the previous lower concentration work of Sugawara et al. In addition an interesting hysteresis phenomenon was observed for $H_2$. It was noted that the temperature of appearance of the side peaks when the $H_2$ is cooled is some 0.15°K lower than the temperature of their disappearance when the temperature is slowly raised. In the case of deuterium, no side peaks were observed for either 33 or 55 per cent para $D_2$ at temperatures down to 0.9°K. $T_1$ was measured roughly for the two concentrations. For n-$D_2$, $T_1$ was found to be 7.6 ±3 sec. This compares well with the theoretical value of 8 sec given by Moriya and Motizuki. For 55 per cent para $D_2$, a value of 3 ±1 sec was found. The theory of Moriya and Motizuki gives 5 sec.

Use of Nuclear Magnetic Resonance in Crystal Analysis - See 8588

Nuclear Magnetic Resonance in Superconduction Pb - See 8755

8845 EXCHANGE INTERACTIONS IN THE PARAMAGNETIC RESONANCE SPECTRUM OF RUBY by M.J. Weber, L. Rimai, H. Statz, G.A. Demars (Raytheon), and G.F. Koster (MIT); Bull. Am. Phys. Soc., Ser. II, Vol. 5, p. 157(A), Mar. 21, 1960

The paramagnetic resonance spectrum of ruby crystals with chromium concentrations ranging up to 1 per cent at 16 kMc was discussed. In addition to the spectrum of isolated $Cr^{3+}$ ions, a very complex spectrum of weak lines has been observed. The intensities of these additional lines and their dependence on chromium concentration suggest that they arise from coupled $Cr^{3+}$ ions. Nearest-neighbor Cr-Cr pairs in $Al_2O_3$ may interact by a superexchange mechanism via the intervening oxygen atoms. It a pair of chromium ions is coupled by an isotropic exchange interaction of the form $JS_1 \cdot S_2$, states of resultant spin S = 3, 2, 1, 0 are formed with energies of 6J, 3J, J, and 0, respectively. The spectrum was studied in the temperature range from 1.6° to 300°K. Measurements of the temperature dependences of several lines have been compared with the temperature dependences predicted for transitions within the various S multiplets, assuming antiferromagnetic coupling. A value of $J \sim 250$ $cm^{-1}$ is obtained. The presence of other ferro- and anti-ferromagnetically coupled pairs was discussed.

8846 PARAMAGNETIC RESONANCE OF NICKEL IN $Al_2O_3$ by S.A. Marshall (Armour Res. Found.); Bull. Am. Phys. Soc., Ser. II, Vol. 5, p. 158(A), Mar. 21, 1960

A magnetic resonance absorption spectrum observed at room temperature in $Al_2O_3$ single crystals doped with nickel was described. The spectrum was attributed to nickel in the divalent state. From the symmetry of the magnetic spectrum it was suggested that the divalent nickel ions are located at sites normally occupied by aluminum ions. The parameters of the spin Hamiltonian are temperature dependent with $g_{||} = 2.196$, $g_\perp = 2.187$, D = 1.375 $cm^{-1}$ at room temperature and g = 2.156, D = 1.312 $cm^{-1}$ at 77°K. Total nickel concentration, determined by neutron activation analysis, is $6.0 \times 10^{17}$ atoms/cc of $Al_2O_3$. The absorption intensity of the divalent nickel magnetic resonance indicates a concentration of $1.5 \times 10^{17}$ ions/cc of $Al_2O_3$.

8847 PARAMAGNETIC RESONANCE AND OPTICAL SPECTRA OF SINGLE CRYSTAL OXIDES CONTAINING PARAMAGNETIC IMPURITIES by W. Low (Hebrew U.); Solid State Phys. Electronics and Telecommun., Vol. 3, Academic Press, 1960, pp. 540-551

Following a brief introduction to paramagnetic resonance and a brief discussion of the characteristics desirable in a paramagnetic substance for maser operation, the paramagnetic resonance spectra of $Cr^{3+}$, $Fe^{3+}$, $Mn^{2+}$, $V^{2+}$, $Ni^{2+}$, $Co^{2+}$, and Gd in single crystal oxides are analyzed to determine their usefulness in maser applications. The paramagnetic resonance spectra of $Cr^{3+}$ and $V^{2+}$ in MgO, $Cr^{3+}$ in $SrTiO_3$, $Mn^{2+}$ in MgO, $Fe^{3+}$ in MgO and $SrTiO_3$, $Ni^{2+}$ in MgO, $Co^{2+}$ in MgO, $Fe^{2+}$ in MgO, $Gd^{3+}$ in $ThO_2$, $Cr^{3+}$ in MgO, $Cr^{3+}$ in $Al_2O_3$, and of $BaTiO_3$ are considered. No evidence of the Jahn-Teller effect has been found in paramagnetic single crystals.

Electron Paramagnetic Resonance of $Eu^{2+}$ in the Phosphor SrS-Eu, Sm - See 8879

Spin Resonance of:
Ni, Pd, and Pt in Si - See 8770
$Mn^{++}$ in CdTe - See 8771
Charge Carriers in Graphite - See 8772

## DIAMAGNETISM

8848 THE MAGNETIC SUSCEPTIBILITY OF THE DEFECT ELECTRONS IN SILICON AND GERMANIUM [in German] by D. Geist (U. Koeln); Z. Physik, Vol. 157, No. 4, pp. 490-498, 1960

The contribution of the free carriers to the magnetic susceptibility of semiconductors is discussed. Holes in silicon (density $10^{18}$ to $10^{19}$ $cm^{-3}$) have a small paramagnetic susceptibility at 297° and 141°K. In contrast, calculations from cyclotron mass parameters for 4°K indicate a strong diamagnetic susceptibility. Holes in germanium (density $4 \times 10^{17}$ and $4 \times 10^{19}$ $cm^{-3}$) have a diamagnetic susceptibility which is smaller than is indicated by cyclotron resonance masses. Small concentrations of neutral boron atoms at 141°K contribute to the susceptibility.

8849 DE HAAS-VAN ALPHEN OSCILLATIONS IN MAGNESIUM by W.L. Gordon, A.S. Joseph and T.G. Eck (Case Inst. Tech.); Bull. Am. Phys. Soc., Ser. II, Vol. 5, p. 149(A), Mar. 21, 1960

Observations of de Haas-van Alphen oscillations in the magnetic susceptibility of single crystals of magnesium in magnetic fields up to 17 kgauss using a null deflection torsion balance

were reported. The dependence of the periods and amplitudes of these oscillations on angle between magnetic field and hexagonal axis of the crystal was obtained for several orientations of crystalline axes relative to a vertical suspension axis at temperatures from 2.3° to 4.2°K. These data are in agreement with the few periods mentioned by other investigators but are not consistent with a simple ellipsoidal description of the detail of the Fermi surface. Comparison was made with current theories of the Fermi surface.

## OPTICAL PROPERTIES

### GENERAL

8850 PHOTON MEMENTUM EFFECTS IN THE MAGNETO-OPTICS OF EXCITONS by J.J. Hopfield and D.G. Thomas (Bell Labs.); Phys. Rev. Lett., Vol. 4, pp. 357-359(L), Apr. 1, 1960

Two magneto-optic effects on excitons due to the small, finite wave vector of visible light are discussed. In the first effect, weak lines in the magneto-optic absorption spectrum become stronger and the strong lines become weaker when the magnetic field is reversed. This effect has been observed in hexagonal CdS at 1.6°K. In the second effect a quasi-electric field $(1/c)\,\vec{v} \times \vec{H}$ should act on excitons in a uniform magnetic field due to the exciton center-of-mass velocity. This effect, however, has not been observed in CdS.

8851 MAGNETO-OPTIC PROPERTIES OF IRON-NICKEL AND NICKEL-COPPER ALLOYS IN THE INFRARED RANGE [in Russian] by G.S. Krinchik and R.D. Nuralieva; Vestnik, Moscow U., Ser. III, Fiz.-Astron., No. 4, pp. 43-47, 1960

Measurements of the magneto-optic characteristics of Fe-Ni and Ni-Cu alloys in the 1 - 8 μ wavelength range are reported. The characteristic singularities of the curves obtained are explained by the change in the energy band structure in the alloys. The influence of distortion in the periodicity of the lattice potential and the change in the magnitude of the spin-orbital interaction constant on the magneto-optic properties of the alloys are discussed.

### ABSORPTION (TRANSMISSION)

8852 ANHARMONIC FORCES IN THE GaP CRYSTAL by D. A. Kleinman (Bell Labs.); Phys. Rev., Vol. 118, pp. 118-127, Apr. 1, 1960

The infrared properties and the thermal expansion of gallium phosphide are treated on the basis of a simple model of the anharmonic forces. In this model, the anharmonic forces are nearest neighbor central forces characterized by a single parameter. The value of this parameter for GaP is obtained from the integrated absorption recently measured for certain infrared combination bands. It is shown that the observed width of the fundamental resonance (reststrahl) and the observed shift with temperature of the combination bands are consistent with the absorption. This is presented as evidence that the anharmonic mechanism is predominantly responsible for the infrared absorption in the combination bands. It is also shown that the observed thermal expansion is consistent with the same anharmonic model.

Photoelectric Analysis of Optical Absorption in CdS Type Crystals - See 8591

8853 FAR INFRARED TRANSMISSION THROUGH SUPERCONDUCTING FILMS by D.M. Ginsberg and M. Tinkham (U. California); Phys. Rev., Vol. 118, pp. 990-1000, May 15, 1960

Measurement of the far infrared transmission through films of superconducting and normal lead, tin, indium, and mercury in the wavelength region between 0.1 and 1.1 mm is reported. The transmission data have been analyzed to find the ratio of the complex conductivity in the superconducting state to that in the normal state as a function of frequency. The width of the energy gap at 0°K may be estimated from the frequency of the extrapolated cutoff of the real part, $\sigma_1(\omega)$, of the superconducting conductivity. The values so obtained are 4.0 ± 0.5, 3.3 ±0.2, and 3.9 ±0.3 $kT_c$ for lead, tin, and indium, respectively. These values are in good agreement with those obtained in other experiments on bulk samples. The frequency dependence of $\sigma_1(\omega)/\sigma_N$ is in qualitative agreement with the results of a calculation by Mattis and Bardeen based on the theory of Bardeen, Cooper, and Schrieffer, except for an unexpected hump in $\sigma_1(\omega)$ for lead and (tentatively) mercury at low frequencies. This hump may be due to the production of collective excitations or an anisotropy in the energy gap. It has also been found that a magnetic field as high as 8000 gauss applied in the plane of a lead film about 12 A thick has only a very small effect on the electromagnetic properties of the film.

8854 ON THE RELATION BETWEEN THE THICKNESS DEPENDENCE OF OPTICAL ABSORPTION AND THE SURFACE LAYERS OF BARIUM TITANATE SINGLE CRYSTALS by P. Coufova and H. Arend (Inst. of Physics, Prague); Czech. J. Phys., Vol. B10, p. 663, 1960

Single crystals of $BaTiO_3$, prepared by crystallization in the system $BaCl_2$-BaO-$BaTiO_3$ show a dependence of the optical absorption coefficient on the sample thickness. The observed thickness dependence of the absorption coefficient can be explained by the existence of a surface layer with optical properties differing from those of the inner part of the crystal. By means of an etching method a direct determination of the thickness of the surface layer of crystals in the thickness range of 0.075 to 0.178 mm has been carried out. The value found is (6.0 ± 0.2) x $10^{-4}$ cm.

Wave Functions for Electron-Excess Color Centers in Alkali Halide Crystals - See 8593

8855 INFRARED LATTICE ABSORPTION OF GaP by D.A. Kleinman and W.G. Spitzer (Bell Labs.); Phys. Rev., Vol. 118, pp. 110-117, Apr. 1, 1960

An analysis of transmission and reflectivity measurements on GaP in the wavelength region 1 to 40 μ which was undertaken to obtain information on the lattice vibrations is reported. The fundamental reflection band has been fitted by dispersion to theory and the strength, width, and resonance wavelength (27.3 μ) have been determined. The dielectric constant is found to be 8.5 ±0.2 in the range K $\lambda < 12$ μ and 10.2 for $\lambda > 40$ μ. The background absorption in n-type samples due to free carriers was reduced by copper diffusion to make possible accurate transmission measurements of the lattice combination bands. An assignment scheme using five frequencies is proposed to explain the combination bands. The temperature dependence of the bands is consistent with theory for two-phonon

processes. One band is observed which appears to be due to molecular vibrations of an impurity not yet identified. From the integrated absorption it is concluded that the principal mechanism for the combination bands is the anharmonic potential energy.

8856 EXPERIMENTAL STUDY OF THE SHAPE OF THE F-BAND ABSORPTION IN KCl by J.D. Konitzer and J.J. Markham (Zenith); J. Chem. Phys., Vol. 32, pp. 843-856, Mar. 1960

Measurement of the optical absorption due to F centers in KCl at temperatures between 4° and 377°K is reported. It is believed that the K band has been eliminated, and that the absorption due to transitions from the ground to the first excited state has been obtained. The method of preparing "pure" F centers is discussed. The half-width, the point of maximum absorption, and the zeroth, first and second moments have been measured in the above temperature range. The data establish Smakula's formula on a firm experimental basis for this center. The half-width in ev is given by the relation $0.163 [\coth (71.0/\theta)]^{1/2}$ while the point of maximum absorption is at $2.340 - 0.027 \coth (71.0/\theta)$, where $\theta$ is the absolute temperature. An equation has been found from which one may calculate the F band absorption. The shape of the band is temperature independent and is approximated by the low temperature form predicted by Pekar. The data on the whole support a generalized theory. The F band shape is believed to be due to the interaction of the F electron with localized modes whose average ground state frequency is $2.96 \times 10^{12}$ sec$^{-1}$.

8857 LOW-TEMPERATURE PROPERTIES OF H, V, and F CENTERS IN KCl AND KBr by J. Cape and G. Jacobs (U. Illinois); Phys. Rev., Vol. 118, pp. 946-949, May 15, 1960

Measurements of the optical absorption produced by irradiation from potassium chloride and potassium bromide crystals exposed to X-rays at 10°K and of the changes in optical absorption produced by subsequent annealing at higher temperatures are reported. The temperatures at which changes in optical absorption occurred have been correlated with the temperatures at which free electrical charge appears, and thermoluminescence has been observed. The absorption band at 345 mμ, in KCl, which has been named the H band, is shown to result from the superposition of two or more bands, one of which is the absorption band due to self-trapped holes. In KCl, the self-trapped hole band bleaches thermally at 43°K with a release of free electrical charge. H centers disappear at 56°K with a release of free charge. The optical absorption band of the H center is shown to have its maximum at 335 mμ. In KBr, the thermal release of free charge at 30°K is attributed to the disappearance of H centers. No charge burst was observed in KBr which may be attributed to the destruction of self-trapped holes.

8858 EFFECT OF PRESSURE ON THE SPECTRA OF COLOR CENTERS by R.A. Eppler and H.G. Drickamer (U. Illinois); J. Chem. Phys., Vol. 32, pp. 1418-1422, May 1960

The effect of pressure on the spectra of certain color centers produced in the alkali halides by X-irradiation has been measured to pressures as high as 166,000 atm. For the F center a shift to higher energies with increasing pressure is observed. The slope of the shift versus density is at least twice the value that would be predicted from Ivey's relation at low pressure, and decreases with increasing pressure. This indicates that the compressibility in the neighborhood of the F center is greater than in the bulk crystal, particularly at low pressure. For the M center in LiCl a shift to higher energy with increasing pressure is observed, about one-fifth as great as the shift observed for the F center.

8859 RELATION BETWEEN X-RAY COLORATION AND OPTICAL BLEACHING OF CKI CRYSTALS by W.E. Bron (IBM Res. Ctr.); Phys. Rev., Vol. 119, pp. 1853-1863, Sept. 15, 1960

Changes in the absorption of KCl crystals in the spectral region of 200 mμ which have been observed during room temperature X-ray irradiation and subsequent bleaching with F light are discussed. Both coloration and bleaching of the F band occur in two stages. Secondary centers such as M, T, and $V_3$ centers grow primarily during the second stage of coloration, and the rate of growth of these centers during the second stage is enhanced by plastic deformation in a manner similar to that of the F band. It is found that the absorption change at the F band during the first stage of bleaching approximately equals that during the first stage of coloration. Furthermore, the initial rate of bleaching of the F band is proportional to the initial F band absorption in samples irradiated only into the first stage of coloration, but is essentially independent of the initial F band absorption in samples irradiated into the second stage of coloration. It is concluded from this and other evidence that the center responsible for the first stages of coloration and bleaching differs from the center responsible for the second stages of coloration and bleaching. A major point of difference is that the first stage centers are considered to be located in the bulk of the crystal, whereas the second stage centers are located in the vicinity of dislocations. It is observed that M centers which are formed from F centers during the first stage of bleaching can be bleached with F light. To explain the observations concerning this M band bleaching, it is proposed that M as well as F centers are bleached when they are joined by mobile defects, possibly vacancy pairs. Some of the second stage centers located in the vicinity of dislocations are thought to compete with the centers located in the bulk of the crystal for the mobile defects.

8860 THE THEORY OF PHOTO IONIZATION OF F-CENTERS by Yu. E. Perlin and M.E. Palistrant; Optics and Spectrosc., Vol. 9, pp. 320-323, Nov. 1960

The states of the continuous spectrum of an F center are interpreted to be polarons moving in the screened Coulomb field of an anion vacancy and the probability for a phototransition from the ground state of an F center into such ionized states is calculated. It is shown that since photons take part in the phototransition, the dependence of the probability of ionization on the frequency of the adsorbed light has the form of an asymmetrical curve with a maximum. On the long wavelength side of the maximum, the curve coincides with Pekar's curve for phototransitions in the discrete spectrum. On the short wavelength side, it decreases more smoothly. As the temperature rises, the height of the photoionization maximum decreases while the half-width of the curve increases.

8861 INFRARED ABSORPTION IN N-TYPE ALUMINUM ANTIMONIDE by W.J. Turner and W.E. Reese (IBM); Phys. Rev., Vol. 117, pp. 1003-1005, Feb. 15, 1960

Determination of the optical absorption constants of tellurium and selenium doped n-type AlSb in the spectral region 0.7 - 38 μ at 300° and 78°K is reported. A 4.3 μ band exists at 300°K for which the absorption constant varies linearly with electron concentration. This band may be explained by an 0.3 ev spin-orbit split off conduction band or alternatively by

multivalleyed conduction band with a central minimum 0.3 above the lowest minima. A transition from the highest lence bands to the lowest conduction level could account for e observed absorption starting at 1.33 ev. At wavelengths eater than 8-10 μ free carrier absorption exists with a $\lambda^2$ pendence and a calculated effective mass of 0.3 m. Lat- e bands are present at 11.2, 13.5, 16.5, 22.9, 27.8, and .8 μ.

62 INFRARED ABSORPTION IN IRRADIATED SILICON, XYGEN INDEPENDENT by H.Y. Fan and A.K. Ramdas urdue U.); Bull. Am. Phys. Soc., Ser. II, Vol. 5, p. 197 ), Mar. 21, 1960

studying crucible grown and floating zone samples bombard- together, irradiation introduced absorption bands at 1.8, 3, 3.9, 18.2, and 20.5 μ were found to be independent of e oxygen content in the samples. The oxygen content was ecked by the strength of the 9 μ absorption band. The 20.5 d the newly found 18.2 lattice bands and the 3.9 electron citation band were observed in neutron bombarded samples. e 20.5 band was found to be also independent of other dop- g impurities. The 3.3 band was observed in n-type samples ith electron as well as neutron irradiations. Its production is ndependent of the oxygen content and the donor impurity. he 1.8 band is also independent of the doping impurity. How- ver, with neutron irradiation it is produced with equal in- ensity in both floating zone and crucible grown samples, but ppears only in the crucible grown samples with electron ir- adiation. The absence of 1.8 band in floating zone samples annot be attributed to high density of dislocation that is ommon to such samples.

8863 INFRARED ABSORPTION IN IRRADIATED SILICON, OXYGEN-DEPENDENT by A.K. Ramdas and H.Y. Fan (Purdue U.); Bull. Am. Phys. Soc., Ser. II, Vol. 5, p. 197 A), Mar. 21, 1960

everal additional lattice absorption bands have been observ- d in electron or neutron bombarded silicon between 9-14 μ. Wavelengths of the peaks in microns are: 9.79, 9.97, 10.35, 0.42, 11.42, 11.56, 11.98, 12.33; strong peaks are underlined. hese bands were not observed in bombarded, floating zone amples. Two of the bands, 9.97 and 12.33 were not found n all samples; they decreased considerably after 1/2-hr an- nealing at 100°C. Annealing at 200°C was made for different ime intervals. The 9.79 band annealed the fastest, the 10.35 nd 10.42 bands annealed slower, and the 11.42, 11.56, and 1.98 bands decreased only slightly after 5-1/2 hrs of anneal- ng. With annealing at 200°C, new bands appeared at 10.28, 0.5, 10.95, 11.29, and 11.68 μ, respectively. The 10.95 band grew steadily with annealing whereas the other three ncreased little after the first 1/2 hr. Two observations are oteworthy: (a) the bands appear to saturate with bombard- ment with little decrease of the normal 9 μ oxygen band, (b) he bands are very weak if the sample is preheated at 1000°C nd the 9 μ band is suppressed.

8864 INFRARED PROPERTIES OF GOLD IN GERMANIUM by L. Johnson and H. Levinstein (Syracuse U.); Phys. Rev., Vol. 117, pp. 1191-1203, Mar. 1, 1960

An investigation of the fundamental parameters of Au in Ge between 60° - 300°K by absorption, photoconductivity, and lifetime studies is reported. Photoconductivity measurements reveal the following capture cross sections for electrons and holes at 80°K (subscript refers to carrier being captured; superscript to charge state of Au center):

$$\sigma_h^- \simeq 1\times10^{-13}\ \text{cm}^2,\ \sigma_e^0 \simeq 6\times10^{-14}\ \text{cm}^2,\ \sigma_e^- \simeq 10^{-17}\ \text{cm}^2.$$

Lifetime studies on n-type samples show the existence of an 0.018 ev Coulomb barrier at singly charged sites and indicate that a thermal (phonon) mechanism is involved in the electron capture process. The lifetime also manifests itself in the noise spectrum. The photoconductive absorption cross section at 80°K of p-type Au-doped Ge (0.15 ev level) is found to be $2\times10^{-16}$ cm$^2$ at 1.8 microns. It is suggested that differences between the absorption and photoconductive spectra are due to departure from spherical symmetry of valence band contours away from k = 0.

8865 ABSORPTION EDGE IN β-SILICON CARBIDE by R. Dalven (Raytheon); J. Phys. Chem. Solids, Vol. 13, pp. 163-164(L), May 1960

Optical absorption measurements performed at 20°C in the range 2.3-2.9 ev in a cubic silicon carbide single crystal are reported. Measurements were made at three successive thicknesses, 0.257, 0.174, and 0.113 mm. The value of the energy gap was determined by plotting the cube root of the absorption coefficient vs the photon energy since Kobayasi has indicated that indirect transitions take place. A value of 2.2 ±0.1 ev was found.

8866 FINE STRUCTURE OF THE FUNDAMENTAL ABSORPTION EDGE IN SINGLE CRYSTALS OF CADMIUM SELENIDE by E.F. Gross and V.V. Sobolev (Physicotechnical Inst.); Soviet Phys.-Solid State, Vol. 2, pp. 379-385, Sept. 1960

The line structure of the absorption and reflection spectra of single crystal CdSe has been investigated at T = 77.3° and 4.2°K in the region of the long-wave absorption edge. The line structure of the absorption spectra of isomorphic CdSe and CdS crystals are compared and are found to be in good agreement .

8867 PREPARATION AND PROPERTIES OF HgTe AND MIXED CRYSTALS OF HgTe-CdTe by W.D. Lawson, S. Nielson, and A.S. Young (Roy. Radar Estab.); Solid State Phys. in Electronics and Telecommun., Vol. 2, Academic Press, 1960, pp. 830-835

The electrical and optical properties of HgTe and mixed crystals of HgTe-CdTe are described. The compounds HgTe and CdTe are prepared by direct synthesis of the elements, in vacuum, in sealed silica crucibles. The purification of Hg is discussed; Te and Cd are purified by repeated distillation along a silica tube under vacuum or in a low pressure stream of hydrogen followed by zone refining in sealed silica crucibles. The mixed crystals are grown in sealed silica crucibles in a horizontal apparatus. HgTe and CdTe both crystallize in the zinc-blende structure with lattice parameters of 6.460 and 6.480 A.U., respectively. Measurements of the variation of the Hall coefficient with magnetic field in n-type HgTe and of the variation of Hall coefficient and conductivity with temperature in an n-type HgTe-CdTe specimen are reported. Absorption curves of several HgTe-CdTe crystals are given. Photoconductivity has been observed in several mixed crystal filaments. The melting point of the mixed crystals shows a continuous nearly linear variation with composition between the melting point of HgTe (600°C) and that of CdTe (1106°C). A curve of the absorption edge of HgTe-CdTe crystals vs composition is given.

8868 α AND β BANDS IN NaF, NaCl, AND KCl by R. Onaka and I. Fujita (Tokyo U.); Phys. Rev., Vol. 119, pp. 1597-1598, Sept. 1, 1960

Vacuum spectrophotometer measurements of α and β bands in NaF, NaCl, and KCl irradiated by soft X-rays are reported. At liquid nitrogen temperature, the positions of the α band are $9.4_3$ ev in NaF, $7.1_6$ ev in NaCl, and $6.9_5$ ev in KCl, and the positions of the β band are $9.7_5$ ev in NaF, $7.3_8$ ev in NaCl, and $7.3_1$ ev in KCl. The doublet structure of the β band in NaCl, expected by Fuchs' theory, has not been detected. This may be due to the fairly wide bandwidth of the component bands.

8869 SEMICONDUCTOR ABSORPTION AND OPTICAL FILTERING by N. Thomas (Electro-Optical Systems); J. Opt. Soc. Am., Vol. 50, p. 502(A), May 1960

The optical properties of certain oxide-type semiconductors were discussed with a view of their use as low-frequency pass filters. It was also shown how, from the classical theory of electronic oscillation, the principle of a high-frequency pass filter can be deduced. This filter seems to be realizable experimentally in the form of long-wavelength reflecting films (NESA glass) which have been developed empirically in the past. The foregoing results can be utilized to minimize radiation losses from solar collectors of relatively extended area and to construct a new type of filter with broad bandpass characteristics.

8870 SOME OPTICAL PROPERTIES OF CADMIUM TELLURIDE by P.W. Davis and T.S. Shilliday (Battelle Mem. Inst.); Phys. Rev., Vol. 118, pp. 1020-1022, May 15, 1960

Measurements of some optical properties of CdTe samples having a carrier concentration of the order of $10^{15}$ $cm^{-3}$ are reported. The index of refraction in the infrared was determined to be 2.61. Values of the absorption coefficient α as a function of frequency were obtained at various temperatures. By plotting $\alpha^{1/2}$ and $\alpha^2$ against frequency, it was found that at room temperature the minimum energy for direct transitions is 1.50 ev; that for indirect transitions is 1.44 ev. The temperature dependencies between 77° and 373°K are given by $(1.66 - 5.6 \times 10^{-4}T)$ev for direct transitions and $(1.56 - 4.1 \times 10^{-4}T)$ev for indirect transitions.

## RADIATION (LUMINESCENCE)

8871 ON THE INFRARED EMISSION IN ZnS:Cu — EFFECT OF SULFUR PRESSURE AND ALUMINUM by E.F. Apple and J.S. Prener (GE Res. Lab.); J. Phys. Chem. Solids, Vol. 13, pp. 81-87, May 1960

An investigation of the intensity of the infrared emission in ZnS:Cu phosphors as a function of the sulfur pressure under which the phosphors are heated at high temperatures and of Al concentration in the phosphors is discussed. The observed dependence is interpreted using a model in which the infrared absorption and emission arises from hole transitions between states of a normally unionized Cu acceptor and the valence band, and in which sulfur vacancies behave as doubly ionizable donors in ZnS. The effect of Al impurities also follows from the model.

8872 RADIATIVE RECOMBINATION IN GALLIUM PHOSPHIDE POINT-CONTACT DIODES by H.C. Gorton, J.M. Swartz, and C.S. Peet (Battelle Mem. Inst.); Nature, Vol. 188, pp. 303-304(L), Oct. 22, 1960

An investigation of the recombination radiation emitted by reverse biased point contact GaP diodes is described. The energy spectrum of the recombination radiation was measured by means of an arrangement consisting of a diffraction grating attached to the 50 mm extension bellows of an Exakta 35 mm camera and a 100 μ slit in the focal plane of the lens. The energy of the recombination radiation was observed to be between 1.96 and 2.19 ev, with a peak density at 2.12 ev. The maximum energy, 2.19 ev, agrees with the room temperature energy gap determined by optical absorption measurements. Direct interband transitions cannot be inferred from these results since the exact operating temperature of the device was not known. A correlation between the onset of luminescence at isolated points in the breakdown region and discontinuities in the slope of the reverse characteristics was observed.

8873 TEMPERATURE DEPENDENCE OF EDGE EMISSION IN CADMIUM SULFIDE by D.C. Reynolds (Wright-Patterson AFB); Phys. Rev., Vol. 118, pp. 478-479, Apr. 15, 1960

An investigation of the temperature dependence of the blue and the green emission in cadmium sulfide in the temperature range from 77° to 300°K is reported. The blue emission shifts to longer wavelengths as the temperature is increased above 77°K with a temperature coefficient of $4.9 \times 10^{-4}$ ev/°C. The intensity of the green emission falls off exponentially above 77°K with very little shift in the spectral position of the green peaks.

8874 THE INTERACTION BETWEEN ACTIVATOR AND NONTOTALLY SYMMETRIC LOCAL VIBRATIONS by N.N. Kristofel; Optics and Spectrosc., Vol. 9, pp. 324-326, Nov. 19

The interaction between activator and nontotally symmetric local vibrations (the Jahn-Teller effect) is considered as exemplified by the $^3P_1$ state of the luminescence center in the KCl:Tl phosphor. Certain problems connected with it are discussed.

8875 ELECTRONIC-VIBRATIONAL PROCESSES IN THE LUMINESCENCE CENTERS OF IONIC CRYSTALS by C.B. Lushchik, N.E. Luschik, and K.K. Shvarts; Optics and Spectrosc., Vol. 9, pp. 113-117, Aug. 1960

A study of the emission spectra, absorption spectra, and quantum yield of luminescence from alkali halide crystals as functions of the frequency of the exciting light ($\nu_{exc}$) and temperature indicated that radiative and nonradiative transitions in luminescence centers take place after an equilibrium distribution of excited states with respect to storage of vibrational energy is established with the crystal. The luminescence quantum yield of the crystals has a steplike dependence of $\nu_{exc}$. The yield is independent of $\nu_{exc}$ in the neighborhood of individual fundamental electronic-vibrational absorption bands. Generally speaking, however, the quantum yields are different near different fundamental absorption bands.

8876 LUMINESCENCE OF IMPURITY CENTERS. Part I. by A.M. Ratner and G.E. Zil'berman (Inst. of Chem. Reagents); Soviet Phys.-Solid State, Vol. 1, pp. 1551-1559, May 1960

The spectral dependence of the absorption coefficient and of the emitted radiation for phosphors which contain impurity

uminescence centers is calculated. The motion of the ions is reated classically. Changes in equilibrium locations of the ons during electronic transitions, and in the elastic constants f the lattice are taken into account. A relation between changes in elastic constants and the deviation of the absorption and luminescence spectra from mirror symmetry, and also from a gaussian shape, is derived. It is shown that neglecting the changes in elastic constants is permissible only when the "mirror symmetry rule" is obeyed. Results are applicable to both rystalline and amorphous or liquid phosphors (independent of the existence of local oscillations).

8877 LUMINESCENCE OF IMPURITY CENTERS. Part II. by A.M. Ratner (Inst. of Chem. Reagents); Soviet Phys.-Solid State, Vol. 1, pp. 1560-1568, May 1960

The probability of thermal transitions between discrete levels associated with the presence of an impurity center is calculated. The motion of the ions is treated classically. The displacements of the ions from their equilibrium sites and changes of elastic constants during electronic transitions are included in the calculations. The relation between the shapes of the absorption and emission spectra and the probability of thermal transitions is established. It is shown that, when elastic constants are taken into account, the results of the calculation are, generally speaking, affected fundamentally. A qualitative comparison is made between theory and experiment. With the help of the results obtained, qualitative conclusions about the mechanism for energy transfer from the lattice to the impurity atoms are given for the case of excitation of the crystal by hard radiation.

8878 USE OF ELECTRON PARAMAGNETIC RESONANCE FOR STUDY OF Eu-ACTIVATED SrS PHOSPHORS by V.G. Dubinin and Z.A. Trapeznikova; Optics and Spectrosc., Vol. 9, pp. 245-248, Oct. 1960

The light sums stored during excitation and given off during de-excitation by Eu-activated SrS phosphors are compared with the aim of determining the fraction of the quenching processes occurring in phosphors after ionization of the activator. It was found that in a phosphor without flux only about half of the recombinations lead to emission, whereas in phosphors with flux almost all the recombinations are accompanied by emission.

8879 AN ELECTRON PARAMAGNETIC RESONANCE INVESTIGATION OF THE VALENCE CHANGE OF THE ACTIVATOR DURING EXCITATION OF THE PHOSPHOR SrS-Eu, Sm by V. G. Dubinin and Z.A. Trapeznikova; Optics and Spectrosc., Vol. 9, pp. 187-189, Sept. 1960

Upon photoexcitation of the phosphor SrS-Eu, Sm in the absorption band of $Eu^{++}$, a decrease in the paramagnetic resonance absorption of the $Eu^{++}$ is detected. It is concluded that upon excitation of the phosphor SrS-Eu, Sm ionization of the activator from $Eu^{++}$ to $Eu^{+++}$ takes place.

8880 ON THE RELATION BETWEEN THE LUMINESCENT, ELECTRICAL AND CHEMICAL PROPERTIES OF ZINC OXIDE [in Russian] by I.K. Vereshchagin (Chernovits U.); Izv. VUZ Fiz., No. 2, pp. 31-36, 1960

Measurements of the intensity of electro- and photoluminescence, the electrical conductivity and the concentration of excess zinc in ZnO samples, roasted at 100° - 200°C under different conditions are discussed. On the basis of the existence of a relation between all the investigated quantities as well as between the magnitude of the catalytic activity and the brightness of the electroluminescence, the possibility of the participation of a double electrical layer on the surface, formed as a result of adsorption of the gas molecules, in the process of exciting electroluminescence is considered. Certain deductions are made on the electroluminescence mechanism in ZnO.

8881 MAIN PEAKS IN THE LIGHT PULSES OF ELECTROLUMINESCENCE by A.N. Georgobiani and M.N. Fok; Optics and Spectrosc., Vol. 9, pp. 407-411, Dec. 1960

By investigating the shape of the light pulse, it is shown that at high voltages the process of electron release is regulated basically by the field. Electron liberation takes place at low temperatures by collision ionization and at high temperatures by tunneling through a potential barrier (Zener effect). A comparison of experimental and theoretical temperature dependence curves of the fields at which a total release of electrons is obtained has made it possible to calculate the value of optical phonons in ZnS and the energy depth of localized levels. These values are in good agreement with the value of the optical phonon obtained from the vibrational structure of the edge emission spectrum, and with the energy depth of levels calculated from the equilibrium concentration of donor free electrons in an electroluminescent ZnS-Cu crystal.

8882 ELECTROLUMINESCENCE AT GRAIN BOUNDARIES IN GALLIUM PHOSPHIDE by G.F. Alfrey and C.S. Wiggins (U. Birmingham); Solid State Phys. in Electronics and Telecommun., Vol. 2, Academic Press, 1960, pp. 747-750

The electroluminescence of GaP is discussed. A few volts of direct current applied to the crystal is sufficient to produce some electroluminescence. For greater luminescent intensity, pulsing techniques are used to avoid overheating the crystal, since its impedance falls rapidly with increasing current. The electroluminescence is shown to occur at grain boundaries. As the current grows, the electroluminescence tends to grow throughout the boundary inside the crystal. Not all boundaries are electroluminescent, and almost all voltage drops occur at grain boundaries. The impedance across a grain boundary is nonlinear. The use of a scanning electron microscope technique to investigate voltage barriers at a grain boundary is described. Segregation of donor impurities at grain boundaries is discussed.

8883 SOME EXPERIMENTS ON ZINC SULPHIDE CRYSTALS by G.F. Alfrey, I. Cooke, and K.N.R. Taylor (U. Birmingham); Solid State Phys. in Electronics and Telecommun., Vol. 2, Academic Press, 1960, pp. 816-818

Several experiments on the electroluminescence of crystals are described. Electroluminescence in ZnS is related to the barrier field and the bulk properties of the crystal. The process which causes reduction in the height of scintillation pulses in ZnS crystals with an applied field is discussed. Differences between ac and dc electroluminescence are considered. A theory to account for the variety of electroluminescent light waveforms and for the variation of electroluminescence with frequency is presented.

8884 ELECTROCHEMILUMINESCENCE AT A SILICON ANODE IN CONTACT WITH AN ELECTROLYTE by A. Gee (Texas Instr.); J. Electrochem. Soc., Vol. 107, pp. 787-788, Sept. 1960

The light emission observed during the anodic oxidization of an amorphous Si film on the surface of p-type Si is discussed. The film is prepared by treating a chemically polished and etched surface with a 49 per cent HF solution containing about 0.1 per cent $HNO_3$ until a blue interference color is visible. Emission is produced by anodic oxidation of the film in different electrolytes such as 1 M solutions of KCl, LiCl, $H_2SO_4$, $HNO_3$, and $HC_2H_3O_2$. Passivation always sets in as soon as the luminescence disappears. The faint, reddish glow usually starts at a single point, expands to cover the entire surface, and then contracts to a point away from the area where it started. Luminescence has not been observed on film covered n-type Si.

Voltage Dependence of Cathodoluminescence - See 8730

8885 THE EFFECT OF ANNEALING ON THERMOSTIMULATED PROCESSES OF COLOURED SODIUM CHLORIDE CRYSTALS by A. Bohun (Czech. Acad. Sci.); Czech. J. Phys., Vol. 10B, No. 5, pp. 360-365, 1960

It is shown experimentally that after annealing samples of NaCl the thermoluminescence in the high-temperature maxima not only increases, which is in agreement with the results of other authors, but that simultaneously the thermoemission decreases. It follows from a discussion of the results that this effect is probably caused by the formation of a surface layer which takes place during the evaporation of the sodium and prevents the rise of the electrons from the crystal. The vacancies left in the crystal by the sodium increase the concentration of the V centers and thus the probability of luminescence.

8886 THE ROLE OF M-, R-, AND F'-COLOR CENTERS IN THE INFRARED FLUORESCENCE OF F-CENTERS IN ALKALI HALIDE CRYSTALS by I. I. Ezhik and S. T. Shovlo; Optics and Spectrosc., Vol. 9, pp. 405-407, Dec. 1960

An experimental investigation of the role of F'-, M-, and R-centers in the infrared fluorescence of F-centers in additively colored KCl and KBr crystals is discussed. The infrared fluorescence of F-centers in the crystals was measured by a) simultaneous excitation by light in the F- and M-absorption bands, b) simultaneous excitation by light in the F- and F'-absorption bands and c) F-, F'-, and M-absorption bands. Comparison with the ultra-violet and visible luminescence of these crystals indicates that the peaks in the infrared F-center fluorescence correspond to thermal decomposition of M- and F'-centers. A mechanism for the formation of the intrared fluorescence peaks is proposed.

8887 CHANGE IN STRUCTURE OF BLUE AND GREEN FLUORESCENCE IN CADMIUM SULFIDE AT LOW TEMPERATURES by L. S. Pedrotti (AF Inst. of Tech.) and D. C. Reynolds (Aero. Res. Lab.); Phys. Rev., Vol. 119, pp. 1897-1898, Sept. 15, 1960

The two fundamental fluorescences observed in cadmium sulfide crystals subjected to ultraviolet excitation at low temperatures are classified according to wavelength. Photographs of the two fluorescences at 4.2° and 77°K are given and their structures are compared. Experimental evidence on the change in structure of the green emission near 5130A between 4.2° and 77°K is presented and used to confirm an explanation for the apparent "green" shift in cadmium sulfide proposed by D. G. Thomas and J. J. Hopfield.

8888 THE INFLUENCE OF TEMPERATURE ON TWO SERIES BANDS IN THE GREEN FLUORESCENCE SPECTRUM OF PURE CADMIUM SULFIDE AT LOW TEMPERATURE by M. Bancie-Grillot, E. F. Gross, E. Grillot and B. S. Razbirin; Optics and Spectrosc., Vol. 9, pp. 287-288, Oct. 1960

An investigation of the temperature dependence of the band intensity of two series in the green luminescence spectrum of pure CdS crystals between 4° and 77°K is reported. One series of bands has maxima located at $\nu_1 = 19450 - 300\,n\ cm^{-1}$ (Series 1) and the other has maxima at $\nu_2 = 19310 - 300\,p\ cm^{-1}$ (Series 2) where n and p are small integers. In crystals which show only series 2 at 4°K the bands become weaker on heating but remain in their original positions. Weak bands of the first series whose intensity increases with temperature are also observed. The intensities of the two bands become comparable at a particular temperature, the bands of the second series disappear near the boiling point of liquid nitrogen, and the intensity of the first series approaches that of the second series at 4°K. When crystals which exhibit only bands of the first series at 4°K are heated from 4° to 77°K, the bands of the second series do not appear. The bands of the first series do not change their position and the band intensity does not change substantially with increase in temperature. In crystals containing both series at 4°K a redistribution of intensities occurs on heating. A similar redistribution occurs on the application of an electric field to a crystal immersed in liquid helium.

8889 SOME SIMPLE FEATURES OF THE MÖSSBAUER EFFECT by H. J. Lipkin (U. Illinois); Ann. Phys., Vol. 9, pp. 332-339, Feb. 1960

A simple description of the change in the state of a crystal lattice upon emission or absorption of a nuclear gamma ray is given. A sum rule for the average energy transfer to the lattice is derived and the probability of zero energy transfer is calculated. The results are general and do not assume a particular model for the crystal. Simple principles which may be useful as a guide to experimentalists are presented.

8890 PHOTO-DIELECTRIC EFFECT IN A ZnS-Cu, Fe PHOSPHOR. Part I. TEMPERATURE DEPENDENCES [in Russian] by P. E. Ramazanov (SFTI, Tomsk U.); Izv. VUZ Fiz., No. 3, pp. 9-18, 1960

Measurements of the temperature dependences of the photodielectric effect in a ZnS-Cu, Fe phosphor under excitation by ultraviolet light and at different stages of the damping of the afterglow of the phosphor are reported. The relaxation character of the effect is shown and an assumption is made on its relation to the repeated localization of the electrons and holes in an excited crystal phosphor which is oriented by the external field.

8891 EMISSION OF ACTIVATED CADMIUM SELENIDE PHOSPHORS by M. Avinor and G. Meijer (Philips); J. Chem. Phys. Vol. 32, pp. 1456-1458, May 1960

The emission bands of cadmium selenide activated by silver, gold, and copper, at liquid nitrogen temperature are discussed. The silver, copper, and gold bands were found at 0.92, 1.20 and 1.45μ, respectively. The silver band is completely quenched at room temperature. A near edge emission of CdSe was found at 0.72μ. In general the bands follow the same pattern as in the sulfide phosphors. However, no additional band is found for activation by excess activator over coactivator.

8892 LOW-TEMPERATURE LUMINESCENCE AND PERSISTENCE OF SILICA GEL [in Russian] by I. K. Musatov (Moscow Inst. Exact. Chem. Tech.); Izv. VUZ, Fiz., No. 4, pp. 46-50, 1960

Measurements of the luminescence spectrum of silica get at the temperature of liquid nitrogen are given. A curve of the decay of persistence at room temperature has been obtained. The persistence spectrum is investigated at −163°C.

## PHOTOELECTRONIC PROPERTIES

8893 PARAMAGNETIC RESONANCE DETECTION OF TRAPPING IN A PHOTOCONDUCTOR by R. S. Title (IBM); Phys. Rev. Lett., Vol. 4, pp. 502-503(L), May 15, 1960

Observations of trapping in ZnS:Gd at room temperature by means of electron paramagnetic resonance are reported. A large increase in the $Gd^{3+}$ paramagnetic resonance signal was observed when the sample was irradiated with light near 385 mμ. The $Gd^{3+}$ resonance decreased to half in approximately an hour and to a tenth in a few days after removing the light. The resonance could be quenched by irradiating the sample with light between 475 and 900 mμ and between 280 mμ and 335 mμ. A green fluorescence was produced by irradiation at 385 mμ and a green phosphorescence on the removal of this irradiation. It is suggested that the normal $Gd^{2+}$ is changed to $Gd^{3+}$ by the 385 mμ light which releases an electron from the $Gd^{2+}$ site to the conduction band. The freed electron is then trapped at an unknown site near the conduction band. The recombination at $Gd^{3+}$ sites of electrons thermally released from these traps causes the green phosphorescence and explains the slow decrease in the magnitude of the $Gd^{3+}$ EPR spectrum. The quenching of the $Gd^{3+}$ resonance by radiation between 475 and 900 mμ is explained. The photocurrent which should flow because of the electrons in the conduction band was measured. A peak in the photoconductivity corresponding to the excitation peak of the $Gd^{3+}$ resonance was observed.

8894 INTERBAND PHOTOCONDUCTIVITY IN GERMANIUM by T. S. Moss and T. D. H. Hawkins (Roy. Aircraft Estab.); Proc. Phys. Soc., Vol. 76, pp. 565-566, Oct. 1960

Photoconductivity due to transitions between the valence bands of germanium is discussed. It was found that the photoconductive signal at liquid nitrogen temperature exceeded that at room temperature for wavelengths between 3.2 μ and 4.1 μ and that the cold sample gave a significantly higher signal in the 3.8 μ region. At wavelengths just outside this range the room temperature signal was higher than the low temperature signal. The time $\tau$ spent in the $V_3$ split off band before returning to the $V_1$ heavy hole band is estimated to be $4\text{-}14 \times 10^{-12}$ sec.

8895 ON THE THEORY OF THE F-CENTER. Part I. WAVE-FUNCTIONS AND ENERGY EIGENVALUES IN THE DYNAMIC ELECTRON-LATTICE COUPLING [in German] by M. Wagner; Z. Naturforsch., Vol. 15a, pp. 889-908, Oct. 1960

To bridge the hitherto extreme theoretical positions of Pekar (an infinite number of oscillators) and Williams (one single oscillator) it is necessary to describe the dynamic coupling of the electron-wave functions at the center of the disturbance by physically real lattice eigen-oscillations. The eigen-oscillations connected with the coupling are chosen in this procedure from the symmetry of the local wave function $\psi_n$, and consequently all display central symmetry in addition to the special symmetry of the wave-function, (s,p,d, etc.). It then becomes possible - in the sense of closing a circle - to determine the normal amplitude (eigen-vectors) of the retarded eigen-oscillations by the electric field of the electron-charge distribution $e\,|\psi_n|^2$. Owing to the fact that at transitions between two electron states only two electron wave functions have to be described simultaneously, it is always possible to reduce the dynamic electron-lattice coupling at the F-center to the coupling of two lattice oscillators which have the symmetry of the two wave functions and which are physically real to a good approximation. A theory based on these fundamentals is able to explain the characteristics of the F absorption- and emission-bands, in good agreement with experimental results. Furthermore it can be employed on transitions without radiation so that questions regarding quantum efficiency and photoconductivity can be investigated.

8896 ELECTRICAL AND PHOTOELECTRICAL PROPERTIES OF GRAIN BOUNDARY LAYERS by O. Weinreich, H. F. Mataré and B. Reed (Sylvania); Solid State Phys. in Electronics and Telecommun., Vol. 1, Academic Press, 1960, pp. 97-108

A theory explaining the presence of a potential drop and a photoconductive effect across a natural grain boundary in Ge is extended by considering three regions across the grain boundary space charge. In the confirmatory experiments, two properties of grain boundaries were investigated – photoeffect transverse to the boundary and conduction along the grain boundary region (sheet conductance). The experimental results support the belief that it is not segregation of impurities but lattice misfit at the grain boundary which is the predominant factor in the formation of a Schottky type barrier in Ge bicrystals.

8897 PROPERTIES AND APPLICATIONS OF INDIUM ANTIMONIDE by R. E. J. King and B. E. Bartlett (Mullard); Philips Tech. Rev., Vol. 22, No. 7, pp. 217-225, 1960-61

The semiconducting III-V compound InSb has a small band gap and is therefore a good photoconductor. The Mullard ORP 10 InSb cell is sensitive to wavelengths up to 7.5 μ, i.e., to further in the infrared than any other cell. The liquid-nitrogen-cooled cell ORP 13 is characterized by a particularly high sensitivity, viz., 14 mv per μw at 4 μ. The time constants of these two cells are, respectively, < 1 μsec and < 10 μsec. The electron mobility in pure InSb is very high (650,000 $cm^2/vs$ at 77°K), so that it is also a very suitable material for Hall effect devices. Still other applications depend on the large magneto-resistance effect in InSb. Very pure InSb single crystals are prepared by melting together purified In and Sb, zone-melting the compound, and then crystal-pulling on the (211) plane. P-type material is made by doping, e.g., with germanium.

8898 PHOTOCONDUCTIVITY IN LEAD SELENIDE by D. H. Roberts (Caswell Res. Labs., England); Solid State Phys. in Electronics and Telecommun., Vol. 2, Academic Press, 1960, pp. 819-824

An investigation of photoconductivity in PbSe is reported. With solid filaments, the photoconductive spectral response shows constant quantum efficiency from 1 to ~4μ, with cutoff at ~4.6μ with no peaks. The lifetime has been found from the photoconductive-photoelectromagnetic radio method to be 0.4 μsec. No edge emission is observed. The effect of oxygen on evaporated films, the wavelength dependence of flicker noise, a method of depositing and sensitizing PbSe films in an orthodox vacuum evaporation plant, the presence of potential

barriers in PbSe films, and the spectral response of PbSe films are discussed.

8899 PHOTOCONDUCTIVITY OF CdS-ZnS MIXED CRYSTAL by M. Kikuchi and S. Iizima (Electrotech. Lab., Tokyo); J. Phys. Soc. Japan, Vol. 15, p. 357(L), Feb. 1960

Measurements of photoconductivity in mixed CdS-ZnS single crystals are discussed. The single crystals were obtained by cleaving crystals prepared by mixing luminescent pure CdS and ZnS powders in sealed, evacuated quartz ampoules and heating the ampoules at 1250°C for 72 hrs. In a sample cleaved from a crystal grown from a mixture of 26.5 gm CdS powder and 4 gm ZnS powder the photoconductivity had a peak at 491 mμ. The photoconductivity in a pure CdS crystal peaked at 516 mμ. Peaks were also observed in both crystals at about 600 mμ. This peak is probably due to oxygen in the powder or ampoule. It was found that the band gap of the mixed crystal can be varied continuously by adding ZnS to CdS.

8900 PHOTOCONDUCTIVITY IN GALLIUM SULFO-SELENIDE SOLID SOLUTIONS by R. H. Bube and E. L. Lind (RCA); Phys. Rev., Vol. 119, pp. 1535-1537, Sept. 1, 1960

The photoconductivity characteristics of solid solutions of GaSe and GaS have been investigated for proportions of GaS between 10 and 50 per cent. The difference between the room temperature band gaps of GaSe and GaSe (50).GaS(50) is 73 per cent of the total difference between the band gaps of GaSe (2.03 ev) and GaS (2.58 ev). The optical quenching energy and the thermal quenching energy of sensitizing centers are independent of the solid solution composition, thus giving additional evidence that these centers are associated with the crystal cation and that the photoconductivity observed is associated with holes.

8901 PHOTOCONDUCTION IN TERNARY V-VI-VII COMPOUNDS by R. Nitsche and W. J. Merz (RCA Labs.,Ltd.); J. Phys. Chem. Solids, Vol. 13, pp. 154-155, May 1960

Some photoelectric properties of single crystals of ternary compounds of the type V-VI-VII (V = Sb, Bi; VI = S, Se, Te; VII = Cl, Br, I) are discussed. The wavelengths of maximum photocurrent, $\lambda_{max}$, shift in a regular way towards longer wavelengths with increasing atomic weight of the components. For the compounds SbSBr and SbSI the dependence of photocurrent, dark current and $\lambda_{max}$ on temperature was measured between -140° and +120°C.

8902 SOME PHOTOELECTRIC PROPERTIES OF ZnS SINGLE CRYSTALS by W. J. Merz (RCA Labs., Ltd.); Solid State Phys. in Electronics and Telecommun., Vol. 2, Academic Press, 1960, pp. 811-815

The photoelectronic properties of ZnS single crystals and their anisotropy are discussed. Photoconduction is large parallel to a striation and much smaller perpendicular to it. The photovoltaic effect is small parallel to the striation, but extremely high (a few hundred volts) perpendicular to it. The temperature dependence of the photovoltage for a fixed light intensity of the 3130 A line is given and the photovoltage is plotted as a function of light intensity. A theoretical band structure for cubic-hexagonal ZnS is proposed on the basis of the experimental evidence.

8903 PHOTOCONDUCTIVITY OF CUPROUS OXIDE IN RELATION TO ITS OTHER SEMICONDUCTING PROPERTIES by F. L. Weichman (Northwestern U.); Phys. Rev., Vol. 117, pp. 998-1003, Feb. 15, 1960

The strong dependence of at least two of the three known peak in the photoconductivity vs wavelength curve of $Cu_2O$ on the oxygen content of the material is shown. The peak near 600 m can be shifted from shorter to longer wavelengths by exposing the sample to relatively low oxygen pressures at 860°C. The peak near 800 mμ is found to increase in magnitude relative to the others under these circumstances, in apparent contrast to the results of previous investigators. It is further shown that both results are consistent with the values of the high temperature activation energy of the conductivity process, as well as with the change in bandgap as a function of temperature as obtained from optical absorption measurements under the assumption that $Cu_2O$ can be classified as a nonpolar semiconductor.

8904 COAGULATION, OPTICAL ABSORPTION AND PHOTOCONDUCTIVITY OF COLLOID CENTRES IN ALKALI HALIDE by W. T. Doyle (U. Southampton); Proc. Phys. Soc., Vol. 7 pp. 649-663, May 1960

The effects of optical illumination and impurities on colloid formation in additively colored KCl and in NaBr colored by ultraviolet light are discussed. It is shown that at elevated temperature additively colored KCl behaves as an auto-sensitized photographic system. A theory of the colloid band which takes account of ion core polarization and harmonic mean effective mass for arbitrary ellipsoidal particles is presented. The colloid band is identified as a bounded plasma resonance, shifted into the visible region by the boundary conditions. Plasma frequencies computed from the positions of the colloid bands are in good agreement with other estimates. The spectral dependence of photoconductivity associated with the colloid band is related to the band structure of the host medium.

Photoconductivity of:
- Au-Doped Ge - See 8864
- Grey Tin - See 8586
- CdS-Type Crystals - See 8591
- ZnO - See 8612

8905 ON THE CONTROL OF THE SPECTRAL CHARACTERISTICS OF COMBINED PHOTO-CATHODES FOR THE ULTRAVIOLET REGION OF THE SPECTRUM [in Russian] by V. N. Kostin and M. I. Zabara (Kharkov U.); Izv. VUZ, Fiz., No 4, pp. 110-116, 1960

The possibility of controlling the integral photosensitivity and the spectral characteristics of photo-cathodes of different kind of pure metals is shown. The reasons for the inconstancy of the photoresponse of Al, Cu and Cd cathodes are clarified and a method of ionic treatment which guarantees the stabilization of this quantity is found. The use of a standard conversion apparatus to photon counters is completely justified.

## ELECTROMAGNETIC PROPERTIES

8906 INFLUENCE OF ELECTRON MAGNETIC RESONANCE ON THE OPTICAL PROPERTIES OF FERROMAGNETIC AND PARAMAGNETIC SOLIDS [in Russian] by P. S. Zyrianov, T. G. Iziumova and G. V. Skrotskii (Ural Polytech. Inst.); Izv. VUZ Fiz., Vol. 3, pp. 32-38, 1960

efractive indices are calculated for a gyrotropic medium under magnetic resonance conditions. These calculations are performed on the basis of a system of macroscopic equations which take account of spin-orbital interaction. For transparent paramagnetic and ferromagnetic solids, the dependence function between the rotation angle of a light wave's polarization plane and the amplitude and frequency of the radio-frequency field has been obtained. The influence of ferromagnetic resonance on the Kerr optical effect is investigated, and a comparison is made with experimental results.

8907 THE OPTICAL PROPERTIES OF BULK BISMUTH IN THE 3-36μ REGION by M. N. Markov and A. S. Khaikin; Optics and Spectrosc., Vol. 9, pp. 253-256, Oct. 1960

A determination of the optical constants n and $\kappa$ of Bi in the 3-36 μ region by measuring its reflectance is reported. An absorption band was found in the vicinity of 27 μ. The concentration of conduction electrons was found to be $5 \times 10^{19} cm^{-3}$. The properties of Bi were treated from the band model viewpoint, with a forbidden band gap $\Delta E_0 = 0.04$ ev.

8908 OPTICAL CONSTANTS OF MONOCLINIC α-SELENIUM by V. Prosser [in Czech]; Cs. cas. fys., Vol. 10A, pp. 35+, 1960

A method for growing single crystals of monoclinic α-selenium is proposed. Their structure is verified and measurements of the optical constants in the region of the intrinsic absorption edge are given.

8909 GENERALIZED FRESNEL EQUATIONS FOR THE SURFACE OF A CRYSTAL, TAKING ACCOUNT OF ANISOTROPY IN THE EFFECTIVE EXCITON MASS by B. E. Tsekvava (Kiev Phys. Inst.); Soviet Phys.-Solid State, Vol. 2, pp. 447-453, Sept. 1960

The Fresnel equations for the transmission of light through a vacuum-crystal boundary are generalized. Equations are obtained for the reflectivity of light from the surface of the crystal, as well as expressions for the coefficients of transparency, reflection, and attenuation of the light intensity in passing through a plane-parallel plate. Experiments for verifying the optical anisotropy of cubic crystals are described.

8910 ON THE THEORY OF THE DAMPING EFFECT IN IONIC CRYSTALS [in Russian] by V. V. Mitskevich (Vil'nius U.); Izv. VUZ, Fiz., No. 4, pp. 6-12, 1960

The infrared dispersion of ionic crystals is analyzed. A computation is made of the damping due to the anharmonicity of the crystal lattice vibrations by quantum-mechanical methods, using a statistical density matrix. The temperature behavior of the absorption line is investigated: at high temperatures the wings of the line increase in proportion to the temperature and the center of absorption diminishes in inverse proportion to the temperature.

8911 INFRA-RED FARADAY EFFECT DUE TO CONDUCTION ELECTRONS IN INDIUM ANTIMONIDE by S. D. Smith and T. S. Moss (Roy. Aircraft Estab.); Solid State Phys. in Electronics and Telecommun., Vol. 2, Academic Press, 1960, pp. 671-679

The theory of the Faraday effect is discussed. Measurements of the Faraday effect rotation in intrinsic and n-type InSb are used to determine the effective mass of the carriers. Experimental results show that accurate measurement of the Faraday effect may be made with carrier concentrations varying by a factor of at least 30. Large rotation is obtained with moderate fields, thus making possible the practical application of the Faraday effect as a high-frequency modulator or chopper of infrared radiation.

8912 INFRA-RED FARADAY ROTATION IN InAs AND InP by I. G. Austin (GE Ltd.); J. Electronics Control, Vol. 8, pp. 167-169, Mar. 1960

Determinations of the effective mass of charge carriers in InAs and InP by means of infrared Faraday rotation measurements in the wavelength region 2-17μ are reported. The measurement technique was slightly different from that used by other workers. The wavelength and magnetic field dependence of rotation ($\theta$) predicted by $\theta = 1.52 \times 10^{-11} \frac{N\lambda^2 B}{n(m^*)}$ deg/m, where N is the free carrier concentration, $\lambda$ is the wavelength, B is the magnetic induction, n is the refractive index, and $m^*$ is the effective mass was found, except near the absorption edge in the wavelength case. The effective mass of carriers in InAs and InP were found to be 0.043 and 0.10, respectively.

## THERMAL PROPERTIES

8913 DEBYE CHARACTERISTIC TEMPERATURE OF SOLIDS by S. K. Joshi and S. S. Mitra (Allahabad U.); Proc. Phys. Soc., Vol. 76, pp. 295-298, Aug. 1960

The Debye characteristic temperatures, $\theta$, for a number of solids belonging to cubic, hexagonal, tetragonal, and trigonal crystal systems, including AgBr, AgCl, GaAs, GaSb, NaBr, NaI, PbS, ZnS, and $TiO_2$, are calculated from their elastic constants using series expansion and numerical methods. Experimental values of $\theta$ determined from specific heat measurements are also given when available.

8914 THE HEAT CAPACITY OF BISMUTH TELLURIDE AT LOW TEMPERATURES by E. S. Itskevich (Inst. Phys. High Pressures); Soviet Phys.-JETP, Vol. 11, pp. 255-260, Aug. 1960

Measurements of the heat capacity of p-type $Bi_2Te_3$ between 1.37° and 65°K are reported. At temperatures below 2.5°K the heat capacity can be described by a linear term with $\gamma = 17 \times 10^{-5}$ joule-deg$^{-2}$(g-atom)$^{-1}$ and a cubic term with $\theta_0 = 155.5$°K. Between 2.5° and 8°K the heat capacity is proportional to a power of the temperature greater than three. The heat capacity of the laminar $Bi_2Te_3$ lattice is not consistent with the calculations performed for lattices with a larger difference between the elastic moduli in the layer and between the layers. Data on measurements of the Hall effect and resistivity of $Bi_2Te_3$ at a number of temperatures between 2° and 300°K are presented. The linear term of the heat capacity is ascribed to holes and the hole mass is estimated to be 1.46 $m_0$.

8915 FREQUENCY DISTRIBUTION AND THE SPECIFIC HEAT OF NaCl AT LOW TEMPERATURES by E. M. Arase and R. D. Hatcher (New York U.); J. Chem. Phys., Vol. 33, pp. 1704-1708, Dec. 1960

Using the Kellerman model of the NaCl crystal, the eigenfrequencies at 0°K are found from those at room temperature by a first-order perturbation theory. From this the frequency distribution at 0°K is obtained and is compared with the room-

temperature frequency spectrum. The specific heat and apparent Debye temperatures below 100°K based on both distributions as well as a linearly weighted average are given.

Specific Heat of KCl at Elevated Temperatures - See 8937

Calculation of the Specific Heat of Si - See 8665

8916 THE LATTICE THERMAL CONDUCTIVITY OF ALLOYS by W. R. G. Kemp and P. G. Klemens (CSIRO); Austl. J. Phys., Vol. 13, pp. 247-254, July 1960

Information about the nature of the electron-proton interaction in alloys and about the density of their dislocations, obtained from the lattice thermal conductivity at liquid He temperatures, is presented. It appears that in Cu, Ag, and Au the electrons interact with transverse as well as with longitudinal lattice waves. The lattice conductivity also varies with alloy composition; it is not clear whether this variation should be ascribed to changes in the electron density or to the presence of dislocations, locked into stable configurations by the solute atom. If the latter view is adopted, the density of dislocations in annealed alloys is typically of the order of $10^{10}$ to $10^{11}$ lines/cm$^2$. Changes of the lattice thermal conductivity of deformed alloys are compared with stored energy release; this suggests that the theory underestimates the scattering of phonons by dislocations by a factor of 3 to 6.

8917 INVESTIGATION OF THE THERMAL PROPERTIES OF SUPERCONDUCTORS. Part III. ANISOTROPY OF THE THERMAL CONDUCTIVITY OF GALLIUM by N. V. Zavaritskii (Inst. Phys. Problems); Soviet Phys.-JETP, Vol. 10, pp. 1069-1076, June 1960

The thermal conductivity of gallium in the normal and superconducting states along different crystallographic directions is discussed. The anisotropy observed in the temperature dependence of the electron thermal conductivity in the superconducting state is related to the anisotropy in the gap width in the excitation energy spectrum. The results of measurement of the critical magnetic field of gallium are presented.

8918 THERMOELECTRICITY AND THERMAL CONDUCTIVITY IN THE LEAD SULFIDE GROUP OF SEMICONDUCTORS by D. Greig (Natl. Res. Counc., Ottawa); Bull. Am. Phys. Soc., Ser. II, Vol. 5, p. 264(A), Apr. 25, 1960

Measurements of the thermal conductivity, thermoelectric power, and electrical conductivity of six specimens of PbS and one each of PbSe and PbTe in the temperature range 4° to 100°K were reported. The samples varied from very polycrystalline natural galena to synthetic specimens of each type containing only a few single crystals. Previous measurements of thermoelectric power above 30°K had indicated no phonon drag effect in the carrier concentration range in which it is most pronounced in the elemental semiconductors. However, the present results show the typical "drag" maxima in the thermoelectric power below 29°K in the specimens of highest charge carrier concentration. A rather detailed investigation of the phonon scattering processes is required to explain this phenomenon. The thermal conductivity was similar in all samples at 100°K but varied by as much as two orders of magnitude at 10°K. In order to explain both this and the thermoelectric power results, it has been necessary to consider dislocation and free electron scattering among the processes which restrict the flow of phonons.

8919 THE THERMAL CONDUCTIVITY AND THERMOELECTRIC POWER OF BISMUTH TELLURIDE AT LOW TEMPERATURES by P. A. Walker (GE Ltd.); Proc. Phys. Soc., Vol. 76, pp. 113-126, July 1960

Measurements of the thermal conductivity and thermoelectric power in n- and p-type $Bi_2Te_3$ single crystals between 6° and 200°K are discussed. The observed lattice conductivity can be interpreted in terms of scattering by the tellurium isotopes. Measurements on the iodine doped samples showed the existence of appreciable impurity scattering. Interpretation of the thermoelectric power results suggest a multiband structure for $Bi_2Te_3$.

Thermal Conductivity and Seebeck Coefficient of an Organic Semiconductor - See 8735

8920 THERMOELECTRICITY AND RESISTIVITY IN METAL ALLOYS AT LOW TEMPERATURES by C. A. Domenicali (Minn.-Honeywell); Phys. Rev., Vol. 117, pp. 984-992, Feb. 15, 1960

A simple model for the "resonant scattering" of electrons from foreign atoms in a crystal lattice is proposed. The model assumes the existence of highly selective scattering mechanisms characterized by widths of the order of $10^{-4}$ electron volts and larger; in this sense it is similar to the model of Korringa and Gerritsen, although the present model makes use of only the general analytical characteristics of the relaxation time and does not specify the details of the scattering mechanism. Mott's well-known approximation formula for the absolute thermoelectric power of a metal alloy is strictly valid and physically meaningful only at temperatures $kT \ll a$, where $2a$ is the width of the resonance. At temperatures $kT \gg a$ the formula leads to useful and valuable information on the thermoelectric properties of alloys, but the formula in this temperature region has only a rather artificial physical meaning. In the intermediate temperature region where kT is comparable to a, the Mott formula is entirely invalid. But it is in precisely this intermediate temperature range that the resistance and thermoelectric anomalies occur, so that Mott's approximation cannot be used for the treatment of these anomalies. The model satisfactorily explains many of the details of this anomalous behavior. It is suggested that the solvent metals used in the experimental studies of these effects will have to be much purer than those presently available before it will be possible to specify unambiguously the effects of a given kind of impurity.

8921 THEORY OF THERMOELECTRIC POWER OF IONIC CRYSTALS. Part IV. by E. Haga (Niigata U.); J. Phys. Soc. Japan, Vol. 15, pp. 1949-1954, Nov. 1960

The thermoelectric power Q associated with the movement of silver ions in $Ag_2X$ (X = S, Se, Te) is discussed, where Q is obtainable by measuring the potential difference between silver electrodes in an arrangement as $Ag(T_1) \mid AgI(T_1) \mid Ag_2X \mid AgI(T_2) \mid Ag(T_2)$. When a temperature gradient is applied, Q in general changes with time because of the thermal diffusion of both electrons and silver ions and then reaches its steady value. Information on the heat of transport of a silver ion is obtained from the comparison between theory and experiment. An explanation on the heat of transport in ionic crystals is given taking into account the variation of lattice vibration frequency due to the presence of defects. The theory is compared with the experimental data on silver halides and $Ag_2X$ available at present.

3922 TRANSMITTED PHONON DRAG MEASUREMENTS IN SILICON by K. Hubner and W. Shockley (Clevite); Phys. Rev. Lett., Vol. 4, pp. 504-505(L), May 15, 1960

An experimental investigation of the dependence of transmitted phonon drag in silicon on the intermediate layer thickness is discussed. The experimental arrangement is described. The samples were 15 mm in length, 1 mm in width, and varied in thickness from 50 to 200 microns. Probe spacings for the input field $E_1$, output field $E_2$, and the current source were 10 mm, 3 mm, and 13 mm, respectively. The ratio $E_2/E$ was found to decrease exponentially with thickness of the intermediate layer. Several other possible phonon drag experiments are discussed.

3923 ON THE THEORY OF THE THOMSON EFFECT IN SEMICONDUCTORS [in Russian] by F. G. Serova (Gor'kii Pedinst.); Izv. VUZ, Fiz., Vol. 3, pp. 123-129, 1960

The dependence of the current carrier mean free path in semiconductors on the energy, and the effect of electron entrainment by photons on the magnitude and sign of the Thomson coefficient, are analyzed.

8924 THE VOLUME-GRADIENT THOMSON EFFECT by P. I. Baranskii (Kiev Inst. of Phys.); Soviet Phys.-Solid State, Vol. 2, pp. 413-423, Sept. 1960

The thermogalvanic phenomena which occur in a nonhomogeneous semiconductor upon the passage of current are analyzed including the volume-gradient Thomson effect which is associated with inhomogeneities of the resistivity ρ in the body of the semiconducting single crystal. A method of measuring the volume-gradient Thomson effect is proposed and tested experimentally in germanium single crystals. The existence of this effect was experimentally observed and its current dependence was studied at room temperature. It is noted that the methods used for investigating the volume-gradient Thomson effect can be applied successfully to the study of the volume Peltier effect, where it opens up new research possibilities.

8925 RADIATION EFFECTS ON THERMOELECTRIC POWER IN $Bi_2Te_3$ by R. A. Levy (U.S. Navy Rad. Def. Lab.); Bull. Am. Phys. Soc., Ser. II, Vol. 5, p. 168(A), Mar. 21, 1960

Results of bombarding samples of n-type $Bi_2Te_3$ with 2-Mev electrons from a Van de Graaff accelerator at beam currents ranging from 1 to 85 μa were reported. Total dosages ranged up to 100 μamp-hr. Thermoelectric power and resistivity measurements were made before, during, and after radiation by means of standard dc techniques using Chromel-Alumel thermocouples. Thermoelectric power decreased up to 50 per cent during bombardment and recovered afterward. Temperature effects prevented an adequate determination of the effect of radiation on electrical resistivity. Other than surface oxidation or melting from the high temperatures produced by the bombarding electrons, no permanent effects were observed in the samples. All measurements were made on flat rectangular wafers sliced parallel to the axis of polycrystalline cylindrical ingots.

8926 EFFECT OF γ IRRADIATION ON THERMOELECTRIC POWER OF BISMUTH TELLURIDE by R. A. Artman (Bucknell U.) and A. N. Goland (Brookhaven Natl. Lab.); Bull. Am. Phys. Soc., Ser. II, Vol. 5, p. 168(A), Mar. 21, 1960

Measurements of changes produced in thermoelectric power and electrical conductivity of n- and p-type polycrystalline bismuth telluride and bismuth by γ irradiation from $Co^{60}$ were reported. N-type samples measured in situ at room temperature show a thermoelectric power and conductivity which decrease with irradiation. The effect saturates at less than $6 \times 10^6$ r and anneals out in less than 3 hr. Near dry-ice temperatures the thermoelectric power increases with irradiation. The initial rate of increase is approximately 2 per cent per $10^6$ r. The increase anneals out with a half life of 29 hr at 230°K. Conductivity decreases approximately 1 per cent for a dose of $6.8 \times 10^6$ r. P-type samples near dry-ice temperatures show thermoelectric power also increasing with irradiation. The initial rate of increase matches that of the n-type. No data were taken on the annealing rate. The conductivity shows an increase of less than 0.2 per cent for a dose of $25.2 \times 10^6$ r. Generally irradiation has the same effect upon thermoelectric power as increasing the temperature. Bismuth shows no change in thermoelectric power near dry-ice temperature for a dose of $12.4 \times 10^6$ r.

8927 EFFECT OF REACTOR IRRADIATION ON THERMOELECTRIC PROPERTIES OF PbTe AND $Bi_2Te_3$ by J. C. Corelli, R. T. Frost and F. A. White (Knolls Atomic Power Lab.); Bull. Am. Phys. Soc., Ser. II, Vol. 5, p. 168(A), Mar. 21, 1960

Irradiation of specimens of commercially available PbTe and $Bi_2Te_3$ at a temperature of 60° ± 20°C to a total flux-time of $1.0 \pm 0.3 \times 10^{19} cm^{-2}$ of neutrons having energy greater than 1 Mev was described. Duplicate samples irradiated with and without cadmium shields allowed a search for effects of transmutations caused by an integrated thermal neutron flux-time of $1.5 \pm 0.5 \times 10^{20} cm^{-2}$. Preliminary comparison of Hall coefficients of irradiated and unirradiated n-type PbTe indicates a decrease in carrier concentration by a factor 4.5 ± 0.5. Seebeck coefficients at 30°C of the n- and p-type PbTe and n-type $Bi_2Te_3$ increased by factors of 1.8, 1.6, and 1.1, respectively, with no significant differences observable between cadmium shielded and unshielded specimens. The p-type $Bi_2Te_3$ (no initial impurity doping) exhibited an n-type Seebeck coefficient subsequent to the irradiation, and its magnitude was changed by a factor of 0.7 for the shielded and 1.8 for the unshielded specimen. The room temperature electrical resistivity of shielded and unshielded n-type PbTe increased by a factor of 10 as a result of the irradiation.

8928 BISMUTH TELLURIDE AND ITS THERMOELECTRIC APPLICATIONS by D. A. Wright (GE Ltd.); Solid State Phys. in Electronics and Telecommun., Vol. 2, Academic Press, 1960, pp. 699-705

The performance of thermo-junctions as refrigerators is discussed. Semiconductor thermo-junctions made of $Bi_2Te_3$ and PbTe generate the greatest thermoelectric power, due to a high lattice component of thermal conductivity and high atomic weight. The preparation of $Bi_2Te_3$ is described and its properties are detailed. The energy gap at 290 degrees Kelvin is near 0.13 electron volts. The lattice component of thermal conductivity is plotted as a function of Sb or Se concentration in $Bi_2Te_3$. The applications of thermoelectric cooling to Ge diodes and triodes, infrared detectors and oil diffusion pump baffles are discussed. The use of thermoelectric generators in the communication industry for radio equipment supplies is also considered; the thermoelectric power delivered is 200-300 μv/degree.

8929 THERMOELECTRIC PROPERTIES OF PRESSED $Bi_2Te_3$ POWDERS by C. Kolm and J. J. Giacalone (Lincoln Lab.);

Properties of Elemental and Compound Semicon., (Interscience), pp. 287-293

An investigation of the effect of grain sizes on the electrical and thermoelectric properties of $Bi_2Te_3$ is reported. A sharp increase in resistivity together with a corresponding decrease in both the thermoelectric power and the figure of merit was found for compacts with a grain size less than 400μ. Annealing of the powders caused a decrease in the resistivity, an increase in the thermoelectric power, and relatively no change in the figure of merit.

8930 ADDITIONAL EXPERIMENTS ON THE THERMOELECTRIC POWER OF MAGNESIUM TERNARY ALLOYS by E. W. Kammer and E. I. Salkovitz (U.S. Naval Res. Lab.); Bull. Am. Phys. Soc., Ser. II, Vol. 5, p. 150(A), Mar. 21, 1960

An investigation of the electron transport properties of dilute magnesium binary alloys demonstrated that the magnitude and sign of such properties are dependent on the electron concentration of these alloys. Then, by adding equal amounts of monovalent silver and trivalent indium to magnesium, a series of ternaries with relatively constant electron concentration was obtained. The thermoelectric power for these alloys behaved similarly to a previously studied MgCd series. Extending this work, new results have been obtained on magnesium ternaries, containing both silver and quadrivalent tin; these behave in such a manner that the thermoelectricity curve is similar to that of the previously studied Mg-In binary alloys. X-ray lattice parameter measurements have been made of the binary and ternary series and comparisons were made.

8931 THERMAL AND ELECTRICAL PROPERTIES OF SOME SILICIDES by S. E. Mayer and A. I. Mlavsky (Transitron); Properties of Elemental and Compound Semicon., (Interscience), pp. 261-274

Measurements of the thermoelectric power and electrical resistivity of p-type MnSi, n-type MnSi, p-type $CrSi_2$, and n-type CoSi from -200° to 1000°C are compared with earlier work on these compounds. The systems CoSi-FeSi and CoSi-NiSi have also been studied. Detailed descriptions of the methods of preparation and of measurement are given. Some tentative explanations are offered for the behavior of these compounds.

8932 THERMAL, ELECTRICAL, AND OPTICAL PROPERTIES OF (In, Ga) As ALLOYS by M. S. Abrahams, R. Braunstein and F. D. Rosi (RCA Labs.); Properties of Elemental and Compound Semicon., (Interscience), pp. 275-285

The (In, Ga) As system exhibits complete solid miscibility. Homogeneous alloys have been produced across the entire system by using the method of zone leveling. Physical measurements show that the lattice thermal conductivity decreases markedly with alloying and exhibits a minimum value of about 0.05 w $deg^{-1}$ $cm^{-1}$ at an alloying composition of about 50 per cent. The thermoelectric power varies linearly with the logarithm of the carrier concentration for nondegenerate crystals, and from this data it appears that the "density of states mass" is independent of alloying. The mobility of electrons decreases monotonically with increasing percentages of GaAs, up to about 70 per cent. The band gap varies continuously with composition and a concave upward dependence is observed on going from InAs to GaAs.

Thermoelectric Power of:
Grey Tin - See 8586
BP - See 8732
Iron Oxides - See 8733

Thermoelectric Properties of Pb-Te, Pb-Se, Pb-S and Pb-Te-Se - See 9034

8933 THERMO AND GALVANOMAGNETIC EFFECTS IN InS [in Russian] by D. Kh. Amirkhanova, Izv. AN AzSSR, Fiz-Mate, Tekh. Nauk Ser., No. 1, pp. 45-56, 1960

Results of an investigation of the longitudinal and lateral Nernst-Ettingshausen effect and the galvanomagnetic effects in p- and n-InSb in the 77°-400°K range in magnetic fields to 26,000 oe are reported. The dependences of the thermomagnetic effects on the magnetic field intensity in the impurity region for p-InSb are explained on the basis of the two-hole model. The effect of phonon entrainment on the thermomagnetic effects in the 77°K region is described. The temperature dependences of the Nernst-Ettingshausen field which have been obtained in both the impurity and the intrinsic conduction regions are explained in the $\frac{uH}{c} >> 1$ case on the basis of the theory of thermomagnetic effects. It is shown that the current carriers in InSb are dissipated primarily by the acoustic vibrations of the crystal lattice in the whole temperature range investigated.

8934 THE THERMAL EXPANSION OF A SILICON SINGLE CRYSTAL by R. R. Berss and R. J. Horne (Imperial Coll.); Proc. Phys. Soc., Vol. 75, pp. 793-795, May 1960

Measurements of the thermal expansion of single crystal silicon in a <111> direction from -195° to 100°C are discussed. Details of the experimental apparatus and techniques are given. The experimental data is compared with that of Gibbons. Below -150°C a region in which the coefficient of thermal expansion and therefore the Grueneisen factor, is negative was found. At low temperatures there is a discrepancy between the two sets of data. Considerable effort has been expended to determine experimental errors which could cause this disagreement. None however, has been found.

Thermal Expansion of:
GaP - See 8852
Triglycine Sulphate - See 8692

## MECHANICAL PROPERTIES

8935 ULTRASONIC MEASUREMENT OF THE ELASTIC MODULI OF RUTILE by G. L. Vick and L. E. Hollander (Lockheed); J. Acoust. Soc. Am., Vol. 32, pp. 947-949, Aug. 1960

Measurements of the elastic moduli of rutile are reported. Four of the elastic moduli were determined by measuring the velocity of 10 Mc ultrasonic waves. They are $C_{11} = 2.48 \pm 0.08 \times 10^{12} d/cm^2$, $C_{33} = 4.52 \pm 0.08 \times 10^{12} d/cm^2$, $C_{44} = 1.20 \pm 0.0$ $\times 10^{12} d/cm^2$, and $C_{66} = 1.6 \pm 0.1 \times 10^{12} d/cm^2$. The remaining two, $C_{12} = 2.0 \pm 0.1 \times 10^{12} d/cm^2$ and $C_{13} = 1.4 \pm 0.1 \times 10^{12} d/cm^2$, were computed from the given data and Bridgman's compressibility data. These values are, with the exception of $C_{33}$, in good agreement with values computed from force constant data. No change in elastic moduli was noted upon reduction to a resistivity of 0.2 ohm cm. It was noted that attenuation was greater in reduced than in fully oxidized rutile and was considerably greater in the a than in the c crystallographic direction.

8936 ELASTIC CONSTANTS OF SYNTHETIC SINGLE CRYSTAL CORUNDUM AT ROOM TEMPERATURE by J. B. Wachtman, Jr., W. E. Tefft, D. G. Lam, Jr. and R. P. Stinchfield (Natl. Bu. Stand.); J. Am. Ceram. Soc., Vol. 43, p. 334(L), June 1960

Elastic compliances and constants of single crystal corundum measured at 25°C by a resonance technique and at frequencies in the range 1 to 45 kc are tabulated. Values measured by other workers are also listed. There is disagreement between the old and the new values, but the latter are believed to be correct.

8937 BEHAVIOR OF THE PRINCIPAL ELASTIC MODULI AND SPECIFIC HEAT AT CONSTANT VOLUME OF KCl AT ELEVATED TEMPERATURES by F. D. Enck (U. Maryland and Franklin and Marshall Coll.); Phys. Rev., Vol. 119, pp. 1873-1877, Sept. 15, 1960

Measurements of the adiabatic elastic constants of potassium chloride (KCl) have been made in the region 300°K to the melting point (1043°K) by a dynamical method developed by Balamuth. Recently determined values of the specific heat at constant pressure ($C_p$) have been used to calculate the isothermal values of the compressibility. Values of the specific heat at constant volume ($C_v$) have been obtained, using recent values of the coefficient of thermal linear expansion (α), the above mentioned values of $C_p$, and the isothermal compressibilities. The results indicate that there is a slight rise in $C_v$ above the Dulong-Petit value above 725°K. This rise is not significant, since the estimated error interval incloses the Dulong-Petit value, and consequently the D-P law is most likely valid up to the melting point.

8938 THE TEMPERATURE DEPENDENCE OF THE YIELD STRESS OF NaCl CRYSTALS by C. W. A. Newey and P. L. Pratt (Imperial Coll.); Acta Cryst., Vol. 13, p. 1113(A), Dec. 1960

The yield stress of single crystals of NaCl, of high purity and also containing known concentrations of $Cd^{++}$ and $Ca^{++}$, has been measured in compression over the temperature range -196° to 550°C. After annealing at 650°C and slowly cooling, the yield stress of the pure crystals was found to decrease rapidly as the temperature was increased from -196° to 0°C, (450 g $mm^{-2}$ to 60 g $mm^{-2}$), and then more gradually at higher temperatures. A 0.1 proof stress varied in a similar way except that a wide peak occurred between 200° and 400°C. Crystals containing 0.05 at. per cent $Cd^{++}$ were translucent after a slow cool from 650°C, and electrolytic conductivity and density measurements showed that some of the $Cd^{++}$ was in precipitate form. These crystals had increased yield stresses at all testing temperatures, (e.g., 750 g $mm^{-2}$ at room temperature), and a maximum of 1300 g $mm^{-2}$ was observed at 265°C. After an aircool from 300°C, the crystals were transparent and their yield stress was increased further, by about 500 g $mm^{-2}$, at temperatures below 300°C; a maximum of 1700 g $mm^{-2}$ occurred at 240°C. A similar addition of $Ca^{++}$ produced no obvious precipitation; the room temperature yield stress of both slowly-cooled and air-cooled crystals was about 4000 g $mm^{-2}$ and a peak at higher temperatures was not observed.

8939 A LOW TEMPERATURE YIELD INSTABILITY IN IRON by J. B. Lean (Central Res. Labs., N.S.W.); Austl. J. Phys., Vol. 13, pp. 359-375, July 1960

The testing of polycrystalline specimens of a 0.07 per cent C steel in tension at liquid air temperatures is described and the results are analyzed. Under particular conditions of temperature and strain rate, following the upper yield point, the recorded stress descended below the lower yield stress, then returned to the lower yield stress quasi-elastically, thus forming a serration of the stress-strain curve. The magnitude of the serration depended on the difference between the upper and lower yield stresses, on the rigidity of the testing machine employed, and on the applied strain rate. In the discussion the mechanical stability of the tensile test during the yield point load drop is examined. The effect of adiabatic temperature increase in specimens deformed at low temperatures in boiling liquids is also discussed.

Effect of Dislocations on:
the Deformation Properties of Solids - See 8599, 8602
Hardening in Crystals - See 8600, 8601, 8606

Annealing of X-Ray Induced Surface Hardening in NaCl - See 8650

8940 ACOUSTIC ATTENUATION IN SINGLE CRYSTAL LiF AND POTASSIUM CHROME ALUM by M. H. Norwood (Rice Inst.); Bull. Am. Phys. Soc., Ser. II, Vol. 5, p. 105(A), Mar. 4, 1960

Sound attenuation studies at high frequencies in single crystals of dielectrics were described. The measured apparent attenuation in LiF (of order 2 db/echo) seems to be almost independent of frequency from 10 mc to 90 mc and of temperature from 150°K to room temperature. It is believed that this apparent attenuation can be attributed not to the LiF specimen but almost entirely to the binder and transducer interface, diffraction, and other corrections. The intrinsic attenuation is too small to be measured accurately by the pulse technique. This result is not surprising in view of another measurement and indicates that LiF may be used as a zero loss medium for studying the effects causing the apparent attenuation. Much larger attenuation (of order 12 db/echo) has been observed in a paramagnetic salt, potassium chrome alum. Preliminary results indicate that an interesting behavior of attenuation as a function of temperature may exist.

8941 EXCITATION AND ATTENUATION OF HYPERSONIC WAVES IN QUARTZ by H. E. Bommel and K. Dransfield (Bell Labs.); Phys. Rev., Vol. 117, pp. 1245-1252, Mar. 1, 1960

A method for the generation and detection of hypersonic waves is discussed in some detail together with some absorption measurements in quartz. Further measurements of the hypersonic absorption in quartz at different crystal orientations and after neutron irradiation are reported. The results are in qualitative agreement with the phonon-phonon relaxation process.

8942 PHOTOSENSITIVE ULTRASONIC ATTENUATION IN CdS by H. D. Nine (Genl. Motors); Phys. Rev. Lett., Vol. 4, pp. 359-361(L), Apr. 1, 1960

The effect of white light radiation on ultrasonic wave propagation in CdS single crystals is discussed. In one crystal (B) the ultrasonic attenuation at 5800A increased linearly with light intensity and in another crystal (A) decreased linearly with light intensity. These attenuation effects differed by an order of magnitude. Compressional waves propagated along the c-axis over the frequency range 10 to 200 Mc were used. Ultrasonic attenuation and photoconductance were measured simultaneously as a function of wavelength. The ultrasonic attenuation effect was observed over the same wavelength region as the response region for the photoconductance effect. The attenua-

tion effect was quenched to the dark value by infrared radiation in crystal B but not in crystal A. Little difference was found between the two crystals by means of a semiquantitative spectrographic analysis. Two possible mechanisms for the ultrasonic attenuation changes are presented.

8943 ANOMALIES IN INTERNAL FRICTION AND MODULUS OF ELASTICITY IN FERROMAGNETICS NEAR THE CURIE POINT by K. P. Belov, G. I. Kataev and R. Z. Levitin (Moscow State U.); Soviet Phys.-JETP, Vol. 10, pp. 670-673, Apr. 1960

The temperature dependence of Young's modulus and internal friction measured in elinvar (Fe-Ni-Cr) and coelinvar (Fe-Co-Cr) alloys, and in nickel and nickel-zinc ferrite is discussed. An internal friction peak, a jump in Young's modulus, and an effect of the magnetic field on the dynamic Young's modulus have been detected near the Curie point in alloys possessing the large paraprocess magnetostriction. It is shown that these phenomena are due to redistribution of spins within the domains induced by elastic stresses.

8944 INTERNAL FRICTION IN SYNTHETIC QUARTZ by C. S. Brown (GE); Proc. Phys. Soc., Vol. 75, pp. 459-460, Mar. 1960

Measurements of internal friction in synthetic quartz as a function of growth rate are discussed. Crystals were grown at rates varying from 0.10 to 0.55 mm/day. It was found that the internal friction in synthetic quartz approaches that in natural quartz at growth rates below 0.15 mm per day. In crystals grown on different seed orientations by slightly varying processes it was found that the losses were relatively independent of the growth process for a given growth rate. For applications such as frequency standards where highest possible Q is required, the crystals should be grown at low growth rates.

8945 INTERNAL FRICTION IN GERMANIUM AND SILICON. Part I. ELECTRON AND IMPURITY RELAXATION by P. D. Southgate (Mullard Res. Labs.); Proc. Phys. Soc., Vol. 76, pp. 385-397, Sept. 1960

The internal friction of single crystal silicon and germanium at 100 kc/s shows a relaxation peak near 0.56 of the melting temperature. The peak is electronic in origin and the relaxation time is the carrier lifetime. At the peak temperature, in many of the specimens measured, intrinsic recombination and intrinsic conduction are the dominant mechanisms, and the peak height at any given frequency depends only upon specimen orientation. If impurities are introduced so that the extrinsic lifetime becomes less than the intrinsic lifetime at the peak temperature, then the peak height is reduced. From the shape of the electronic peak and from its shift with frequency, the temperature variation of both intrinsic and extrinsic lifetime may be deduced. The activation energy of recombination of carriers in silicon appears to be 1.45 ev and in germanium about 1.15 ev, although it is difficult to reconcile these values with existing theories. The height of the peak gives the deformation potential constant; in silicon it is 2.3 ev and in germanium 6.5 ev per unit dilatational strain, which values are of the same order as those derived from hydrostatic measurements. In silicon crystals containing oxygen, having a [111] vibration axis, an internal friction peak appears at 1030°C (100 kc/s). The peak is not present if the silicon is oxygen free or has a [100] axis, and can be attributed to the movement of dissolved oxygen. The activation energy is 2.55 ev. The peak height varies, but in most crystals grown from silica crucibles the maximum logarithmic decrement is of the order $3 \times 10^{-4}$. In germanium a small peak appears in some specimens at 770°C (100 kc). No reduction of its height has been observed on annealing and its shape is consistent with that of impurity relaxation.

8946 INTERNAL FRICTION IN GERMANIUM AND SILICON. Part II. OXYGEN MOVEMENT AND DISLOCATION DAMPING by P. D. Southgate (Mullard Res. Labs.); Proc. Phys. Soc., Vol. 76, pp. 398-408, Sept. 1960

Measurements of the magnitude of electronic and oxygen impurity relaxation peaks in single crystal silicon yield values for the extrinsic carrier lifetime and the relative oxygen concentration, respectively. This method is used to study the production of recombination centers associated with oxygen impurity, and the internal precipitation of oxygen. Recombination centers are induced when oxygen-containing silicon is cooled rapidly from above 1000° to 650°C, reducing the lifetime to less than 0.35 μsec, which then recovers at a rate which increases with successive heat treatments. Precipitation onto internal particles at 1025°C occurs in the order of 3 hours for 2.7 Ωcm aluminum-doped silicon, and considerably longer for a purer sample, indicating that aluminum acts as an efficient precipitation nucleus. A 2 per cent plastic deformation of the aluminum-doped specimen does not greatly reduce the precipitation time. Analysis of the precipitation curve form indicates that stresses around the precipitate particles may be important in determining the precipitation rate. Dislocation relaxation produces a rise in internal friction at elevated temperatures, an activation energy of 1.1 ev in germanium and 1.5 ev in silicon being associated with the rise. In silicon and germanium specimens which have been plastically deformed by about 2 per cent the process becomes predominant above 0.6 of the melting temperature. Undistorted ('as-grown') specimens show a rise at higher temperatures, which varies in magnitude between specimens, and which could be due to the same process as that in deformed specimens. Oxygen in silicon appears to inhibit the loss process. Experimental results are discussed in the light of three possible theories, and it is concluded that there is insufficient evidence to indicate which one is applicable.

8947 MECHANICAL DAMPING OF GERMANIUM AND SILICON CONTAINING IMPURITY OXYGEN by P. D. Southgate (Mullard Res. Labs.); Solid State Phys. in Electronics and Telecommun., Vol. 1, Academic Press, 1960, pp. 240-250

Measurements of internal friction in Ge and Si made over the temperature range of 100°-1300°C and the frequency range of 100 to 300 kc are reported. The log decrement $\Delta = \frac{\pi}{Q} = \frac{\delta W}{W}$ (where $\delta W$ is the loss per cycle of mechanical energy W) is found. Values of $\Delta$ are very low and changes in the elastic constant associated with the loss peak were difficult to measu

# SOLID STATE DEVICES

## DIODES AND RECTIFIERS

### POINT CONTACT

8948 ON THE QUESTION OF THE ELECTRICAL SHAPING OF POINT GERMANIUM DIODES [in Russian] by V.M. Lavrika, S.S. Gutin, V.M. Matoshin, and M.G. Serbulenko (Novosibirsk Electrotek. Inst.); Izv. VUZ Fiz., No. 4, pp. 103-106, 1960

The physical phenomena involved in the electrical shaping of whiskers for point contact Ge diodes are discussed and the use of stepped current pulses is described. Diodes with predetermined parameters may be fabricated by this method.

8949 ELECTRICAL CHARACTERISTICS OF DIODES by C.W. Mueach and R.L. Crone (Hughes Aircraft); U.S. Pat. 2,894,184, Issued July 7, 1959

The fabrication of point contact diodes with high reverse voltage by electrically forming a point contact touching the semiconductor surface and simultaneously covering the resulting p-n junction with an insulating coating is described. In an example a Mo wire coated with successive layers of In and Ge is brought into contact with an n-type Ge wafer and an electrical forming current is passed through the whisker and crystal. The In produces a p-type region in the n-type semiconductor adjacent to the point contact and the $GeO_2$ on the surface of both the wafer and the layer of Ge on the whisker forms a continuous insulating layer over the p-n junction at the surface.

8950 CRYSTAL RECTIFIERS by M.C. Waltz (Bell Labs.); U.S. Pat. 2,835,810, Issued May 20, 1958

A technique for increasing the bandwidth of a microwave diode by improving the impedance match of the diode is described. The impedance of the whisker wire contact can be reduced by increasing its capacitance and reducing its inductance. Inductance is reduced by using a c-bend rather than an s-bend in the lead, since the c-bend is shorter. Capacitance is increased by enclosing the whisker in a rectangular metal channel, with the plane of the c-bend in a plane through the center of the channel in its long direction. Capacitance is further increased by filling the channel with a material having a high dielectric constant.

Whisker Mounting on Point Contact Diodes - See 9016

8951 CALORIZED POINT CONTACT ELECTRODE FOR SEMICONDUCTING DEVICES by T.E. LeLoup (GE); U.S. Pat. 2,861,230, Issued Nov. 18, 1958

Fabrication of Pt or W whiskers for Al bonded diodes is described. Pointed and shaped whiskers are placed in a 10 - 20 per cent Al-$Al_2O_3$ mixture and heated in a nonoxidizing atmosphere at 400°-600°C. The whiskers are then removed and reheated in a nonoxidizing atmosphere at 800°-1000°C. Diodes are formed by pulsing for 0.25 sec at 40 volts. A decrease in forward voltage was observed in n-type bulk point contact diodes employing the Al-coated whiskers.

8952 GLASS SEALED CRYSTAL RECTIFIER by J.N. Carman, Jr. (Pacific Semicon.); U.S. Pat. 2,881,369, Issued Apr. 7, 1959

The fabrication of an hermetically sealed point contact rectifier is described. A subassembly consisting of a semiconductor crystal soldered to a metal plug is inserted into one end of a glass cylinder which has Kovar-glass seals at each end. The plug, which is crimped to the Kovar, is made of a metal which has both high thermal and electrical conductivities such as Cu. The plug is clad with a layer of a metal which welds easily to Kovar. Another subassembly consisting of another metallic plug with an attached point contact is inserted into the other end of the glass cylinder and crimped. The device is sealed by seam welding the plugs to the Kovar. The resulting heat is not high enough to harm the device. Detailed descriptions of all the steps in the fabrication process are given.

8953 SEMI-CONDUCTOR ELECTRODE SYSTEM by W.A. Roovers and O.L.V. Steenis (Philips); U.S. Pat. 2,835,853, Issued May 20, 1958

A technique for the fabrication of glass packaged point contact diodes which feature increased heat dissipation is described. In order that the chip be mounted close to the package end in a glass diode body, it is first alloyed to a fabricated metal base plate and the base plate is then soldered to the end of the projecting lead. The fabricated plate has a socket on one face for attachment to the lead and projecting metal fingers that contact the insides of the glass body. The plate is soldered to the lead by heating the external end of the lead, with the chip and plate resting on a jig.

### JUNCTION

8954 HIGH FREQUENCY NEGATIVE RESISTANCE DEVICE by W.T. Read, Jr. (Bell Labs.); U.S. Pat. 2,899,652, Issued Aug. 11, 1959

Four-layer high frequency negative resistance diodes are described. Negative resistance is achieved by the phase shift between current and voltage due to the transit of field generated charge carriers across a space charge region. The field must be distributed so that the hole-electron pairs are generated in a limited region and the carriers should move through the space charge region with an average transit time which results in a negative product of current and voltage. The latter criterion requires that the average charge carrier transit time in the space charge region be greater than one-half a cycle and less than one cycle when the carriers are generated only at the maximum of an applied signal. In this case maximum negative resistance is obtained when the average transit time in the space charge region is three quarters of a cycle.

8955 PROPERTIES OF HEAVILY-DOPED GERMANIUM AND NARROW p-n JUNCTIONS by L. Esaki (Sony Corp., Tokyo); Solid State Phys. in Electronics and Telecommun., Vol. 1, Academic Press, 1960, pp. 514-523

The preparation of heavily doped uniform Ge single crystals and the fabrication of narrow alloyed p-n junctions from this material are discussed. Data on the current voltage characteristics and junction width are given. The current-voltage curve shows inverted rectification and negative resistance characteristics which would enable the realization of low-level, high-speed switching and oscillator devices. The junction has no transit or minority storage time since the negative resistance does not rely on the minority carrier mechanisms involved in transistor-like device operation; the junction is also independent

of ambient gas and incident light and is relatively insensitive to temperature variations.

8956 GALLIUM ARSENIDE TUNNEL DIODES by K.G. Hambleton, J.J. Low, and R.J. Sherwell (Services Electronics Res. Lab.); Nature, Vol. 185, pp. 676-677(L), Mar. 5, 1960

The characteristics of GaAs tunnel diodes fabricated by alloying tin pellets ranging in diameter from 0.003 to 0.015 inch are discussed. The diodes exhibit negative resistances of between 0.1 and 4 Ω and peak currents from 70 ma to 7 amp. Peak to valley current ratios as high as 30:1 have been observed, with the average value being about 15:1. The voltages at which the peak and velley currents occur are found to vary from device to device. The diodes switch across the unstable negative resistance region in less than 1 nμsec. Relaxation oscillations are observed in diodes mounted in a strip line designed to resonate at 400 Mc. The fundamental frequency varies with dc bias voltage between 360 and 560 Mc and in all cases harmonics have been observed up to 1 kMc, the limit of the receiver. 5 mw of output power has been obtained.

8957 TEMPERATURE DEPENDENCE OF TUNNEL DIODE CHARACTERISTICS by Y. Furukawa (Electrical Commun. Lab., Tokyo); J. Phys. Soc. Japan, Vol. 15, p. 1130(L), June 1960

The temperature dependence of the maximum current $I_{max}$ in the forward direction for As- and Sb-doped Ge tunnel diodes is discussed. Measurements verified the theoretical prediction that $I_{max}$ has a positive temperature coefficient at low temperatures and that the temperature dependence decreases as the carrier concentration increases. The temperature coefficient of the energy gap was found to be $\beta = 3.7 \times 10^{-4}$ ev/°K in the Sb-doped sample. Appreciable differences in the characteristics of Sb- and As-doped diodes were observed. For the same electron concentration and at room temperature, the Sb-doped diode shows positive temperature dependence while the As-doped diode shows negative dependence. Differences are tentitively regarded as due to the degeneracy of the conduction band.

8958 ELECTRICAL PROPERTIES OF HEAVILY DOPED N-TYPE GERMANIUM by Y. Furukawa (Electrical Commun. Lab., Tokyo); J. Phys. Soc. Japan, Vol. 15, p. 1903(L), Oct. 1960

The electrical properties at 4.2°K of tunnel junctions fabricated in Ge doped with both As and Sb are discussed. Indirect tunneling associated with longitudinal acoustic phonons has been observed in samples in which the ratio of the As concentration to the total donor concentration, r, is very much larger than 0.2 and the As concentration is $\sim 10^{19}$ cm$^{-3}$. No tunneling associated with transverse acoustic phonons has been observed. The relation between resistivity and electron concentration was also investigated in As-Sb-doped crystals with different values of r.

8959 SEMICONDUCTOR NONLINEAR CAPACITANCE DIODE by A. Uhlir (Bell Labs.); U.S. Pat. 2,884,607, Issued Apr. 28, 1959

The fabrication of a high power nonlinear capacitance diode having high impedance at microwave frequencies is described. The diode has 12 alternating p- and n-type regions, although any number, odd or even, of regions may be used. The junctions are alternate graded and semi-step junctions. The device is formed by rate growing, each region being 0.007 inch thick and the completed diode being only 0.012 inch thick. Ohm contacts are made to the two end regions. Under suitable bi the space charge extension across the graded p-n junction de creases its capacitance faster than the space charge decrease across the abrupt n-p junction increases its capacitance. Th multiple junctions increase the impedance and nonlinearity.

8960 OPTIMUM FIGURES OF MERIT OF VARACTORS by H. G. Rudenberg (Transitron); Proc. NEC, Vol. 15, pp. 79-82, Oct. 12-14, 1959

Practical designs which maximize the F = nQf product or fig of merit of diodes are described. Semiconductor and ferroelectric voltage variable capacitors (varactors) have general been characterized by their capacitance-voltage coefficient n and by their circuit Q at a given frequency f. As most cir cuit applications involve trimming or padding with low-loss capacitors, it can be shown that a low-Q varactor of large voltage coefficient can give results equivalent to a high-Q varactor of small voltage coefficient. These concepts lead t special diffused semiconductor designs having very high capa itance-voltage coefficients. A high figure of merit is achie by different approaches in low frequency and very high frequ cy circuits, depending on the circuit requirements for n, Q, and equivalent varactor series resistance. Design considerations provide useful junction structures for low capacitance microwave parametric amplifier diodes, for audio-frequency capaciture modulators, and for intermediate ranges of frequencies.

8961 SPACE-CHARGE-LIMITED CURRENTS IN CYLINDRIC AND SPHERICAL INSULATOR DIODES by B. Meltzer (U. Edinburgh); J. Electronics Control, Vol. 8, pp. 171-176, Mar. 1960

Equations for space-charge-limited currents in cylindrical a spherical diodes are derived. The equations are then used t calculate space-charge-limited currents in cylindrical and spherical diodes fabricated from pure CdS, for which the mo bility and permittivity are taken as 0.01 m$^2$/v-sec and $10^{-8}$/ $36\pi$ f/m, respectively. The space charge limited currents i planar diodes are also calculated. For planar, cylindrical, and spherical diodes with anode-cathode spacing of 80 μ, curr of 0.70 a/cm$^2$, 3.2 a/cm$^2$, and 12.0 a/cm$^2$, respectively, v calculated.

8962 ON THE INDUCTIVE CHARACTER OF P-N JUNCTIO DIODE IMPEDANCE AT HIGH CURRENT DENSITIES IN THI FORWARD DIRECTION by L.I. Baranov (Saratov State U.); Radio Engrg. Electronics, Vol. 5, No. 6, pp. 173-179, 19

The voltage transient caused by the inductance of a p-n junc tion diode switched into the forward direction at high curren densities is analyzed. The inductance is caused by the varia tion of the semiconductor bulk conductivity by the injected carriers. It is found that the magnitude of the peak and the duration of the voltage decline to steady-state value increas with increase of $L_0/L$, where $L_0$ is the distance between the junction and the ohmic contace and $L = \sqrt{D_p \tau\, 2b/b+1}$, wi $b = \mu_n''/\mu_p$. This agrees with experimental data. The analy also shows that under the conditions considered the leading trailing edges of the transient will be different. This differe has been observed experimentally.

8963 HIGH FORWARD CURRENT FLOW IN JUNCTION DI ODES by A.K. Jonscher (GE Ltd.); Solid State Phys. in Ele tronics and Telecommun., Vol. 1, Academic Press, 1960, p 524-531

The theory of current flow at high-injection levels in junction diodes is discussed. The proposition that the high-injection-level flow of current in a p-n junction is space-charge limited is confirmed by a number of experimentally observed facts. Kinks in the square root of the current vs the voltage ($I^{1/2}$ vs $V$) characteristics at low temperatures are discussed. A pulse technique of measuring the characteristics without heating the specimens is described.

8964 LOW REVERSE LEAKAGE GALLIUM ARSENIDE DIODES by J. Halpern and R.H. Rediker (Lincoln Lab.); Proc. IRE, Vol. 48, pp. 1780-1781(L), Oct. 1960

Diffused mesa GaAs diodes which exhibit reverse leakage currents between $10^{-12}$ and $5 \times 10^{-11}$ amp and rectification ratios above $10^{10}$ are discussed. The current-voltage characteristics of two diodes are presented. The forward current in both shows an exp(qv/2kT) voltage dependence over a relatively large range of voltage. In one the rectification ratio at 2 v is $1.3 \times 10^{10}$ and in the other it is $2.5 \times 10^{11}$. Calculations utilizing the space charge generated saturation current determined from these measured characteristics indicate a carrier lifetime of the order of $1 \times 10^{-9}$ sec. The voltage-current characteristics were measured as a function of ambient and temperature. The lowest reverse currents have been obtained in dry nitrogen or in vacuum. Exposure to dry oxygen increases the reverse current by an order of magnitude and exposure to wet nitrogen increases it by three to four orders of magnitude. The original low reverse currents can be restored by vacuum baking. The fabrication of the devices is described.

8965 REVERSE CURRENT JUMPS IN P-N JUNCTION SILICON DIODES by R. Mutabzija (Inst. Ruder Boskovie, Zagred); Solid State Phys. in Electronics and Telecommun., Vol. 1, Academic Press, 1960, pp. 532-540

Measurements on the reverse dc current-voltage characteristics of a Si junction diode are reported. A negative slope near the saturation region of the I-V breakdown curve was observed. Oscillograph observations show that the negative slope was due to conduction instability or oscillation.

8966 EFFECT OF A STRONG FIELD IN GERMANIUM p-n JUNCTIONS [in Russion] by V.I. Gaman, V.A. Perkal'skaia and G.V. Kallestinov (SFTI, Tomsk U.); Izv. VUZ Fiz., No. 2, pp. 3-9, 1960

Voltage pulse measurements of the reverse currents in industrial diodes are analyzed. A rise in the reverse current was observed in strong electric fields ($E = 10^5$ v/cm) because of the Zener effect. The influence of the pulse duration on the reverse branch of the I-V characteristic has been detected in both weak and strong electric fields.

8967 MULTIPLICATION OF ELECTRONS AND HOLES IN p-n JUNCTIONS by B.M. Wul and A.P. Shotov (Phys. Inst. Acad. Sci., Moscow); Solid State Phys. in Electronics and Telecommun., Vol. 1, Academic Press, 1960, pp. 491-497

Theoretical considerations governing the multiplication of electrons and holes in p-n junctions are presented. Impact ionization has been studied by investigating the multiplication of additionally injected electrons or holes in the p-n junction. The multiplication of both electrons and holes has been measured by the same p-n diffusion junction, specially prepared for this purpose. The additional electrons and holes were injected by irradiation of the p-n junction through filters to cut off the long-wave part of the irradiation. The investigations of the p-n junctions in high electrical field gave evidence of the avalanche processes owing to the impact ionization in crystals.

8968 MAXIMUM AVALANCHE MULTIPLICATION IN P-N JUNCTIONS by D.J. Hamilton (U. Arizona); Proc. IRE, Vol. 48, pp. 1787-1788(L), Oct. 1960

Avalanche multiplication in reverse-biased junctions is analyzed. It is shown that the multiplication factor M has a maximum value $M_{max}$. The analysis indicates that $M_{max}$ is proportional to the ratio of the optimum bias current to thermally generated current with the junction temperature equal to the ambient temperature, and that at a given ambient temperature the optimum bias current for obtaining $M_{max}$ varies inversely with the breakdown voltage. A Ge junction with a breakdown voltage of 42 v, a thermally generated current of 5 μa at the ambient temperature, and a temperature coefficient of $0.5 \times 10^3$ °C/w has $M_{max}$ of ~ 40 and $I_{opt}$ of ~ 0.54 ma.

8969 1/f NOISE IN GERMANIUM DIODES by T.B. Watkins (Mullard Res. Labs.); Solid State Phys. in Electronics and Telecommun., Vol. 1, Academic Press, 1960, pp. 565-574

Experiments verifying current theories of 1/f noise in Ge filaments are described. Fast states and noise have been measured as a function of bias current and barrier height. The theories of McWhorter and Bess are explored by artificially varying the surface barrier height. A tentative explanation of 1/f noise in Ge devices is given on the basis of the experimental evidence.

Fabrication of Grown Junctions - See 8996

8970 SEMICONDUCTOR P-N UNITS AND METHOD OF MAKING THE SAME by R.N. Hall (GE); U.S. Pat. 2,822,308, Issued Feb. 4, 1958

A vertical technique for forming grown p-n junctions by variation of the crystal growth rate is described. Since the effective segregation coefficient of an impurity is dependent on the growth rate (temperature gradient) of the crystal, variation of the growth rate causes a variation of the effective segregation coefficient and consequently a variation in the conductivity of the crystal. To this end, a semiconductor melt is doped with sufficient quantities of opposite type dopes that the crystal, grown at some fixed rate, will be intrinsic. Variations above and below this growth rate will then cause the crystal type to be changed, forming a p-n junction.

8971 METHOD OF PREPARING SEMICONDUCTIVE MATERIALS by J.W. Rutter and W.A. Tiller (Canadian Patents and Development); U.S. Pat. 2,824,030, Issued Feb. 18, 1958

A technique for producing grown junctions and grown junction devices is described. The procedure is based on the impurity concentration build-up behind the freezing interface, in the absence of stirring. A semiconductor preform is doped with two impurities of opposite type and different segregation coefficient. The concentration of one impurity is less than that of the other impurity; the product of its concentration and segregation coefficient is greater than the corresponding product of the other impurity. A zone is grown, solidification is stopped and the liquid is stirred, thus producing a p-n junction and readying the system for another p-n junction.

8972 METHOD OF PRODUCING A SEMICONDUCTOR ALLOY JUNCTION by B.A. Leinfelder and L.D. Favro (Clevite); U.S.

Pat. 2,835,615, Issued May 20, 1958

A technique for fabricating large-area Ge alloy junctions for high-current rectifiers is described. A suitable metal base is placed in a carbon jig, covered with a preform of n-doped alloy (such as Pb-Sn eutectic), an n-type Ge chip, a thin In preform and a smaller diameter piece of Al foil. The stack is covered with a heavy carbon plug. As the assembly is heated in the furnace, the In wets the Ge and starts to dissolve. At the same time the Al starts to melt and mix with the alloy. The molten Al is an efficient scavenger of oxygen and effectively removes all oxygen or oxides from the system, allowing complete wetting of the In.

8973 FUSED JUNCTION SILICON SEMICONDUCTOR DEVICE by R.A. Gudmundsen (Hughes); U.S. Pat. 2,829,999, Issued Apr. 8, 1958

Fabrication of high injection efficiency alloy junctions in Si by the use of a boron doped Al impurity dot is described. Since boron has a higher melting point than Si, it cannot be alloyed directly. However, up to 3 per cent boron can be dissolved in Al. This concentration is sufficient (since the boron segregation coefficient is near unity) to give a heavily doped recrystallized region whose resistivity is constant with depth. The dot is placed on a chip and alloyed at some high temperature, after which it is cooled slowly to give a doped recrystallized region. The metal button is etched off after alloying.

8974 MICROALLOY JUNCTION FOR SILICON by L. Maissel (Philco); J. Electrochem. Soc., Vol. 107, pp. 933-934, Nov. 1960

The dip alloying technique for forming a microalloy junction in Si is discussed. The Si, with a dot of plated Sb on its surface, is plunged into a fused salt bath. A crust of the salt freezes on the surface of the cold Si when it enters the bath. Since the melting point of the bath is higher than that of Sb, the salt provides a tough close-fitting jacket which constrains the Sb long enough for it to undercut the oxide on the Si surface through pores in the oxide. Successful alloying has been obtained in both KCl and KBr baths.

8975 METHODS OF SURFACE ALLOYING WITH ALUMINUM-CONTAINING SOLDER by L.D. Armstrong and M.J. Bentivegna (RCA); U.S. Pat. 2,833,678, Issued May 6, 1958

A technique for fabricating Al doped alloy junctions that operate at high emitter efficiencies is described. A three-layer impurity disk, consisting of two outer layers of In-Cu (0.2 - 2 per cent) and a center layer of In-Al (1 - 2 per cent) is alloyed to the chip at 525°C in a nonoxidizing atmosphere. The outer In layer melts first and, with the help of the Cu, wets the chip before the center layer containing the Al melts. Thus the problems associated with wetting Al onto the chip are eliminated and the heavy doping advantages of Al are retained. Alternately a homogenous dot of In-Cu (2 per cent)-Al (1 per cent) may be used, but at some sacrifice in wettability.

Fabrication of:

Alloyed Junctions - See 8997, 8998, 8999, 9000
Alloy Diffused Junctions - See 9001
Alloyed Hook Junctions - See 9002 and 9003

8976 SEMICONDUCTIVE DEVICE AND METHOD OF MANUFACTURE by W.E. Bradley (Philco); U.S. Pat. 2,885,608, Issued May 5, 1959

The preparation of highly efficient rectifying surface barrier contacts on Si and Ge is discussed. The semiconductor is electrolytically etched with an electrolyte containing a metal which can produce the conductivity type opposite to that of the semiconductor. The polarities of the semiconductor and electrolyte are then reversed, causing the metal to be deposited on the electrolytically-produced oxide layer on the semiconductor surface. The metal is also incorporated substitutionally in the oxide layer. A detailed discussion of the physical mechanism responsible for the production of rectifying contacts by this technique is presented.

8977 GOLD-GERMANIUM EUTECTIC JUNCTIONS [in Polish] by J. Pultorak; Arch. Elektrotech., Vol. 9, No. 2, pp. 281-303, 1960

A technique for forming Au-Ge eutectic junctions in Ge with Au wire is described. A eutectic is formed at the end of a Au wire and then the wire is alloyed with the Ge. The shape and depth of penetration of the junctions formed by this technique can be readily controlled. Preparing microsections of the eutectic junctions and photographing the microsections are discussed.

Fabrication of:

Diffused Junctions - See 9004
Outdiffused Junctions - See 9006

8978 METHOD FOR PRODUCING JUNCTIONS IN SEMICONDUCTOR DEVICES by J.H. Myer (Hughes); U.S. Pat. 2,828,232, Issued Mar. 25, 1958

A technique for fabricating broad-area diffused ohmic and rectifying junctions in Si and Ge is reported. The prepared semiconductor chip is dipped in a molten salt of the impurity to be diffused and either heated in the salt for a given time or removed from the salt bath and heated in a container of carbon dust. Alternately, a dry salt may be melted on the chip surface and then heated in a container of carbon dust. The diffusion temperature should be as high as possible but less than the melting point of the crystal or the decomposition temperature of the salt.

Fabrication of Epitaxial Junctions - See 9007

8979 PROCESS FOR MAKING FUSED JUNCTION SEMICONDUCTOR DEVICES WITH ALKALI METAL-GALLIUM ALLOY by J.H. Myer and W.P. Waters (Hughes); U.S. Pat. 2,829,993, Issued Apr. 8, 1958

A procedure for fabricating alloy junction devices by the use of a self fluxing impurity dot is described. The impurity dot consists of a quantity of active impurity, an alkali metal or alkaline earth and, in some cases, a solvent metal. The dot is alloyed to the chip at elevated temperature in a nonoxidizing atmosphere, cooled and the solvent metal dot removed. Hence Ga is a particularly useful solvent metal although Bi, Th, and Pb may also be used. The active impurity may be the solvent metal in some cases. The alkali metal or alkaline earth reacts with the oxide on the semiconductor surface when the dot melts, allowing full wetting.

8980 SEMICONDUCTIVE ALLOYS OF GALLIUM ARSENIDE by D.A. Jenny (RCA); U.S. Pat. 2,830,239, Issued Apr. 8, 1958

A technique for the formation of GaAs-Ge alloys and device applications of the alloys are discussed. The alloys are prepared by heating pure Ge and GaAs in a sealed quartz tube at the melting point of GaAs and then gradient freezing at the end of the reaction. The energy gap was 1.25 ev in the composition range of 10-75 per cent Ge; the hole mobility was greater than that of GaAs. The as-prepared material was n-type and two phase structure exists in alloys containing more than 10 per cent Ge.

Ohmic and Rectifying Diffused Contacts - See 9010

8981 HIGH-TEMPERATURE BASE-TAB FOR SILICON by L. Maissel (Philco); J. Electrochem. Soc., Vol. 107, pp. 1007-1009, Dec. 1960

A contact to Si which can be utilized at temperatures exceeding 800°C is described. A tab of Mo is plated first with Pt and then with a layer of Ni. The thickness of the Ni layer is about a third the thickness of the Pt layer. The contact is made by heating the Si in contact with the Mo in an inert atmosphere. The pressure between the two is provided by two tungsten probes pressing on the Mo tabs. A heating current also passes between the two probes. Optimum results were obtained by heating at ~1000°C for 10-15 sec. Low resistance ohmic contacts were obtained with p-type Si but not with n-type Si. The mechanism responsible for the production of strain-free ohmic contacts which can be temperature cycled is discussed.

8982 TREATMENT OF TANTALUM SEMICONDUCTOR ELECTRODES by V. Sils (Westinghouse); U.S. Pat. 2,957,112, Issued Oct. 18, 1960

A method of improving the wetting characteristics of Ta components of semiconductor devices is described. The method involves precoating the Ta to a thickness of 10-500 x $10^{-6}$ in with a vaporized metal selected from the group Au, Ag, In, and Sn. A description of the vacuum deposition process is included. Most satisfactory coating resulted when temperatures from 1200° to 1500°C were used for 3-7 minutes at pressures of $10^{-4}$ mm Hg.

Stabilization of Junctions - See 9012

8983 SEMICONDUCTOR DIODE by F.L. Howland and J.W. West (Bell Labs.); U.S. Pat. 2,897,419, Issued July 28, 1959

A production line technique for sealing junction diodes in hermetically-sealed containers is described. A subassembly is first constructed by brazing an insulating ceramic washer between a nickel base and a nickel washer. The ceramic washer is concentric with a hollow cylinder at the center of the base. A diode is dropped into the hollow cylinder and a cover is sealed on the subassembly by thermocompression bonding. The thermocompression bonding also produces ohmic contacts between the diode and projections from both the base and cover.

8984 DIODE by G. Eannarino (Sarkes Tarzian); U.S. Pat. 2,958,020, Issued Oct. 25, 1960

A method for readily connecting a diode into a circuit without the use of tools and insuring easy replacement and proper polarity is described. The assembly of a suitable diode having a tubular insulating housing whose opposite ends have dissimilar extending terminal members capable of fitting into correspondingly dissimilar spring clips of a connector is discussed. The spring clips are substantially U-shaped and are spatially and dimensionally arranged to provide a resilient contact to the diode while insuring a proper polarity-insertion of the diode.

8985 IMPROVEMENT OF SEMICONDUCTOR SURFACES BY LOW MELTING GLASSES, POSSIBLY FUNCTIONING AS ION GETTERS by S.S. Flaschen, A.D. Pearson, and I.L. Kalnins (Bell Labs.); J. Appl. Phys., Vol. 31, pp. 431-432 (L), Feb. 1960

Improvements in the reverse currents and breakdown voltages of diffused junction $n^+$-p diffused junction Si diodes produced by coating the devices with low-melting sulfide and iodide inorganic glasses are discussed. Diodes were etched and washed and the reverse currents were measured at ~80 per cent of the breakdown voltage in a dark vacuum chamber. The diodes were then coated with glass and the reverse currents were remeasured. A reduction from $10^{-7}$ to $10^{-9}$ amp was observed. Another group of diodes was exposed to a mixture of deleterious vapors after etching and cleaning. The reverse currents after contamination were in excess of $10^{-6}$ amp and the breakdown voltages were erratic over the range 40 - 50 v. Immersion in a glass melt for 90 sec reduced the reverse currents to $10^{-8}$ from $10^{-7}$ amp and improved the breakdown voltages. Further aging of the diodes in the glass melts at 275°C reduced the reverse currents to $10^{-9}$ amp and raised the breakdown voltages to their full value.

## AREA CONTACT

8986 SELENIUM RECTIFIER AND METHOD OF MAKING SUCH RECTIFIER by R.B. Johnson (IBM); U.S. Pat. 2,832,014, Issued Apr. 22, 1958

Fabrication of a bank of coplanar Se rectifiers in a unitary flat assembly is described. A large Al blank is suitably stamped to provide a number of squares with contact tabs and interconnected with narrow strips. The plate is then coated with Se which is converted to the crystalline form. An insulating layer with square holes, slightly smaller than the Se squares, is placed on the Se side of the plate and another insulating layer is placed on the back of the plate. These layers are pressed into the plate, filling its depressions. Counter-electrodes are then sprayed through the square openings and the interconnecting strips are drilled out.

8987 COMPOSITE RECTIFIER ASSEMBLY by E. Lidow (Intl. Rectifier); U.S. Pat. 2,837,703, Issued June 3, 1958

A rectifier consisting of a series connected Se cell and a Ge cell is described. The composite rectifier is less susceptible to voltage surges than a Ge rectifier and less temperature sensitive than a Se rectivier. The Ge rectifier is packaged in the head of the mounting stud that then passes through the Se rectifier plate. In this construction the Se plate also functions as a heat radiator for the Ge rectifier. Pressure contact to the Se rectifier is made by a convoluted metal disk. Because its temperature characteristics more closely match Se, Ge is preferred to Si for this purpose.

AREA CONTACT (Cont'd)

8988 POWER TRANSMISSION by P.N. Caldwell (Vickers); U.S. Pat. 2,881,371, Issued Apr. 7, 1959

The fabrication of high voltage Se rectifiers which can operate at high temperatures is described. A layer of crystalline Se is deposited on a base plate of a metal such as Ni, steel, or Al. The layer may be formed by subjecting a layer of powdered, amorphous Se to heat and pressure to produce a partially crystallized layer which is then completely crystallized by heat treatment. A thin layer of a semiconducting sulfide, selenide, telluride, or a solid solution of at least two of these compounds is then evaporated on the Se layer. This layer may consist, for example, of the sulfides, selenides, or tellurides of Cd, Sn, Bi, Tl, Ge or solid solutions of these compounds. The evaporated layer is coated with a cellulose base lacquer, and the device is electrically formed.

8989 METAL OXIDE RECTIFIERS by R.D. Laughlin (U.S. Army); U.S. Pat. 2,827,401, Issued Mar. 18, 1958

Fabrication of CbO(NbO) rectifiers with large current capability and high temperature stability is described. A thin film of Cb metal is vacuum evaporated onto an inert metal base plate and given a partially reduced oxide coating by heating in water vapor for 3 hrs at 550°-600°C. Air oxidation produces a less suitable oxide. The counterelectrode is then electroplated onto the oxide layer from either a copper sulphate or silver cyanide bath. Rectifiers so constructed, with an area of 0.1 $cm^2$, had a forward resistance of 20 ohm at 1.3 v and a reverse resistance of 1.2 megohm at 5 v.

8990 ARSENIC TELLURIUM ALLOYS by B. Kopelman (Sylvania); U.S. Pat. 2,829,321, Issued Apr. 1, 1958

A technique for preparing microwave diodes and area rectifiers of polycrystalline As-Te alloys is described. The powdered elements, in 1-1 or 2-1 As-Te ratios, are heated in a carbon crucible with 0.5 per cent Sn in a neutral atmosphere or vacuum at 550°C for 2 hrs. One face of the resultant crystal is then polished and this surface is contacted with either a pointed whisker or a soft metal plate. The device is a barrier layer rectifier whose rectification ratio is improved by the addition of Sn or other element from Group IV or VII. The rectifiers feature high reverse breakdown and current capacity.

8991 ENCAPSULATED SELENIUM RECTIFIERS by L.W. Burton and J.R. Thurell, Jr. (GE); U.S. Pat. 2,883,592, Issued Apr. 21, 1959

The encapsulation of Se rectifiers which can eliminate shorts between the counter-electrode and the Al baseplate as they occur is described. A Se rectifier stack is coated with a thin silicon oil so that the counterelectrodes are completely covered by the oil. The oil is allowed to dry to form a film on the counterelectrode surfaces. The coated stack is then placed in a mold which is heated to about 100°C. An epoxy resin which has the same coefficient of thermal expansion as the Al baseplate is heated to between 45° and 60°C and poured into the heated mold. The ends of the stack are left exposed in order to make electrical connections. The resin is cured and the rectifier is cooled before it is removed from the mold. The same technique can be used with copper oxide rectifiers.

8992 SOLID METALLIC RECTIFIER by J.L. Bonanno (Lionel); U.S. Pat. 2,966,620, Issued Dec. 27, 1960

An economical solid metallic rectifier utilizing inexpensive spacers and leads, and enabling simplified plug-in connection is described. Uniform distribution of pressure on the rectifier plates is achieved by the use of a spring washer. Rigid input and output leads extending in substantially the same direction are used.

## TRANSISTORS

### GENERAL

8993 CIRCUIT FOR MEASURING ALPHA OF TRANSISTORS by G. Raisbeck (Bell Labs.); U.S. Pat. 2,897,448, Issued July 28, 1959

A circuit for accurately determining the magnitude and phase angle of a at any frequency is presented. An alternating current is applied to a transistor in a grounded-emitter configuration having a small load. This current is passed through a variable impedance across which is developed a voltage out of phase with the voltage across the load. By varying the impedance, the net voltage across the load and variable impedance, connected in series, is reduced to zero. When a null is obtained, the magnitude and phase angle of a may be determined from an expression involving only the values of the load resistor and the impedance. The magnitude and phase angle of a may be obtained for any desired frequency in a relatively broad band merely by substituting the desired frequency in the aforementioned expression.

### POINT CONTACT

8994 ELECTRODE SYSTEM by P.J.W. Jochems and L.J. Tummers (N.A. Philips); U.S. Pat. 2,887,631, Issued May 19, 1959

The preparation of fixed distance, closely spaced, rigid point contact assemblies for use in point contact transistors is discussed. The point contacts are kept a fixed distance apart by means of an insulating bridge, e.g., by a bead formed from a droplet of polystyrene in benzene. The spacing is first set by placing the thin electrodes in a jig. The contacts are made resilient by bending them above the bridge. The fabrication of a pair of contacts from a single wire is described.

### JUNCTION

Current Flow in Junctions - See 8963

8995 ELECTRIC FIELD IN A SEMICONDUCTOR BETWEEN JUNCTIONS ACCORDING TO THE TYPE OF CONDUCTIVITY [in Russian] by Iu. S. Riabinkin (Tomsk Polytech. Inst.); Izv. VUZ Fiz., No. 2, pp. 140-147, 1960

An equation which describes the electric field distribution and the potential between fused p-n or pi junctions for arbitrary injection levels is derived. An approximate solution of this equation is given under boundary conditions corresponding to a triode base. The potential, field, volume charge, minority carrier distributions and the field and diffusion components of the current along the base are found. The volt-ampere characteristic, the base transfer coefficient and the emitter efficiency are calculated.

Avalanche Multiplication in p-n Junctions - See 8967, 8968

Fabrication of Grown Junctions - See 8970, 8971

8996 GROWN JUNCTION TYPE TRANSISTORS AND METHOD OF MAKING SAME by M.E. Jones and W.A. Adcock (Texas Instr.); U.S. Pat. 2,845,372, Issued July 29, 1958

The fabrication of a grown junction n-p-n Si transistor is described. The collector region is grown first by pulling a seed from a melt containing Sb-doped Si. A thin p-type base region is then grown by adding sufficient Al to the melt and the emitter region by adding sufficient As to the remaining melt. The crystal is cut into bars about 0.040" x 0.040" by 0.200" containing all three regions. The bars are etched in a mixture of hydrofluoric acid, nitric acid, acetic acid, and bromine to delineate the three regions and electrodes are attached to each region. Following the etch, the emitter appears shiny, the collector rough, and the base as a definite line between them.

Fabrication of Alloyed Junctions - See 8972, 8973, 8974, 8975

8997 JUNCTION TYPE SEMICONDUCTOR DEVICE AND METHOD OF ITS MANUFACTURE by C.W. Mueller (RCA); U.S. Pat. 2,836,522, Issued May 27, 1958

A technique for fabricating high frequency Ge alloy p-n-p transistors with low collector capacitance and flat junctions with thick transition regions is described. The technique is based on the addition of 2-6 per cent Al to In and utilization of this alloy as the dot material. The disk-shaped dots are alloyed at 500°-525°C for 3-5 min. A chip 0.002 thick is used and the collector dot, 0.005 x 0.025 diam, is first soldered on at 450°-500°C for 1 min followed by alloying of the collector and an 0.005 x 0.010 diam emitter. The Al diffuses to give a thick transition region and forms a flat junction whose penetration is more easily controlled than in the case of pure In.

8998 FUSED JUNCTION TRANSISTORS WITH REGROWN BASE REGIONS by J.N. Carman, Jr. (Hughes); U.S. Pat. 2,821,593, Issued Jan. 28, 1958

A technique for fabricating point contact and alloy junction Ge transistors whose base region is a recrystallized layer is described. A suitable dot containing an impurity of the type opposite that of the wafer is alloyed into the wafer in a box containing an inert gas. The alloying is accomplished by a heater placed slightly above the dot. When the wafer is cooled slowly, 10°/min, most of the Ge is regrown on the wafer. Contact wires may then be put on the base for emitter and collector or emitter and collector dots may then be alloyed to the regrown region. These dots or the base dot may be alloyed with Ge first to limit penetration.

8999 SEMICONDUCTOR TRANSLATING DEVICE by R.A. Gudmundsen and J. Maserjian (Hughes); U.S. Pat. 2,834,701, Issued May 13, 1958

A technique for fabricating multiple Si p-n-p transistors, with increased mechanical strength, on a single wafer is described. An 0.015 Si chip is alloyed with a regular pattern of Al collectors, the excess Al is etched off and a solderable contact is fused to the recrystallized region. The collector face of the wafer is then gold-eutectic alloyed to another 0.015 degenerate Si wafer having holes in register with the collectors. The opposite face of the original chip is lapped to 0.005 and emitters are alloyed opposite the collectors. The wafer is then cut into individual transistors. The degenerate backing plate is used as the base contact.

9000 SEMI-CONDUCTOR DEVICE by P.J.W. Jochems (Philips); U.S. Pat. 2,926,290, Issued Feb. 23, 1958

Fabrication of alloy junction semiconductor devices whose leads are integral with the junctions is described. The junctions are formed by alloying nonhomogenous wires of the proper diameter. The wires consist of a high melting metal and a low melting metal in intimate contact. This construction may be achieved by cladding, coring, electroplating or tinning. Lengths of the composite wire are alloyed to the opposite faces of the chip or the wire may be formed into a ring with the chip slipped between its open ends. The low melting metal melts and alloys while the high melting metal maintains the shape of the wire.

9001 METHOD OF MAKING JUNCTION TRANSISTORS by R.L. Longini (Westinghouse); U.S. Pat. 2,836,520, Issued May 27, 1958

A technique for fabricating alloy diffused junctions and devices utilizing these junctions is described. The basis of the technique is gradient cooling of the molten dot to deposit a thin layer of recrystallized semiconductor, doped to the conductivity type of the molten dot, and subsequent diffusion of this impurity into the semiconductor body. The gradient cooling is accomplished by making the thermal mass on top of the dot greater than the mass under the chip, so that the chip is cooler than the dot. Uniform dot wetting is extremely important and is accomplished by very slow heating, by plating the semiconductor before alloying or by adding semiconductor to the dot.

9002 HOOK COLLECTORS AND METHOD OF PRODUCING SAME by R.L. Longini (Westinghouse); U.S. Pat. 2,836,521, Issued May 27, 1958

Fabrication of alloy diffused hook collectors is described. A dot consisting of a rapidly diffusing element doping one conductivity type and a slow diffusing element doping the opposite conductivity type in a matrix of a third metal (if necessary) is alloyed to a chip and gradient cooled slightly to form a thin double doped recrystallized region from which the two impurities diffuse to form two regions of opposite conductivity type under the dot, which retains the conductivity type of the nearest diffused region. Transistors with hook collectors, controlled rectifiers, and diodes with improved characteristics may be fabricated employing this technique.

9003 SEMI-CONDUCTOR DEVICES AND METHODS OF MAKING SAME by J.I. Pankove (RCA); U.S. Pat. 2,861,229, Issued Nov. 18, 1958

Techniques for fabricating hook electrodes and devices using such electrodes are described. In one case, a large In dot is alloyed into the surface of an n-type chip and the excess In is etched off. A smaller Pb-10 per cent Sb dot is then alloyed into the center of the In doped recrystallized region. By proper regulation of the alloying temperature, two closely spaced p-n junctions are thus obtained. This structure can be directly used as a high frequency n-p-n transistor or a p-doped emitter may be added to the other side to form a transistor with hook collector. A diffused structure of this type may be obtained if the dots are replaced by evaporated films.

9004 A P-N-P HIGH-FREQUENCY SILICON TRANSISTOR by W.A. Little (Texas Instr.); J. Electrochem. Soc., Vol. 107, pp. 789-791, Sept. 1960

The fabrication of double-diffused Si p-n-p high frequency transistors by means of oxide masking is discussed. A two step process is employed to produce a diffused n-type layer with a surface concentration between $10^{17}$ and $10^{19}$ atoms/cm$^3$. A thin concentrated n-layer is first deposited on a 1-3 ohm cm p-type wafer by an open-tube diffusion process. The source of phosphorus is then removed from the combustion tube and wet oxygen is used to grow an oxide layer 5000 - 8000 A thick. Diffusion of the n-layer to a depth of 4-5 μ occurs during growth of the oxide. Selected regions are then removed from the oxide mask by forming a photoresist on the surface and etching the exposed oxide. A p-layer 2-3 μ deep with a surface concentration of about $10^{20}$ atoms/cm$^3$ is then formed on the n-layer by the open tube diffusion process. Gold emitter and base stripes are evaporated through a mask and are alloyed by heating in an RF heater at about 750°-850°C. The wafers are then etched to form mesas and diced into squares. The collector is bonded to the header, leads are bonded to the emitter and base stripes, and the device is encapsulated. The electrical characteristics of a transistor fabricated by these techniques are presented.

9005 TRANSISTOR PROCESS AND PRODUCT by T.E. Pardue (Motorola); U.S. Pat. 2,947,923 and 2,947,924, Issued Aug. 2, 1960

The design and fabrication of a diffused base, intrinsic collector, high frequency transistor are described. The intrinsic collector zone decreases collector capacitance and increases collector breakdown. Jet etched-plated rectifying contacts are formed on the surface layer and high resistivity cavity regions of the device.

9006 MANUFACTURE OF SEMICONDUCTIVE DEVICES by C.S. Fuller (Bell Labs.); U.S. Pat. 2,836,523, Issued May 27, 1958

A technique for fabricating p-n-p, n-p-n, p-n-i-p, n-p-i-n, and p-n-p-n devices by the use of outdiffusion and gettering is described. The technique is based on the outdiffusion of a fast diffusing dope from a doubly doped semiconductor chip and gettering action of a surface metal on the fast diffusing impurity. The fast diffusing impurity is generally Cu or Zn for Ge and Li, Au, Zn or Fe for Si. The slow diffusing impurities generally are from Groups III and V. Normally a single doped chip is diffused through with the fast impurity. A metal such as Pb, Sn, In, or doped gold is plated on the surface and heated for a short time. This clears a thin region of the fast impurity.

Fabrication of Diffused Junctions - See 8978

9007 MANUFACTURE OF TRANSISTORS by H.W. Parker; U.S. Pat. 2,840,494, Issued June 24, 1958

A technique for fabricating transistors by controlled epitaxial deposition of semiconductor films is described. The method is based on the complete vaporization of a semiconductor wire in a vacuum chamber by the passage of a high current through it. By using suitably doped rods, films of opposite types are deposited successively to form the three layers of the transistor. Masks are interposed between the rods and the substrate to limit the geometry of the layers. The substrate may be either Si, Ge, or SiC. Each film is approximately $4 \times 10^{-6}$ cm thic and must be annealed to form a single crystal before the next layer is deposited.

9008 TRANSISTOR by P.J.W. Jochems (Philips); U.S. Pat. 2,827,599, Issued Mar. 18, 1958

A technique for fabricating power transistors with reduced collector saturation current and high alpha at large emitter a collector currents is reported. The device geometry is such th the emitter and collector are on the same side of the base. Th principle utilized is that of interposing a nonconducting regio between part of the emitter and/or collector and the base. To this end slots are cut into the face of the chip or holes are bored through it. The contacts are then alloyed over the slot or holes to give ring emitters and/or collectors. By using mul tiple elements, each emitter perimeter will ring a base regio and each base an emitter region.

9009 ETCHING OF SEMICONDUCTOR MATERIALS by D.L. Cox (Texas Instr.); U.S. Pat. 2,827,367, Issued May 18, 195

An etch for exposing the junctions in grown junction transisto and a method of contacting their base regions are described. Si grown junctions are etched 10-60 sec at room temperature in a solution of 300 ml nitric, 200 ml HF and 200 drops of 1 p cent KI in water. Ge is processed under the same conditions as above in a solution of 300 ml nitric, 180 ml HF and 120 dro of 1 per cent KI in water. The surfaces of the bars must be relatively smooth for good results. This etch is somewhat fast than CP-4 and leaves a smoother surface. A lead is attached to the base region of the bar by passing a current through the lead and bar, thus fusing the lead.

High Temperature Mo-Si Contacts - See 8981

9010 METHOD OF SURFACE-TREATING SEMI-CONDUCTO by P.W. Haayman (Philips); U.S. Pat. 2,835,613, Issued Ma 20, 1958

A technique for fabrication of both ohmic and rectifying dif fused junctions in Si, Ge, SiC and III-V compounds is described. The procedure is based on diffusion from a suitably confined liquid source containing the doping agent. The requirement of the system is that the liquid does not alloy with the semiconductor. For high melting semiconductors like Si and SiC, metal such as lead may be used. Glasses or mixed oxides may also be used. Pb-2 per cent P, diffused at 1150°C is suitable for Si while Sn-2 per cent P, diffused at 1500°C, is suitable for SiC. The solidified dot is mechanically remove when the diffusion is completed.

9011 COOLING ARRANGEMENT FOR TRANSISTOR by B. Cornelison and E.A. Wolff (Texas Instr.); U.S. Pat. 2,958,0 Issued Oct. 25, 1960

A liquid-vapor heat exchange cycle for cooling a power tran sistor is described. The collector side of a diffused base tran sistor is exposed to the inside of a tube through a copper mou ing plate. The tube has a plurality of externally mounted radial cooling fins and contains a refrigerant which can be readily vaporized by the heat given off by the transistor. He is removed to the ambient by the process of vaporization and passage of the heat to the heat fins by the hot vapors, with subsequent condensation of the vapors and recirculation back to the liquid. Suitable refrigerants include Freon CC/4 alco hols and halogenated hydrocarbons containing one or more fl orine atoms.

9012 METHODS OF PRODUCING STABLE TRANSISTORS by J.J.A. Ploos van Amstel (Philips); Philips Tech. Rev., Vol. 22, No. 6, pp. 204-214, 1960-61

Methods of controlling the surface state of Ge transistors are discussed. The occupation of the surface by water molecules is shown to affect the amplification factor, and is thought to have an optimum value. A favorable water occupation may be maintained in all operating conditions by incorporating in the encapsulant a buffer substance — a stabilizer — which provides the appropriate water-vapor pressure as a function of temperature. Better results are obtained with a buffer whose water-vapor pressure is initially too low. After the transistors have been heated for several days at 140°C, they are found to have stable characteristics. The process is described as "surface forming." There are other substances that resemble water in their effect on the surface. Results obtained with one such substance (arsenic) are briefly discussed.

9013 METHOD OF ENCASING A TRANSISTOR AND STRUCTURE THEREOF by I.E. Levy, E.S. Mockus, and A.B. Spyut (Raytheon); U.S. Pat. 2,827,598, Issued Mar. 18, 1958

Fabrication of a hermetically sealed transistor package is described. The cylindrical package consists of a tubular base with leads passing through a glass-to-metal seal at one end and a cylindrical cap with either a hole or tubulation at the closed end. The lower tube is short with the lead wires extending well above its edge. The semiconductor device is supported on the lead wires. The two halves of the package are clamped in opposing collets that are fabricated from a metal having a high thermal conductivity, brought together and rotated in synchronism under a Heli-Arc torch. The package is sealed later by plugging the hole or pinching-off the tubulation.

Protective Glass Coatings for Junctions - See 8985

## SURFACE BARRIER

9014 SEMICONDUCTOR DEVICE by W.E. Bradley (Philco); U.S. Pat. 2,846,346, Issued Aug. 5, 1958

Fabrication of surface barrier and MAT transistors by controlled jet etching is described. The jet etching process is controlled by the high resistance of the space charge layer associated with a reverse biased junction. A conventional jet, pump, electrolyte and reversible polarity power supply is used to plate a collector on a chip after sufficient etching to clean the surface. For a p-type chip, the collector should be alloyed in. The chip, in a ring tab, is then placed in a jet etcher and the collector is back biased. Etching of the emitter hole proceeds rapidly until the limit of the space charge region is encountered. The cavity diameter then grows with further etching.

9015 SEMICONDUCTOR DEVICE by R.A. Williams and J.W. Tiley (Philco); U.S. Pat. 2,885,571, Issued May 5, 1959

The fabrication of high frequency transistors which utilize surface barrier emitters is described. An extremely close spacing (less than the minority carrier diffusion length) is achieved between the collector and emitter by means of electrolytic etching. High collection efficiency without the need for high collector voltages results from this close spacing. The minority carrier lifetime, the crystal orientation, and the resistivity of the base material are not extremely important parameters in the fabrication of surface barrier high frequency transistors. Detailed descriptions of the fabrication of Si and Ge devices are presented.

9016 CONTACTING ARRANGEMENT FOR SEMICONDUCTOR DEVICE, AND METHOD FOR THE FABRICATION THEREOF by J.W. Stineman and S.A. Robinson (Philco); U.S. Pat. 2,825,015, Issued Feb. 25, 1958

A method of anchoring whisker wires on microwave diodes and surface barrier transistors is described. Previous cementing techniques required a great deal of care and even then shrinkage of the cement could shift the point. The diode whisker wire is reshaped so that it has a knee bend near the chip surface. This knee is cemented to the chip before the diode is adjusted and aged. In the surface barrier units, the whisker leads are soldered to the junctions, brought down and cemented to the thick part of the chip and then drawn over to the lead posts.

9017 METHOD FOR ELECTROPLATING SELECTED REGIONS OF n-TYPE SEMICONDUCTIVE BODIES by G.L. Schnable (Philco); U.S. Pat. 2,893,929, Issued July 7, 1959

A method for electroplating only the n-type base region of an alloyed junction p-n-p transistor or a surface barrier transistor without the necessity of masking the emitter and collector regions of the device is described. The method is illustrated by the Au plating of a surface barrier Ge transistor. The transistor is cleaned by etching and rinsing in distilled water. The emitter and collector electrodes of the device are then both connected through a variable resistor to the positive terminal of a battery and the base electrode is connected to the negative terminal of the battery to produce a potential of about 1.5 v between the emitter and collector electrodes and the base electrode. The device is immersed for 2 min in a plating solution and etched and washed following the plating operation. The mechanisms believed to be responsible for the selective deposition are discussed.

## MAGNETOELECTRIC DEVICES

9018 PRINCIPLES AND APPLICATIONS OF HALL-EFFECT DEVICES by M. Epstein, L.J. Greenstein, and H.M. Sachs (Armour Res. Found.); Proc. NEC, Vol. 15, pp. 241-252, Oct. 12-14, 1959

The Hall effect and its utilization in engineering applications are described. The development of semiconductor materials with high-mobility carriers and their use as Hall-effect sensors is discussed. Considerations and problems relative to design and construction of Hall-effect sensors are described. Results indicate that high sensitivities can be obtained; measurements of magnetic field intensities of the order of $10^{-4}$ oe, independent of frequency, have been achieved. When used in conjunction with permeable materials, sensitivities of $10^{-6}$ oe have been obtained. Both the design and experimental results of an Armstrong phase-shift modulator and the utilization of the principle of multiplication, inherent in the Hall-effect devices, in the design of various communication circuits are investigated.

9019 MODERN APPLICATIONS OF HALL EFFECT IN SEMICONDUCTOR COMPOUNDS by M.J.O. Strutt (Swiss Fed.

Inst. Tech.); Solid State Phys. in Electronics and Telecommun., Vol. 2, Academic Press, 1960, pp. 706-722

The application of the Hall effect in semiconductor compounds to the construction of various electronic devices is described. The theory and design of Hall effect wattmeters, oscillators, flux density meters, and superheterodyne receivers using Hall probes are discussed. Frequency dependence of the Hall coefficient and temperature dependence of the Hall voltage are also reported.

InAs Hall Plates - See 8760

9020 HALL EFFECT DEVICE by F. Kuhrt (Siemens AG); U.S. Pat. 2,877,394, Issued Mar. 10, 1959

A means for preventing the occurrence of an inductive component in a Hall circuit by appropriate arrangement of the Hall electrodes is described. The Hall electrodes are placed at opposite ends of the Hall device; one of the electrodes leading to one of the Hall voltage tap-off points is led out in the direction of the other tap-off point. It preferably lies directly on a face of the device and is insulated from the surface. It is then extended, together with the other electrode, in an interlocking, twisting manner such that an effective induction surface in relation to the magnetic field flux of the device is avoided.

## OTHER CONDUCTIVE DEVICES

9021 CONTROLLED NON-LINEAR SEMICONDUCTOR RESISTANCES by O.M. Kudriautsev and V.I. Pruzhinina; Radio Engrg. Electronics, Vol. 5, No. 6, pp. 180-184(L), 1960

The characteristics of controlled nonlinear semiconductor resistances are described. The devices utilize the property that in a polycrystalline nonlinear semiconductor resistance, the application of an electric field in one direction changes the electrical conductivity not only in that direction but in other directions through the crystal. One particular device, in which a control voltage $V_1$ is applied in a direction perpendicular to a controlled voltage $V_2$ is discussed. The gradient of the controlling electric field is much greater than that of the controlled electric field. In this device the resistance in one direction was varied over two orders of magnitude, from 9.1 Ω to 0.0147 Ω, when the voltage in that direction was kept constant and the voltage in the other direction was varied from 0 to 80 v. Devices which utilize electrodes in three mutually perpendicular directions are also described.

## PHOTODEVICES

9022 CURRENT FLUCTUATIONS IN PbS CELLS by J. Blok and F.M. Klaassen (Vrije U., Amsterdam); Solid State Phys. in Electronics and Telecommun., Vol. 1, Academic Press, 1960, pp. 541-547

Possible mechanism of photoconduction in Pbs photocells, involving the barrier and one-carrier (majority-carrier) theories of photoconductivity, are described. Measurements were made on the noise spectrum and photoresponse of the cells; the noise spectrum was analyzed using the Fourier components of the square of the current fluctuations.

9023 PHOTOELECTRIC DEVICE by J.C. Marinace and U. Cocca (GE); U.S. Pat. 2,885,562, Issued May 5, 1959

A self-contained and compact photoelectric device having photovoltaic and photoconductive characteristics is discussed. The device consists of a p-type Se layer and an n-type silver actuated CdSe or CdS layer. A counter-electrode is deposited onto the n-type phosphor (CdSe). High energy radiation incident on the counter-electrode passes through into the n-type phosphor, generating light. Current flows through an external circuit in the presence or absence of an applied potential as a measure of the amount of radiation. The photovoltaic character of the device enables operation without the use of power supplies or amplifiers. Where accessory equipment is conveniently used, the photoconductive effect can be utilized. The device is particularly useful in the detection of high quantum energy electromagnetic radiation.

9024 PHOTOSENSITIVE DEVICES by S. Pakswer and C.S. Szegho (Rauland); U.S. Pat. 2,879,182, Issued Mar. 24, 1959

Photosensitive cells of the photoconductor type in which the photoconductor comprises sintered CdS, CdSe, or a mixture of the two is described. A substrate is coated with a photoconductor consisting primarily of at least one compound of a group including either CdS or CdSe. The photoconductor includes minor portions of a donor element selected from the third and seventh columns of Periodic Table and of an inhibitor element selected from Cu, Ag, or Mn. The coated substrate is fired in an atmosphere controlled by the presence of at least one of the compounds and at a temperature above 650°C for a period of time sufficient to sinter the photoconductor coating to the substrate and to develop photoconductive properties in the coating. Two spaced conductive elements are applied to the photoconductor to form a pair of electrodes electrically interconnected by the sintered photoconductive coating. The resulting devices exhibit a high sensitivity to radiation in the red portion of the spectrum.

9025 INFRARED DEVICES AND METHODS by Y.A. Rocard and B.E. Bartels (Hupp); U.S. Pat. 2,884,345, Issued Apr. 28, 1959

Photocells of the evaporated layer type which provide improved response to infrared radiations, improved stability, high sensitivity, and low time constant are discussed. Wet and dry methods for producing the PbS powder are presented. In producing the PbS sensitive area, the sublimation and oxidation operations are separated into distinct steps providing greater control over activation of the sublimed PbS and resulting in cells of substantially identical characteristics. A cell is evacuated to $10^{-5}$ — $10^{-6}$mm Hg and heated to 200°C for 1-2 min if electrical testing shows the standards for light and dark currents are not met. Spectral sensitivity curves of a PbS cell is included showing wavelengths of 3 microns at room temperature and 4.5 microns at -180°C. The time constant is $10^{-4}$ sec at 20°C and the signal-to-noise ratio ranges from 300:1 to 500:1.

9026 METHOD OF PRODUCING PHOTOCELLS by B.E. Bartels (Hupp); U.S. Pat. 2,892,250, Issued June 30, 1959

The fabrication of coolable chemically deposited PbS cells which have a high spectral response in the 3.5 - 4.2 μ wavelength region is discussed. The details of the cell glass envelope construction are given. The novel features of this construction are that the inner cylinder is formed from a single piece of glass rather than two pieces (this results in a high signal-to-noise ratio) and a very thin convex glass window

which is highly transparent to radiation up to 6 μ is used. The electrodes from the lead wires to the sensitive surface are preferably made of alternate layers of Au and Pt with the outer layer being Au but it can also consist of separate layers of either Au or Pt. Two chemical reactions for producing the PbS film are described. After deposition the films are photosensitized by heating the cell in an oven at a temperature between 125° and 150°C until a maximum resistance is reached. The cell is then sealed off.

9027 HIGH FREQUENCY LIGHT MODULATION by R.L. Williams (Canadian Armament Res. and Dev. Estab.); J. Sci. Instr., Vol. 37, pp. 205-208, June 1960

A system which can be used to measure the short response times of semiconductor infrared detectors is described. High frequency light modulation is achieved by using a magnetically driven rotor suspended by a magnetic field in a vacuum chamber. With a rotor 1 inch in diameter having 180 reflecting faces, modulation frequencies in the megacycle region can be readily obtained. The design of the rotor, and the driving and suspension circuit is discussed. A time constant measurement for an indium antimonide sample is given as an illustration of the system.

9028 PHOTOSENSITIVE DEVICE by R.L. Meyer (Rauland); U.S. Pat. 2,879,362, Issued Mar. 24, 1959

The fabrication of a CdSe photoconductive device which exhibits high sensitivity to radiation in the red portion of the spectrum is described. The device is manufactured by coating a substrate with a material consisting primarily of CdS. The coated substrate is fired at a temperature above 650°C for a period of time sufficient to sinter to the substrate. The sintered coating is then coated with a photoconductor consisting primarily of CdSe. The double-coated substrate is fired at a temperature above 650°C for a period of time sufficient to sinter the CdSe coating to the CdS coating and to develop photoconductive properties in the CdSe coating. Two spaced conductive elements are applied to the photoconductor to form a pair of electrodes electrically interconnected by the sintered CdSe coating.

9029 PHOTOCONDUCTIVE DEVICE HAVING A SILICON DIOXIDE PROTECTIVE LAYER AND METHOD OF MAKING SAME by A.L. Floyd, Jr. (Lane-Wells); U.S. Pat. 2,879,360, Issued Mar. 24, 1959

The fabrication of a highly sensitive photoconductive cell in which the photoconductive surface is fully protected by a film of fused $SiO_2$ is described. A surface film of a photoconductor material (CdS) is vacuum deposited over and between the electrodes of the device. The photoconductor is then baked to a state of high photosensitivity prior to application of the protective material. SiO is applied to the photoconductor surface by vacuum sublimation and condensation. By suitable heat treatment (approximately 200°C) in the presence of oxygen, the SiO is converted to $SiO_2$ to form a substantially impervious transparent cover.

9030 PHOTOCELLS by O.T. McIlvaine; U.S. Pat. 2,899,659, Issued Aug. 11, 1959

The fabrication of a multielement photocell is described. Holes are drilled at regular intervals in an insulating material such as mica or glass, electrodes are inserted into the holes, and a photosensitive layer such as PbS, Ge, or Si is deposited by any one of several techniques on the insulator surface in contact with the electrodes. A circuit is completed when light shines on a spot between any two electrodes. A transparent conductive layer may also be applied to the semiconductor layer. In this case a cell is formed between the transparent layer and each pin. An array of phototransistors can also be constructed utilizing the same technique.

9031 SEMICONDUCTING DEVICE by J.E. Jacobs (GE); U.S. Pat. 2,856,541, Issued Oct. 14, 1958

Fabrication of an X-ray sensitive plate usable as an image orthicon is described. The active element is powdered crystalline CdS, HgS, or CdSe in a suitable organic binder. The active film is deposited over a metal base or a thin metal film on a glass base, air dried and then vacuum baked. A thin layer of Mo, Ag, or Al is then evaporated or sputtered over the semiconductor layer for the other contact. Stacked arrays may be used for greater response. X-ray irradiation of these semiconductors cause the release of large numbers of electrons, thus giving an amplification. The released electrons decrease the impedance of the layer.

9032 THE REGENERATIVE IMAGE INTENSIFIER AND ITS APPLICATION TO THE LUMINESCENT CHAMBER by M.L. Perl and L.W. Jones (U. Michigan); Advances Electronics and Electron Phys., Vol. 12, Academic Press, 1960, pp. 153-182

The theory and design of regenerative image intensifiers are discussed. Four special types of regenerative image intensifiers are considered: (1) forced-registry, (2) registered, (3) non-registered, and (4) flip-flop. The luminescent chamber is described in detail. It records the image of particle tracks passing through scintillating crystals and has advantages in time resolution, lack of dead time, and the fact that an image tube can be gated so that only pictures of desired events may be recorded.

9033 IMAGE INTENSIFIER DEVELOPMENTS IN THE RCA ELECTRON TUBE DIVISION by R.G. Stoudenheimer (RCA); Advances in Electronics and Electron Phys., Vol. 12, Academic Press, 1960, pp. 41-58

A two-stage developmental image intensifier is described. Two sizes were built. They are made with P-11 (blue) and P-20 (yellow) output screens. The tubes have multialkali cathodes in the first stage and antimony-cesium cathodes in the interstage coupling "sandwich." The theoretical conversion gain is calculated, and methods for measuring the conversion gain are discussed. The variation of the resolution over the area of the cathode, fluctuation noise, screen background, and pincushion distortion are considered. Two recent single-stage image intensifier tubes and a three-stage image intensifier are discussed.

Electroluminescent Typewriter - See 9124

Oxide Semiconductors for Optical Filters - See 8869

## THERMAL DEVICES

9034 THERMOELECTRIC HEAT PUMP by R.W. Fritts and S. Karrer (Minnesota Mining and Mfg.); U.S. Pat. 2,896,005, Issued July 21, 1959

Semimetallic compositions employed as thermoelectric elements

in single or multiple junction heat pumps are described. Binary alloys or compositions of Pb-Te, Pb-Se, Pb-S, and Pb-Te-Se serve as basic materials for the device; other substances are added as impurities to act as "promoters" for negative or positive polarity and for electrical parameters. Tables of percentage by weight compositions of the basic and impurity materials vs Peltier EMF, thermal conductivity, electrical resistivity, and performance factor are cited. Temperature suppression of 25°C at the cool junction and elevation of 100°C at the hot junction have been attained with a single element heat pump. Pumping rates approaching 0.2 watts at a current density in excess of 25 a/cm$^2$ have been observed.

Use of Thermojunctions for Refrigeration - See 8928

## FERRO- AND FERRIMAGNETIC (FERRITE) DEVICES

9035 MICROWAVE SWITCHES USING CUTOFF PHENOMENA IN FERRITE LOADED WAVEGUIDE by D. Caswell (Monogram Precision Ind.); Solid State Phys. in Electronics and Telecommun., Vol. 3, Academic Press, 1960, pp. 270-274

The performance of microwave transverse switches which utilize a new type waveguide cutoff attenuator is discussed. In the attenuator a ferrite is located against a waveguide wall and a controllable magnetic field is applied to the ferrite in a direction transverse to the waveguide. The magnetic field can be adjusted to make permeability of the ferrite negative. The negative permeability reduces the apparent width of the waveguide. If the apparent width is reduced sufficiently, the waveguide is cut off and energy introduced into the waveguide is reflected. Two transverse switches, one formed by locating a cutoff attenuator in the two output arms of a "Y" junction and another formed by locating cutoff attenuators in the two output arms of a shunt "tee" have been investigated. These studies indicate that a transverse switch between two ports with a switching time of 5 msec, a bandwidth of 5 per cent, and insertion loss to the "on" arm of less than 1 db and an insertion loss to the "off" arm of greater than 50 db, can be built as a practical device. Appreciably higher insertion losses to the "off" arms can be achieved at the expense of increased insertion loss to the "on" arm.

9036 FERRITE SHAPE CONSIDERATIONS FOR UHF HIGH-POWER ISOLATORS by E. Stern (GE); IRE Trans., Vol. MTT-8, p. 656(L), Sept. 1960

The design of high power UHF ferrite isolators is discussed. It is shown that coincidence between the main and subsidiary resonances can be avoided if the length and width dimensions of the ferrite slab are properly chosen. The critical frequency ratio for the onset of main and subsidiary resonance coincidence is plotted as a function of ferrite shape. The dimensions of a YIG 400 Mc high power isolator are then determined.

9037 RECENT ADVANCES IN MAGNETIC DEVICES FOR COMPUTERS by D.H. Looney (Bell Labs.); J. Appl. Phys., Vol. 30, Suppl., pp. 38S-42S, Apr. 1959

Magnetic elements which may replace ferrite toroids in memory matrices are described. Ferrite materials are being used as sheets and multiaperture devices. The sheets show great promise in achieving a cost reduction. The multiaperture devices in memory applications offer the advantages of increased speeds, a wider operating temperature range, and nondestructive readout. The ferromagnetic materials are used in the form of thin films and wrapped wire. The films are capable of increased switching speeds at nominal current drives. The use of magnetic wire as a storage element offers new fabrication technology, a wider operating temperature range, and new functional structures. A comparison is made to illustrate the device characteristics of the various structures.

9038 INHIBITED FLUX — A NEW MODE OF OPERATION OF THE THREE-HOLE MEMORY CORE by J.A. Baldwin, Jr. and J.L. Rogers (Bell Labs.); J. Appl. Phys., Vol. 30, Suppl., pp. 58S-59S, Apr. 1959

A new method of operation of the three-hole memory core is reported. As in the case with the coincident-flux scheme developed by IBM, read and write times may be made very short. However, by using single-line drive rather than coincident current, only one conductor is required through each hole. A description of a small memory array which uses this method is given.

9039 STUDY OF THE RESIDUAL STATES OF FERRITE CORES IN COMPUTER MEMORY OPERATION by W.M. Overn and V.J. Korkowski (Remington Rand Univac); J. Appl. Phys., Vol. 30, Suppl., pp. 52S-53S, Apr. 1959

The two complimentary residual states of magnetic induction used to represent binary information in a ferrite core storage system are discussed. The flux density found at the two states depends on any large fields which may have saturated the core in the past, as well as on the nature of the driving fields employed in the system. The partial-select noise amplitude is a function of the residual magnetic induction and saturation history. By applying this information, "delta" noise can be eliminated. The role of the post-write disturb pulse in preventing errors under certain abnormal operating conditions has been determined.

9040 REVERSIBLE COMPONENT OF MAGNETIZATION by R.W. MKay (U. Toronto); J. Appl. Phys., Vol. 30, Suppl., pp. 56S-57S, Apr. 1959

A method of nondestructive sensing of a ferrite-core memory which depends on the variation of the reversible component of magnetization with the state of the core is reported. Measurements of this reversible component were made for two types of cores. It was found that the reversible component varies nearly three to one between the remanent state and the demagnetized state. The effects of finite core-wall thickness and of flux-leakage are discussed.

9041 EFFECT OF SMALL ADDITIONS OF RARE EARTH OXIDES ON THE MAGNETIC BEHAVIOR OF A VARIETY OF SQUARE-LOOP FERRITE CORES [in Chinese] by G.-D. Li, X.-L. Wang, and F.-K. Xiao; Acta Physica Sinica, Vol. 16, No. 5, pp. 272-280, 1960

The effect of small additions (0.1, 0.5, and 1.0 weight per cent) of rare earth oxides ($La_2O_3$, $CeO_2$, $Sm_2O_3$, $Gd_2O_3$) and $Y_2O_3$ on the static hysteresis loop and the signal to noise ratio of square-loop Mg-Mn ferrite containing some ZnO and CuO is discussed. The samples were prepared by the usual oxide method, sintered 2 hrs in air at 1300°C and quenched from 950° or 1050°C. Preliminary results showed that $La_2O_3$ and $Gd_2O_3$ increased the squareness ratio and the signal to noise ratio. In contrast, $CeO_2$, $Sm_2O_3$, and $Y_2O_3$ additions did not

show these effects. The saturation magnetization and the Curie point were not appreciably affected by the introduction of the rare earth oxides. The influence of the core size and the quenching temperature on the squareness ratio and the signal to noise ratio was also noted.

9042 MILLIMICROSECOND MAGNETIC SWITCHING AND STORAGE ELEMENT by D.A. Meier (Natl. Cash Register); J. Appl. Phys., Vol. 30, Suppl., pp. 45S-46S, Apr. 1959

A magnetic rod suitable for performing the logical switching and storage functions required in a digital computer is described. The magnetic element consists of a silver-coated glass rod upon which is electroplated an Fe-Ni alloy several thousand angstrom thick. A single element for a coincident-current memory requiring two inputs, an inhibit winding, and a sense winding consists of four single separate layer concentric selenoids wound over the magnetic rod. Memory matrices, each consisting of many selenoids, are stacked and simultaneously threaded with the rod. The switching speed of the element operating in a coincident-current mode is approximately 70 μsec. The output voltage generated across a ten-turn sense winding is 200 to 500 mv depending upon the alloy thickness. The rod is also suitable as a multi-input logical switch. Separate inhibiting windings wound over the rod perform the NOR function of its input literals. A total of thirty separate inhibiting windings have been demonstrated in the laboratory. Satisfactory operation in the 2- to 5-Mc range using transistors in conjunction with the rod has been shown to be practical. Continuous plating and testing in conjunction with automatic machine winding techniques make the rod appear economically attractive in digital computer applications.

9043 A BROAD-BAND FERRITE REFLECTIVE SWITCH by C. M. Johnson and J.C. Wiltse (Electronic Commun.); IRE Trans., Vol. MTT-8, pp. 466-467(L), July 1960

A reflective ferrite switch consisting of a short section of heavily loaded coax, stripline, or waveguide is described. When an axial magnetic field of sufficient magnitude is applied to the switch, the effective permeability of the ferrite approaches zero and electromagnetic waves are strongly reflected. The device is small, borad-band, requires only a moderate magnetic field whose magnitude can be varied over a wide range, and can be used over much of the UHF and SHF frequency regions by choosing a ferrite with proper saturation magnetization.

9044 STABILITY OF MAGNETS COMPOSED OF ELONGATED SINGLE-DOMAIN IRON PARTICLES by E.J. Yamartino, H.R. Broadley, Jr., and R.C. Lever (GE); J. Appl. Phys., Vol. 30, Suppl., pp. 144S-145S, Apr. 1959

The magnetic and physical stability of permanent magnets compacted from elongated single domain Fe particles in metallic and organic matrices under various environmental conditions are reported. Changes resulting from two years exposure to 95 per cent relative cycling humidity and 100°C were measured. The influence of powder compacting temperatures, pressures, powder size, and additives are described. Compacts with Pb matrices exposed to 100°C and 95 per cent relative humidity showed gradual magnetic and dimensional changes from insignificant variations after one month to maximums of 0.5 per cent over a two-year period. These results compared favorably with results obtained for Alnico V magnets subjected to identical conditions. Temperatures of 200° and 250°C produced magnetic changes in the order of 1 per cent after one month with physical degradation occurring after two months at 250°C. Magnetic changes of 1 per cent and weight and volume changes in the order of 2 per cent occurred in organic matrix magnets after one month at 100°C. The magnetic changes resulted from a slow oxidation of the Fe particles which caused a small decrease of intrinsic saturation induction and an increase in coercive force.

9045 NOVEL LIGHT-WEIGHT MOLDABLE PERMANENT-MAGNET MATERIAL by L.I. Mendelsohn and R.S. Norman (GE); J. Appl. Phys., Vol. 30, Suppl., pp. 142S-145S, Apr. 1959

A lightweight, moldable permanent-magnet material consisting of elongated-single-domain (ESD) particles of iron-cobalt coated with a thermosetting plastic which serves as a matrix is described. The particles are aligned while the plastic is in a liquid phase. The matrix is then solidified, and the agglomerate is ground to a -30 mesh freeflowing powder. Each of the particles of this powder consists of submicroscopic elongated aligned particles. The freeflowing powder can then be directionally pressed in conventional presses to produce magnets of complex shape held to precise dimensions. Energies of $2.0 \times 10^{-6}$ gauss-oersteds have been achieved in magnets whose density is 4 g/cm$^3$ and whose temperature coefficient is 0.008 per cent C. The properties of the material make it well suited to applications where a lightweight, high-energy, precision-dimensioned easily fabricated magnet, capable of withstanding adverse environmental conditions is required. An excellent application of this material is the moving-magnet-instrument rotor.

## PARAMAGNETIC DEVICES (Masers and Lasers)

9046 METHOD FOR CALCULATING SIMULTANEOUS RESONANCE CONDITIONS IN A THREE-LEVEL RUBY MASER by M.A. Garstens (U.S. Naval Res. Lab.); J. Appl. Phys., Vol. 30, pp. 976-977, July 1959

The external magnetic field and crystal orientation necessary to match a given pair of frequencies in the operation of a 3-level maser are discussed. In the case of $Cr^{3+}$ a 4$^{th}$-degree secular equation determines the four energy levels for each value of external field H and crystal orientation. Determination of the latter two variables, given two desired frequencies of operation, ordinarily involves either the solution of a tremendous number of fourth-degree equations and extrapolation towards the required solution, or determination of the matching conditions by experimental methods. A method that allows direct calculation of H and O by transformation of the secular equation is described.

9047 EFFECT OF NUCLEAR POLARIZATION ON THE BEHAVIOR OF SOLID STATE MASERS by G. Makhov, L.G. Cross, R.W. Terhune, and J. Lambe (U. Michigan); J. Appl. Phys., Vol. 31, pp. 935-938(L), May 1960

Changes produced in a ruby maser amplifier and oscillator as a result of the application of RF power and the subsequent changes in the polarization of the Al nuclei are discussed. The gain of the maser amplifier increased from 15 db to 35 db and the mode of operation of the oscillator changed from the cw mode to the relaxation mode on the application of RF power at 4.5 Mc. The

measurements were made on ruby containing 0.1 per cent chromium. A two turn coil was wound about the ruby and the assembly was placed in a doubly resonant microwave cavity and located so that the axis of the coil was perpendicular to the direction of the dc magnetic field and the polar angle was ~60°. The system was cooled to 4.2°K, a K-band pump was used to saturate the 1-3 transition and X-band emission was obtained in the 3-2 transition. The recovery of a solid state maser from saturation or from fluctuations in pumping power is characterized by two time constants, a rapid recovery determined by spin-lattice relaxation and a slow recovery determined by nuclear-electronic relaxation.

9048 ELECTRONICALLY-TUNABLE TRAVELLING-WAVE MASERS AT L AND S BANDS by S. Okwit, F.R. Arams, and J.G. Smith (Airborne Instr. Lab.); Proc. IRE, Vol. 48, pp. 2025-2026(L), Dec. 1960

An experimental investigation of the tunability of traveling-wave masers in the L- and S-band regions is discussed. A comb structure in which the active ruby (the chromium content nominally 0.05 per cent) was placed on both sides of the comb was used. The ruby c-axis was oriented parallel to the direction of propagation and the active length of each of the three structures investigated was $1^{7}/_{8}$ inch. The measurements were made at 1.6° to 1.8°K. Over the ranges 1120 to 1370 Mc, 1850 to 2150 Mc, and 2100 to 2400 Mc, electronic tuning ranges and average electronic gains of 20 per cent and 6.5 db, 15 per cent and 9.4 db, and 13 per cent and 9.1 db, respectively, were measured. All the measurements were made by varying only the applied magnetic field and the pump frequency.

9049 PULSED FIELD MILLIMETER WAVE MASER by L.R. Momo, R.A. Myers, and S. Foner (Lincoln Lab.); J. Appl. Phys., Vol. 31, p. 443(L), Feb. 1960

Improvements in a previously-described pulsed field ruby maser which permit operation in the 70 kMc range and a power output of several mw are described. Operation in the mm wave region was achieved by systematically increasing the peak pulsed magnetic field applied to the crystal and a larger power output was achieved by increased cavity coupling and greater pump power. Oscillations at the two lowest $TE_{10n}$ modes, 12.7 kMc and 19.2 kMc have been identified and the highest frequency attained has been 75 ± 5 kMc. As many as 14 different emission frequencies have been observed in the 12 to 70 kMc range. Peak output power of more than 2.5 mw has been obtained at 12.7 and 19.2 kMc and more than 0.025 mw at ~ 40 kMc. The upper limits of the magnetic field dependence of the spin-lattice relaxation time in ruby are estimated from the experimental results.

9050 RUBY AS A MASER MATERIAL by C. Kikuchi, J. Lambe, G. Makhov, and R.W. Terhune (U. Michigan); J. Appl. Phys., Vol. 30, pp. 1061-1067, July 1959

The reasons for the initial choice of ruby as a maser material are outlined and some measurements of the parameters in the spin Hamiltonian and of spin relaxation times are reported. The relative merits of single- and double-pump modes of operation of a four-level maser are discussed and measurements of the oscillator power for the two cases are included.

Maser Communication Systems - See 9109



Figures of Merit of Ferroelectric Varactors - See 8960

9051 CAPACITOR by Y. Ishikawa, Y. Sasaki, and I. Sato (Nippon Electric); U.S. Pat. 2,836,776, Issued May 27, 1958

The fabrication of a p-n junction capacitor with large capacitance per unit area and wide operating temperature limits is described. The device is a p-i-n diode consisting of doped layers of tantalum oxide. A Ta foil plate is cleaned and anodically oxidized in 7 per cent ammonium carbonate at 4 ma/cm$^2$. A thin film of high purity Ge is then evaporated over the oxide layer and covered with an evaporated Al film. The initial oxide deposit on the metal is n-type while the successive layers are intrinsic. The Ge layer converts that part of the intrinsic oxide it contacts to p-type and the Al layer is used as a low resistance contact.

9052 RADIATION EFFECTS ON QUARTZ OSCILLATORS by O. Renius and D. Rees (Ord. Tank-Automotive Command); Proc. IRE, Vol. 48, p. 1340(L), July 1960

The frequency shift of quartz oscillators as a function of the total dose, the dose rate, and the level of X- and γ-ray incident energy is discussed. Oscillators utilizing BT cut crystals were irradiated by 28, 100, and 300 kvp X-ray sources and multi-Curie gamma emitting isotope sources of 0.66 and 1.25 Mev. Dose rates varied from $9 \times 10^3$ R/hr to $147.6 \times 10^3$ R/hr, with total doses up to $1 \times 10^6$ R. The frequency was found to change more rapidly at a low total dose than at a high total dose. At a dose level of 300,000 R, the frequency shift increased directly with the increase in the peak energy of the incident X-radiation. The frequency shifts were not found to be dependent on dose rate.

9053 REVERSIBLE, DIODELESS, TWISTOR SHIFT REGISTER by A.H. Bobeck and R.F. Fischer (Bell Labs.); J. Appl. Phys., Vol. 30, Suppl., pp. 43S-44S, Apr. 1959

A twistor shift register which has been built and operated successfully is described. The design utilizes interaction effects which exist between magnetized regions on a magnetic wire. Only a single magnetic wire is required for a complete register. The information is stored as magnetically polarized zones which can be moved along the wire by means of a five phase pulse source. No diodes are required. Therefore, drive powers can be greatly decreased since the only threshold consideration is the magnetic material itself. Bidirectional operation is easily secured. The upper frequency limit has not been established; however, a several hundred kilocycle bit rate should be possible. Physically, the register could be made of no more than magnetic and copper wire. This should make fabrication considerably cheaper than conventional shift registers.

# BASIC SOLID STATE DEVICE CIRCUITS

## GENERAL

9054 PRACTICAL APPLICATIONS OF SIGNAL FLOW GRAPHS USING AN ARRAY OF NON-TOUCHING LOOPS by G.S. Axelby and R.H. Plath (Westinghouse); Proc. NEC, Vol. 15, pp. 1044-1055, Oct. 12-14, 1959

A systematic, practical method of drawing and using signal flow diagrams is discussed. The method features a simple, tabular array from which various combinations of nontouching loops may be found and used to determine transfer characteristics directly from the flow graphs. This simple device eliminates the usual duplication or neglect of loop combinations which are not obvious. Signal flow graphs provide a more efficient method of solving certain types of problems than do other conventional methods using determinants or matrices, and flow graphs replace tedious manual calculations with shorter and more rapid mental tasks.

9055 TRANSMISSION AND HYBRID PARAMETERS FOR n-PORT NETWORKS by L.P. Huelsman (U. California, Berkeley); Proc. NEC, Vol. 15, pp. 920-927, Oct. 12-14, 1959

A theorem which states the conditions under which any arbitrary set of parameters of an n-port network may be realized from any other given set is presented. This theorem overcomes the difficulties inherent in applying 2-port techniques to the n-port case. The general solution determines the transmission parameters of the n-port network from the Z, Y or hybrid parameters of the network. The theorem is applied to a specific 3-port network to illustrate the method.

9056 THE EFFECT OF ELEMENT TOLERANCES ON CASCADED FOUR TERMINAL NETWORKS by E.A. Worrell and H.J. Yost (Westinghouse); Proc. NEC, Vol. 15, pp. 945-958, Oct. 12-14, 1959

A general equation for a circuit consisting of theoretically identical cascaded sections with element tolerances included is derived. The difficulty of multiplying a large number of nonidentical matrices, which is the case with tolerances included, is overcome by a matrix transformation and splitting. The resulting equation is in a single matrix form, from which any of the circuit functions may be taken. The voltage transfer function is given in a series, whose successive terms contain a higher order of tolerance. A statistical study results in the derivation of the mean and standard deviation of the voltage transfer function. Examples are given to show the application of the general equation to practical circuits.

9057 TRANSFER FUNCTION OF GROUNDED TWO-PORTS WITH ONE INDUCTOR by S.L. Hakimi (U. Illinois); Proc. NEC, Vol. 15, pp. 937-944, Oct. 12-14, 1959

A proof that any RLC realizable transfer function which has no more than one pair of complex poles can be realized as an RC network terminated in a series combination of an inductor and a resistor is presented. It is shown that available inductors which are inherently lossy may be used to terminate the RC network. Emphasis is on the realization of voltage transfer functions but open-circuit impedance and short-circuit admittance transfer functions can be realized in a similar manner.

9058 THE CIRCUITRY FOR SCATTERING MATRIX SYNTHESIS by K.L. Su (Georgia Inst. Tech.); Proc. NEC, Vol. 15, pp. 928-936, Oct. 12-14, 1959

A collection of scattering matrix combinations and their corresponding network interconnections is presented. Among them are several novel suggestions. They include a scheme that averages two scattering matrices, a means to add two matrices with different relative weights, and a device to add two matrices directly. The application of this technique to actual circuits is discussed.

9059 CASCADE SYNTHESIS OF RECIPROCAL AND NON-RECIPROCAL LOSSLESS 2-PORTS by W.L. Rubin (Polytech. Inst. Brooklyn); Diss. Abstr., Vol. 21, p. 1507(A), Dec. 1960

A new and more general 2-port synthesis procedure, in terms of the scattering matrix, was developed. The development cycle of (1) construction of a simplest scattering matrix, (2) computation of a residual scattering matrix, and (3) development of canonic 2-port configurations, was fully described. The results indicate the possibility of extending this synthesis procedure to the cascade synthesis of lossy 2-ports as a cascade of lossless and lossy canonic 2-ports. Examples of the new synthesis procedure for lumped and distributed nonreciprocal 2-port lossless networks were presented.

## AMPLIFIERS

9060 GAIN CONTROL CIRCUIT FOR SEMICONDUCTOR AMPLIFIERS by W.F. Chow (GE); U.S. Pat. 2,898,411, Issued Aug. 4, 1959

A circuit which controls the operating point of a transistor amplifier in accordance with the strength of the signal being amplified is described. A detector circuit provides a dc voltage which is direct coupled to the emitter-base circuit. This control signal is then amplified together with the information signal, providing an output which shifts the operating point of the collector circuit of the amplifier in a direction such as to maintain the magnitude of the output substantially constant, independent of the magnitude of the input.

9061 TRANSISTOR AMPLIFIER HAVING SIMULTANEOUS GAIN AND SELECTIVITY CONTROL by A.J.W.M. Van Overbeek (N.A. Philips); U.S. Pat. 2,890,293, Issued June 9, 1959

A transistor amplifier with gain control in which the selectivity varies to a desired extent with changes of the control current, while the effect on the resonant frequency remains negligible, is described. The series resonant circuit consists of a capacitor, an inductor and the input impedance, $Z_i$, of a transistor. Connected in parallel with $Z_i$ is an impedance having a value which lies between the minimum and maximum of $Z_i$, the latter being controlled manually or automatically by a current source. Gain and selectivity control are achieved if the transistor is operated in grounded base connection and if the external impedance has mainly the nature of a resistor. The circuit is applicable in the HF and IF sections of a receiver.

9062 CASCADED TETRODE TRANSISTOR AMPLIFIER by R.J. Zelinka (Minn.-Honeywell); U.S. Pat. 2,897,295, Issued July 28, 1959

A compound tetrode junction transistor circuit which is relatively insensitive to ambient temperature variations and which possesses nearly linear transconductance characteristics is described. The total leakage current of the circuit is limited to the arithmetic sum of the individual leakage currents, $Ic_o$, and the leakage of one unit is not amplified by the succeeding units. A hard back bias between the emitter electrode and one base electrode maintains the linearity of the transconductance, and the low leakage current obviates the need for external feedback to improve stability. A suggested physical configuration for a two-tetrode compound unit utilizing annular electrodes is given.

9063 NON-LINEAR DISTORTION IN TRANSISTOR AMPLIFIERS WITH AUTOMATIC AMPLIFICATION CONTROL by Ye. P. Dement'yev; Radio Engrg., Vol. 14, No. 11, pp. 78-90, 1959

The causes of the nonlinear distortions which arise when the amplification is conrrolled either by varying the emitter current or the collector voltage are examined. Operation using active and resonant loads are examined and the principal quantitative relationships are established.

9064 SEMICONDUCTOR AMPLIFIER CIRCUITS by H.C. Lin (RCA); U.S. Pat. 2,896,029, Issued July 21, 1959

A transistor amplifier circuit which efficiently provides a high power output, a wide frequency range and low distortion is described. An input signal is applied to both parallel connected bases of a pair of opposite conductivity-type transistors. These transistors provide the required out of phase signals to drive the output stage. The output stage consists of a pair of like conductivity-type transistors connected as a push-pull power amplifier and arranged in a parallel single-ended relation for supplying output currents to a utilization device. No coupling transformer is required. The basic circuit and a modification to permit application of bias to the transistors are described. Class B operation is utilized to provide high power output in an efficient manner. Effective application may be made of this circuit for audio amplifiers in radio and television receivers.

9065 SEMI-CONDUCTOR AMPLIFIERS by R. Chapman and L.E. Robinson (Intl. Stand. Elect.); U.S. Pat. 2,901,556, Issued Aug. 25, 1959

A stabilized hearing-aid amplifier having minimal power consumption in the stabilizing network is described. The multistage transistor amplifier employs dc negative feedback to achieve stabilization against temperature changes and a constant power output for a wide range of transistor parameters. Additional ac negative feedback adds to the signal stabilization factor. Step-down auto-transformers are used for interstage coupling. Seven circuits embodying the feedback design are shown using from two to four transistors.

9066 TRANSISTOR AMPLIFIER CIRCUITS by R.R. Webster (Texas Instr.); U.S. Pat. 2,901,558, Issued Aug. 25, 1959

A transistorized RF amplifier with neutralization of the interelectrode capacitance is described. The neutralization feedback network is connected between a secondary coil of the output transformer and the primary coil of the input transformer of the amplifier circuit. An optimum power level of the feedback signal is thus achieved; the feedback capacitor in this circuit is sufficiently large for variations of the stray capacitance in the amplifier to be neglected.

9067 DIODE AMPLIFIER by W.A. Ogletree (Burroughs); U.S. Pat. 2,892,979, Issued June 30, 1959

A diode pulse amplifier with low standby power requirements is described. The device uses the dynamic impedance characteristic displayed by a Ge junction diode when it changes its conductive state. Current carriers, injected by a forward voltage, are swept out by a reverse voltage. The diode is used as a nonlinear impedance in a divider circuit, and the forward signal current controls the voltage division of a reverse potential. An AM pulse train can be generated by varying the amount of forward current flow. A current gain of 20 and a voltage gain of 8 have been obtained.

9068 SEMI-CONDUCTOR SIGNAL TRANSLATING CIRCUITS by J.P. Jones, Jr. (Navig. Computer); U.S. Pat. 2,897,378, Issued July 28, 1959

A transistor pulse-amplifier which produces a pulse output with rapid rise and fall time in response to a pulse input is described. The input pulse is coupled to a damped parallel resonant circuit which produces a sinewave pulse whose half sinewave interval is approximately equal to the duration of the applied pulse. This sinewave first drives the transistor into the saturation region and subsequently into the cutoff region in a rapid fashion, thus achieving a high frequency response. Stability and reliability is attained by adding damping in the resonant circuit.

9069 GAIN AND BANDWIDTH CONSIDERATIONS IN REACTANCE UP-CONVERTER PARAMETRIC AMPLIFIERS by A. J. Holub (Purdue U.); Diss. Abstr., Vol. 21, p. 1504(A), Dec. 1960

An analysis of reactance up-converter parametric amplifiers with special emphasis on operation in the lower UHF range was presented. The gain of these amplifiers is equal to the maximum theoretical gain only when a parameter a, involving a product of the signal frequency, upperside band frequency, load impedance and nonlinear diode coefficient, is unity. This value of a is very difficult to achieve. After theoretical discussion of an optimum amplifier, the performance of an experimental amplifier was described and analyzed.

9070 MAGNETIC FILM PARAMETRIC AMPLIFIERS by A.A. Read and A.V. Pohm (Iowa State U.); Proc. NEC, Vol. 15, pp. 65-78, Oct. 12-14, 1959

The use of thin film inductive elements as nonlinear low-loss reactances for parametric amplifiers is discussed. An experimental parametric amplifier having a pump frequency in the 20 - 30 Mc range has been constructed. Signal gains in the 20 db range have been obtained as well as superregenerative detection of very low level signals. Thin film parametric amplification has been discussed both graphically and analytically in terms of a quasi-static model. At frequencies below VHF this is satisfactory. At higher frequencies a model with losses must be considered. Such a model indicates that operation up to 100 Mc or higher should be feasible with moderate pumping powers.

9071 CLASS B TRANSISTOR AMPLIFIER by A.I. Aronson (RCA); U.S. Pat. 2,892,045, Issued June 23, 1959

An improved Class B transistor amplifier is described. The amplifier, which may be used in either a single-ended or push-pull configuration, employs capacitative coupling while maintaining relatively distortion-free amplification. This accomplished by the use of a degenerative feedback resistor in the emitter circuit and by shunting the emitter-to-base junction with an external resistor, thereby maintaining a substantially linear input impedance. Design equations are given.

## OSCILLATORS

9072 TRANSISTOR OSCILLATORS by E.M. Jones and C.F. Winder (Baldwin Piano); U.S. Pat. 2,902,655, Issued Sept. 1, 1959

A common-base pulse oscillator in which the frequency is stabilized by an L-C series resonant circuit is described. The frequency of oscillation may be varied in response to a control signal of low frequency. The circuit is suitable as a master oscillator of electronic musical instruments to drive a chain of 2:1 frequency dividers or to provide an output waveform rich in harmonic content.

9073 MAGNETIC COUPLED MULTIVIBRATOR by T. Erb (Sperry Rand); U.S. Pat. 2,894,210, Issued July 7, 1959

A self-exciting multivibrator having magnetic circuit control is described. The circuit consists of one transistor and a saturable core. Self-excitation is produced by the recurring unidirectional charging of a condenser connected at the input of the saturable core. The condenser charge is sufficient to remove the blocking bias voltage at the transistor base when the flux state in the magnetic circuit is stabilized. The frequency of the generated pulses is controlled by a variable resistor in series with a control winding of the reactor. The circuit delivers uni-directional power pulses with a substantially constant volt-time area.

9074 TRANSISTOR OSCILLATOR FOR VIBRATO PURPOSES by M.B. Gregory (Baldwin Piano); U.S. Pat. 2,899,648, Issued Aug. 11, 1959

A one-transistor sub-audio oscillator which may be used to frequency modulate multiply-connected master audio oscillators is described. The circuit is of the Hartly type and is so designed that the amplitude of the sub-audio oscillator signals may be varied without affecting either the frequency of this oscillator or the frequency or amplitude of the master oscillator. The circuit is employed as a vibrato signal generator in an electronic musical instrument.

9075 OSCILLATOR CIRCUIT FOR TRANSISTORS by T. Grewe (Intl. Stand. Elect.); U.S. Pat. 2,896,170, Issued July 21, 1959

A transistor oscillator circuit in which any phase shift due to load change is avoided and which includes a limiter for the control current is described. The control current is obtained from a direct current source through a dropping resistance and is divided into two paths; one comprising a rectifier and the other comprising the emitter-base path. The current is controlled in part by a voltage feedback and is divided into two pulsating direct currents of which the current flowing through the base-emitter path controls the transistor. By this means the collector-to-emitter voltage cannot be reduced to zero and the output circuit will be highly resistive irrespective of phase conditions. The basic circuit and several modifications are described.

9076 TRANSISTORIZED VOLTAGE CONTROLLED OSCILLATOR by R.K. Dahlin (NA Aviation); U.S. Pat. 2,898,557, Issued Aug. 4, 1959

An oscillator whose frequency is controlled by a dc input voltage is described. The input voltage charges a capacitor through a series resistance. When the capacitor voltage exceeds a predetermined level, a normally nonconductive diode is rendered conductive, transmitting a pulse which is then amplified and applied to a blocking oscillator. This produces an output pulse, part of which is fed back to the base of a transistor connected to the charging capacitor. This turns on the transistor and discharges the capacitor through the collector-emitter circuit to ground, thus re-establishing the zero-reference level. Since the amplitude of the input signal determines the charging rate of the capacitor and thus the pulse rate of the blocking oscillator, the frequency of the output signal is effectively controlled by the amplitude of the input signal.

9077 STABLE TRANSISTOR OSCILLATOR SYSTEM by E.J.H. Bussard (Avco Mfg.); U.S. Pat. 2,894,211, Issued July 7, 1959

A transistor oscillator system which will give frequency stable performance and be tunable over a wide frequency range, and which can use the various types of commercial transistors with good efficiency is discussed. A dominant positive feedback circuit is employed using a high Q and a capacitive voltage divider to provide regeneration. Self adjustment of the transistor to its best operating conditions and stable power flow is established by a combination of a fixed base bias and employment of a negative feedback emitter resistor. The emitter resistor can be made variable to control the output power over a wide range. The resonant circuit consists of a tapped winding to minimize the effects of transistor parameters. The oscillator circuit may be incorporated as the local oscillator in a superheterodyne receiver.

9078 TRANSISTOR MULTIVIBRATOR by A.H. Faulkner (Genl. Tel. Labs.); U.S. Pat. 2,900,606, Issued Aug. 18, 1959

A transistorized multivibrator having separate and independent controls for varying the cycle period and the pulse width ratio is described. The conduction biasing potential, and hence the operating frequency, is controlled by a voltage applied jointly to the emitter electrodes; the resistors in the time constant networks are connected via a common potentiometer in a way that permits their ratio to be varied inversely, thus varying the ratio of the conduction periods of the two transistors.

9079 REDUCTION OF MULTIVIBRATOR RECOVERY TIME by G.L. Haugen (Bendix Aviation); U.S. Pat. 2,898,478, Issued Aug. 4, 1959

A means of reducing the recovery time of a transistor monostable multivibrator is described. The recovery time is largely determined by the charging rate of the coupling capacitor between the two transistors. This charging rate is in turn limited by the resistance in the collector circuit of the first or input transistor; the resistance serves to provide a conductive path for the transistor during its astable condition. An inductive component is added in series with the resistance so that the energy stored in its magnetic field during the astable period is sufficient to charge the coupling capacitor. This effectively bypasses the collector resistance and thus reduces the charging time. A diode may be added in parallel across this combination so as to afford a low impedance discharge path for the inductor during the portion of the cycle.

Hall Effect Oscillators - See 9019

## SWITCHING CIRCUITS

9080 TRANSISTOR SWITCH by W. Shockley (Consol. Electrody.); U.S. Pat. 2,891,171, Issued June 16, 1959

Methods of eliminating spurious signals introduced by a switching circuit are shown. The connections to emitter and collector are reversed to achieve a high alpha which in turn reduces the value of the saturation voltage. A bias voltage equal and opposite to the saturation voltage is effective in eliminating spurious voltages since the saturation voltage is independent of the control voltage applied to the base and relatively insensitive to temperature changes. Balanced circuits in which the spurious voltages cancel because of symmetry are described. Balance is provided by an additional pair of p-n junctions that are either in series or in parallel with the transistor.

9081 DESIGN OF A BROADBAND UHF DIODE SWITCH by J.H. Hendershot (Electronic Commun.); Electronic Design, Vol. 9, pp. 124-127, Nov. 22, 1959

A high speed low-power SPST coaxial switch operating from 100 to 1000 Mc is described. A diode is connected in series with the center conductor of a 50 ohm coaxial line. When the diode is biased "on" with a positive voltage, it presents a low impedance to the incident RF power. For a negative applied voltage, the diode impedance is very large and nearly all the incident RF power is reflected. Circuit diagrams and characteristics are given, and a discussion of diode selection is presented. The 1N100 diode was selected because of its high ratio of reverse-to-forward resistance, small physical size, low cost and reasonably low barrier capacitance. A multiport 6-throw switch is also discussed. The switches are useful for switching low-power signals in such receiver applications as frequency channel selection or antenna switching. They have alternate application as modulators, choppers, and attenuators.

Flip-Flop Switching Circuits - See 9101

9082 TRIGGER CIRCUIT FOR USE IN TIME DIVISION MULTIPLEX SYSTEMS by R.B. Trousdale (Genl. Dynamics); U.S. Pat. 2,898,526, Issued Aug. 4, 1959

A trigger circuit with sufficient power to maintain a relay operated so long as control pulses persist in a single time position in repetitive time position frames is described. The circuit consists of a bistable multivibrator which is completely conducting or completely nonconducting, and a two-input AND gate which controls the state of the multivibrator. A continually recurring reset pulse is applied to the emitter of one transistor of the multivibrator; these pulses occur in a position immediately prior to the control pulse time position frames, and maintain the multivibrator in the "off" position. When the two control pulses appear in overlapping positions, they are gated through the AND gate to the base of the multivibrator, turning it on and closing the relay. The relay remains closed until the control-pulses are removed and the next reset pulse causes the multivibrator to return to the "off" or nonconducting state.

9083 TRANSISTOR SWITCHING CIRCUIT by C. Huang (Sylvania); U.S. Pat. 2,901,638, Issued Aug. 25, 1959

Bistable circuits utilizing multiple-emitter transistors in which each emitter is capable of switching the transistor from the "off" to the "on" state are described. AND, OR and AND/OR building blocks utilizing this device perform reliably and are of less complexity than conventional circuits. A serial binary adder in which such logical functions as OR, "reset" and "inhibition" are achieved uses a single transistor of the multiple-emitter type, eliminating plural external gating diodes.

9084 GATING CIRCUITS FOR ELECTRONIC COMPUTERS by A.D. Scarbrough (Thompson RW); U.S. Pat. 2,892,103, Issued June 23, 1959

A group of gating circuits which can translate either pulse type or steady state output signals of a bistable circuit or other two state device into pulses representing the state of the device is described. The bi-level control signal of the two state device is utilized to control a gating device (a grounded emitter transistor) connected in series with the primary section of a transformer. Timing pulses are then applied across this primary to pass current through the gating device when it is closed in response to one of the levels of the control signal. No pulse passes through the transformer when the two state device is in its other state and the associated gating device is open. This technique avoids the needs for pulse shaping and synchronization on an extensive scale when pulse type signals are used, and does not draw excessive power from the bistable device when steady state signals are used. The required power is drawn from the clock or synchronizing pulses under control of the bistable device.

9085 COINCIDENCE GATE TRANSISTOR CIRCUIT by E.S. McVey (U.S. Navy); U.S. Pat. 2,892,953, Issued June 30, 1959

A transistor coincidence gate circuit which produces output pulse signals of a magnitude equivalent to that of the smaller of two coincident input pulses is described. The circuit consists of two normally conducting transistors. Their emitters are in parallel and are connected to a load across which the output signal is developed. Application of a negative pulse to one transistor to decrease conduction will cause the other transistor to increase its conduction because of the positive bias in common to the emitters of these transistors. If negative pulses are applied to both transistors, each is attenuated in conduction during coincidence and a negative output pulse is developed across the load. The circuit has power gain since the input impedance is high and the output low. The circuit is applicable in radar ranging devices wherein video signals can be applied to produce output pulses for operation of tracking or lock-on discriminator circuits.

9086 TRANSISTOR-SATURABLE REACTOR RELAY WITH OVER FREQUENCY CUTOUT by R.J. Price; U.S. Pat. 2,894,180, Issued July 7, 1959

An apparatus for operating a relay or other load by a large central current which is controlled by a single trigger pulse or group of pulses is described. A saturable reactor is employed to control current through the load. In the absence of an input trigger pulse, current through both halves of a control winding of the reactor sets up opposing flux which tends to neutralize the field and to cause the reactor to present a high impedance to the load current. An input signal triggers a transistor blocking oscillator which produces a discharge of an output capacitor to effect saturation of the reactor. The output of the blocking oscillator is also applied to another capacitor through a resistor which provides an adjustable time constant. When the frequency of the incoming signal is high enough, the second capacitor voltage is applied to another reactor winding to effectively disable the first winding and thus prevent saturation.

9087 THREE-STATE ELECTRONIC CIRCUIT by E.L. Wolf (Gen Dynamics); U.S. Pat. 2,901,641, Issued Aug. 25, 1959

A three-state (trinary) circuit using two neon diodes and a transistor is described. The potentials across the neon diodes are arranged in such a way that the diodes fire consecutively upon application of pulses of a discrete amplitude. The first input pulse causes diode 1 and the transistor to conduct, producing an output pulse as well as an indication of the state of the scale-of-three. The second input pulse extinguishes diode 1 and causes diode 2 to conduct, while the differentiated third input pulse causes the circuit to revert to its original state.

## SIGNAL CONVERTERS

Frequency Modulators - See 9101

9088 APPARATUS FOR GENERATING FREQUENCY MODULATED SIGNALS by D.C. Erdman (Electrocircuits); U.S. Pat. 2,902,658, Issued Sept. 1, 1959

An apparatus for generating frequency modulated signals for use in measuring the propagation time of waves along a path is described. Two waves are produced in time sequency having frequencies which sweep periodically in a similar manner. The second wave starts at a later time and is offset in frequency from the first wave. To produce these waves a negative resistance transistor oscillator is employed which has a sawtooth wave applied to one electrode to provide a sweep in frequency and a square wave applied to another electrode to cause the frequency of oscillation to change abruptly from one level to another. One or both of the waves may be transmitted from the source to a reflecting target, and the reflected waves are mixed with one or both of the waves which are then being produced by the source. An indicator arrangement provides an indication of the occurrence of heterodyne signals having a certain frequency. A block diagram and discussion are given for the entire wave propagation measuring device. The device is useful in producing ultrasonic waves such as are employed in the nondestructive testing of materials to detect hidden flaws for physical research.

Hall Effect Phase-Shift Modulators - See 9019

9089 DETECTOR AND AGC SYSTEM by R.W. Bradmiller (Avco Mfg.); U.S. Pat. 2,891,145, Issued June 16, 1959

A power detector circuit used as a demodulator in a transistor receiver system is described. Isolation between the receiver detector diode and its load is achieved by means of an emitter follower of high input impedance. The following advantages are derived: (1) distortion-free low level signal detection, (2) distortion-free high percentage modulation detection, (3) transformerless audio circuitry, (4) one or two orders of AGC control power more than is usually available from a simple diode detector, and (5) a demodulation process unaffected by varying audio or AGC loads.

9090 DISCRIMINATOR by R.M. Tillman (Burroughs); U.S. Pat. 2,900,508, Issued Aug. 18, 1959

A solid state subcarrier discriminator whose linearity and stability are independent of variations in the supply voltage over a wide range is described. The discriminator is of the pulse averaging type, and the voltage-time product of the pulses generated is maintained constant by employing a magnetic core with a substantially rectangular hysteresis loop. The circuit is particularly suited for telemetry.

9091 DETECTOR CIRCUIT by R.P. Crow (Motorola); U.S. Pat. 2,891,156, Issued June 16, 1959

A transistor frequency selective detector is described. In the basic circuit one input signal is applied between the base and emitter of a transistor so that this signal will be detected and tend to cause unidirectional current flow to the collector of the transistor. A second input signal is applied between the base and collector of the same transistor. This signal is detected and tends to cause unidirectional current flow in the opposite direction to the emitter electrode. A load impedance in the emitter-collector circuit is used to derive the difference between the two currents. By constructing the input circuits with particular characteristics the apparatus may be made very selective and responsive only to a particular relationship between input signals. Circuit applications as a narrow band amplifier, a detector circuit used in a radio control system for operating a garage door, or as a detector for frequency modulated signals are illustrated.

9092 TRANSISTOR PHASE DISCRIMINATOR by J.G. Hinsdale (Lear); U.S. Pat. 2,897,379, Issued July 28, 1959

A transistor phase discriminator which supplies an output to a split load impedance is described. A single transistor is employed, and diode rectification is used to supply unidirectional current pulses to one or the other of the load impedances in accordance with the phase of the input signal with respect to the reference signal. Transformer coupling is used for both the input and reference signals, resulting in a stability factor of less than two. Two discriminators may be connected in parallel to supply successive current pulses to the load and reduce the need for supplemental filtering where inductive loads are used. The circuit may also be modified to supply current pulses to both impedances, with the amplitude of the pulse supplied to each depending on the phase characteristics of the signal and reference voltages.

9093 PHASE SHIFT DETECTOR by L.E. Dwork and C. Huang (Sylvania); U.S. Pat. 2,901,612, Issued Aug. 25, 1959

A phase-shift detector in which the output signal varies proportionately to the phase shift, is described. The circuit utilizes a pair of complementary transistors and is suitable for use as a discriminator in a frequency modulation receiver.

9094 SAMPLING CIRCUIT by S.C. Rogers (Bell Labs.); U.S. Pat. 2,900,507, Issued Aug. 18, 1959

A pulse-position demodulator with sampling and storage circuits for converting a pulse position code into a direct current potential is described. The sampling switch has a low closed-circuit impedance so that the signal to be sampled is not attenuated in the switch, while maintaining a high open circuit impedance to eliminate false outputs due to leakage through the switch. The storage circuit will handle both positive and negative signals, and combines the two by means of an adder circuit which gives a single output voltage for use as a control potential.

9095 FREQUENCY HALVER by J.F. Reuther and S.D. Silliman (Westinghouse); U.S. Pat. 2,892,102, Issued June 23, 1959

A bistable multivibrator which produces a square wave output pulse for alternate square wave input pulses is described. Diode steering is used to trigger the circuit from one stable state to another, using pulses supplied from a common trigger circuit.

Short trigger pulses of the order of one microsecond are obtained from the discharge of a capacitor initiated by the application of a pulse from the square wave generator.

9096 AN INVESTIGATION OF HARMONIC GENERATION USING SEMICONDUCTOR JUNCTION DIODES by J.W. Rood (Cornell U.); Diss. Abstr., Vol. 21, p. 1507(A), Dec. 1960

The effects of loss and finite voltage range on harmonic generation efficiency and power handling ability, utilizing a nonlinear reactance in the form of semiconductor junction diodes, were described. The possibility of designing the semiconductor junction itself to increase the power handling ability was discussed. Results were presented showing overall efficiencies of over 50 per cent for generation of second harmonic power from a 400 Mc input power level of 1 watt.

9097 A TRAVELING WAVE HARMONIC GENERATOR by D. L. Hedderly (Brit. Telecommun. Res.); Proc. IRE, Vol. 48, p. 1658(L), Sept. 1960

A traveling wave harmonic generator which generates only the desired harmonics is described. Power at the fundamental frequency F is provided at the input of a propagating structure containing n diodes and (n-1) sections. If only one diode at a time conducts as the fundamental wave travels down the structure and the delay per section is {1/n F} sec, the principal component of the voltage across the load will be at a frequency of nF. Attenuation in the fundamental wave as it travels down the line can be compensated by progressively reducing the dc bias on the diodes.

9098 LINEAR VOLTAGE-TO-FREQUENCY CONVERTER by W.N. Toy (Bell Labs.); U.S. Pat. 2,894,215, Issued July 7, 1959

A circuit for a multivibrator wave generator whose output frequency can be varied linearily under the control of one or more external signals is described. The circuit consists of a bistable multivibrator which is triggered back and forth between its two stable states of equilibrium by an external timing circuit. Each stage is triggered from its ON condition since the base potential is better defined than in the corresponding OFF state. The timing circuit is reset after each triggering of the bistable multivibrator by a transistor switch connected between the timing capacitor and a source of reference potential. When the transistor switch is open, the timing capacitor is isolated from the reference source and the potential across it is free to change toward the level determined by the input signal. When the transistor switch is closed, the timing capacitor is clamped to a reference potential. The circuit exhibits an increased frequency range and less dependence upon incoming signal amplitude.

## WAVE GENERATORS

9099 SEQUENTIAL PULSE GENERATOR by S. Paull; U.S. Pat. 2,891,170, Issued June 16, 1959

A magnetic core pulsed circuit which operates in the manner of a blocking oscillator or flip-flop circuit is described. No "clock" or other auxiliary source of potential is required to initiate the operation of the pulser, which uses the power supply only during switching of the magnetic cores from one state of remnance to another. Since the trigger pulse above initiates the operation of the pulser, the pulses can be supplied in any frequency, or at any arbitrary time, limited only by the minimum time required between the arrival of the first input pulse and the completion of the resetting of the cores to the zero state after all the stages have been operated. The reset is automatic and occurs after the $n^{th}$ stage has been switched from its "0" to "1" condition. The circuit has possible applications in time delay units and telemetering devices.

9100 RAMP FUNCTION TRANSISTOR CIRCUIT by E.S. McVey (U.S. Navy); U.S. Pat. 2,892,952, Issued June 30, 1959

A bootstrap semiconductor circuit for producing linear ramp voltages in direct correspondence to the time interval of applied input gating pulses is described. A negative gate is applied to the base of a normally heavily conducting transistor producing a sharp cutoff of conduction. The collector voltage of this transistor begins to rise. The voltage rise is applied directly to the base of an emitter follower transistor. The emitter voltage rise of the second transistor feeds back a current to keep the voltage across the charging resistor constant. The current through the charging resistor is applied to storage capacitors to produce a linear ramp output voltage. Modifications of the basic circuit to compensate for temperature effects and to improve frequency response are given. The circuit may be employed as a component of a radar range unit.

9101 TRANSISTOR WAVEFORM GENERATORS by G.N. Webb and R.N. Glackin (Johns Hopkins U.); 1959 IRE Natl. Conv. Rec., Part 9, pp. 51-55

Three basic transistor circuits are described, their operation is explained, and their critical design features are outlined. The units are: a positive or negative going linear ramp, a pulse generator and a flip-flop. Ways of interconnecting these building blocks to make (1) a voltage controlled frequency modulator, (2) a triggered, linear sawtooth with duration from 100 μsec to 200 sec, (3) trapezoid stimulating waveforms with separately controlled rise, dwell and fall time, and (4) delay units for physiological stimulating programs are illustrated. Construction features which help to minimize temperature effects are shown. Performance characteristics under operating conditions are presented.

## OTHER CIRCUITS

9102 TEMPERATURE STABILIZED TWO-TERMINAL SEMICONDUCTOR FILTER CIRCUIT by J.E. Lindsay (RCA); U.S. Pat. 2,892,165, Issued June 23, 1959

Means for stabilizing filter circuits utilizing opposite conductivity-type semiconductor devices are given. A circuit arrangement which permits connecting the collector electrode of a transistor of one conductivity-type directly with the base electrode of a transistor of an opposite conductivity-type is described. Phase shifts which might accompany the use of capacitive coupling are thus eliminated and the possibility of circuit oscillations under certain operating conditions is prevented. A pair of diodes is connected in the base emitter circuit of the first transistor to temperature stabilize the circuit.

9103 LIMITING CIRCUIT by J.M. Cluwen (Philips); U.S. Pat. 2,885,575, Issued May 5, 1959

A transistorized signal limiter having an input resonant circuit is described. Dynamic limiting is produced by a rectifier and RC filter circuit connected across the input of the resonant circuit. The filter has a long time constant and is insensitive to unwanted amplitude variations. A voltage proportional to the mean signal voltage is applied to the collector of the operational transistor. Polarities of the rectifier are so chosen that when the instantaneous amplitude is reached, at which limitation of the dynamic limiter begins, the instantaneous value of the collector-base voltage periodically becomes substantially zero. Hence, the transistor is operated in collector limitation. This involves a periodic increase in the input impedance of the transistor which causes the input resonant circuit to be periodically damped in a sense to further suppress the unwanted amplitude modulation. Other configurations are presented and some circuit detail is given.

9104 TRANSISTOR SIGNAL TRANSLATING CIRCUIT by C. C. Bopp (Avco Mfg.); U.S. Pat. 2,894,150, Issued July 7, 1959

A transistor amplitude limiting circuit which may be arranged to provide signal amplification is described. Signal limiting action is accomplished by biasing the emitter electrode at a low value of current. Input signals of sufficient strength cause the emitter to rectify which, due to a long time constant, changes the emitter bias and makes it proportional in magnitude to the applied signal. An alternate method is given whereby the emitter is heavily biased in a forward direction to prevent rectification but the collector bias is relatively low. The load is adjusted such that the load line would terminate near cutoff. In this case driving the emitter with a signal greater than a given magnitude does not appreciably increase the collector voltage. A combination of both limiting modes is also given. Pulse limiting operation may be enhanced by connecting a varistor between the emitter and the base of the transistor. The circuit is useful in frequency modulation receivers in which the inclusion of added gain at no cost in transistor complement is advantageous.

9105 AN INVESTIGATION INTO SOME ASPECTS OF DIODE QUANTIZING CIRCUITS by H.V. Bell and W. Alexander (U. Nottingham); Electronic Engrg., Vol. 31, pp. 594-598, Oct. 1959

The construction and application of diode quantizing circuits is described. Formulae for the degradation (departure of the actual quantizer transfer characteristics from the ideal linear-step relation) are given, and the calculated results are shown to be in good agreement with measured results. Circuits for four-level and ten-level quantizers are given, together with a display of their transfer characteristics. Examples of the quantization of sine-waves and speech-waves are given. The need for diodes with low forward resistance and high backward resistance is shown.

# APPLICATIONS OF SOLID STATE DEVICES

## COMMERCIAL AND SPACE

9106 IGNITION SYSTEMS by R.L. Jaeschke (Eaton Mfg.); U.S. Pat. 2,898,392, Issued Aug. 4, 1959

A transistorized automotive ignition system is described. The automotive generator supplies an ac signal having a frequency and amplitude which are functions of engine speed. The signal is then applied to a transistor switch which closes at a predetermined value to establish an oscillatory current of high frequency (15 kc) in a tank circuit. The inductance in this tank circuit forms the primary of a step-up transformer which generates a voltage of 10 to 15 kv in the transformer secondary winding, where it is then available for distribution to the spark plugs.

Automotive Generator Regulators - See 9129

9107 ELECTRONIC TRACK CIRCUIT FOR RAILROADS by J. H. Auer, Jr., C.S. Wilcox, and M.E. Hoff, Jr. (Genl. Rwy. Sig.); U.S. Pat. 2,896,068, Issued July 21, 1959

An electronic track circuit system which may be superimposed without interference upon the usual track circuits employed in railway signaling practice is described. The circuit comprises a high audio frequency transmitter whose output appears across the secondary winding of a transformer. This winding and the primary winding of a transformer associated with a receiver are connected in series across the track rails. The series circuit can be completed only by a shunt of the track rails as produced by a railway vehicle. When the rails are properly shunted, energy is coupled from the transmitter to the receiver and results in the actuation of a track relay. By proper adjustment of circuit parameters a relatively uniform sensitivity characteristic over a predetermined length of track rail is possible. A full description of the circuit including its application with a system for the control of a switch lock is given.

9108 INSTRUMENTATION FOR A THERMAL RADIATION BUDGET SATELLITE by R.J. Parent, H.H. Miller, V.E. Suomi, and W.B. Swift (U. Wisconsin); Proc. NEC, Vol. 15, pp. 824-839, Oct. 12-14, 1959

Transistorized circuitry for the Explorer VII Thermal Budget Satellite is described. The unit includes both resistor and thermistor sensing devices which are sampled by a 9-channel commutator. Two ten stage binary scalers receive the information, are sampled and the data is recorded for later transmission. A general description of the overall system is given and the circuits are discussed in some detail.

9109 ULTRA-LOW-NOISE ANTENNA AND RECEIVER COMBINATION FOR SATELLITE OR SPACE COMMUNICATION by R.W. DeGrasse, D.C. Hogg, E.A. Ohm, and H.E.D. Scovil (Bell Labs.); Proc. NEC, Vol. 15, pp. 370-379, Oct. 12-14, 1959

A traveling-wave solid-state maser and a low-side-lobe horn-reflector antenna combined to realize an ultra-low-noise receiving system are described. Overall input temperatures as

low as 17.6°K have been observed at 5.65 kMc where this figure comprises the noise contribution due to the sky, the antenna, and the maser-preamplifier. Noise contributions from the following stages can easily be made negligible. The ultimate limitation in sensitivity of an earth-based receiving system is set by noise generated in the earth's atmosphere. A zenith sky temperature of 2.7°K at 6 kMc has been calculated. The actual value was measured using the low-noise receiving system. From this measurement a zenith sky temperature of $2.5 \pm 0.75$°K was determined. Thus it seems advisable to attempt even a lower receiving system noise temperature. It appears that, by reduction of waveguide and coax losses in the present system, a system noise temperature of 10°K could be realized at 6 kMc, while a noise temperature of 7°K is expected at 2 kMc, both for the vertical antenna position.

## RADIO AND TELEVISION

9110 TRANSISTOR RADIO APPARATUS by R.C. Koch (I.D. E.A.); U.S. Pat. 2,892,931, Issued June 30, 1959

A superheterodyne transistor circuit which consumes a minimum of current is described. A battery powered biasing circuit serves one transistor stage and an auxiliary biasing circuit operates off normal transistor current to produce bias for another transistor stage. This reduces power consumption and prolongs battery life. The circuit is applicable for miniature commercial receivers as lower power consumption allows a decrease in battery size while maintaining an acceptable battery lifetime.

9111 THE USE OF RADIO NOISE FROM THE SUN FOR CALIBRATING RADIO RECEIVING SYSTEMS by M.E. Armstrong (Collins), G.W. Swenson, Jr., R.L. Sydnor, and H.D. Webb (U. Illinois); Proc. NEC, Vol. 15, pp. 380-393, Oct. 12-14, 1959

A modified Dicke radiometer utilizing solid state diodes in the antenna switch and a transistorized phase sensitive detector is described. The 413 Mc strip line antenna switch cycles at 30 cps. The phase detector is of standard design utilizing a regenerative reference signal amplifier with a Zener diode limited output and a regenerative signal amplifier to drive the balanced diode phase detector.

9112 RADIO RECEIVER WITH TRANSISTORIZED AUDIO-DETECTOR AND AUTOMATIC GAIN CONTROL CIRCUITRY by S. Kagan (Avco Mfg.); U.S. Pat. 2,895,045, Issued July 14, 1959

A radio receiver with improvements in automatic gain control and in detector-audio circuitry is described. A bridge-type signal attenuator including an automatic gain control amplifying transistor in one of its branches is provided. The amplifying transistor has its emitter connected to a delay voltage point and its base connected to the audio output emitter load via a filter. The detector-audio circuit provides the source of AGC control voltage. Power detection is employed to utilize the advantage of both voltage and current amplification in the detector. The detector is directly coupled to an emitter follower output amplifier in such a manner that neither transistor is conductive in the absence of received signals. A discussion of novel circuit features and their application in a complete portable broadcast radio receiver is given.

9113 RETRACE DRIVEN DEFLECTION CIRCUIT FOR CATHODE RAY TUBES by W.B. Guggi (RCA); U.S. Pat. 2,896,115, Issued July 21, 1959

A transistor deflection circuit for cathode ray tubes is described. Energy is circulated among various low resistance reactive elements through low dissipation on-off switches. Assuming that energy has been transferred into the sweep coil during the preceding retrace cycle, then during the sweep period energy is transferred from the sweep coil into a large sweep capacitor or constant voltage source which provides a linear decrease of sweep current. At the same time, energy is also transferred from this capacitor or constant voltage source into a storage inductor. During the latter part of the sweep period, this energy is stepped up to a higher voltage level by charging a small retrace capacitor and then is returned to the sweep coil during the retrace cycle. Design considerations and a description of circuit operation is given. The circuit requires less power, eliminates most of the transient difficulties and has good linearity. It may be employed in deflection circuits for cathode ray tubes used in television.

## TELEPHONY

9114 TELEPHONE SET by H. Kunckel; U.S. Pat. 2,894,075, Issued July 7, 1959

A portable telephone set which is operated from local battery power supply is presented. The device is constructed of lightweight material and the conventional carbon microphone is replaced by a microphone which operates with a battery. Amplification is provided to boost the signal to a level approximately 1 néper above that of the carbon microphone, while requiring only one-fourth of the dc power required by the carbon microphone. The transistor amplifier stage can be made to oscillate and operate as an AF ringer. In a similarly constructed called station, a sensitive receiver may be energized by the AF ringing current to produce a loud ringing signal. Thus, the need for a hand generator and bell is eliminated. The device may be keyed to send code. A schematic and a diagram illustrating physical construction of the telephone set are given.

9115 THE APPLICATION OF DIGITAL COMPUTER TECHNIQUES TO ELECTRONIC AUTOMATIC TELEPHONE SWITCHING SYSTEMS by D.K. Melvin (Genl. Tel.); Proc. NEC, Vol. 15, pp. 593-605, Oct. 12-14, 1959

The basic principles of crosspoint and time-division-multiplex electronic telephone switching systems are discussed with an emphasis on the digital computer techniques used in controlling the voice transmission paths. The requirements for logic, temporary and permanent memory, recirculating memories, registers, and buffer storage are considered. Time sharing of control equipment which enables dial pulses from many subscriber's telephones to be registered simultaneously is also possible with these high speed techniques. A recirculating magneto-striction delay line which records dial pulses and remembers the appropriate time-slot to be used for multiplex transmission is compared with a recirculating ferrite core memory which serves a similar purpose. The advantages of using Boolean algebra in the design of electronic telephone systems for reducing the number of components and simplifying the resulting circuitry are pointed out.

9116 A FULLY ELECTRONIC PRIVATE AUTOMATIC TELEPHONE SWITCHBOARD by J.G. Van Bosse (Genl. Tel.); Proc. NEC, Vol. 15, pp. 585-952, Oct. 12-14, 1959

A fully electronic solid state automatic telephone switchboard designed to serve as a private automatic exchange for up to 100 subscribers is described. Voice frequency connections between subscribers are made in a four stage switching network, using p-n-p-n diodes as switching elements. Control actions in the system are performed by centralized equipment which is time-shared by all subscribers.

## OTHER COMMUNICATIONS TYPE APPLICATIONS

9117 A LIGHT TELEMETRY MOLECULAR SYSTEM by G. Strull (Westinghouse); Proc. NEC, Vol. 15, pp. 640-644, Oct. 12-14, 1959

A unique light telemetry system which involves only a single block of appropriately-doped semiconductor material, a power supply, and a load is described. In darkness the system generates a sawtooth oscillation. When visible light is incident upon the active element, the frequency of oscillation varies inversely with the light level. This is achieved with virtually no amplitude modulation. All other semiconductor devices interpret light with a change in dc level. To telemeter such data, the light must be chopped — a process involving additional circuit elements. In the unique molecular system described, the information is directly in a form suitable for transmission.

9118 EYEGLASS HEARING AID by E.B. Passow (Zenith Radio); U.S. Pat. 2,901,551, Issued Aug. 25, 1959

A transistorized hearing aid which utilizes a solar battery consisting of series-connected photovoltaic cells (both to operate the hearing aid and to recharge the nickel-cadmium battery which operates the hearing aid when there is not sufficient light) is described. The solar cells are mounted on the top of one of the ear-pieces. One battery is used to operate the aid while the other is being recharged. The two batteries can be switched when necessary. When the solar battery develops power in excess of that needed to operate the hearing aid, the excess power is used to recharge a battery and consequently a damaging current surge does not occur.

Hearing Aid Amplifiers - See 9065

9119 PROBLEMS ENCOUNTERED IN WIDE-BAND FREQUENCY MODULATION by D.D. Wilcox (Ampex); Proc. NEC, Vol. 15, pp. 173-181, Oct. 12-14, 1959

The use of transistorized FM systems for recording very wide-band signals on magnetic tape is discussed. The difficulties involved in detecting the frequency modulated components and the various factors which contribute to the problem are considered. It is shown that the success of a frequency modulated wideband recorder depends upon careful consideration of several unusual design factors as circuit design proceeds. Use of transistors in the circuits is discussed, and it is shown that carefully designed transistorized circuits can do a creditable job when frequency modulated wideband recording is used.

9120 A COMPATIBLE TAPE CARTRIDGE by M. Camras (Armour Res. Found.); Proc. NEC, Vol. 15, pp. 119-128, Oct. 12-14, 1959

A new magnetic tape cartridge of very low cost, which is compact and fully protects the record, is described. The cartridge is completely automatic when used on a machine specifically designed for it, but will operate manually on present tape recorders. Various machines are described, and stereophonic playback from an automatic machine is discussed. A general survey of magnetic tape characteristics is given.

## COMPUTERS

9121 TRANSISTOR-RESISTOR LOGICAL CIRCUITS by P.D.T. Hawker (Mullard); Electronic Applic., Vol. 21, No. 1, pp. 32-40, 1960-1961

The operation of a basic transistor-resistor logic circuit including the design and performance equations is discussed. The simplicity of the circuit leads to economy, reliability and ease of design. By way of illustration, circuits using the switching transistors types OC46 and OC47 are designed. Modifications to the basic circuit which give greater gain or faster operations are included.

9122 TRANSISTOR COUNTER by E.D. Ostroff and M.A. Meyer (LFE); U.S. Pat. 2,902,609, Issued Sept. 1, 1959

An efficient and relatively inexpensive bistable circuit which is substantially independent of wide variations of transistor characteristics and is suitable for cascading to form a counter is described. The circuit utilizes a switching transistor and a magnetic core having a first and second stable state and four windings: signal (set), reset, switching, and output. Alternate pulses only switch the transistor because the impedance of the set winding changes according to the state of the core. The number of windings can be reduced to three when employing complementary transistors in adjacent bistable circuits. Details of a 30 kc counter are given.

Adder Circuits - See 9083

9123 TRANSISTOR BINARY ADDER by F.C. Williams (Natl. Res. Dev., London); U.S. Pat. 2,895,673, Issued July 21, 1959

A transistor binary adder of the analog type is described. Input signals produce a single signal having one of four possible magnitudes analogous to the four combinations of two digits (A and B) together with any carry digit ($C_D$) resulting from the combination of the next less significant pair of digits. The circuit comprises a first and second transistor with their emitters connected in parallel to an input terminal. A current $I_0$, $I_1$, $I_2$, or $I_3$ is fed into this terminal in ascending order of magnitude as A + B + $C_D$ has the value 0, 1, 2, or 3, respectively. The transistors are biased such that corresponding to $I_0$ both are cut off. For $I_1$ the first transistor is on, the second is off. For $I_2$ the first transistor is off, the second is on. For $I_3$ both transistors are on. An arrangement comprising a plurality of binary adding circuits is given.

9124 ELECTROLUMINESCENT TYPEWRITER by T. Hamburger (Westinghouse); Proc. NEC, Vol. 15, pp. 575-584, Oct. 12-14, 1959

A new display system utilizing electroluminescent alpha-numeric indicators and ferroresonant storage and switching is discussed. A present embodiment of the system consists of a standard typewriter keyboard upon which information is entered and a sequential display panel, with a capability of five characters, where the information appears. Possible uses are: (1) to read-in or read-out computer information, (2) as a display board, or (3) for communication between two or more remote locations.

9125 TRANSISTOR ACTUATED DEVICE by H.E. Tompkins (Burroughs); U.S. Pat. 2,896,130, Issued July 21, 1959

An improved means for stopping a print bar of a keyboard printing machine at a position representative of the number to be printed is described. The operation of the circuit is initiated by either a mechanical opening of a switch or an equivalent electrical signal at the input. This impulse is fed into a transistor to drive it into conduction. The resulting output pulse is applied to cut off the second transistor collector current. The second transistor is normally held in saturation to maintain an energized state of a pawl actuating relay. The release time is about 5 milliseconds. Design considerations of both electrical and mechanical aspects of the device are given. It is faster, smaller, and requires less power than corresponding circuits employing thyratron tubes. The device is applicable for use in business machines.

Magnetic Rod Memory Units - See 9042

9126 OPERATING CHARACTERISTICS OF A THIN FILM MEMORY by J.I. Raffel (Lincoln Lab.); J. Appl. Phys., Vol. 30, Suppl., pp. 60S-61S, Apr. 1959

The design, construction, and testing of an experimental thin film memory with 32 ten bit words are described. Circular spots of 1/16 inch diameter and 600 A thick are evaporated on two pieces of glass, each comprising a 16 x 16 array. Transistorized circuitry is employed for driving and sensing and the memory uses external register selection from a core-diode matrix. Word selection is provided by a transverse field and a digit winding conditions the information written by applying a longitudinal field in the "1" or "0" direction. An operating cycle time of less than 1/2 μsec appears possible and an extension to sizes of the order of 1000 words is planned.

9127 TRANSISTOR MEMORY CIRCUIT by T.E. Billings, C.P. Keshler, Jr., and H.W. Wainwright (GE); U. S. Pat. 2,902,674, Issued Sept. 1, 1959

A transistor memory circuit capable of maintaining a voltage level established during a short gating period is described. The voltage level is gated by means of a gate circuit, gate pulse source and signal source so as to charge a capacitor. The voltage across the capacitor is applied to the base of an emitter follower and a readout voltage appears across the emitter load. A voltage proportional to the output voltage level is amplified and fed to another transistor which acts as a current source in such a manner as to provide a constant current directly proportional to the voltage level established across the input capacitor. The constant current is designed to supply the current that leaks off the input capacitor into the finite resistance of the emitter follower and thus maintain a constant voltage level. The memory circuit is particularly applicable to computer and radar type circuitry wherein the circuits serve the function of providing short term memory.

Twistor Shift Registers - See 9053

9128 CLOCK PULSE CIRCUIT FOR TRANSISTOR FLIP-FLOP by M.R. McElroy (Hughes Aircraft); U.S. Pat. 2,898,479, Issued Aug. 4, 1959

A circuit for coupling a clock pulse into a transistor flip-flop is described. Coupling is achieved by means of a clock-pulse transformer connected into the base-emitter circuit of the flip-flop, with the emitters tied together. Using this scheme, the effect of the clock-pulse on the flip-flop is determined by the condition of the two inputs to the flip-flop. This system provides increased sensitivity and a reduction in power requirements. Using this scheme, the clock-pulse need provide only 3-4 ma of current to the circuit in order to achieve an effective output.

## POWER APPLICATIONS

9129 GENERATOR REGULATING APPARATUS by R.D. Sommer (Essex Wire); U.S. Pat. 2,892,143, Issued June 23, 1959

An improved regulating apparatus using semiconductor devices to control and regulate the output of an electric generator is described. A transistor circuit which regulates the output voltage by controlling the shunt field current of the generator is discussed. The circuit is substantially independent of ambient temperature variations. It is energized solely by the low voltage generator which it regulates, can be easily adjusted and does not require re-adjustment. A modification of the basic circuit provides means to limit the current output of the generator and to prevent the discharge of battery current through the generator. The system constitutes a generator regulating apparatus employing no electromagnetic relays or other moving parts. It has a longer lifetime and is especially applicable for use with the low voltage generator of an automotive vehicle.

9130 ELECTRICAL GENERATOR CONTROL APPARATUS by L.R. Lowry, Jr. and G.W. Ernsberger (Westinghouse); U.S. Pat. 2,896,149, Issued July 21, 1959

A transistor apparatus which regulates electrical generators by controlling the field excitation current of a dynamoelectric machine is described. By applying low level control signals to the regulation system the excitation current may be started or stopped. The regulator system comprises an error detecting circuit which produces a dc error signal proportional to the difference between the output terminal voltage and a reference voltage. A pulse width modulator produces output pulses whose width varies with the error voltage from the error detecting circuit. The output pulses are amplified and applied to the field winding of the exciter. A discussion of the complete circuit is given. The apparatus is particularly suited for aircraft applications due to its small size, weight, and resistance to environmental conditions.

9131 SEMICONDUCTOR JUNCTION-TYPE RECTIFIER SYSTEMS by L. Filberich, D.V. Haebler, and H. Nagorsen (Siemens AG); U.S. Pat. 2,895,100, Issued July 14, 1959

Methods of preventing large transient reverse leakage currents characteristic of semiconductor rectifier systems are described

The temporary increase in reverse leakage currents is apparently due to the lifetime (about 1 msec) of the forward conducting charge carriers. One or more current-controlling circuit components which modify the wave shape of the inverse voltage so as to delay its commencement and/or reduce its rate of increase are connected with the rectifiers in individual phase circuits. A switching means which keeps the inverse blocking voltage away from the rectifier member during a portion of the cycle period is also provided. Either mechanical or magnetic switches are employed for this purpose.

9132 ELECTRICAL SIGNAL REGULATOR by J.M. Jackson (GE); U.S. Pat. 2,897,432, Issued July 28, 1959

A three-transistor voltage regulator is described. The circuit uses two Zener diodes as reference elements, and maintains the output voltage constant to within 1/2 per cent for an input voltage variation of 30 per cent, a significant improvement over prior regulators. This performance is achieved by supplying the voltage requirements of the amplifier units from both the regulated output and the unregulated input, combining the two by means of a Zener diode.

9133 STATIC CONTROL FOR A MECHANICALLY REGULATED D-C SUPPLY by H.J. Abrams and J.F. Brubaker (Westinghouse); Proc. NEC, Vol. 15, pp. 698-706, Oct. 12-14, 1959

A voltage regulator for a 40 kv dc power supply, using two high-gain transistor-magnetic amplifier bistable amplifiers and a varistor detector, is described. The control system is very similar to the well known balanced beam relay control, except that all-static components are used. Power gains of $10^8$ with 20 msec response time and a drift level of $10^{-8}$ w in the bistable amplifiers reduces the system accuracy to the accuracy of the varistor reference. Over a limited ambient temperature range (25° to 55°C), trip point accuracy of the system can be held to better than 0.1 per cent.

9134 DIRECT CURRENT VOLTAGE REGULATOR by R.P. Putkovich and G.J. Thompson (Westinghouse); U.S. Pat. 2,987,433, Issued July 28, 1959

A voltage regulator particularly suited for working from direct current generators is described. The regulator system provides a unidirectional current which varies inversely with the input voltage and which is added to this input to maintain a substantially constant output. The regulator employs two inverters and a magnetic amplifier to provide an incremental voltage of proper magnitude. This technique has the advantage that the regulator itself handles only a portion of the power supplied by the source to the load, thus maintaining a relatively high efficiency without suffering from excessive power dissipation problems.

9135 SUPPLY CIRCUIT TRANSISTOR CURRENT CONTROL FOR ELECTRIC LOADS by P.J.W. Jochems (Philips); U.S. Pat. 2,897,429, Issued July 20, 1959

A transistor constant-current power supply is described. The circuit makes use of the fact that a fixed base current, when applied to a transistor in the common-emitter configuration, will cause a collector current to flow which is substantially independent of the collector voltage over a wide range of values. The circuit is shown as applied in three-phase power supplies, multiple loads, and push-pull amplifiers.

9136 STABILIZED TRANSISTOR ELECTRICAL POWER SUPPLY by J.T. Winkel (Philips); U.S. Pat. 2,897,430, Issued July 28, 1959

A transistor electric power supply which provides a constant voltage is described. The transistor is used in the common-base configuration, with the load in the emitter circuit, the power source in the collector circuit, and a control voltage in the base circuit. The circuit has no regulation other than that provided by the single transistor alone.

9137 VOLTAGE STABILIZING CIRCUIT by E. Wolfendale (Philips); U.S. Pat. 2,897,431, Issued July 28, 1959

A transistorized voltage regulator of low output impedance is described. The circuit utilizes two transistors in the grounded collector configuration; the first acts as a constant base-current supply, while the second supplies the load which is connected in its emitter circuit. The circuit has the advantage of requiring a low current drain from the reference supply voltage which is preferably a battery.

9138 THE DESIGN OF TRANSISTOR PUSH-PULL D.C. CONVERTORS by W.L. Stephenson, L.P. Morgan, and T.H. Brown (Mullard); Electronic Engrg., Vol. 31, pp. 585-589, Oct. 1959

The design formulae for a low to high voltage dc convertor which utilizes a transistor square wave oscillator controlled by a saturating transformer are derived in terms of operating parameters. Most of the practical limitations and difficulties are outlined but are not discussed in detail, as individual solutions are usually required.

9139 NAVY STATIC INVERTER USES TUNNEL DIODES by J.M. Marzolf (U.S. Naval Res. Lab.); Electronic Design; Vol. 9, pp. 28-31, Nov. 22, 1959

A static inverter consisting of two tunnel diodes and a square-loop magnetic core transformer is described. It has provided square waves from low-voltage, high current dc inputs reliably over reasonably wide ambient conditions. The tunnel diodes are employed as switches rather than as amplifiers. Some of the diodes are experimental units with peak currents ranging as high as 27 amp. Power-handling capability of the inverters has exceeded 2w. A detailed description of how the tunnel diode static inverter works is presented. The device is intended for use with such power sources as thermoelectric, thermionic, and fuel-cell generators.

## CONTROL APPLICATIONS

9140 PRECISE CONTROL OF HIGH VOLTAGE DC USING MAGNETIC CONTROLS by P.W. Covert (Magnetics) and M. Kramer (Aluminum Co.); Proc. NEC, Vol. 15, pp. 691-697, Oct. 12-14, 1959

A system using sensitive magnetic amplifiers which is employed as the basic element in a dc bus voltage regulator is described. The magnetic amplifiers are preferred over the usual voltage sensitive relays because they allow easier changing of bus voltage settings, elimination of recalibration, reduction of maintenance, and improved ruggedness of the basic sensing device. This new method allows setting of the voltage limits by turning rheostats which vary the reading on miniature indicating meters. One meter reads directly in terms of the minimum

and maximum voltage to be tolerated. The other meter reads the "deadband" in terms of the voltage swing to be tolerated. Thus the switchboard operator may readily adjust the meters to the desired limits and the control scheme regulates to these limits. The observed sensitivity is ±3/4 v over an operating range 500 - 700 v with no deadband set in.

9141 ANALOG COMPUTER DESIGN OF MAGNETIC AMPLIFIERS by L.A. Gregory (Magnetic Controls); Proc. NEC, Vol. 15, pp. 679-690, Oct. 12-14, 1959

Fundamental techniques in the analog-solution of equations that occur in the design of magnetic amplifiers are cited. The simultaneous solution of several equations involving common variables can be more quickly accomplished by substituting variable voltages as the counterpart of mathematical variables in these equations. The combination of these voltages according to mathematical rules can be read or recorded on any electrical measuring device and transformed back into original mathematical language to attain the desired design data.

9142 TRANSISTOR CONTROLLED MAGNETIC AMPLIFIER by L.H. Rowley and H. Milenbach (Sperry Rand); U.S. Pat. 2,902,547, Issued Sept. 1, 1959

A transistor amplifier which provides impedance matching between a high impedance signal source and a magnetic amplifier is described. The particular magnetic amplifier circuit shown operates the load on alternate half cycles of line current. The transistors serve to precondition the magnetic circuit cores on the nonconducting half cycles for either high or low impedance on the conducting half cycle. The preconditioning current is supplied by the signal controlled transistors which are powered by batteries or by bias resistors placed in parallel across the line and poled oppositely to the main reactor circuits.

9143 INTERRUPTED FLASH GENERATOR by J.W. Crownover and N.R. Smith; U.S. Pat. 2,895,081, Issued July 14, 1959

A transistor interrupted flash generator circuit which provides increased visibility of interrupted flashes without increasing the weight or bulkiness of the flasher is described. In one version the output of a blocking oscillator is stepped up and transformer coupled to a gas discharge tube. By varying the time constant at the base of the blocking oscillator the time duration of the flash of light emitted by the tube and the time elapsing between successive flashes may be varied in any desired manner. The apparent brightness of the glow or flash of light emitted by the tube is increased by connecting a wire loop around the tube. The loop is connected across the secondary of the oscillator transformer and induces an alternating electromagnetic field within the gas when voltage is transmitted to the tube. The barricade flasher is useful at night in and around open areas of construction activity as a signal or warning device.

9144 THYRATRON CONTROL CIRCUIT by J. Rywak (Northern Elect.); U.S. Pat. 2,898,515, Issued Aug. 4, 1959

A transistor circuit for controlling the operation of a thyratron is described. The circuit may be used with either one- or two-grid thyratron tubes and employs two transistors, one to control the conditioning voltage, the other to control the firing voltage. The thyratron is protected from firing by spurious voltage pulses through the use of the control circuit and protective diodes associated with it.



Hall Effect Wattmeters - See 9019

9145 AN IMPROVED TRANSISTORIZED WAVE ANALYZER by J.R. Petrak (Hewlett-Packard); Proc. NEC, Vol. 15, pp. 874-883, Oct. 12-14, 1959

The design of a transistorized wave analyzer for the 20-50,000 cps range is discussed. Specific problems concerning the design of a stable oscillator, a low distortion amplifier and the selective crystal filter are considered. The instrument is compact, requires no warmup time and may be used portably. Output provision is made for a controlled 1 v signal over the operating range.

Hall Effect:
Magnetometers - See 9018
Flux Meters - See 9019

9146 TECHNICAL CONSIDERATIONS FOR AN ULTRA-SENSITIVE BRIDGE TO MEASURE RF POWER AND VOLTAGE by L.J. Greenstein, R.B. Schulz, M. Epstein, and D. Fryberger (Armour Res. Found.); Proc. NEC, Vol. 15, pp. 896-906, Oct. 12-14, 1959

The basic considerations in the design of a dc operated, temperature compensated, balanced thermistor bridge which is used in the measurement of low level radio-frequency power and voltage are discussed. The bridge is maintained at balance in the presence of RF power by removing from the the thermistor an equal and easily measured amount of dc power. The RF and dc calibrating signals are applied simultaneously in pulses in order to diminish the effect of dc drift in the bridge output. The relationship between these signals is derived and the source of error are discussed. The thermistor response to pulsed energy is analyzed on the basis of thermal equilibrium considerations.

9147 LIGHT METER by F.F. Offner; U.S. Pat. 2,897,720, Issued Aug. 4, 1959

A transistorized photoelectric light meter composed of a barrier layer photoelectric cell, a transistor amplifier, and a suitable current meter is described. The current meter is shown incorporated in several configurations, among which is the balanced bridge arrangement; this allows compensation for temperature variation and provision for meter zero setting. The unit is especially suited for photography applications when low light-levels are to be measured.

9148 TRANSISTORIZED FREQUENCY STANDARD by R.L. Denton; U.S. Pat. 2,882,404, Issued Apr. 14, 1959

A transistorized frequency standard which can be operated by a storage battery and thus eliminates the need for an external power source is described. Frequency standardization is accomplished by means of a crystal oscillator operating at 100 kc, a series of regenerative frequency dividers, a series of binary dividers and a power amplifier driving a 50 cps electric clock. A feedback loop from the output of one of the binary dividers is employed to reset a portion of the preceding dividers to divide the frequency in the ratio of 5:1 instead of the expected 8:1. Circuit details are given including schematics and a block diagram of the device, which has a frequency stability of the order of one part in $10^8$ per day. Several accurately known frequencies in the audio frequency range are also available by tapping off the desired frequency from the output of the appropriate frequency divider stage.

9149 ELECTRONIC TIMING SET (TIME ENCODER) by J. Brazda (Hallicrafters); Proc. NEC, Vol. 15, pp. 860-873, Oct. 12-14, 1959

The Time Encoder, a self contained electronic time piece designed for those systems requiring real time information, is described. The accuracy of within ±1 second per day is achieved with a crystal controlled oscillator. Continuous output signals suitable for audio or graphical recording are provided with timing marker pulse frequencies of 6000 cycles per second, 60 cycles per second, and 1 cycle per second. The real time of day as a digitized pulse output in serial binary coded decimal form is available during each second interval of a 24 hour period. A six digit numerical time display is driven from a common source to insure identical time readings at up to 10 remote positions with a resolution of one second. Synchronous clock operation from a 110 volt source with similar resolution capabilities is available. Associated equipment synchronization is possible with the use of 6 kc, 120 cps, or 1 cps outputs. Circuit features are binary chains as frequency dividers, diode program logic, and flip-flop as storage devices.

9150 SILICON p-n JUNCTIONS AS PARTICLE SPECTROMETERS by J.M. McKenzie (Chalk River Labs.); Bull. Am. Phys. Soc., Ser. II, Vol. 5, p. 355(A), June 15, 1960

The use of Si p-n junctions as particle spectrometers was discussed. The sensitive thickness of the detector is controlled by choosing Si of the appropriate resistivity and operating the detector at a suitable bias voltage. This enables a junction to be made which will permit heavy ionizing particles, such as oxygen ions, to be detected in the presence of equal energy protons or alpha particles. The thickness of the junction is adjusted to be less than the range of the latter particles. A resolution of 16 kev (width at 1/2 maximum) for 6.04 Mev alpha particles was obtained with a junction of sufficient thickness to stop 10 Mev alpha particles. The two well-know beta lines at 115 and 129 kev from $Co^{57}$ have been resolved using a junction made from 12,000 ohm-cm Si.

**Announcing the Availability of Bibliographic and Information Retrieval Services**

Our highly experienced scientific abstracting staff, composed of people with substantial professional qualifications and representing many branches of the sciences, is ready to work with you in these areas.

For more detailed information, write a brief description of your problem or project and a member of our scientific staff will review it. Our reply will be prompt.

Write directly to:

**Dr. Geoffrey Knight, Jr., President**
**Cambridge Communications Corporation**
238 Main Street
Cambridge 42, Massachusetts

**REQUEST FOR PAPERS**

Cambridge Communications Corporation has initiated publication of original review articles pertaining to the solid state. Manuscripts (with bibliographies) reviewing topics in the fields of solid state physics and metallurgy, solid state device technology, and circuit applications of solid state devices are requested. Interested parties should contact the Assistant Editor for further information.

# SUBJECT INDEX


A

Absorption:
  Coefficient of Phosphors 8876
  Edge of:
    CdSe 8866
    SiC 8865
Absorption in:
  Alkali Halides 8858
  AlSb, Infrared 8861
  $BaTiO_3$ 8854
  CdTe 8870
  GaP, Infrared 8855
  Ge, Infrared 8864
  HgTe and HgTe-CdTe 8867
  KBr 8857
  KCl,
    Color Center 8859
    F-Band 8856
  KCl: 8857, 8868
    and KBr 8839
  NaCl 8868
  NaF 8868
  Si, Infrared 8862, 8863
  SiC 8865
  ZnO 8612
Absorption-Emission Spectra 8876, 8877
Acoustic Attenuation in LiF and $CrK(SO_4)_2 \cdot 12H_2O$ 8940
Adder Circuits 9083
Adders, Binary 9123
Alkali Halide:
  Color Centers, Wave Functions of 8593
  Crystals, Growth of High Purity 8618
Alkali Halides,
  Absorption in 8858
  Fluorescence in 8886
Alkali Metal-Gallium Alloy as Dot Material 8979
Alloy-Diffused Junction Transistors, Fabrication of 9001
Alloyed Junctions,
  Boron-Selenide 8973
  Fabrication of 8998, 8999
Alpha of Transistors, Circuit for Measurement of 8993
Alumina, Dielectric Properties of 8678
Aluminum,
  Nuclear Spin Relaxation in Superconducting 8843
  Photoresponse of 8905
Aluminum Antimonide,
  Absorption in 8861
  Diffusion of Cu in 8624
Aluminum Oxide,
  - See also Ruby
  PMR of:
    Ni in 8846
    Transition Metals in 8847
Amorphous Solids, Energy Levels in 8657
Amplifier Gain Control 9060, 9061
Amplifiers,
  Audio 9064, 9065
  Cascaded 9062
  Class B 9071
  Hearing Aid 9065
  Magnetic 9140, 9141, 9142
  Nonlinear Distortion in 9063
  Parametric: 9069
    Magnetic Film 9070
  Pulse 9067, 9068
  RF 9066
Amplitude Modulation Detectors 9089
Anisotropic:
  Conduction: 8723
    in Ge 8722
Annealing of:
  Irradiated Al and Cu 8651
  X-Ray:
    Induced Surface Hardening in NaCl 8650
    Radiation Damage in LiF, Low Temperature 8647
Antiferromagnetic:
  $FeVO_3$, Preparation and Properties of 8631
  MnF, NMR in 8808
  Transition Temperatures of $MnF_2$ and $CoF_2$ 8820
Antiferromagnetism of:
  $CrF_2$ and $CrCl_2$, Neutron Diffraction Studies of 8821
  Rare Earth-Iron 8822
Antimony, Chemical Analysis of 8615
Antimony-Sulfur-Bromine Compound, Photoconductivity of 8901
Antimony-Sulfur-Iodine Compound, Photoconductivity of 8901
Antimony Telluride, Dislocations in 8598, 8603
Attenuators, Ferrite 9035
Audio:
  Amplifiers 9064, 9065
  Oscillators, Sub- 9074
Auger Recombination in Semiconductors, Overlap Integrals for 8697
Automatic Gain:
  Control 9060
  Control, Radio Receiver 9112
Automotive:
  Generator Regulators 9129
  Ignition System 9106
Avalanche Multiplication in Junctions 8967, 8968

B

Band Dynamics of Semiconductors 8705
Bandwidth in Point Contact Diodes, Increasing 8950
Barium Ferrite, Ferrimagnetic Linewidth of 8812
Barium Titanate,
  Absorption in 8854
  Barkhausen Pulses in 8683
  Coercive Field of 8685
  Conductivity of 8682
  Dielectric Constant of 8684
  Effects of Impurity Additions on Dielectric Properties of 8686, 8687, 8688
  PMR of Transition Metals in 8847
  Space Charge:
    Fields in 8680
    Limited Currents in 8681
Barkhausen Pulses in $BaTiO_3$ 8683
Base Transfer Characteristics 8995
Beryllium Superconducting Thin Films 8757
Binary:
  Semiconductors 8653
  System, Electrical Properties of $Ag_2$-Group VI 8734
Bismuth,
  Chemical Analysis of 8615
  Conductivity and Properties of 8727
  Optical Constants of 8907
Bismuth Telluride,
  Dislocations in 8598, 8603
  Energy Band Structure of 8919
  Heat Capacity of 8914
  Thermal Properties of 8919
  Thermoelectric:
    Power of 8925, 8926
    Properties of 8927, 8928, 8929
  Thermo-Junctions of 8928
Bistable Switching Circuits 9083
Bond Structure of ZnS Structure Crystals 8654
Bonding Scheme of ZnSb, Atomic 8589
Boron in Si, Diffusion of 8621
Boron-Aluminum Alloys 8973
Boron Phosphide, Semiconducting Properties of Cubic 8732
Boron-Silicon Alloyed Junctions 8973
Bragg Reflections from Polygrain Metals 8592
Bromine on Se, Effects of 8728

C

Cadmium, Photoresponse of 8905
Cadmium in GaAs, Diffusion of 8623
Cadmium Antimonide, Cyclotron Resonance Absorption in 8768
Cadmium Arsenides, Solid-Vapor Equilibria for 8582
Cadmium Selenide, Absorption Edge in 8866
Cadmium Selenide:
  Phosphors, Emission of 8891
  Radiation Detectors, Fabrication of 9023
Cadmium Sulfide,
  Edge Emission in 8873
  Fluorescence in 8887, 8888
  Magneto-Optic Effects on Excitons in 8850
  Magnetoresistance of 8767
  Photosensitive Ultrasonic Attenuation in 8942
  Piezoelectric Scattering in 8693
  Space Charge Limited Currents in 8681
  Traps in 8702
Cadmium Sulfide Type Crystals, Photoelectric Analysis of Imperfections and Properties of 8591
Cadmium Sulfide-Selenide:
  Photoconductive Device, Fabrication of 9028
  Photosensitive Cells, Fabrication of 9024
Cadmium Sulfide-Zinc Sulfide Mixed Crystals, Photoconductivity of 8899
Cadmium Telluride,
  Absorption in 8870
  Hall and Optical Properties of 8764
  Spin Resonance of $Mn^{2+}$ in 8771
Calcium Fluoride, PMR of 8832
Capacitance Diodes, Fabrication of High-Power Nonlinear 8959
Capacitors, Evaporated Ge-Ta Film 9051
Capture Cross Sections in Si and Ge 8704
Carrier:
  Concentration in InSb 8731
  Distribution in Semiconductors 8696
  Surface Transport 8710
  Transport, Dislocation Effects on 8708
  Transport in:
    Ge 8709
    Solids 8707
Cascaded Amplifiers 9062
Cathodoluminescence, Voltage Dependence of 8730
Ceramics, Characteristic Improvements by Diminishing Inhomogeneity in 8676
Chalcopyrite Crystals, Energy Band Structure of 8656
Chemical Anslysis of Bi-Sb-Te-Se Systems 8615
Chromic Bromide, Magnetic Properties of 8818
Chromium$^{3+}$ in Ruby, PMR of 8845
Chromium Dioxide, Preparation of Ferromagnetic 8630
Chromium Potassium Sulfate, Acoustic Attenuation in 8940
Chromous Chloride, Antiferromagnetic 8821
Chromous Fluoride, Antiferromagnetic 8821
Class B Amplifiers 9071
Cleaning:
  Ge Surfaces, Ion-Bombardment Method for 8637
  InSb Surfaces, Ion-Bombardment Method for 8638
Clock Pulse Circuits 9128
Clocks, Electronic 9149
Cobalt, NMR in 8807
Cobalt:
  Domain Walls, $Co^{59}$ NMR Broadening in 8806
  Magnetic Structure, Thickness Dependence of 8800
Cobalt$^{59}$ NMR Broadening in Co Domain Walls 8806
Cobalt Acetate, Susceptibility of 8819
Cobalt Fluoride,
  Antiferromagnetic Transition Temperature of 8820
  Curie Temperature of 8820
Coercive Field of $BaTiO_3$ 8685
Color:
  Center:
    Absorption in:
      Alkali Halides, Pressure Effect on 8858
      KCl 8859
      KCl and KBr 8857
    Fluorescence in Alkali Halides, Infrared 8886
    Wavefunctions 8895
  Centers, Photo-Ionization of 8860
  Centers in Alkali Halides, Wavefunctions of 8593
Columbium Oxide Rectifiers, Fabrication of 8989

Communication Systems, Maser 9109
Conduction, Dielectric Theory of Impurity 8721
Conductivity,
  Anisotropy in 8723
  Heitler-London Mechanism of 8718
  Voltage Dependence of Electron Bombardment Induced 8730
Conductivity in:
  CdS Type Crystals, Photoelectric Analysis of 8591
  Ge, Anisotropy of 8722
Conductivity of:
  $Ag_2$-Group VI Binaries 8734
  $BaTiO_3$ 8682
  Bismuth 8727
  Dysprosium 8736
  Ge, Low Temperature 8720
  InAs, Heat Treatment Effects on 8726
  InSb 8731
  Ionic Crystals 8713
  Li-Ni-O 8719
  NaCl, Ionic 8729
  p-Phenylenediamine-Chloranil Complex 8735
  PbS and PbSe 8918
  Wustite and Magnetite 8733
  ZnO 8612
Contacts,
  Electroplated 9017
  Ohmic and Rectifying: Diffused 9010
  Preparation of Assemblies of Point 8994
  Surface Barrier Rectifying 8976
Contacts for Si, High Temperature Mo 8981
Converters,
  dc-dc 9138
  Linear Voltage to Frequency 9098
Copper, Photoresponse of 8905
Copper in AlSb, Diffusion of 8624
Corundum, Elastic Compliances and Constants of 8936
Counters 9122
Critical:
  Field, Superconducting 8741
  Field of Superconducting:
    Hg 8748
    In 8748
    Sn: 8748
      Films, Oxygen Content Effects on 8747
  Temperature of:
    Superconducting Alloys 8745
    Superconductors 8746
Crystal Distortion in $Mn^{3+}$ Spinels 8590
Cuprous Oxide, Photoconductivity of 8903
Cuprous Oxide Rectifiers, Encapsulation of 8991
Curie Temperatures of $MnF_2$ and $CoF_2$, Pressure Effects on 8820
Current Flow in Junctions,
  High Injection Level 8963
  Reverse 8965
Currents in Diodes, Reverse 8966
Cyclotron Resonance:
  Absorption in ZnSb and CdSb 8768
  Measurement of Valence Band Parameters in Si 8706
  Negative Effective Mass Experiments 8769

D

Debye Temperature of Solids 8913
Defects in Lead Silicate Glass, Radiation-Induced 8648
Deflector Circuits, TV 9113
deHaas-van Alphen Oscillations in Mg 8849
Delineation of Junctions 9009
Demodulators, Pulse-Position 9094
Detectors,
  AM 9089
  Frequency 9091
  Phase 9093
  Radio Receiver 9112
Diamagnetic Susceptibility in Si and Ge 8848
Diamond, Gas Etching Effects on Single Crystals of 8643
Diamond Lattice, Grain Boundaries in 8611
Dielectric:
  Constant, Measurement of 8670, 8671
  Constant of:
    $BaTiO_3$ 8684
    Ge 8673
    Si and Ge 8672
  Permeability of Insulators, Radiation Effects on 8674
  Properties of:
    Alumina, High Temperature 8678
    $BaTiO_3$ 8686, 8687, 8688
    Insulating Ceramics 8676
    Insulators, Radiation Effects on 8675
    $MnO_2$ 8690
    $MnO_2$, Temperature and Frequency Variation Effects on 8689
    Solid Solution Systems Based on $NaNbO_3$ 8677
  Theory of Impurity Conduction 8721
Dielectrics, Space Charge:
  Distribution in 8679
  Fields in 8680
Diffused:
  Base Transistors, Fabrication of 9005
  Contacts, Ohmic and Rectifying 9010
  Junctions, Fabrication of 8978
Diffusion:
  of Au in Ge 8622
  of B in Si 8621
  of Cd in GaAs 8623
  of Cu in AlSb 8624
  in Semiconductors, Substitutional and Interstitial 8620
  in Solids, Vacancy 8594
Diode:
  Connection Assembly, Polarized 8984
  Impedance, Inductive Character of 8962
Diodes,
  Al Bonded 8951
  Diffused: GaAs 8964
  Four Layer 8954
  Junction:
    High Power (Current) - See Rectifiers
    Packaging of 8983
    Protective Glass Coatings for 8985
  Multi-Layer: Fabrication of 8959
  Noise in 8969
  Point Contact:
    As-Te 8990
    Encapsulation of 8952
    Fabrication of 8949
    Forming of 8948
    Increasing Bandwidth in 8950
    Packaging of 8953
    Whisker Mounting on 9016
  Reverse Current in 8965, 8966
  Space Charge Limited Currents in Insulator 8961
  Tunnel: Characteristics of GaAs 8956
  Varactor: Figures of Merit of 8960
Dip Alloy Technique for Microalloy Junctions in Si 8974
Discriminators,
  Magnetic Core 9090
  Phase 9092
Dislocation:
  Damping in Si and Ge 8946
  Effects on Carrier Transport 8708
  Models of Grain Boundaries 8610, 8611
  Nets in $Sb_2Te_3$ and $Bi_2Te_3$ 8603
Dislocations,
  Climb Motion of 8605
  Continuous Distribution of 8597
  Interactions between: 8608
    Fixed and Moving 8607
    Parallel Edge and Tilt 8606
  Lattice Statics of 8596
  Motion of 8604
Dislocations:
  in Ferroelectric Glycine Sulfate 8609
  in GaAs, Etchants for Revealing 8641
  on Hardening, Effect of 8601
  in Nonmetallic Layer Structures 8598
  in PbTe, Etches for Revealing 8642
  by Spark Discharge, Formation of 8599
  on Strength of Crystalline Materials, Effect of 8602
  on Work-Hardening in fcc Metals, Effect of 8600
Dissociation Pressures of Cadmium Arsenides 8582
Distillation Purification of Ge 8619
Distortion in Transistor Amplifiers, Nonlinear 9063
Distributions in Mg-Mn Ferrites, Ion 8584
Dividers, Frequency 9095
Domain:
  Wall Motion 8801, 8805
  Walls,
    $Co^{59}$ NMR Broadening in Co 8806
    Energy and Entropy of 8802
    Zigzagging in 8804
  Walls in Permalloy Films 8803
Domain-Dislocation Relationship in Ferroelectric Glycine Sulfate 8609
Dysprosium, Conductivity of 8736

E

Edge Emission in CdS 8873
Effective:
  Mass,
    Cyclotron Resonance Measurement of 8769
    Faraday Effect Method of Measuring 8911
  Mass:
    of Carriers in Si-Ge 8824
    of Charge Carriers in InAs and InP, Faraday Effect Method of Measuring 8912
    of Semiconductors 8705
    in Si, Cyclotron Resonance Measurement of 8706
    in ZnSb and CdS, Cyclotron Resonance Measurement of 8768
Elastic:
  Compliances and Constants of Corundum 8936
  Moduli of:
    KCl 8937
    Rutile 8935
Electric Strength of Insulators, Radiation Effects on 8674
Electrical:
  and Optical Properties of GaP 8882
  Properties of InSb 8731
Electrochemiluminescence of Si 8884
Electrodes, Metalizing of Ta 8982
Electroluminescence of:
  GaP 8882
  ZnS 8881, 8883
Electroluminescent Typewriter 9124
Electron:
  PMR:
    Spectra of $K_3Co(CN)_6$, Polytype Effects in the 8831
    in Studies of Activated Phosphors 8878
  Relaxation in Si and Ge 8945
  Spin:
    PMR in LiF 8836
    Resonance of:
      F-Centers in KCl 8840
      S-State Ions 8826
  Tunneling Measurement of Superconducting Energy Gap 8749
Electronic Structure of Crystals, Hartree-Fock Equations of 8668
Emission:
  in CdS, Edge 8873
  of CdSe Phosphors 8891
  in ZnS:Cu, Infrared 8871
Emitter Efficiency Characteristics 8995
Encapsulation of:
  Point Contact Diodes 8952
  Rectifiers 8991
Energy:
  Band:
    in Si-Ge 8824

Energy: Band: (Cont'd)
Structure, Many Electron State 8655
Structure of:
Amorphous Solids 8657
$Bi_2Te_3$ 8919
Chalcopyrite Crystals 8656
Gap:
of CdTe 8764
of SiC 8865
in Superconductors, Electron Tunneling Measurement of 8749
of ZnS Structure Crystals 8658
Level Density in Superconductors 8746
Levels, Surface 8660, 8661, 8662, 8663, 8664
Levels in CdS Type Crystals, Photoelectric Analysis of 8591
Epitaxial:
Si Layers, Growth of 8628
Transistors, Fabrication of 9007
Etchants for Revealing Dislocations in GaAs 8641
Etches for Revealing Dislocations in PbTe 8642
Etching,
Jet 9014
Junction Delineation 9009
Etching:
{111} Surfaces of III-V Intermetallic Compounds 8640
of III-V Intermetallic Compounds, Effect of Polarity on 8639
and its Effect on Semiconductor Surfaces, Gas 8643
Technique for Fabricating Silica Windows 8629
Evaporator, Electron Gun 8627
Exciton Energy Levels in Ge and Si 8695
Excitons in CdS, Magneto-Optic Effects on 8850
Exposure Meters 9147

F

F-Band Absorption in KCl 8856
F-Centers, Photo Ionization of 8860
F-Centers in:
KCl, ESR of 8840
LiF, PMR of 8837
Fabrication of:
Alloy Diffused Junction Transistors 9001
Alloyed:
Boron-Silicon Junctions 8973
Junctions 8975, 9000
Junctions, Large Area 8972
Transistors 8999
As-Te Point Contact Diodes and Rectifiers 8990
CbO (NbO) Rectifiers 8989
Composite Se-Ge Rectifiers 8987
Diffused:
Base Transistors 9005
Junctions 8978
Double Diffused High Frequency Junction Transistors 9004
Eutectic Junctions 8977
Four-Layer Triodes 9006
GaAs Diffused Diodes 8964
Grown Junctions 8970, 8971
Hook Collectors 9002, 9003
Microalloy Junctions in Si 8974
Multielement Photocells 9030
Photocells 9025, 9026
Photoconductive Devices 9028
Photosensitive Cells 9024
Point Contact:
Diodes 8948, 8949
Transistors with Recrystallized Base 8998
Power Transistors 9008
Radiation Detectors 9023
Se Rectifiers 8986, 8988
Solid Metallic Rectifiers 8992
Surface Barrier:
Rectifying Contacts on Si and Ge 8976
Transistors 9014
Surface-Protected Photoconductive Cells 9029
Tunnel Diodes 8955
Vapor Deposited Junction Transistors 9007
Faraday:
Effect Method of Measuring Effective Mass in InSb 8911
Rotation in InAs and InP 8912
Ferrimagnetic:
Garnets, Superexchange Interaction in 8791
Linewidth of $BaFe_{12}O_{19}$ 8812
Resonance, Wall Effect in 8810
Ferrite:
Attenuators 9035
Cores,
Effect of Rare Earth Oxides on the Magnetic Behavior of 9041
Inhibited Flux Operation of 9038
Residual States in 9039
Reversible Magnetization in 9040
Devices for Computers 9037
Isolators, UHF High Power 9036
Loaded Waveguide Microwave Transverse Switches 9035
Switches, Broadband Reflective 9043
Ferrites,
Demagnetization of 8792
Hall Effect in 8763
Ion Distributions and Valencies in Mg-Mn 8584
Magnetic Properties of Mixed 8815
Phase Equilibria of $FeO-MgO-Fe_2O_3$ 8581
Stability of 9044
Temperature Dependence of Magnetostatic Properties in Ni-Zn 8788
Ultrasonic Measurement of Magnetization in Mn 8787
Ferroelectric:
Glycine Sulfate, Dislocations in 8609
Properties of Triglycine Sulfate, Temperature Variation Effects on 8691
Triglycine Sulfate, Transitions in 8692
Ferromagnetic:
Co, NMR in 8807
$CrO_2$, Preparation of 8630
Magnetic Anisotropy, Temperature Dependence of 8794
Particles, Anisotropy Energy and Remanent Magnetization of 8790
Resonance, Anisotropic Elastic Stress Effects on 8809
Resonance Absorption Linewidth, Ferrite Size and Shape Effects on 8811
Superconductors, Intermediate State of 8738
Ferromagnetics,
Internal Friction in 8943
Young's Modulus of 8943
Ferromagnetism in Dilute Alloys, Critical Concentration for Existence of 8785
Ferromagnets,
Degree of Texture Perfection in 8799
Flux Reversal in Soft 8798
Green's Function Applied to 8780
Magnetic State Stability in 8786
Magnetization:
Curve of Heisenberg 8782
in Si-Fe 8805
Magnetostrictive Constants of 8775
Refractive Indices of 8906
Spin Waves in 8781
Transverse Magnetization in 8781
Ferro-Vanadium Oxide, Preparation and Properties of Antiferromagnetic 8631
Field Effect, High Frequency 8773
Field-Emission Microscope for Surface Studies 8633
Field-Ion Microscope for Surface Studies 8633
Figures of Merit of Varactors 8960
Films,
Cross-Tie and Chain Walls in Permalloy 8803
Induced Magnetic Anisotropy in Evaporated Ni-Fe 8795
Magnetic Anisotropy in:
Ni and Permalloy 8797
Permalloy 8796
Oxidation of Thin 8636
Superconducting:
Magnetic Field Penetration in 8754
Tin 8747
Filters, Stabilization of 9102
Flow Graphs Using Array of Non-Touching Loops 9054
Fluorescence in:
Alkali Halides, Color Center 8886
CdS 8887, 8888
Flux Meters, Hall Effect 9019
Forbidden Zone Width of ZnS Structure Crystals 8658
Four Layer Diodes 8954
Frequency:
Dividers 9095
Modulators 9088, 9101
Response of Infrared Detectors, Measurement of the 9027
Standard Units 9148

G

Gadolinium,
Magnetostriction Temperature Dependence of 8777
Thermal Expansion of 8777
Gadolinium$^{3+}$ in Single Crystal Oxides, PMR of 8847
Gain Control, Amplifier 9060, 9061
Gallium in the Normal and Superconducting States, Thermal Conductivity of 8917
Gallium Antimonide, Piezoresistance of 8724
Gallium Arsenide,
Diffusion of Cd in 8623
Etchants for Revealing Dislocations in 8641
Hall Coefficients of Si Doped 8762
Magnetoresistance of 8765
Thermal and Physical Properties of 8932
Gallium Arsenide:
Diodes, Diffused 8964
Tunnel Diodes, Characteristics of 8956
Gallium Arsenide-Germanium Alloys, Device Applications and Growth of 8980
Gallium-Indium Antimonides, Properties of 8725
Gallium Phosphide,
Electroluminescence in 8882
Infrared:
Absorption in 8855
Properties of 8852
Thermal Expansion of 8852
Gallium Phosphide Diodes, Radiative Recombination in 8872
Gallium Sulfo-Selenide, Photoconductivity of 8900
Galvanomagnetic - See Magnetoelectric
Garnets, Superexchange Interactions in Ferrimagnetic 8791
Gas Etching and its Effect on Semiconductor Surfaces 8643
Gating Circuits 9084, 9085
Generator Regulators 9129
Generators,
Harmonic 9096, 9097
Pulse 9099
Ramp Function 9100
Waveform 9101
Germanium,
Absorption in 8864
Capture Cross Sections in 8704
Carrier Transport in 8709
Conductivity of 8720
Conductivity Anisotropy of Hot Electrons in 8722
Dielectric Constant of 8672, 8673
Diffusion in 8620
Diffusion of Au in 8622
Exciton Energy Levels in 8695
Gas Etching Effects on Single Crystal of 8643
Hall Coefficients of 8761
High Energy Electron Irradiation of 8649
Internal Friction in 8945, 8946, 8947
Lifetime of 8700, 8701, 8864
Ohmic and Rectifying Contacts for 9010

Germanium, (Cont'd)
Photoconductivity of: 8864, 8894
Grain Boundaries in 8896
Piezoresistance of 8724
Purification of 8619
Surface Properties of 8774
Susceptibility of 8823, 8848
Germanium:
Surface States 8664
Surfaces, Oxidation of Clean 8637
Germanium-Gallium Arsenide Alloys, Device Applications and Growth of 8980
Germanium-Silicon, Susceptibility of 8824
Glass, Radiation-Induced Defects in Lead Silicate 8648
Glass Coatings for Junctions, Protective 8985
Glycine Sulfate, Dislocations in Ferroelectric 8609
Gold in Ge, Diffusion of 8622
Gold-Germanium Eutectic Junctions 8977
Grain:
Boundaries,
Electroluminescent 8882
Photoconductivity of Ge 8896
Structure and Properties of 8610
Boundaries in Diamond Lattice 8611
Graphite,
Dislocations in 8598
Spin Resonance of Charge Carriers in 8772
Group:
III-V Compounds, Ohmic and Rectifying Contacts for 9010
V-VI-VII Compounds, Photoconductivity of 8901
VI-Silver Compounds, Properties of 8734
Grown Junctions, Fabrication of 8996
Growth of:
- See also Preparation of
Epitaxial Si Layers 8628
GaAs-Ge Alloys 8980
Ge (Heavily Doped) 8955
High Purity Alkali Halide Crystals 8618
Selenium 8908

H

Halides, Structure of 8587
Hall:
Coefficients of:
CdTe 8764
Ge, Anisotropic 8761
InSb 8731
Si Doped GaAs 8762
Constant in CdS Type Crystals, Photoelectric Analysis of 8591
Effect:
Devices 8760, 9020
Devices,
Characteristics and Applications of 9018
Design of 9019
in Ferrites 8763
Hardening, Dislocation Effects on 8601, 8606
Harmonic Generators 9096
Hearing:
Aid Amplifiers 9065
Aids, Solar Powered 9118
Heat:
Capacity of $Bi_2Te_3$ 8914
Dissipation of Power Transistors, Method for 9011
Heitler-London Conductivity Mechanism 8718
Hexagonal Solids, Debye Temperature of 8913
High:
Frequency Transistors, Fabrication of 8998, 9004, 9005
Power Switching Circuits 9086
Hook Collectors, Fabrication of 9002, 9003
Hot Electrons in Germanium, Anisotropy of 8722
Hysteresis Loop of:
$BaTiO_3$ 8685
$MnO_2$ 8690

I

Ignition System, Transistorized 9106
Image Intensifiers 9032, 9033
Impact Ionization in Semiconductors 8717
Impedance of Diodes, Inductive Character of 8962
Imperfections in CdS Type Crystals, Photoelectric Analysis of 8591
Impurities in SiC, Spectrographic Analysis of 8614
Impurity:
Analysis 8615
Analysis, Spectrographic 8613
Conduction, Dielectric Theory of 8721
Interactions in Si, Li-Oxygen 8625
Levels in Semiconductors 8659
Relaxation in Si and Ge 8945
Indium, Superconducting 8748
Indium Antimonide,
Electrical Properties of 8731
Faraday Effect in 8911
Lifetimes in 8698
Magnetoelectric Effect in 8759
Magnetoresistive Effects in 8766
Noise in 8698
Photoconductivity of 8897
Piezoresistance of 8724
Thermomagnetic Effects in 8933
Indium Antimonide Surfaces, Oxygen Adsorption on Clean 8638
Indium Arsenide,
Conductivity of 8726
Effective Mass of Charge Carriers in 8912
Faraday Rotation in 8912
Magnetoresistive Effects in 8766
Properties of 8760
Thermal and Physical Properties of 8932
Indium Phosphide, Effective Mass of Charge Carriers in 8912
Infrared:
Absorption in:
AlSb 8861
GaP 8855
Si 8862, 8863
Color Center Fluorescence in Alkali Halides 8886
Detectors, Measurement of the Frequency Response of 9027
Emission in ZnS:Cu 8871
Photocells, Fabrication of 9026
Properties of:
Au in Ge 8864
GaP 8852
Reflection of Ionic Crystals 8910
Transmission through Normal and Superconducting Films 8853
Inhibition of {111} Surfaces of III-V Intermetallic Compounds 8640
Input-Output Units: Electroluminescent Typewriter 9124
Insulators,
Characteristic Improvements by Diminishing Inhomogeneity in 8676
Radiation Effects on Dielectric Properties of 8674, 8675
Interface Shape upon Melt-Grown Pure Metal Crystals, Effect of Solid-Liquid 8632
Intermetallic Compounds,
Etching of 8639
Etching and Inhibition of {111} Surfaces of III-V 8640
Oxidation Kinetics of III-V 8635
Internal Friction in:
Ferromagnetics, Temperature Dependence of 8943
Ge and Si 8945, 8946, 8947
Synthetic Quartz 8944
Inverters, Tunnel Diode 9139
Ion:
Bombardment Cleaning of:
Ge Surfaces 8637
InSb Surfaces 8638
Distributions and Valencies in Mg-Mn Ferrites 8584
Gauge for Surface Studies, Use of an 8633
Lattices, Polarization Energy in 8669
Ionic:
Crystals,
Conductivity of 8713
Infrared Reflection of 8910
Luminescence in 8875
Mobility in 8713
Nuclear Magnetic Relaxation in 8842
Thermoelectric Power of 8921
Lattice Vibrations 8667
Ionization in Semiconductors, Impact 8717
Iron, Yield Instability in 8939
Iron-Magnesium Oxide Ferrites, Phase Equilibria of 8581
Iron-Nickel,
Magnetic Properties of 8793
Magneto-Optic Infrared Properties of 8851
Iron-Silicon, Dislocation Formation by Spark Discharge in 8599
Ising Problem for Rectangular Lattice, Solution of 8779
Isolators, UHF High Power Ferrite 9036

J

Jahn-Teller Effect in KCl:Tl Phosphors 8874
Junction:
Capacitors, Evaporated Ge-Ta 9051
Characteristics, I-V High Current 8963
Particle Spectrometers, Design and Performance of Si 9150
Junctions,
Alloy-Diffused: Fabrication of 9001
Alloyed:
Boron-Silicon 8973
Fabrication of 8972, 8975, 8998, 8999
Alloyed Hook: Fabrication of 9002, 9003
Delineation of 9009
Diffused:
Fabrication of 8978, 9004
Ohmic and Rectifying 9010
Epitaxial: Fabrication of 9007
Eutectic: Au-Ge 9877
Grown:
Fabrication of 8971, 8996
Vertical Technique for Formation of 8970
Protective Glass Coatings for 8985
Reverse Current in 8965, 8966
Stabilization of 9012
Tunneling in Sb-As Doped Ge 8958
Junctions in Si, Microalloy Fabrication of 8974

K

Kirkendall Diffusion, Nonequilibrium Vacancy 8594

L

Lamp Flashing Generator 9143
Lanthanum, Superconducting Transition Temperature of 8744
Lanthanum Ethyl Sulfate, PMR of $Nd^{3+}$ in 8827
Lattice, Grain Boundaries in Diamond 8611
Lattice:
Constants of $FeO-MgO-Fe_2O_3$ Ferrites 8581
Dynamics, Slow Neutron Interaction Analysis of 8666
Scattering in Si 8716
Thermal Conductivity 8916
Vibrations,
Ionic 8667
Silicon 8665
Vibrations of CdTe 8764
Lead Selenide,
Photoconductivity of 8898
Thermal Properties of 8918
Lead-Selenium, Thermoelectric Properties of 9034
Lead Sulfide,
Photoconduction Mechanisms of 9022
Thermal Properties of 8918
Lead Sulfide Photocells 9025, 9026, 9030
Lead-Sulfur, Thermoelectric Properties of 9034

Lead Superconductors,
  Isotope Effect in 8756
  Resistivity Limit of 8755
Lead Telluride,
  Etches for Revealing Dislocations in 8642
  Thermoelectric Properties of 8927, 8928
  Thermo-Junctions of 8928
Lead-Tellurium, Thermoelectric Properties of 9034
Lead-Tellurium-Selenium, Thermoelectric Properties of 9034
Lifetime, Photoconductive Measurement of 8699, 8700
Lifetime:
  - See also Recombination
  of Ge 8864
  of Ge, Noise Measurement of 8701
Lifetimes in InSb, Temperature Dependence of 8698
Light:
  Meters 9147
  Scattering by Neutron Irradiated Fused Silica 8646
Limiters 9103, 9104
Lithium-Aluminum Ferrites, Magnetic Properties of 8816
Lithium Chloride, Absorption in 8858
Lithium-Chromium Ferrites, Magnetostriction in the Neighborhood of the Compensation Point of 8776
Lithium Fluoride,
  Acoustic Attenuation in 8940
  Electron Spin PMR in 8836
  PMR:
    of F-Centers in 8837
    in Irradiated 8835
    Study of X-Ray Radiation Damage in 8647
Lithium-Nickel Oxides, Conductivity of 8719
Lithium-Oxygen Interaction in Si 8625
Logic:
  Circuits 9083
  Circuits, Design and Performance of Transistor-Resistor 9121
Low Temperature Solid State Physics 8652
Luminescence of:
  CdSe 8891
  Impurity Centers 8876, 8877
  Ionic Crystals, Electronic-Vibrational Processes of 8875
  KCl:Tl Phosphor 8874
  Silica Gel 8892
  ZnO 8612, 8880

M

Magnesium, Susceptibility of 8849
Magnesium Binary and Ternary Alloys, Thermoelectric Power of 8930
Magnesium-Manganese Ferrites,
  Ferrimagnetic Resonance in 8810
  Ion Distributions and Valencies in 8584
Magnesium Oxide, PMR of Transition Metals in 8847
Magnetic:
  Amplifier Control Systems 9140
  Amplifiers,
    Computer Design of 9141
    Transistor Controlled 9142
  Anisotropy:
    in Evaporated Ni-Fe Films, Induced 8795
    of Ferromagnetics, Temperature Dependence of 8794
    in Ni and Permalloy Films 8797
    in Permalloy Films 8796
  Dipole Interactions in Semiconductors 8778
  Field in the Vicinity of a High Permeability Parallelepiped, Determination of 8784
  Film Parametric Amplifiers 9070
  Material for Permanent Magnets 9045
  Properties of:
    $CrBr_3$ 8818
    Fe-Ni Alloys, Radiation Effects on 8793
    Li-Al Ferrites 8816
    Mixed Ferrites 8815
    the Y-Yb Garnet System 8817
  Rod Memory Unit 9042
  Saturation Moment of Ferrimagnetic Garnets 8791
  State Stability in Ferromagnets 8786
  Structure of Co, Thickness Dependence of the 8800
  Tape:
    Cartridges 9120
    Recording, FM Systems for 9119
  Transitions in Dy 8736
Magnetically Polarized Media, Magnetoelastic Wave Propagation in 8783
Magnetite, Conductivity and Thermoelectric Power of 8733
Magnetization:
  Curve in Heisenberg Ferromagnet 8782
  in Mn Ferrites, Ultrasonic Measurement of 8787
  in Si-Fe Ferromagnets 8805
Magnetoelastic Waves, Propagation of 8783
Magnetoelectric:
  Effect in:
    InAs 8760
    InSb 8759
  Properties of Bi 8727
Magnetometers, Hall Effect 9018
Magneto-Optic:
  Effects on Excitons in CdS 8850
  Infrared Properties of Ni-Cu and Fe-Ni 8851
Magnetoresistance of:
  CdS 8767
  GaAs, Impurity Concentration and Radiation Produced Defects Effects on 8765
Magnetoresistive Effects in InSb and InAs 8766
Magnetostatic Properties in Ni-Zn Ferrites, Temperature Dependence of 8788
Magnetostriction of:
  Gd, Temperature Dependence of 8777
  $Li_{0.5}Fe_{0.8}Cr_{1.7}O_4$ 8776
Manganese Binary Structures, Superconductivity of 8758
Manganese$^{2+}$ in CdTe, Spin Resonance of 8771
Manganese Acetate, Susceptibility of 8819
Manganese Dioxide, Dielectric Properties of 8689, 8690
Manganese Ferrites,
  Magnetization in 8787
  Oxidation of 8634
Manganese Fluoride,
  Antiferromagnetic Transition Temperature of 8820
  Curie Temperature of 8820
  NMR in 8808
Maser Communication Systems 9109
Masers,
  Nuclear Polarization Effects on 9047
  Pulsed Field Millimeter Wave 9049
  Ruby: Characteristics of 9050
  Three-Level: Simultaneous Resonance Condition Calculations for 9046
  Traveling-Wave: Tunability of 9048
Masking, Fabrication of Double Diffused Junction Transistors by Oxide 9004
Matrix Synthesis 9058
Memory:
  Cores,
    Inhibited Flux Operation of 9038
    Residual States in 9039
    Reversible Magnetization in 9040
  Units,
    Magnetic Rod 9042
    Thin Film 9126
    Transistor 9127
Mercury, Superconducting 8748
Mercury Telluride, Optical Properties and Preparation of 8867
Mercury Telluride-Cadmium Telluride, Optical Properties and Preparation of 8867
Metal Alloys, Thermoelectric Properties of 8920
Metals,
  Polycrystalline Double-Bragg Reflections from 8592
  Work-Hardening in fcc 8600
Metals Grown from Melt, Effect of Solid-Liquid Interface on Pure 8632
Millimeter Wave Pulsed Field Masers 9049
Mobility,
  Bardeen-Shockley Formula of 8711
  Microwave Measurement of 8714
Mobility:
  in Ionic Crystals 8713
  of Si 8715
  Variation with Applied Electric Field 8712
Modulators, Frequency 9088
Molecular Crystals, PMR in Hydrated and Deuterated 8838
Molybdenum Si Contacts, High Temperature 8981
Mössbauer Effect in Crystals 8889
Multiplication in Junctions, Avalanche 8967, 8968
Multipliers for Analog Computers, Hall Effect 8760
Multivibrators 9073, 9078
Multivibrators, Reduction of Recovery Time of 9079
Muscovite, Dislocations in 8598
Musical Instruments, Oscillators for 9072

N

N-Port Networks, Transmission and Hybrid Parameters for 9055
Neodymium in Lanthanum Ethyl Sulfate, PMR of 8827
Network:
  Synthesis,
    Matrix 9058
    Two-Port 9059
  Theory,
    Flow Graph 9054
    N-Port 9055
    Two-Port 9056, 9057
Neutron Scattering in Lattices, Slow 8666
Nickel:
  in $Al_2O_3$, PMR of 8846
  Films, Magnetic Anisotropy in 8797
Nickel Acetate, Susceptibility of 8819
Nickel-Cadmium Ferrites, Susceptibility of 8825
Nickel-Chromium Ferrites, Composition Effects on Characteristics of 8813
Nickel-Copper, Magneto-Optic Infrared Properties of 8851
Nickel-Copper Ferrites, Resonance Linewidth of 8814
Nickel Ferrites, Ferrimagnetic Resonance in 8810
Nickel-Iron Films, Induced Magnetic Anisotropy in Evaporated 8795
Nickel Oxides, Conductivity of 8719
Nickel-Zinc Ferrites, Magnetostatic Temperature Dependence of 8788
Niobium Oxide Rectifiers, Fabrication of 8989
Noise in:
  Ge Diodes 8969
  InSb 8698
Nuclear:
  Magnetic:
    Relaxation in Ionic Crystals 8842
    Resonance:
      in Antiferromagnetic MnF 8808
      of $Co^{59}$ in Domain Walls of Co 8806
      in Crystal Analysis 8588
      in Ferromagnetic Co 8807
      Measurement of Superconducting Pb Resistivity Limit 8755
      of Solid $H_2$ and $D_2$ 8844
  Spin Relaxation in Superconducting Al 8843

O

Optical:
  Absorption:
    in CdS Type Crystals, Photoelectric Analysis of 8591
    Spectra of KCl and KBr 8839
  Constants of:
    Bi 8907
    Se 8908

Optical: (Cont'd)
Filters 8869
Properties of:
CdTe 8870
HgTe and HgTe-CdTe 8867
Phosphors 8876
Semiconductors 8869
ZnS 8883
Organic Semiconductors, Characteristics of p-Phenylenediamine-Chloranil Complex 8735
Oscillators,
Hall Effect 9019
Multivibrator 9078, 9079
Phase-Locked 9075
Pulse 9072
Radiation Effects on Quartz 9052
Resonant Circuit 9077
Sub-Audio 9074
Variable Amplitude 9074
Voltage Controlled 9076
Outdiffusion in Junction Transistor Fabrication 9006
Oxidation:
of Clean Ge Surfaces 8637
Kinetics of III-V Intermetallic Compounds 8635
of Manganese Ferrites 8634
of SiC 8636
Oxides, Structure of 8587
Oxygen, Radiation Damage in n-Type Si Containing Dissolved 8645
Oxygen Adsorption on Clean InSb Surfaces 8638
Oxygen-Lithium Interaction in Si 8625

P

P-Phenylenediamine-Chloranil Complex, Electrical and Thermoelectric Properties of the 8735
Packaging of:
Diodes 8983
Point Contact Diodes 8952, 8953
Transistors 9013
Paramagnetic:
Particles, Anisotropy Energy and Remanent Magnetization of 8790
Resonance,
Exchange-Narrowed 8828
Nuclear and Electron 8841
Resonance:
Absorption, Saturation Inhomogeneously Broadened 8830
of $Cr^{3+}$ in Ruby 8845
in Hydrated and Deuterated Molecular Crystals 8838
in KCl and KBr 8839
in LiF 8835
in LiF, F-Center 8837
Linewidth in Dilute Crystals with Anisotropic g-Factor 8827
of $Nd^{3+}$ in Lanthanum Ethyl Sulfate 8827
of Ni in $Al_2O_3$ 8846
Spectra of:
$CaF_2$, Annealing Effect on 8832
$K_3Co(CN)_6$, Polytype Effects in the Electron 8831
Studies of Eu and Sm Activators in SrS 8879
Study of X-Ray Radiation Damage in LiF 8647
of Transition Metals and $Gd^{3+}$ in Single Crystal Oxides 8847
Salts, Spin-Lattice Relaxation in 8833
Susceptibility:
of Ni-Cd Ferrites 8825
in Si and Ge 8848
Three and Four Level Systems, Saturation in 8829
Paramagnets, Refractive Indices of 8906
Parametric Amplifiers 9069, 9070
Permalloy Films,
Cross-Tie and Chain Walls in 8803
Magnetic Anisotropy in 8796, 8797
Permanent Magnets, Magnetic Material for 9044, 9045
Permeability - See Susceptibility
Permittivity - See Dielectric Constant
Perovskites, Antiferromagnetic Rare Earth-Iron 8822
Phase:
Detectors 9093
Discriminators 9092
Equilibria:
for $CdAs_2$ and $Cd_2A_3$, Solid-Vapor 8582
of FeO-MgO-$Fe_2O_3$ Ferrites 8581
in the ZnO-$TiO_2$ System 8580
Transformations in $Mn^{3+}$ Spinels 8590
Transitions in:
Solid Solutions 8583
Solids, Gradual 8585
Phase-Locked Oscillators 9075
Phase-Shift Modulator, Hall Effect 9018
Phonon Drag Measurements in Si, Transmitted 8922
Phonon-Phonon Transitions in Si 8716
Phosphor Screens 9031
Phosphors,
Electron PMR Studies of Activated 8878
EPR Studies of Eu and Sm Activators in SrS 8879
Optical Properties of 8876
Phosphors of KCl:Tl, Jahn-Teller Effect in 8874
Photocells,
Fabrication:
and Characteristics of 9025
of Coolable PbS 9026
of Multielement 9030
Photoconduction in PbS, Mechanisms of 9022
Photoconductive:
Cells, Fabrication of Surface-Protected 9029
Devices, Fabrication of 9028
Trapping in ZnS, PMR Studies of 8893
Photoconductivity of:
CdS-ZnS Mixed Crystals 8899
$Cu_2O$ 8903
GaS-Se 8900
Ge: 8864, 8894
Grain Boundaries 8896
Group V-VI-VII Compounds 8901
InSb 8897
PbSe 8898
ZnO 8612
Photo-Dielectric Effect in ZnS-(Cu, Fe) 8890
Photoelectronic Properties of ZnS 8902
Photosensitive:
Cells, Fabrication of 9024
Ultrasonic Attenuation in CdS 8942
Photosensitivity of Photo-Cathodes 8905
Phototransistors, Fabrication of an Array of 9030
Physical Properties of GaSb-InSb 8725
Piezoelectric:
Crystals, Production of Sound in 8694
Scattering in:
CdS 8693
ZnO 8693
Piezoresistance of:
GaSb, Pressure Effects on 8724
Ge, Pressure Effects on 8724
InSb, Pressure Effects on 8724
Polarization Energy in Ion Lattices 8669
Polygrain Metals, Double-Bragg Reflections from 8592
Potassium Bromide,
Absorption in 8839, 8857
PMR in 8839
Potassium Chloride,
Absorption in 8839, 8856, 8857, 8859, 8868
Dislocations in 8596
Elastic Moduli and Specific Heat of 8937
ESR of F-Centers in 8840
Photoconductivity of 8904
PMR in 8839
Potassium Chloride:Tl Phosphor, Jahn-Teller Effect in 8874
Potassium Chrome Alum, Acoustic Attenuation in 8940
Potassium Cobalticyanide, Electron PMR Spectra of 8831
Power:
Generators, Regulators for 9130
Meters, RF 9146
Regulators 9133
Supplies: 9135, 9136, 9137
- See also Voltage Regulators
Transistors, Fabrication of 9008
Preparation of:
- See also Growth of
Ferromagnetic $CrO_2$ 8630
$FeVO_3$ 8631
Ge by Distillation 8619
HgTe-CdTe Crystals 8867
Printers, Control Circuit for 9125
Pulse:
Amplifiers 9067, 9068
Converters 9084, 9085
Generators 9099, 9101
Oscillators 9072, 9073
Position Demodulators 9094
Purification, Modified Boat for Zone 8617
Purification of:
Alkali Halide Crystals 8618
Ge by Distillation 8619
High Vapor Pressure Elements, Vapor-Zone Refining Method of 8616

Q

Quantizers 9105
Quarternary Se and Te Semiconductors 8653
Quartz,
Hypersonic Waves in 8941
Internal Friction in Synthetic 8944
Quartz Oscillators, Radiation Effects on 9052

R

Radiation, Angular Dependence of 8644
Radiation:
Damage in:
Fused Silica, Light Scattering Study of Neutron 8646
LiF, Paramagnetic Resonance Study of X-Ray 8647
n-Type Si, Effects of Dissolved Oxygen on 8645
Detectors, Fabrication of 9023, 9024
Effects in:
Al and Cu, Annealing of 8651
NaCl, Annealing of 8650
in GaP Diodes, Recombination 8872
Induced Defects in Lead Silicate Glass 8648
Radio:
Frequency:
Amplifiers 9066
Power Meters 9146
Receivers,
AGC and Detector Stages of 9112
Battery Operated 9110
Receiving Systems, Calibration of 9111
Railway Track Signaling System 9107
Ramp Function Generators 9100
Rare Earth-Iron Perovskites, Antiferromagnetic 8822
Rare Earth Oxides on the Magnetic Behavior of Ferrite Cores, Effect of 9041
Receivers, Battery Operated 9110
Recombination:
- See also Lifetime
Radiation in GaP Diodes 8872
in Semiconductors, Overlap Integrals for the Calculation of Auger 8697
on Si Surfaces 8703
Recovery Time in Multivibrators, Reduction of 9079
Rectifiers,
As-Te 8990
CbO (NbO) 8989
Encapsulation of 8991
Ge 8972
Se 8986, 8988
Se-Ge Composite 8987
Solid Metallic 8992

Rectifying Circuits 9131
Reflection:
  Equations, Fresnel 8909
  of Ionic Crystals, Infrared 8910
Refractive Indices of Ferro- and Paramagnetic Solids 8906
Regulators,
  dc:
    Power 9133
    Voltage 9134
  Voltage 9132
Resistances, Nonlinear Controlled Semiconductor 9021
Resistivity - See Conductivity
Resonance Linewidth of Ni-Cu Ferrites 8814
Resonant Circuit Oscillators 9077
Reverse:
  Current in Junctions, Jumps in 8965
  Currents in Diodes 8966
Ruby, Paramagnetic Resonance of $Cr^{3+}$ in 8845
Ruby:
  - See also Aluminum Oxide 8846
  Masers,
    Applications and Characteristics of 9050
    Nuclear Polarization Effects on 9047
    Pulsed Field 9049
    Simultaneous Resonance Condition Calculations for Three-Level 9046
    Traveling-Wave 9048
Rutile, Elastic Moduli of 8935

S

Satellite:
  Communication Systems, Maser 9109
  Instrumentation System 9108
Scattering in:
  Lattices, Slow Neutron 8666
  Si, Phonon-Phonon 8716
Selenium,
  Chemical Anslysis of 8615
  Electrical Properties of 8728
  Growth of 8908
  Optical Constants of 8908
Selenium:
  Radiation Detectors, Fabrication of 9023
  Rectifiers,
    Encapsulation of 8991
    Fabrication of 8986, 8988
Selenium-Germanium Composite Rectifiers 8987
Semiconducting Properties of Cubic Boron Phosphide 8732
Semiconductors,
  Band Dynamics of 8705
  Binary and Quartemary 8653
  Carrier Distribution in 8696
  Diffusion in 8620
  Effective Mass of 8705
  Impurity Levels in 8659
  Magnetic:
    Dipole Interactions in 8778
    Susceptibility of Donors in 8823
  Overlap Integrals for the Calculation of Auger Recombination in 8697
  Surface Properties of 8774
  Thomson Effect in 8923, 8924
  Zener Effect in 8705
Shaping Method for Si 8629
Shift Registers, Twistor 9053
Signaling System, Railway 9107
Silica:
  Gel, Luminescence of 8892
  Windows, Selective Etching Technique for Fabricating 8629
Silicides, Thermoelectric Power and Electrical Conductivity of 8931
Silicon,
  Absorption in 8862, 8863
  Capture Cross Sections in 8704
  Dielectric Constant of 8672
  Diffusion in 8620
  Diffusion of Boron in 8621
  Dislocation Interactions in 8608
  Electrochemiluminescence of 8884
  Evaporation of 8627
  Exciton Energy Levels in 8695
  Gas Etching Effects on Single Crystals of 8643
  High Temperature Mo Contacts for 8981
  Internal Friction in 8945, 8946, 8947
  Lattice Vibrations in 8665
  Li-Oxygen Interaction in 8625
  Mobility of 8715
  Ohmic and Rectifying Contacts for 9010
  Oxygen Effects on Radiation Damage in n-Type 8645
  Phonon-Phonon Scattering in 8716
  Shaping Method for 8629
  Specific Heat of 8665
  Spin Resonance of Group VIII Impurities in 8770
  Surface Recombination on 8703
  Susceptibility of 8823, 8848
  Thermal Expansion of 8934
  Transmitted Phonon Drag Measurements in 8922
  Valence Band Parameters in 8706
Silicon:
  Doped GaAs, Hall Coefficients of 8762
  Layers, Epitaxial Growth of 8628
  Surface States 8663, 8664
Silicon-Boron Alloyed Junctions 8973
Silicon Carbide,
  Absorption Edge of 8865
  Energy Gap of 8865
  Ohmic and Rectifying Contacts for 9010
  Oxidation of 8636
  Spectrographic Analysis of 8614
Silicon Dioxide, Light Scattering Study of Neutron Radiation Damage in Fused 8646
Silicon Dioxide Protective Films for Photoconductive Cells 9029
Silicon-Germanium, Susceptibility of 8824
Silicon-Iron,
  Magnetization in 8805
  Susceptibility of 8789
Silver$_2$-Group VI Compounds, Electrical Properties of 8734
Silver (S, Se, Te)$_2$, Thermoelectric Power of 8921
Sintering of ZnO Spheres 8626
Skin Effect, Superconducting 8750
Sodium Bromide, Photoconductivity of 8904
Sodium Chloride,
  Absorption in 8868
  Annealing of X-Ray Induced Surface Hardening in 8650
  Conductivity of 8729
  Specific Heat of 8915
  Thermoluminescence of 8885
  Yield Stress of 8938
Sodium Fluoride, Absorption in 8868
Sodium Niobate, Dielectric Properties of Solid Solution Systems Based on 8677
Solar Powered Hearing Aids 9118
Solid:
  Solutions, Structure of 8583
  Solutions:
    of $Fe_2O_3$ and $FeVO_3$ 8631
    in the System $ZnO-TiO_2$ 8580
  State, Low Temperature 8652
Solids,
  Gradual Phase Transitions in 8585
  Transport Processes in 8707
Space Charge:
  Distributions,
    Effects of Charge Mobility on 8679
    Solids and Liquids Measurement in 8679
    Static 8679
  Fields in $BaTiO_3$ 8680
  Limited Currents in:
    $BaTiO_3$ and CdS 8681
    Insulator Diodes 8961
Specific Heat of:
  KCl 8937
  NaCl 8915
  Si 8665
Spectrographic Analysis of:
  Impurities 8613
  SiC 8614
Spectrometers, Si Junction Particle 9150
Spin:
  Resonance of:
    Charge Carriers in Graphite 8772
    Group VIII Impurities in Si 8770
    $Mn^{2+}$ in CdTe 8771
  Waves in Ferromagnets 8781
Spin-Lattice:
  Relaxation, Measurement of 8834
  Relaxation in Paramagnetic Salts 8833
Spinels, Crystal Distortion and Phase Transformations in $Mn^{3+}$ 8590
Stabilization of Junction Transistors 9012
Strength of Crystalline Materials 8602
Strontium Sulfide, Paramagnetic Resonance Studies of Eu and Sm Activators in 8879
Strontium Titanate, Paramagnetic Resonance of Transition Metals in 8847
Structure,
  NMR Analysis of Crystal 8588
  Slow Neutron Interaction Analysis of 8666
Structure of:
  Clean InSb Surfaces 8638
  Crystals 8587
  Grain Boundaries 8610
  $Mn^{3+}$ Spinels 8590
  Solid Solutions 8583
  ZnO 8612
  ZnSb 8589
Superconducting:
  Al, Nuclear Spin Relaxation in 8843
  Alloys, Critical Temperature Theory of 8745
  Be Thin Films 8757
  Films,
    Far-Infrared Transmission through 8853
    Magnetic Field Penetration in 8754
  Hg, Critical Field of 8748
  In, Critical Field of 8748
  La, Transition Temperature of 8744
  Pb,
    Isotope Effect in 8756
    Resistivity Limit of 8755
  Sn, Critical Field of 8748
  Sn Films, Critical Field of 8747
Superconductivity,
  BCS Theory of 8737
  Coulomb Effects in the Theory of 8740
  Critical Field in 8741
  Strong-Coupling Limit in 8739
  Transitions in 8742, 8743
Superconductivity of $\sigma$- and $\alpha$-Mn Binary Structures 8758
Superconductors,
  Energy:
    Gap in 8749
    Level Density and Critical Temperature of 8746
  Ferromagnetic 8738
  Surface Impedance of 8750, 8751, 8752, 8753
Surface:
  Alloying with Al-Containing Solder 8975
  Barrier:
    Rectifying Contacts 8976
    Transistors,
      Fabrication of 9014, 9015
      Whisker Mounting on 9016
  Impedance of Superconductors 8750, 8751, 8752, 8753
  Properties of Semiconductors 8774
  Recombination on Si 8703
  State of Ge Transistors, Effect of $H_2O$ on 9012
  States on:
    Crystals 8660, 8661, 8662
    Si 8663
    Si and Ge 8664

Surface: (Cont'd)
Studies, New Tools for 8633
Transport 8710
Surfaces,
Gas Etching and its Effect on Semiconductor 8643
Mass Spectrographic Studies of Impurities on 8613
Oxidation of Clean Ge 8637
Oxygen Adsorption on Clean InSb 8638
Surfaces of III-V Intermetallic Compounds, Etching and Inhibition of {111} 8640
Susceptibility of:
$Co(C_2H_3O_2)_2 \cdot 4H_2O$ 8819
Ferrimagnetic Garnets 8791
Mg 8849
$Mn(C_2H_3O_2)_2 \cdot 4H_2O$ 8819
$Ni(C_2H_3O_2)_2 \cdot 4H_2O$ 8819
Ni-Cd Ferrites 8825
Si and Ge 8823, 8848
Si-Fe, Photo-Measurement of 8789
Si-Ge 8824
Three and Four Level Systems, Saturation Effect of 8829
Switchboard, Telephone 9116
Switches,
Broadband Reflective Ferrite 9043
Microwave Transverse Ferrite 9035
Switching:
Circuits,
Bistable 9083
Broadband UHF 9081
Flip-Flop 9101
Gate 9084, 9085
High Power 9086
Stabilization of 9080
Three-State 9087
Trigger 9082
Systems, Design of 9115

T

Talc, Dislocations in 8598
Tantalum Electrodes, Metalizing of 8982
Tape:
Cartridges 9120
Recording, FM Systems for 9119
Telemetry Systems, Light Modulated 9117
Telephone:
Set 9114
Switchboard 9116
Switching Systems, Design of 9115
Television Deflector Circuits 9113
Tellurium, Chemical Analysis of 8615
Ternaries, Photoconductivity of Group V-VI-VII 8901
Tetragonal Solids, Debye Temperature of 8913
Thermal:
Conductivity of:
Alloys 8916
$Bi_2Te_3$ 8919
Ga in the Normal and Superconducting States 8917
PbS and PbSe 8918
Expansion of:
GaP 8852
Gd, Magnetostriction Contribution to 8777
Si 8934
Triglycine Sulfate 8692
Properties of (Ga, In) As 8932
Thermionic Emission of Si 8664
Thermoelectric:
Heat Pump 9034
Materials 9034
Power of:
$Bi_2Te_3$ 8919
$Bi_2Te_3$, Radiation Effects on 8925, 8926
CoSi 8931
Co-Si-FeSi 8931
CoSi-NiSi 8931
CrSi 8931
Ionic Crystals 8921
Mg Binary and Ternary Alloys 8930
MnSi 8931
PbS and PbSe 8918
Wustite and Magnetite 8733
Properties of:
$Bi_2Te_3$ 8929
Metal Alloys 8920
the p-Phenylenediamine-Chloranil Complex 8735
PbTe and $Bi_2Te_3$, Radiation Effects on 8927
Thermo-Junctions of PbTe and $Bi_2Te_3$ 8928
Thermoluminescence of NaCl, Color Center 8885
Thermomagnetic Effects in InSb 8933
Thomson Effect in Semiconductors 8923, 8924
Thorium Oxide, Paramagnetic Resonance of $Gd^{3+}$ in 8847
Thyratron Control Circuit 9144
Timing Device 9149
Tin,
Phase Transformations and Properties of Gray 8586
Superconducting 8748
Tin Films, Superconducting 8747
Titanium Dioxide-Zinc Oxide System, Phase Equilibria in 8580
Transformations in Gray Tin 8586
Transistors,
Characteristics of Base and Emitter in 8995
Circuit for Measurement of Alpha of 8993
Diffused Base: Fabrication of 9005
High Frequency: Fabrication of 9004
Junction: Fabrication of: 8998, 8999
Alloy Diffused 9001
Vapor Deposited 9007
Method for Cooling Power 9011
Methods of Producing Stable 9012
Packaging of 9013
Point Contact: Preparation of Point Contact Assemblies for 8994
Power: Fabrication of 9008
Surface Barrier:
Fabrication of 9014, 9015
Selective Electroplating of 9017
Whisker Mounting on 9016
Transition Metals in Single Crystal Oxides, Paramagnetic Resonance of 8847
Transmission:
Equations, Fresnel 8909
through Normal and Superconducting Films, Far-Infrared 8853
Transport Processes in Solids, Theory of 8707
Trapping in ZnS, Paramagnetic Resonance Studies of 8893
Traps in CdS, Noise and Photoconductivity Measurement of 8702
Traveling Wave:
Harmonic Generators 9097
Masers, Tunability of 9048
Trigger Circuits 9082
Triglycine Sulfate,
Ferroelectric:
Properties of 8691
Transition in 8692
Thermal Expansion in 8692
Trigonal Solids, Debye Temperature of 8913
Tunnel:
Diode Inverters 9139
Diodes, Characteristics:
and Fabrication of 8955
of GaAs 8956
Tunneling:
Current, Temperature Dependence of 8957
in Sb-As Doped Ge Junctions 8958
Twistor Shift Register 9053

U

Ultra High Frequency Broadband Switching Circuits 9081
Ultrasonic:
Attenuation in CdS, Photosensitive 8942
Measurement of Magnetization in Mn Ferrites 8787
Waves in Quartz, Excitation and Attenuation of 8941

V

Vacancy:
Condensation during Cooling of Solids 8595
Diffusion, Nonequilibrium 8594
Valence Band Parameters in Si, Cyclotron Resonance Measurement of 8706
Valencies in Mg-Mn Ferrites, Ion 8584
Vapor-Zone Refining 8616
Varactors, Figures of Merit of 8960
Varistors 9021
Voltage:
Regulators, Direct Current 9134
Regulators: 9132
- See also Power Supplies

W

Wall Effect in Ferrimagnetic Resonance 8810
Wattmeters, Hall Effect 9019
Wave Analyzers 9145
Waveform Generators 9101
Whisker Mounting on Diodes and Transistors 9016
Whiskers,
Impedance Matching of 8950
In-Ge Plated 8949
Whiskers for Al Bonded Diodes 8951
Work-Hardening in fcc Crystals, Orientation Dependence of 8600
Wurtzite Structures, Bond Structure of 8654
Wustite, Conductivity and Thermoelectric Power of 8733

X

X-Ray Induced Surface Hardening in NaCl, Annealing of 8650

Y

Yield:
Instability in Fe, Low Temperature 8939
Stress of NaCl, Temperature Dependence of 8938
Young's Modulus in Ferromagnetics, Temperature Dependence of 8943
Yttrium Iron Garnet, Ferrimagnetic Resonance in 8810
Yttrium-Ytterbium Garnet System, Magnetic Properties of 8817

Z

Zener Effect in Semiconductors 8705
Zinc Antimonide,
Cyclotron Resonance Absorption in 8768
Structure of 8589
Zinc Oxide,
Lattice Structure and Properties of 8612
Luminescence in 8880
Piezoelectric Scattering in 8693
Sintering of 8626
Zinc Oxide-Titanium Dioxide System, Phase Equilibria in 8580
Zinc Sulfide,
Electroluminescence of 8881, 8883
Phase Transitions in 8585
Photoconductive Trapping in 8893
Photoelectronic Properties of 8902
Zinc Sulfide Structure Crystals, Forbidden Zone Width of 8658
Zinc Sulfide-Copper, Infrared Emission in 8871
Zinc Sulfide-Cu, Fe Phosphors, Photo-Dielectric Effect in 8890
Zone Refining,
Modified Boat for 8617
Vapor- 8616

# AUTHOR INDEX


Abe, R. 8685
Abrahams, M.S. 8932
Abrams, H.J. 9133
Abrikosov, A. 8753
Adcock, W.A. 8996
Adrian, F.J. 8593
Aerts, E. 8660,8661, 8662
Ahearn, A.J. 8613
Alexander, W. 9105
Alfrey, G.F. 8882, 8883
Allen, F.G. 8663
Allen, J.W. 8585
Allen, L.C. 8668
Amelinckx, S. 8598, 8603, 8610, 8650
Amirkhanova, D.Kh. 8933
Andrä, W. 8797
Apple, E.F. 8871
Arams, F.R. 9048
Arase, E.M. 8915
Arend, H.T. 8691, 8854
Armstrong, L.D. 8975
Armstrong, M.E. 9111
Aronson, A.I. 9071
Artman, J.O. 8831
Artman, R.A. 8926
Astrov, D.N. 8820
Auer, Jr., J.H. 9107
Austin, I.G. 8912
Avinor, M. 8891
Avramenko, V.P. 8815
Axelby, G.S. 9054

Bady, I. 8812
Baker, W.E. 8622
Baldwin, Jr., J.A. 9038
Balluffi, R.W. 8594
Baltensperger, W. 8778
Bancie-Grillot, M. 8888
Baranov, L.I. 8962
Baranskii, P.I. 8924
Barker, R.S. 8648
Barker, W.A. 8833
Barlow, H.M. 8714
Barnes, J.F. 8713
Bartels, B.E. 9025, 9026
Bartlett, B.E. 8897
Baynham, A.C. 8673
Beattie, A.R. 8697
Becker, J.A. 8633
Bell, H.V. 9105
Belov, K.P. 8763, 8943
Benedek, G.B. 8808
Bengtivegna, M.J. 8975
Berry, C.R. 8631
Berss, R.R. 8934
Berz, F. 8773
Bhide, V.G. 8689, 8690
Billings, T.E. 9127
Birss, R.R. 8775, 8776
Biswas, A.B. 8590
Blaugher, R.D. 8758
Blewitt, T.H. 8651
Blok, J. 9022
Bobeck, A.H. 9053
Bodó, Z. 8696, 8700
Bohun, A. 8885
Bolling, G.F. 8632
Bommel, H.E. 8941
Bonanno, J.L. 8992
Bopp, C.C. 9104
Bose, M. 8735
Bradley, E.M. 8795
Bradley, W.E. 8976, 9014
Bradmiller, R.W. 9089
Braginski, A. 8634
Branwood, A. 8682
Braunstein, R. 8932
Bray, J.P. 8836
Brazda, J. 9149
Brezina, B. 8691
Broadley, Jr., H.R. 9044
Bron, W.E. 8859
Brooks, H. 8672
Brophy, J.J. 8702
Brout, R. 8782, 8785
Brown, C.S. 8944
Brown, J. 8714
Brown, T.H. 9138
Broz, J. 8584
Brubaker, J.F. 9133
Bube, R.H. 8591, 8900
Budnick, J.I. 8743
Burnysheva, A.N. 8809
Burton, L.W. 8991
Busch, G. 8586, 8653, 8824
Bussard, E.J.H. 9077

Cable, J.W. 8821
Cahn, J.W. 8802
Caldwell, P.N. 8988
Camras, M. 9120
Cape, J. 8857
Cardona, M. 8672
Carman, Jr., J.N. 8952, 8998
Caswell, D. 9035
Caswell, H.L. 8747
Chaldyshev, V.A. 8656
Chapman, R. 9065
Chasmar, R.P. 8760
Chechernikov, V.I. 8825
Chen, Z.-R. 8817
Chow, W.F. 9060
Clarebrough, L.M. 8600
Cluwen, J.M. 9103
Cocca, U. 9023
Cohen, E. 8760
Cohen, M.S. 8796
Collins, T. 8812
Coltman, R.R. 8651
Combs, C.M. 8631
Compton, D.M.J. 8622
Cooke, I. 8883
Coopersmith, M. 8785
Corelli, J.C. 8927
Corenzwit, E. 8744
Cornelison, B. 9011
Corner, W.D. 8777
Coufova, P. 8854
Covert, P.W. 9140
Cowan, J.A. 8838
Cox, D.L. 9009
Crocker, A.J. 8641
Crone, R.L. 8949
Cross, L.G. 9047
Crow, R.P. 9091
Crownover, J.W. 9143
Cunnell, F.A. 8623
Cutler, I.B. 8636
Cuypers, R. 8650

Dahlin, R.K. 9076
Dalven, R. 8865
Damle, R.V. 8689, 8690
Davis, P.W. 8870
Dayal, B. 8665
DeBitetto, D.J. 8812
deGraaf, A.M. 8778
DeGrasse, R.W. 9109
Degtyarev, I.F. 8805
Dekeyser, W. 8610
Delavignette, P. 8598, 8603
Demars, G.A. 8774, 8845
Dement'yev, Ye.P. 9063
Denton, R.L. 9148
Dexter, R.N. 8769
Ditzenberger, J.A. 8762
Domenicali, C.A. 8920
Doyle, W.T. 8904
Dransfield, K. 8941
Dresselhaus, G. 8751, 8752
Dresselhaus, M.S. 8751, 8752
Drickamer, H.G. 8858
Drobchenko, L.D. 8788
Dubinin, V.G. 8878, 8879
Duga, J.J. 8765
Dulin, F.H. 8580
Dumke, W.P. 8716
du Pré, F.K. 8812
Dwork, L.E. 9093

Eagles, D.M. 8585
Eannarino, G. 8984
Eck, T.G. 8849
Edmond, J.T. 8726
Elleman, D.D. 8755
Enck, F.D. 8937
Eppler, R.A. 8858
Epstein, M. 9018, 9146
Erb, T. 9073
Erdman, D.C. 9088
Ernsberger, G.W. 9130
Esaki, L. 8955
Ezhik, I.I. 8886

Fan, H.Y. 8862, 8863
Fara, H. 8594
Faulkner, A.H. 9078
Faust, Jr., J.W. 8639
Favro, L.D. 8972
Feher, G. 8706
Filberich, L. 9131
Finnemore, D.K. 8748
Fischer, G. 8759
Fischer, R.F. 9053
Flaschen, S.S. 8985
Flippen, R.B. 8819
Florio, J.V. 8678
Floyd, Jr., A.L. 9029
Fok, M.N. 8881
Folberth, O.G. 8654, 8658
Foner, S. 9049
Frankel, D.R. 8710
Frederikse, H.P.R. 8766
Friedberg, S.A. 8819
Friedman, A.N. 8727
Friedman, E. 8832
Fritts, R.W. 9034
Frood, D.G.H. 8721
Frost, R.T. 8927
Fryberger, D. 9146
Fu-Chouh, Pu. 8780
Fujita, I. 8868
Fuller, C.S. 9006
Furuichi, J. 8684
Furukawa, Y. 8957, 8958

Gaman, V.I. 8966
Ganesan, S. 8692
Garber, R.I. 8602
Garstens, M.A. 9046
Gatos, H.C. 8640
Gee, A. 8884
Geist, D. 8848
Georgobiani, A.N. 8881
Gergely, Gy. 8730
Giacaletto, J.J. 8929
Giaever, I. 8749
Gibson, A.F. 8673
Gilleo, M.A. 8791
Gillett, C.M. 8725
Gindin, I.A. 8602
Ginsberg, D.M. 8853
Glackin, R.N. 9101
Glaister, R.M. 8677
Gobeli, G.W. 8663
Goland, A.N. 8926
Gomi, Y. 8803
Gooch, C.H. 8623
Goodwin, D.W. 8698
Gordon, W.L. 8849
Gor'kov, L.P. 8741, 8745, 8753
Gorton, H.C. 8624, 8872
Gourary, B.S. 8593
Granville, J.W. 8673
Green, H.S. 8779
Greene, R.F. 8710
Greenstein, L.J. 9018, 9146
Gregory, L.A. 9141
Gregory, M.B. 9074
Greig, D. 8918
Grewe, T. 9075
Grika, V.M. 8948
Griunier, A. 8583
Gross, E.F. 8866, 8888
Gualtieri, J.G. 8643
Gudmundsen, R.A. 8973, 8999
Guggi, W.B. 9113
Gutin, S.S. 8948
Gyorgy, E.M. 8798

Haayman, P.W. 9010
Haebler, D.V. 9131
Haga, E. 8921
Haken, H. 8782
Hakimi, S.L. 9057
Hall, P.M. 8736
Hall, R.N. 8970
Halloran, M. 8769
Halpern, J. 8964
Hamada, S. 8764
Hambleton, K.G. 8956
Hamburger, T. 9124
Hamilton, D.J. 8968
Hamming, R.W. 8588
Handler, P. 8664
Haneman, D. 8638
Hargreaves, M.E. 8600
Harrity, J.W. 8649
Harten, H.U. 8703
Hatcher, R.D. 8915
Haugen, G.L. 9079
Hawker, P.D.T. 9121
Hawkins, T.D.H. 8894
Hayes, W. 8839
Heasell, E.L. 8715
Hedderly, D.L. 9097
Heer, R. 8644
Heiland, G. 8612
Hendershot, J.H. 9081
Hensel, J.C. 8706
Hensler, D. 8769
Hildebrandt, A.F. 8755
Hill, D. 8732
Hilsum, C. 8726
Hinsdale, J.G. 9092
Hoff, Jr., M.E. 9107
Hogg, D.C. 9109
Holländer, E.F. 8597
Hollander, L.E. 8935
Hollar, E. 8769
Holub, A.J. 9069
Hopfield, J.J. 8929
Hopkins, D.C. 8850
Horiuchi, S. 8756
Horiye, H. 8621
Horne, R.J. 8649
Hornstra, J. 8934
Hosler, W.R. 8611
Housley, R.M. 8766
Houston, B.B. 8844
Howland, F.L. 8642
Hrivnák, L. 8983
Huang, C. 8711
Hubner, K. 9083, 9093
Huelsman, L.P. 8922
Hulliger, F. 9055
Hulm, J.K. 8653
Hurst, C.A. 8758
Husimi, K. 8779
Hutchison, F. 8787
Hutson, A.R. 8777
Hyde, J.S. 8693
8830, 8835
8710

Iizima, S. 8899
Ingham, Jr., H.S. 8729
Irani, K.S. 8590
Ishikawa, Y. 9051
Ishmukhametov, B. Kh. 8783
Itskevich, E.S. 8914
Ivanov, K.P. 8792
Iziumova, T.G. 8906

Jackson, J.M. 9132
Jacobs, G. 8857
Jacobs, J.E. 9031
Jacobsen, E.H. 8694
Jaeschke, R.L. 9106
Janousek, V. 8671
Janovec, V. 8691
Jenny, D.A. 8980
Jochems, P.J.W. 8994, 9000, 9008, 9135
Johnson, C.M. 9043
Johnson, L. 8864
Johnson, L.R. 8617
Johnson, R.B. 8986
Jones, E.M. 9072
Jones, Jr., J.P. 9068
Jones, L.W. 9032
Jones, M.E. 8996
Jones, R.V. 8807
Jonscher, A.K. 8963
Jorgensen, P.J. 8636
Joseph, A.S. 8849
Joshi, S.K. 8667, 8913

Kagan, S. 9112
Kallestinov, G.V. 8966
Kalnins, I.L. 8985
Kaminow, I.P. 8807
Kammer, E.W. 8930
Kandaurova, G.S. 8800
Kanzaki, H. 8618
Känzig, W. 8647, 8837
Kaplan, R. 8836
Karrer, S. 9034
Kataev, G.I. 8943
Kathan, L.S. 8666
Katz, M.J. 8643
Keldysh, L.V. 8717
Kemp, W.R.G. 8916
Kern, R. 8586
Keshler, Jr., C.P. 9127
Keyes, R.W. 8724
Khaikin, A.S. 8907
Khalatnikov, I.M. 8753
Khlystov, A.S. 8813, 8816
Khromov, B.P. 8789
Kido, K. 8618
Kikuchi, C. 8771, 9050
Kikuchi, M. 8899
Kikuchi, R. 8801, 8802
Kim, Y.W. 8836
King, R.E.J. 8897
Kippenhan, B.W. 8628
Kirenskii, L.V. 8805
Klabunde, C.E. 8651
Klassen, F.M. 9022
Klecak, G.L. 8614
Kleinman, D.A. 8852, 8855
Klemens, P.G. 8916
Klimowski, J. 8686
Koch, R.C. 9110
Koehler, W.C. 8822
Koenig, S.H. 8720, 8727
Kohn, J.A. 8831
Kokin, A.A. 8841
Kolm, C. 8929
Koloskova, N.G. 8827
Kondorskii, E.I. 8786
Konitzer, J.D. 8856
Kopelman, B. 8990
Kopvillem, U.Kh. 8827
Korkowski, V.J. 9039
Koster, G.F. 8845
Kostin, V.N. 8905
Kotiukov, Iu.N. 8809, 8811
Kramer, M. 9140
Krinchik, G.S. 8851
Kristofel, N.N. 8874
Kubota, B. 8630
Kudriautsev, O.M. 9021
Kudriavtsev, I.P. 8799
Kudzin, A. Iu. 8815
Kuhrt, F. 9020
Kunckel, H. 9114
Kurosawa, T. 8718
Kushida, T. 8808

Labes, M.M. 8735
Lam, Jr., D.G. 8936
Lambe, J. 8771, 9047, 9050
Landsberg, P.T. 8659, 8697
Lapluye, G. 8687, 8688
Laughlin, R.D. 8989
Lavine, M.C. 8640
Lawson, W.D. 8867
Lax, M. 8704
Lazarev, B.G. 8757
Lean, J.B. 8939
Lee, E.W. 8775, 8776
Lee, V.J. 8626
Legvold, S. 8736
Leinfelder, B.A. 8972
LeLoup, T.E. 8951
Lever, R.C. 9044
Levinstein, H. 8864
Levitin, R.Z. 8943
Levy, I.E. 9013
Levy, R.A. 8925
Li, G.-D. 8817, 9041
Li, J.C.M. 8606
Libovicky, S. 8599
Lidow, E. 8987
Lin, H.C. 9064
Lind, E.L. 8900
Lindsay, J.E. 9102
Lipkin, H.J. 8889
Little, W.A. 9004
Longini, R.L. 9001, 9002
Looney, D.H. 9037
Lothe, J. 8605
Loudon, R. 8695
Low, J.J. 8956
Low, W. 8832, 8847
Lowry, Jr., L.R. 9130
Ludwig, G.W. 8770
Lushchik, C.B. 8875
Lushchik, N.E. 8875
Lyons, V.J. 8582

MacDonald, J.R. 8679

# AUTHOR INDEX *(Continued)*


Maeda, H. 8761
Mahendroo, P.P. 8842
Maissel, L. 8974, 8981
Makhov, G. 9047, 9050
Mandelkorn, J. 8699
Mapother, D.E. 8748, 8756
Marinace, J.C. 9023
Markham, J.J. 8856
Markov, M.N. 8907
Marshall, S.A. 8846
Marzolf, J.M. 9139
Maserjian, J. 8999
Maslennikova, F.V. 8800
Masuda, Y. 8843
Masumi, T. 8767
Mataré, H.F. 8708, 8896
Matoshin, V.M. 8948
Matsumura, K. 8621
Matthias, B.T. 8744
Maurer, R.D. 8646
Mayer, S.E. 8931
McCall, D.W. 8588
McConkey, E.A.G. 8648
McElroy, M.R. 9128
McIlvaine, O.T. 9030
McKay, R.W. 9040
McKenzie, J.M. 9150
McLean, T.P. 8695
McVey, E.S. 9085, 9100
Meier, D.A. 9042
Meijer, G. 8891
Meltzer, B. 8961
Melvin, D.K. 9115
Mendelsohn, L.I. 9045
Merz, W.J. 8901, 8902
Meyer, M.A. 9122
Meyer, R.L. 9028
Meyers, N.H. 8754
Mikhailova, T.G. 8675
Milenbach, H. 9142
Milevskii, L.S. 8608
Miller, H.H. 9108
Miller, P.B. 8750
Miller, R.C. 8683
Mishin, D.D. 8788
Mitra, S.S. 8667, 8913
Mitsek, A.I. 8794
Mitskevich, V.V. 8910
Miyatani, S. 8734
Miyazawa, H. 8761
Mlavsky, A.I. 8931
Mockus, E.S. 9013
Mollwo, E. 8612
Momo, L.R. 9049
Morgan, L.P. 9138
Morinet, G. 8687, 8688
Morrison, G.H. 8614
Moss, T.S. 8894, 8911
Mueller, C.W. 8997
Murphy, J.C. 8831
Musatov, I.K. 8892
Mutabzija, R. 8965
Myer, J.H. 8978, 8979
Myers, R.A. 9049

Nagorsen, H. 9131
Nakamura, E. 8684
Nash, W.B. 8810
Nekrasov, M.M. 8676
Neugebauer, T. 8669
Newey, C.W.A. 8938
Nicols, G.M. 8839
Nielson, S. 8867
Nine, H.D. 8942
Nishiguchi, K. 8787
Nitsche, R. 8901
Noble, G.A. 8840
Nolle, A.W. 8842
Norman, R.S. 9045
Norr, M.K. 8642
Norwood, M.H. 8940
Novey, T.B. 8644
Novikova, S.I. 8820
Nuralieva, R.D. 8851

Odani, Y. 8803
Offner, F.F. 9147
Ogino, Y. 8621
Ogletree, W.A. 9067
Ohm, E.A. 9109
Okazaki, S. 8701
Oki, H. 8701
Okwit, S. 9048
Olsen, J.L. 8746
Onaka, R. 8868
Orlova, M.P. 8820
Ostroff, E.D. 9122
Overn, W.M. 9039

Paige, E.G.S. 8722
Pake, G.E. 8828
Pakswer, S. 9024
Paladino, A.E. 8581
Palistrant, M.E. 8860
Palla, P. 8687, 8688
Pankove, J.I. 9033
Pardue, T.E. 9005
Parent, R.J. 9108
Parker, H.W. 9007
Parravano, G. 8626
Partovi, F. 8784
Passow, E.B. 9118
Paton, F. 8715
Paul, W. 8672
Paull, S. 9099
Pearson, A.D. 8985
Pedrotti, L.S. 8887
Peet, C.S. 8624, 8872
Pell, E.M. 8625
Pendergast, R.J. 8833
Perkal'skaia, V.A. 8966
Perl, M.L. 9032
Perlin, Yu. E. 8860
Petrak, J.R. 9145
Petrakovskii, G.A. 8813
Phariseau, P. 8657
Pietrzak, J. 8686
Pincus, P. 8781
Plath, R.H. 9054
Ploos van Amstel, J.J.A. 9012
Pohm, A.V. 9070
Pokrovskii, V.N. 8656
Pollak, M. 8724
Potakhova, G.I. 8674
Pratt, Jr., G.W. 8655
Pratt, P.L. 8938
Prener, J.S. 8871
Price, P.J. 8723
Price, R.J. 9086
Prior, A.C. 8709
Prosser, V. 8908
Prutton, M. 8795
Pruzhinina, V.I. 9021
Pultorak, J. 8977
Putkovich, R.P. 9134
Putley, E.H. 8731

Quinn, D.J. 8743

Raffel, J.I. 9126
Raisbeck, G. 8993
Ramazanov, P.E. 8890
Ramdas, A.K. 8862, 8863
Ramsey, J.B. 8627
Rase, D.E. 8580
Ratner, A.M. 8876, 8877
Razbirin, B.S. 8888
Read, A.A. 9070
Read, Jr., W.T. 8954
Redfield, A. 8843
Rediker, R.H. 8964
Reed, B. 8896
Reed, J.F. 8615
Rees, D. 9052
Reese, W.E. 8861
Renius, O. 9052
Reuther, J.F. 9095
Reynolds, D.C. 8873, 8887
Rhys-Roberts, C. 8681
Riabinkin, Iu, S. 8995
Richards, J.L. 8641
Richardson, D.A. 8648
Richardson, J.M. 8707
Rimai, L. 8845
Roberts, D.H. 8898
Robinson, L.E. 9065
Robinson, R.J. 8702
Robinson, S.A. 9016
Rocard, Y.A. 9025
Rogers, J.L. 9038
Rogers, S.C. 9094
Rohrer, H. 8746
Romankevich, V.N. 8728
Rood, J.W. 9096
Roovers, W.A. 8953
Rose, F.W.G. 8715
Rosenberg, A.J. 8635
Rosi, F.D. 8616, 8932
Rösner, O. 8619
Rowley, L.H. 9142
Rubin, W.L. 9059
Rudenberg, H.G. 8960
Rupp, R.L. 8614
Rutter, J.W. 8971
Rywak, J. 9144

Saada, G. 8601, 8607
Sachs, H.M. 9018
Sagar, A. 8639
Salkovitz, E.I. 8793, 8930
Santini, M. 8834
Sasaki, Y. 9051
Sato, I. 9051
Savchenko, M.K. 8805
Scarbrough, A.D. 9084
Schindler, A.I. 8793
Schnable, G.L. 9017
Schulz, R.B. 9146
Schüppel, W. 8797
Schweinler, H.C. 8823
Scovil, H.E.D. 9109
Sehr, R. 8735
Semenenko, E.E. 8757
Serbulenko, M.G. 8948
Serova, F.G. 8923
Sestak, B. 8599
Sharpe, C.B. 8670
Shavlo, S.T. 8886
Shaw, R.W. 8748, 8756
Sherwell, R.J. 8956
Shiklosh, T. 8780
Shilliday, T.S. 8870
Shirkov, D.V. 8740
Shockley, W. 8922, 9080
Shotov, A.P. 8967
Shtrikman, S. 8804
Shur, Ya. S. 8800
Shvarts, K.K. 8875
Sidiakin, V.G. 8728
Silliman, S.D. 9095
Sils, V. 8982
Silvestri, V.J. 8582
Singh, S.P. 8665
Singwi, K.S. 8666
Sinha, A.P.B. 8590
Siniakov, E.V. 8815
Skrotskii, G.V. 8906
Smith, D.O. 8796
Smith, G.W. 8844
Smith, J.G. 9048
Smith, N.R. 9143
Smith, S.D. 8911
Smokotin, E.M. 8811
Smoluchowski, R. 8729
Sobolev, V.V. 8866
Sommer, R.D. 9129
Sonder, E. 8645, 8823
Southgate, P.D. 8946, 8947
Spedding, F.H. 8736
Spitzer, W.G. 8855
Spyut, A.B. 9013
Standley, K.J. 8810
Stankevich, K.S. 8829
Statz, H. 8774, 8845
Steenis, O.L.V. 8953
Stemme, O. 8797
Stephenson, W.L. 9138
Stern, E. 9036
Stevenson, M.J. 8768
Stinchfield, R.P. 8936
Stineman, J.W. 9016
Stockmann, F. 8612
Stone, B. 8732
Stoudenheimer, R.G. 9033
Stratton, R. 8712
Strull, G. 9117
Struthers, J.D. 8762
Strutt, M.J.O. 9019
Su, K.L. 9058
Sudovtsev, A.I. 8757
Suge, Y. 8767
Suhl, H. 8744, 8806
Suomi, V.E. 9108
Suzuki, T. 8787
Svirina, E.P. 8763
Swalin, R.A. 8620
Swartz, J.M. 8872
Swenson, Jr., G.W. 9111
Swift, W.B. 9108
Swihart, J.C. 8754
Sydnor, R.L. 9111
Szegho, C.S. 9024

Tanaka, S. 8767
Tannenbaum, E. 8629
Tannhauser, D.S. 8733
Tansal, S. 8754
Taylor, K.N.R. 8883
Tefft, W.E. 8936
Templeton, L.C. 8645
Terhune, R.W. 9047, 9050
Tewordt, L. 8737
Thomas, D.G. 8850
Thomas, N. 8869
Thompson, G.J. 9134
Thomson, R. 8604
Thouless, D.J. 8739
Thun, R. 8627
Thurell, Jr., J.R. 8991
Tiablikov, S.V. 8780
Tiley, J.W. 9015
Tiller, W.A. 8632, 8971
Tillman, R.M. 9090
Tinkham, M. 8853
Title, R.S. 8893
Toman, K. 8589
Tomik, J. 8671
Tompkins, H.E. 9125
Townes, W.D. 8831
Toy, W.N. 9098
Toyoda, H. 8609
Trapeznikova, Z.A. 8878, 8879
Tredgold, R.H. 8681, 8682, 8713
Treves, D. 8804
Triebwasser, S. 8680
Trousdale, R.B. 9082
Tsekvava, B.E. 8909
Tsubokawa, I. 8818
Tummers, L.J. 8994
Turner, W.J. 8861
Turov, E.A. 8794

Uchaikina, R.F. 8825
Uhlir, A. 8959

Van Bosse, J.G. 9116
Van Houten, S. 8719
van Lint, V.A.J. 8649
Van Overbeek, A.J.W.M. 9061
Veach, C.W. 8949
Vereshchagin, I.K. 8880
Vick, G.L. 8935
Vladimirov, V.I. 8595
Vlasov, K.B. 8783
Vodop'ianov, K.A. 8674, 8675
Vogt, O. 8824
Volger, J. 8652
Vorozhtsov, B.I. 8674, 8675

Wachtman, Jr., J.B. 8936
Waddas, R. 8814
Wadsworth, M.E. 8636
Wagner, M. 8895
Wagoner, G. 8772
Wahl, F. 8596
Wainwright, H.W. 9127
Wajda, E.S. 8628
Walker, P.A. 8919
Waltz, M.C. 8950
Wang, X.-L. 9041
Wannier, G.H. 8705
Warren, B.E. 8592
Watanabe, H. 8826
Waters, W.P. 8979
Watkins, T.B. 8969
Webb, G.N. 9101
Webb, H.D. 9111
Weber, M.J. 8845
Webster, R.R. 9066
Weichman, F.L. 8903
Weinreich, O. 8896
Weisberg, L.R. 8616
Weiss, G.P. 8796
Wells, A.F. 8587
Wentzel, G. 8742
West, F. 8790
West, J.W. 8983
Whelan, J.M. 8762
White, F.A. 8927
White, W.H. 8628
Wieber, R.H. 8624
Wigen, P.E. 8838
Wiggins, C.S. 8882
Wikner, E.G. 8649
Wilcox, C.S. 9107
Wilcox, D.D. 9119
Wilkinson, M.K. 8821, 8822
Willardson, R.K. 8765
Williams, F.C. 9123
Williams, R.A. 9015
Williams, R.L. 9027
Wiltse, J.C. 9043
Winder, C.F. 9072
Winkel, J.T. 9136
Wolf, E.L. 9087
Wolfendale, E. 9137
Wolff, E.A. 9011
Wolff, G.A. 8643
Wollan, E.O. 8821, 8822
Wolsky, S.P. 8637
Woodbury, H.H. 8770
Woolley, J.C. 8725
Worrell, E.A. 9056
Wright, D.A. 8928
Wul, B.M. 8967

Xiao, F.-K. 9041
Xin, H.-W. 8817

Yamaguchi, J. 8621
Yamartino, E.J. 9044
Yamashita, J. 8718
Yeadon, R.E. 8648
Yost, H.J. 9056
Young, A.S. 8867
Young, D.R. 8754

Zabara, M.I. 8905
Zavaritskii, N.V. 8917
Zdanuk, E.J. 8637
Zelinka, R.J. 9062
Zemel, J. 8710
Zharkov, G.F. 8738
Zhiliakov, S.M. 8816
Zil'berman, G.E. 8876
Zimmerman, III, W. 8617
Zlai, C.-Y. 8817
Zuev, A.F. 8815
Zyrianov, P.S. 8906

“Every 24 hours enough technical papers are turned out around the globe to fill seven sets of the twenty-four volume *Encyclopaedia Britannica*. And the output is rising every year. This year's crop: some 60 million papers . . . the laboratory scientist, busy with work of his own, no longer can find enough hours in the day to keep up with all that is published in his field. Even staying on top of the indexes and abstracts of these papers has become an insurmountable task for the lab men. One result is that company after company has found itself duplicating research work that others have done and fully chronicled.”

From the *Wall Street Journal*
Tuesday, December 20, 1960

# COMPUTER ABSTRACTS ON CARDS

## A quick cumulative reference to the Technical Literature on Electronic Computers

C 2.25/1.249

1539 COMPUTER DESIGN OF MULTIPLE-OUTPUT LOGICAL NETWORKS by T. C. Bartee (Lincoln Lab., M.I.T.); IRE Trans. on Electronic Computers, Vol. EC-10, pp. 21-30, March 1961

An important step in the design of digital machines lies in the derivation of the Boolean expressions which describe the combinational logical networks in the system. Emphasis is generally placed upon deriving expressions which are minimal according to some criteria. A computer program which automatically derives a set of minimal Boolean expressions describing a given logical network with multiple-output lines is discussed. The program accepts punched cards listing the in-out relations for the network, and then prints a list of expressions which are minimal according to a selected one of three criteria. The basic design procedure and the criteria for minimality are described.

COMPUTER ABSTRACTS ON CARDS is designed to provide the engineer or scientist with a cumulative reference file to the technical literature on electronic computers, *organized by subject matter*. As a subscriber you would receive, every other month, several hundred 3″ x 5″ cards containing abstracts of recently published papers in the computer field. These abstracts summarize the contents of the papers, enabling you to determine what work has been reported on a given subject and showing you where you can find more detailed information on that subject. In addition to the abstract and the journal reference, each card has a classification number which makes it easy for you to file the card in a *logical sequence* with all previously issued cards. In this way you can continuously group together abstracts of related references, just as the Dewey Decimal System enables a librarian to group together books on related subjects.

This abstract card file corresponds in some ways to the card file which enables the librarian to locate any book or periodical in the library. However, it has additional advantages which result from the information provided by the abstracts themselves and from the logical (as opposed to alphabetical) organization which permits one to browse through references on related topics as one might browse through the books on a library shelf. An alphabetical Pre-Index is provided with this service to direct the user to the part of the file which is devoted to a given topic. In addition, the same abstracts are supplied in a non-cumulative form with subject and author non-cumulative version of the abstracts make it easy to locate information by:

*Logical Sequence*
*Alphabetically by Subject*
*Alphabetically by Author*

COMPUTER ABSTRACTS ON CARDS covers the following topics in the field of electronic computers:

- Logic and Switching Theory (Boolean Functions, Switching Networks, Automata)
- Digital Computers and Systems (Design, Arithmetic Methods, Equipment, Error Detection)
- Devices (Electromechanical, Electron Tube, Semiconductor, Magnetic, Cryogenic, etc.)
- Logic and Waveforming Circuits
- Storage and Input-Output
- Programming and Coding (Programming Languages, Automatic Programming, Algorithms)
- Languages (Natural and Formal Languages, Mechanical Translation)
- Information Retrieval
- Pattern Recognition and Artificial Intelligence
- Mathematics (Number Theory, Numerical Analysis, Probability and Statistics)
- Operations Research and Game Theory
- Information Theory and Noise; Communications Systems
- Analog and Hybrid Computers
- Real-Time Systems and Automatic Control
- Applications of Computers in Science, Engineering, Industry, Government, Business, etc.

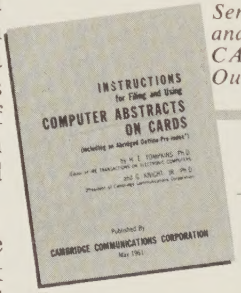


*Send for free booklet — “Instructions for Filing and Using COMPUTER ABSTRACTS ON CARDS” — including Abridged Classification Outline and Pre-Index.*

**CAMBRIDGE COMMUNICATIONS CORPORATION**
236 Main St., Cambridge 42, Mass.

Please send me a copy of “Instructions for Filing and Using COMPUTER ABSTRACTS ON CARDS”.

NAME _____

TITLE _____

COMPANY _____

ADDRESS _____

CITY _____ ZONE _____

STATE _____

**in'for·ma'tion re·triev'al,** *n.* **1.** rapid location of technical information on specific topics.

# information retrieval system for the solid state:

# SOLID STATE ABSTRACTS ON CARDS

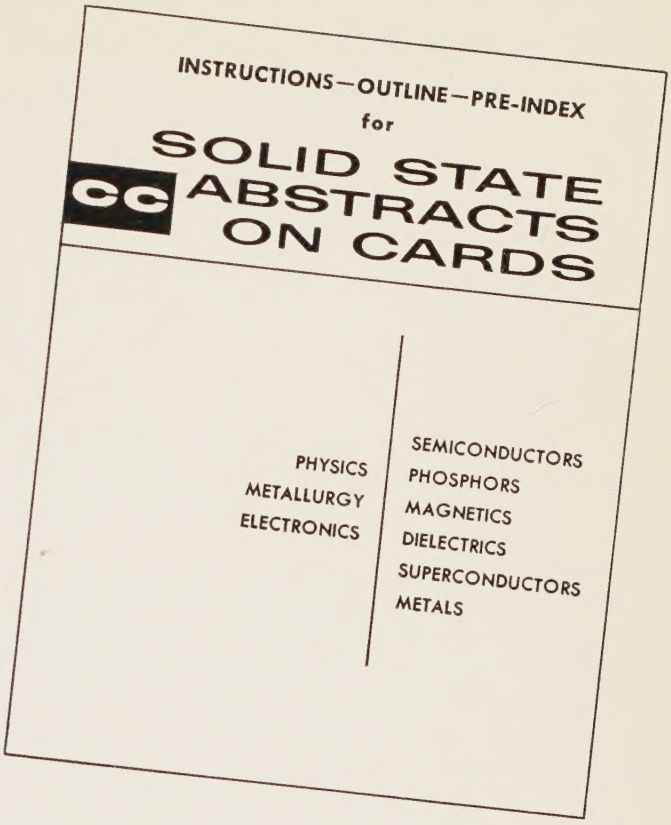


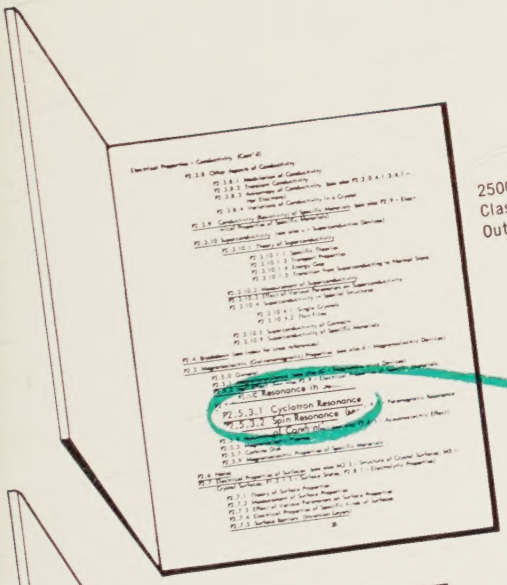

2500-Topic Classification Outline

Send for your free copy of our new 120 page book describing this unique system which is now being used in more than 300 solid state laboratories throughout the world.

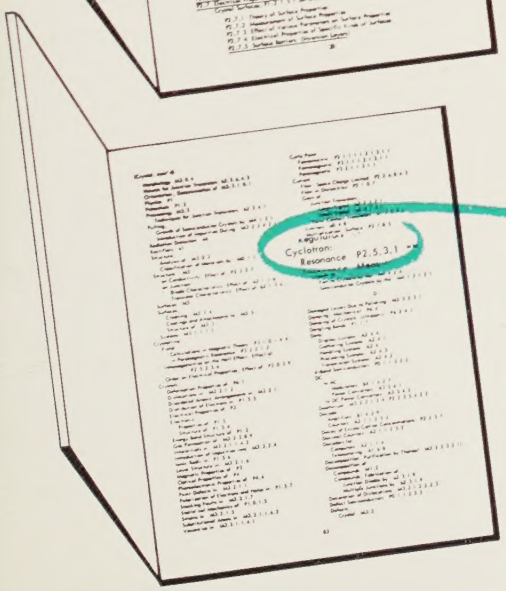

4000-Entry Alphabetical Pre-Index

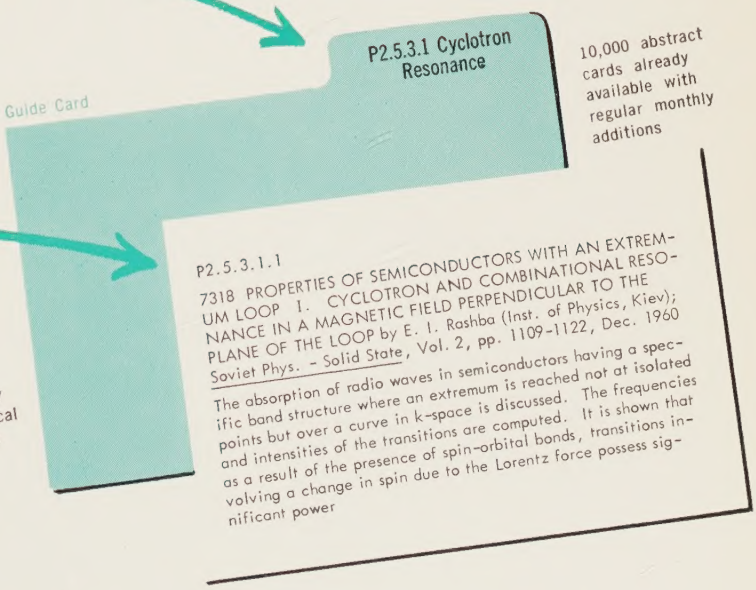
P2.5.3.1 Cyclotron Resonance
Guide Card
10,000 abstract cards already available with regular monthly additions
P2.5.3.1.1
7318 PROPERTIES OF SEMICONDUCTORS WITH AN EXTREMUM LOOP I. CYCLOTRON AND COMBINATIONAL RESONANCE IN A MAGNETIC FIELD PERPENDICULAR TO THE PLANE OF THE LOOP by E. I. Rashba (Inst. of Physics, Kiev); Soviet Phys. - Solid State, Vol. 2, pp. 1109-1122, Dec. 1960
The absorption of radio waves in semiconductors having a specific band structure where an extremum is reached not at isolated points but over a curve in k-space is discussed. The frequencies and intensities of the transitions are computed. It is shown that as a result of the presence of spin-orbital bonds, transitions involving a change in spin due to the Lorentz force possess significant power

**CAMBRIDGE COMMUNICATIONS CORPORATION**

236 MAIN STREET • CAMBRIDGE 42, MASSACHUSETTS • Tel. 491-0710

# Pre-publication Announcement

A BOOK
OF CLASSIFIED
ABSTRACTS
ON

# ORGANIC SEMICONDUCTORS

FEATURING

- Over 1000 Abstracts
- Subject Index
- Material Index
- Author Index

You save money by ordering now at the pre-publication price of $20^{00}$

Payment will not be due until the book is issued in the Fall of 1962.

SEND YOUR ORDER TODA Y TO

**CAMBRIDGE COMMUNICATIONS CORPORATION**
238 Main St., Cambridge 42, Mass.

Please enter our Pre-publication Order for ORGANIC SEMICONDUCTORS to be published in the Fall of 1962, at the special price of $20.00.

Name .....
Position .....
Company .....
Division, if any .....
Address .....
City ..... Zone ..... State.....